Volume 2 Figures and Tables

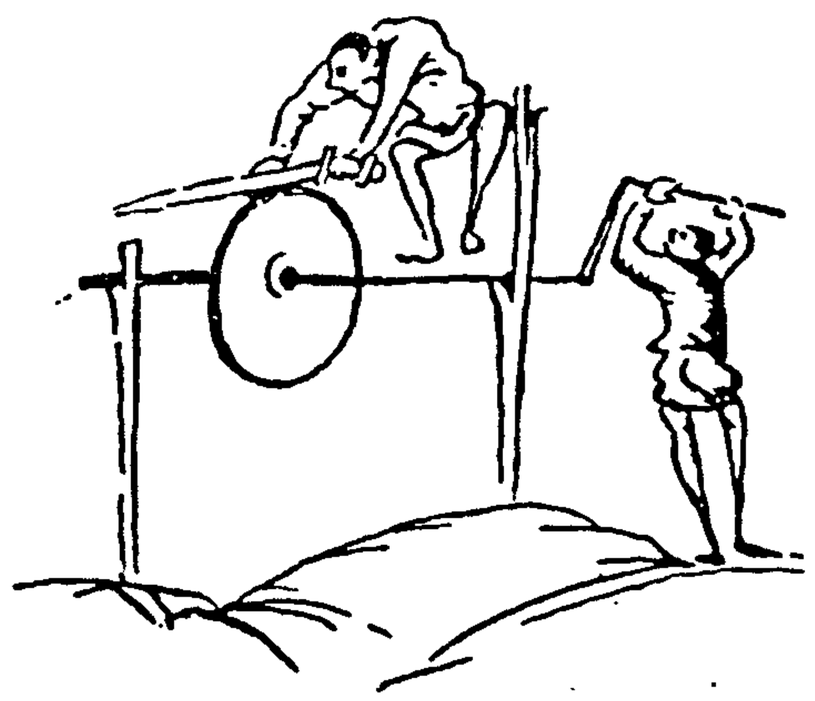

Fig 1 Wheel and hand grinding and polishing of sword blades; from the Utrecht Psalter AD 820 (Chapter 2.2)

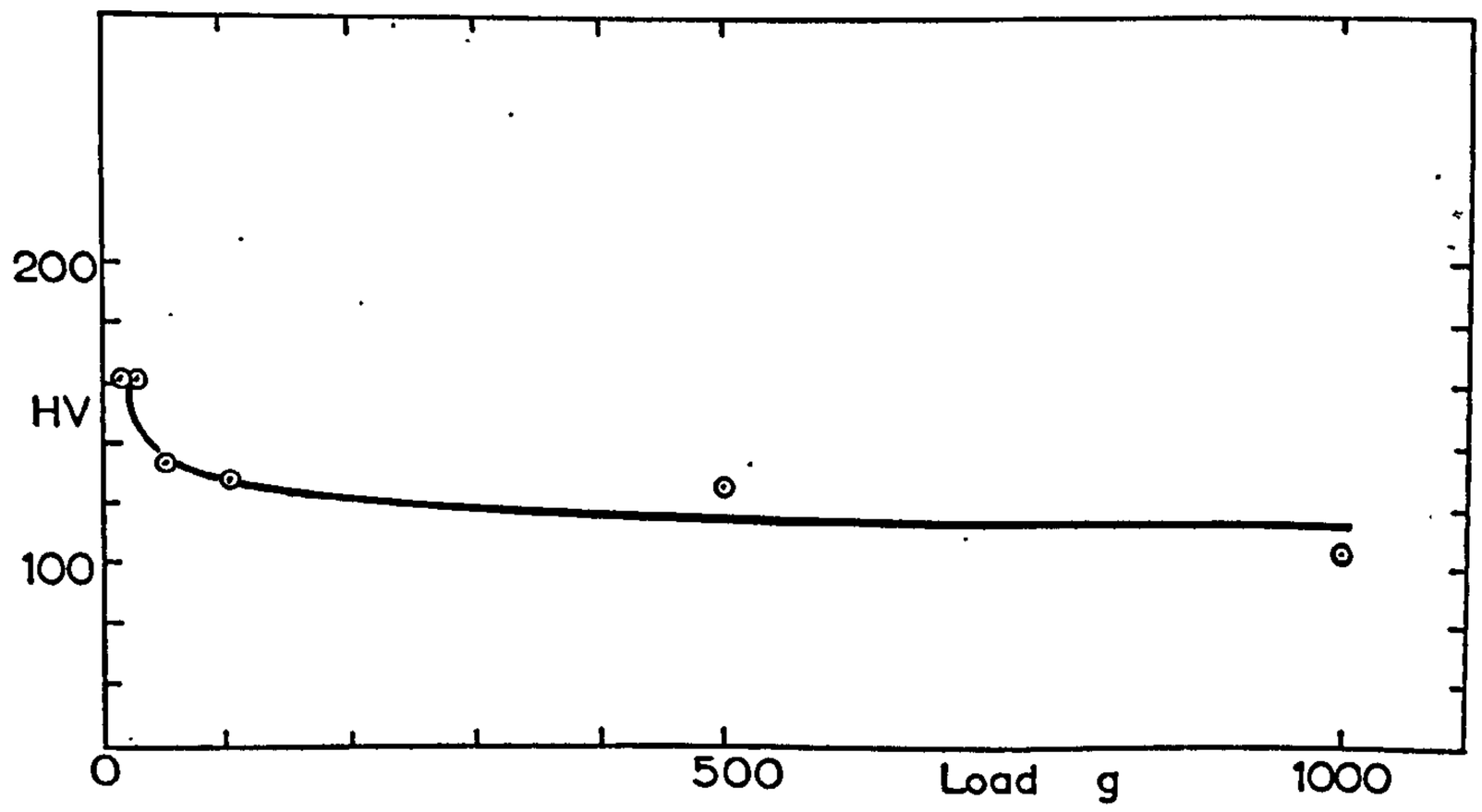

Fig 2 Variation of micro-hardness with load (Chapter 3.3.3)

IRON-CARBON SYSTEM

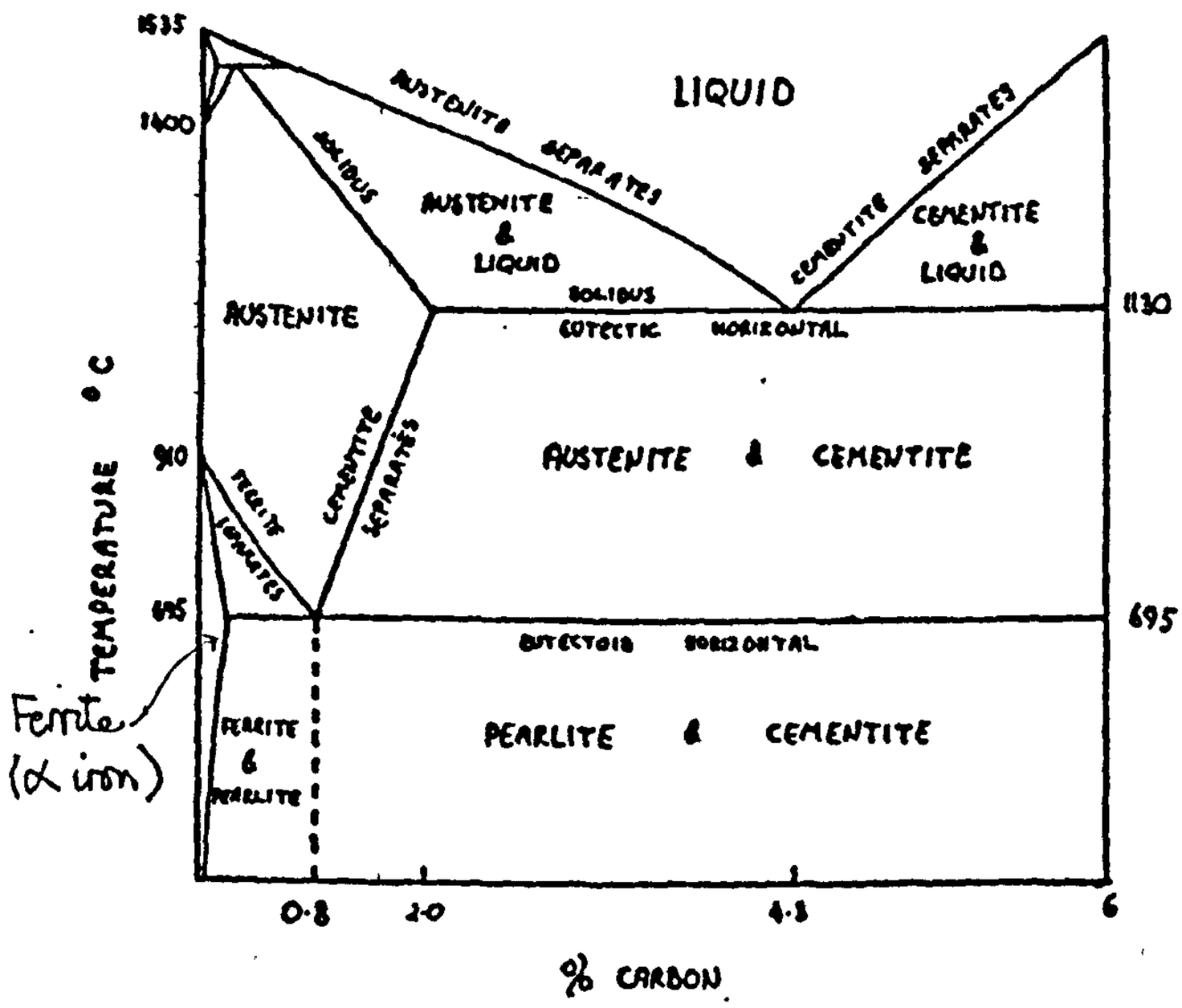

1 THE COMPLETE IRON - CARBON DIAGRAM

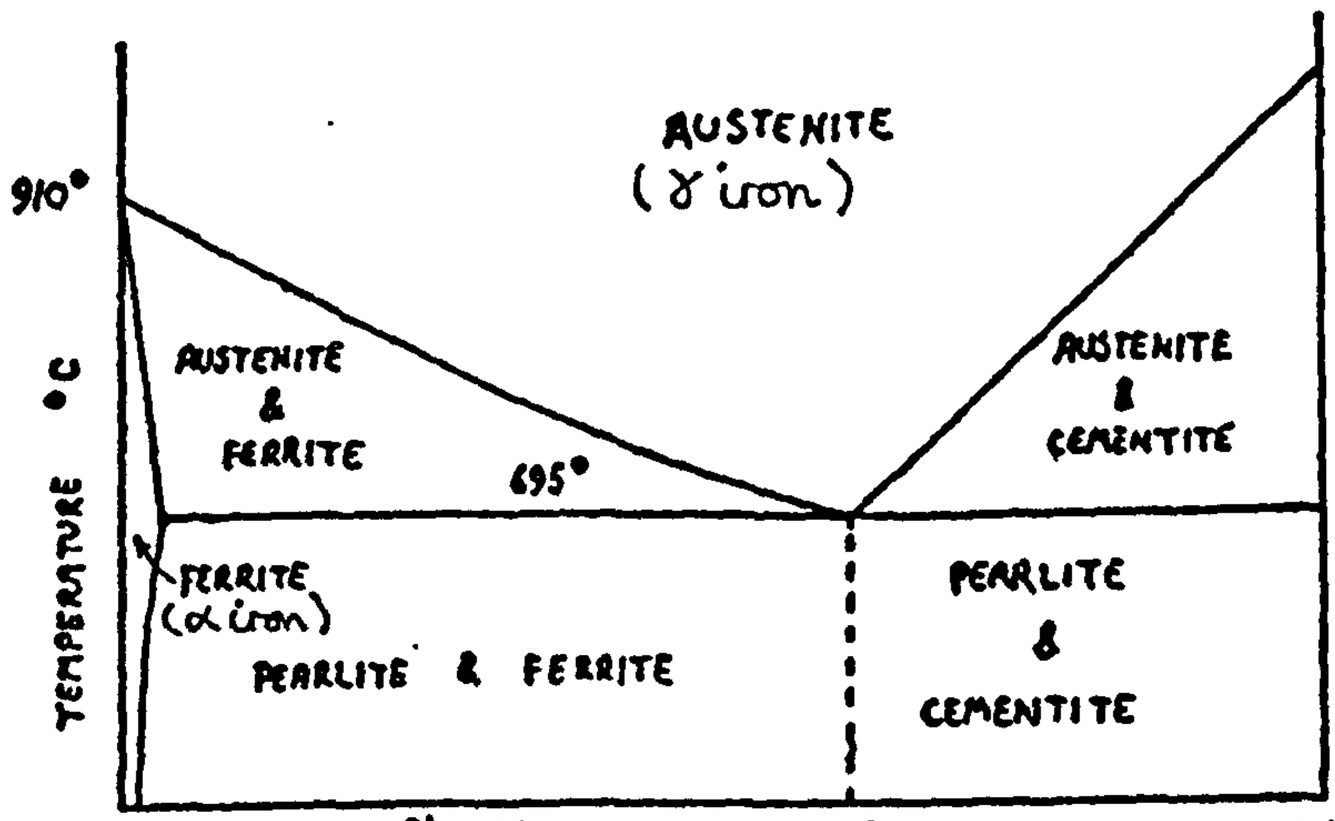

ii THE 'STEEL PORTION' OF THE IRON - CARBON DIAGRAM

Fig 3 i. Iron-carbon equilibrium diagram (Chapter 4)

ii Expanded steel portion of the iron-carbon diagram (Chapter 4)

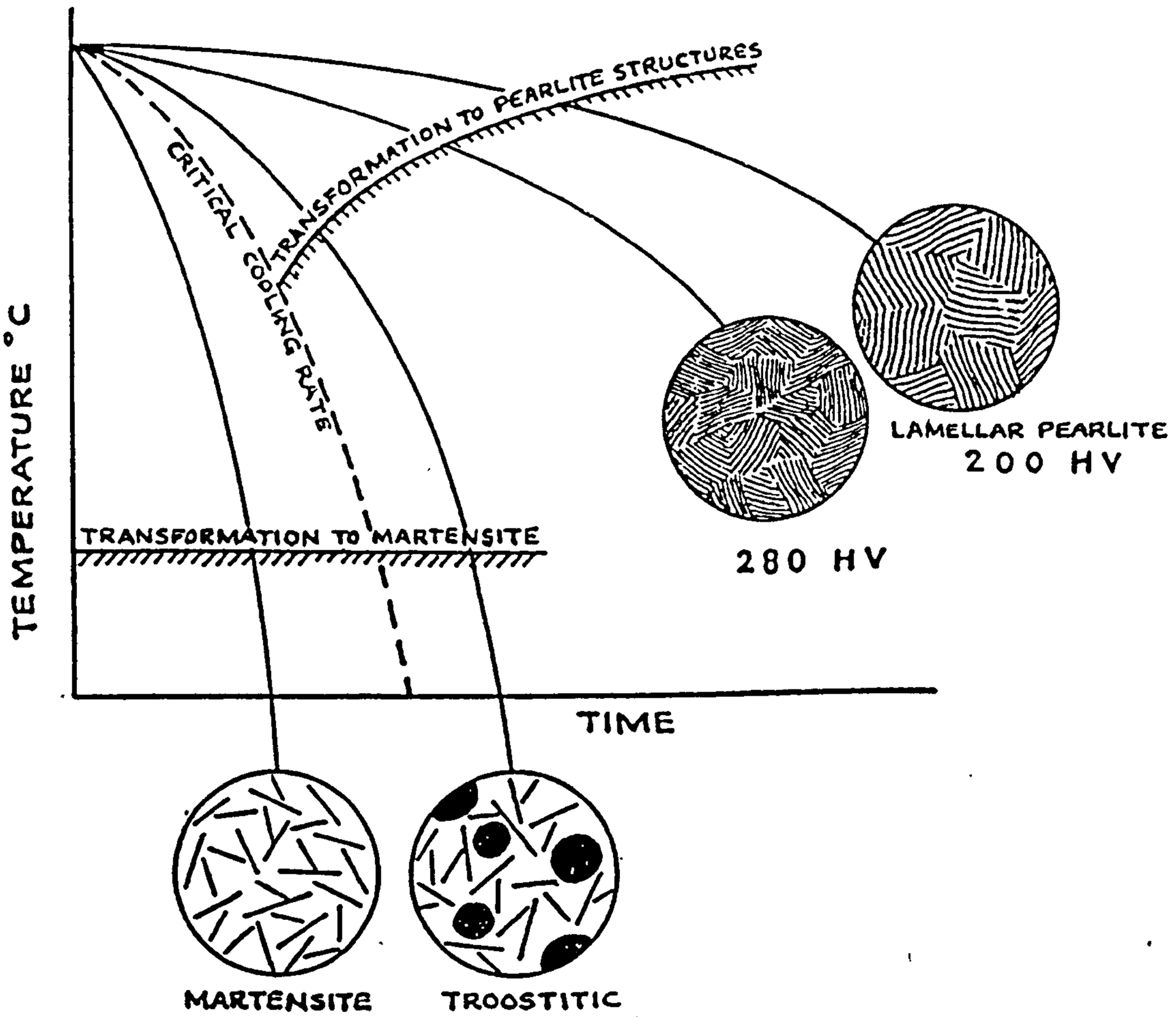

Fig 4 Continuous cooling time/temperature transformation (TTT) diagram: the transformation effects of different cooling rates for eutectoid steel - 0.8% carbon (Chapter 4.7.6 - 4.7.10)

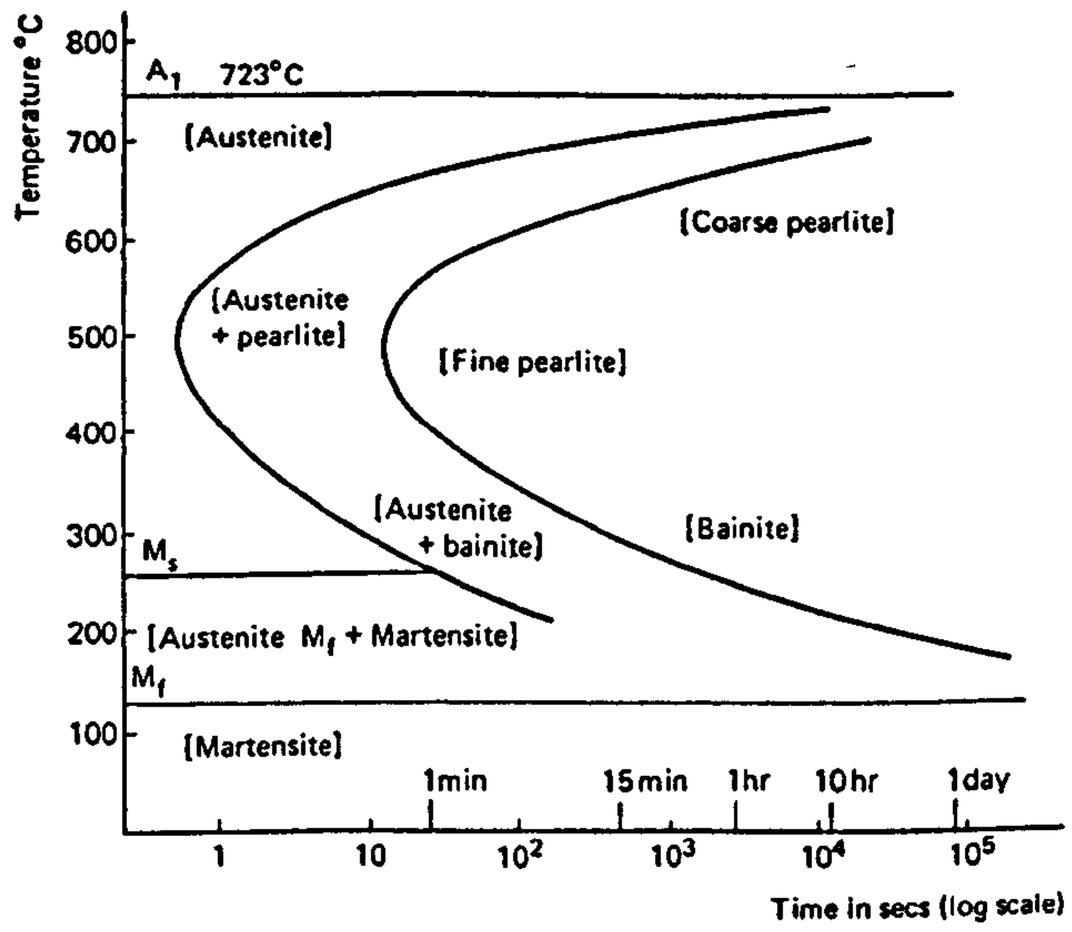

Fig 5 Isothermal TTT diagram for eutectoid steel (Chapter 4.7.10)

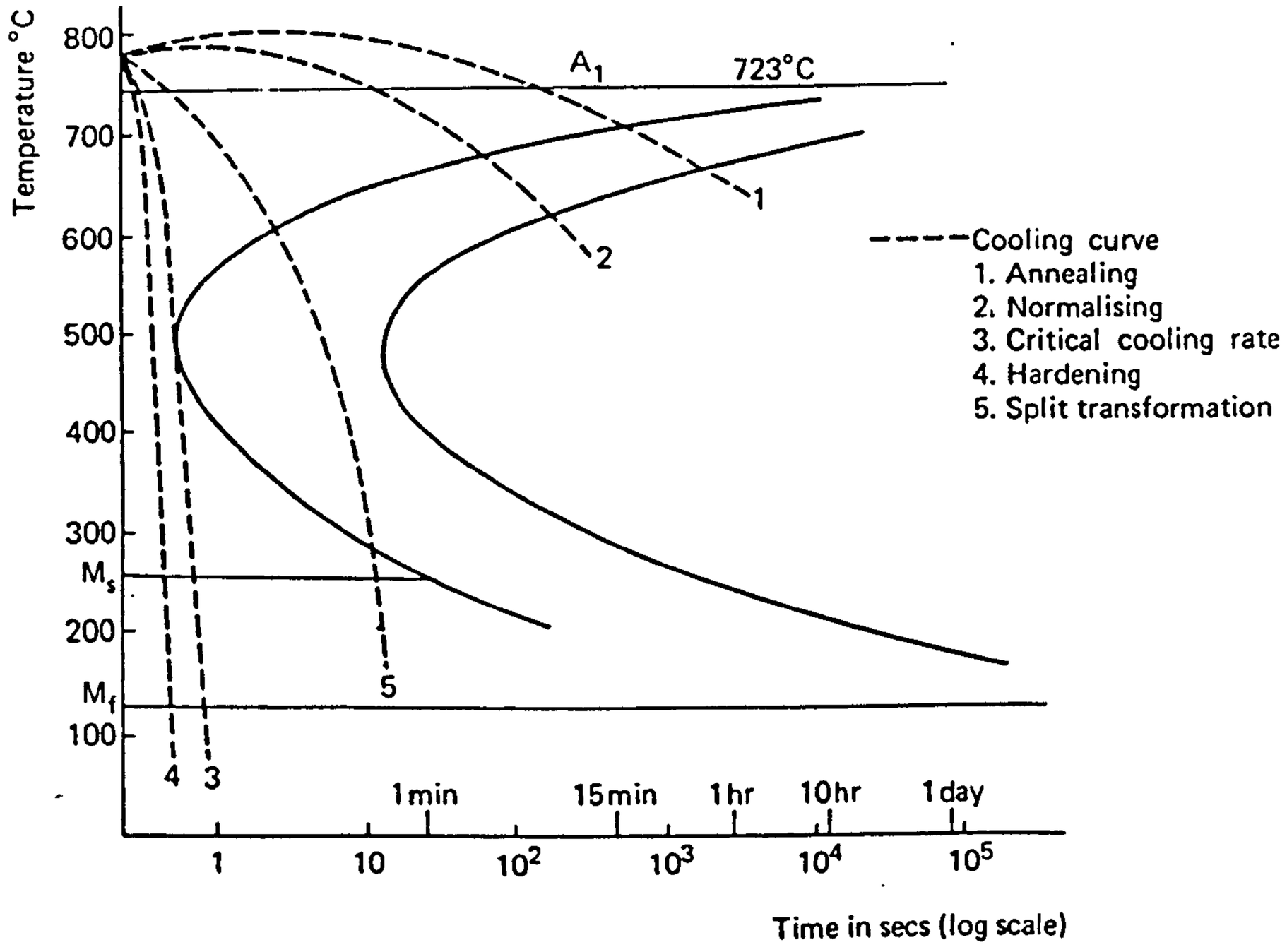

Fig 6 Superimposed continuous cooling and isothermal TTT diagrams (Chapter 4.7.10)

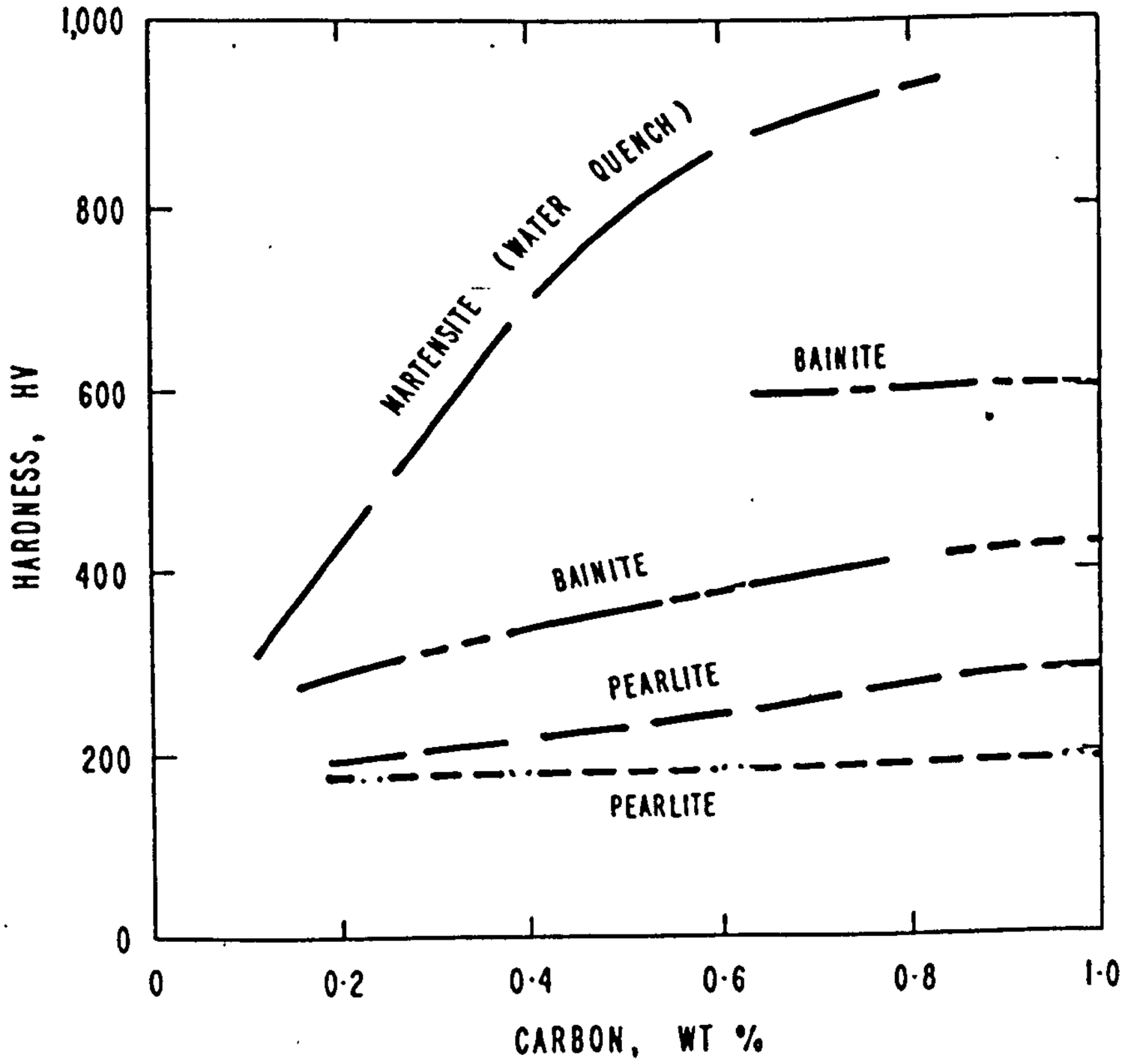

Fig 7 Variation of hardness with carbon content for different structures found in plain carbon steel (Chapter 4.7)

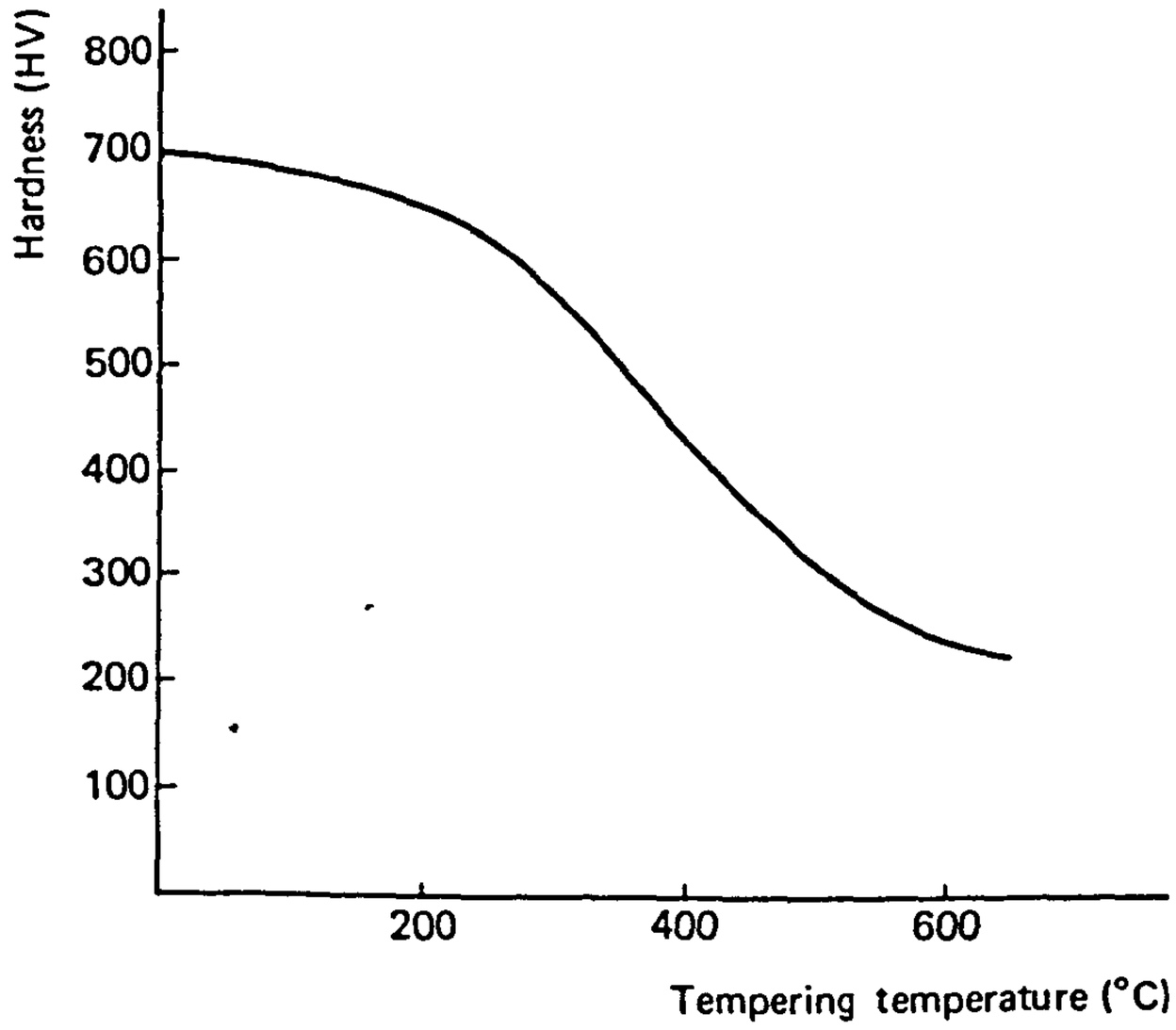

Fig 8 Variation of hardness with tempering temperature for a 0.4% carbon steel tempered for 30 minutes (Chapter 4.7.11)

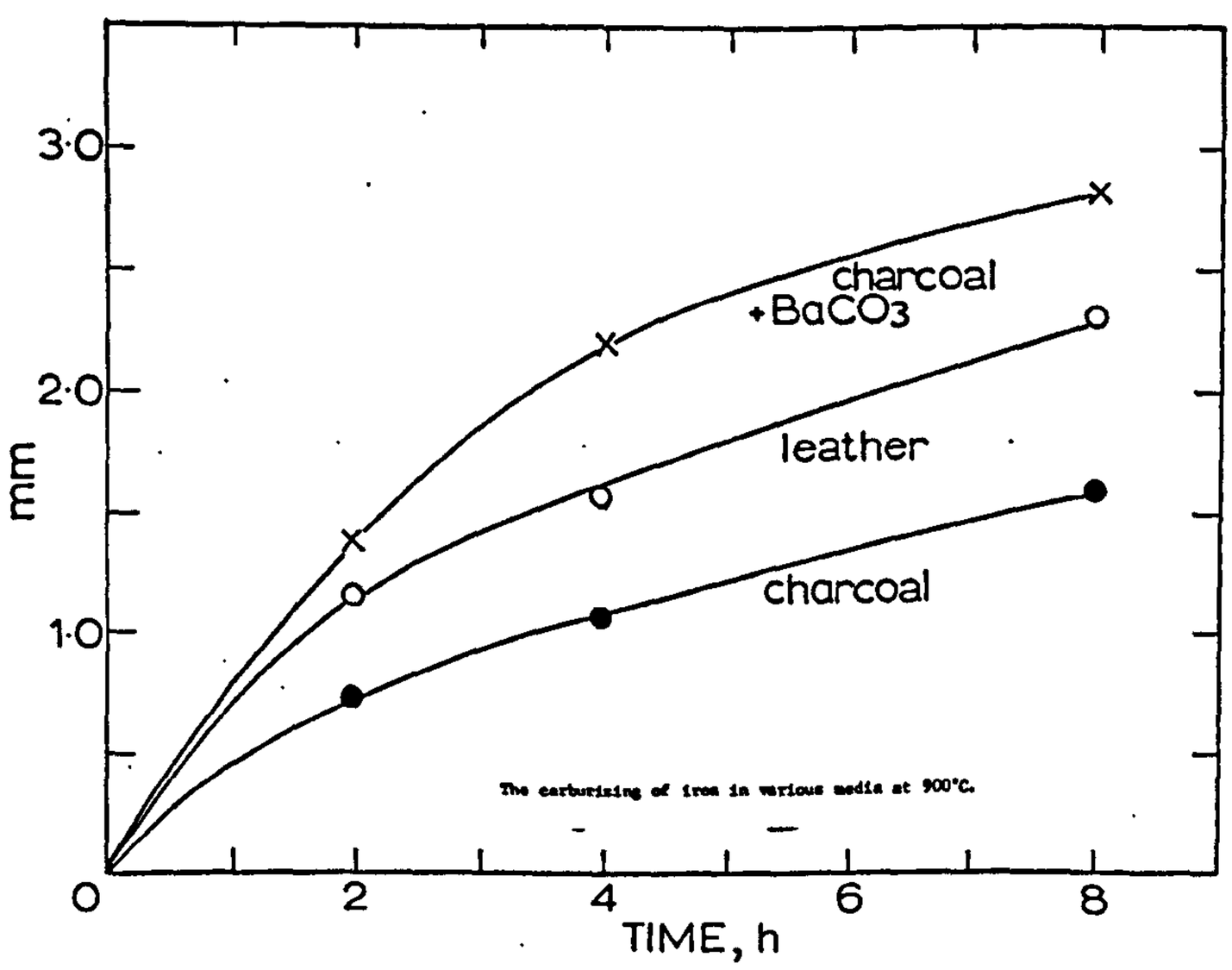

Fig 9 Variation of depth of carburisation with temperature (Chapter 5.10)

Positions of sections scale bars 10 cm

S1

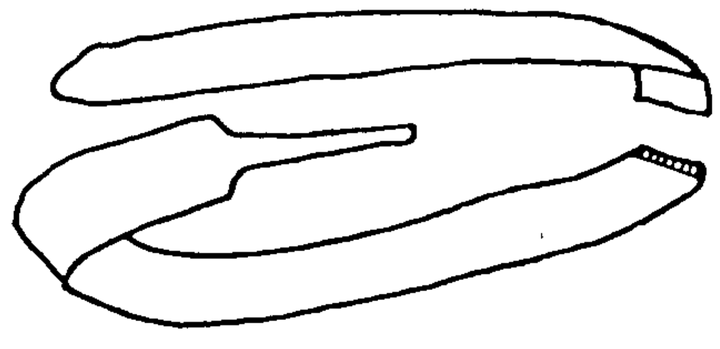

S7

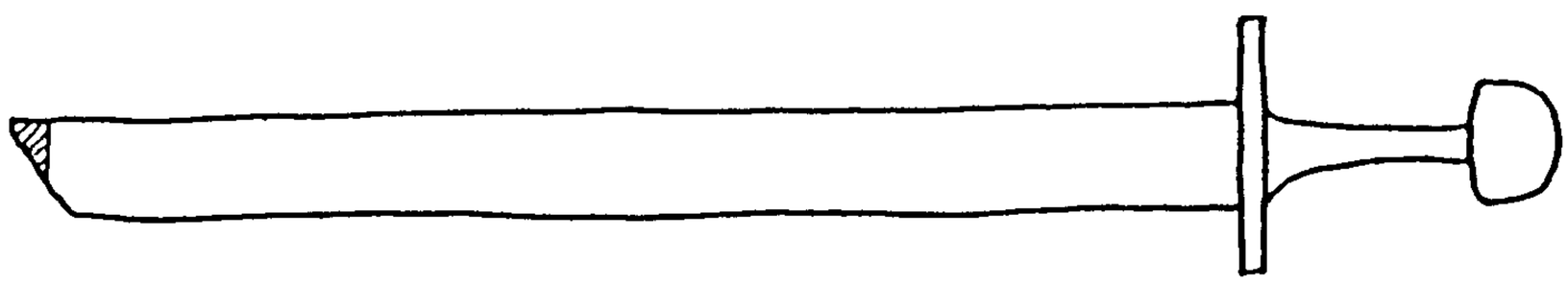

S8

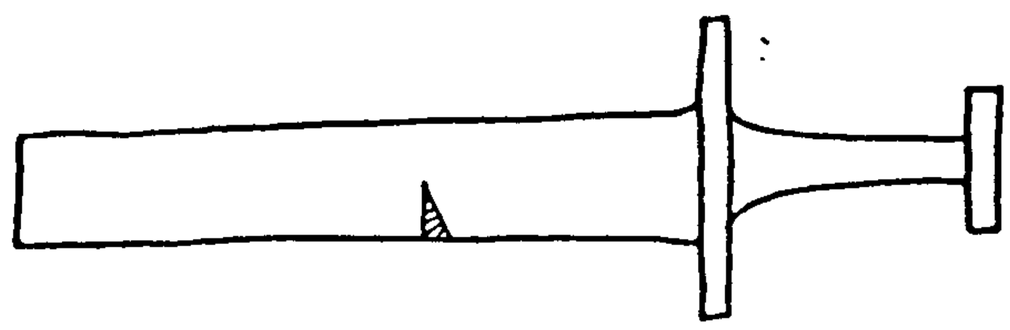

S10

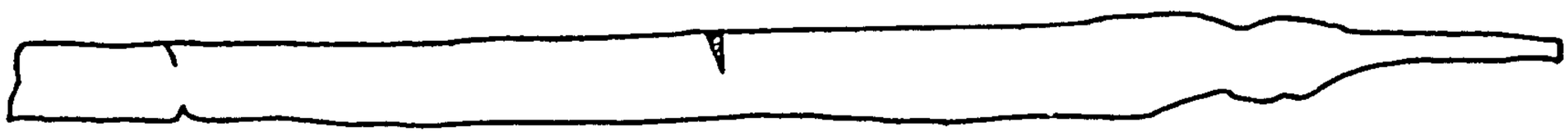

S12

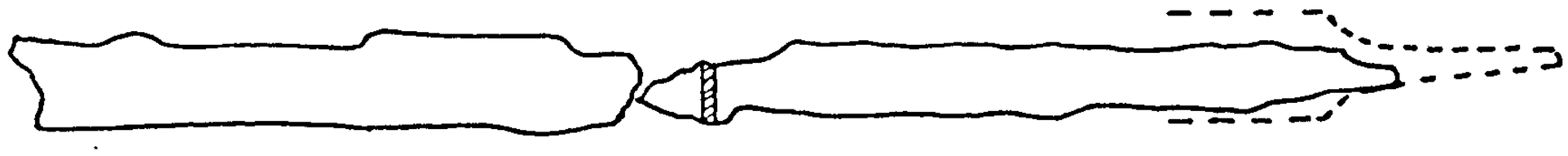

S13

S14

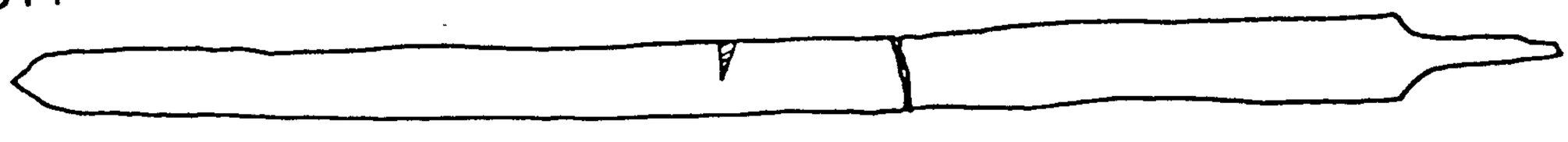

Fig 10 Outlines of swords with positions of sections (Chapter 6)

S15

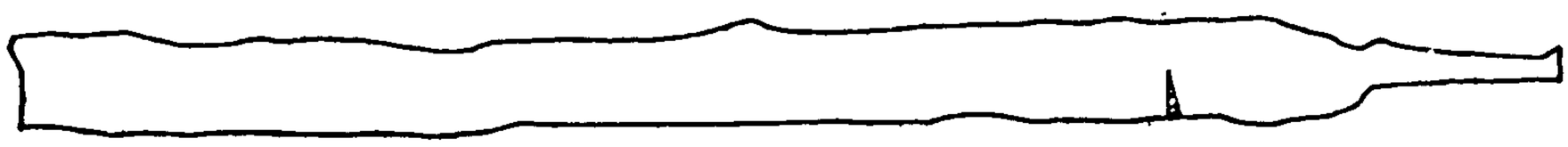

S16

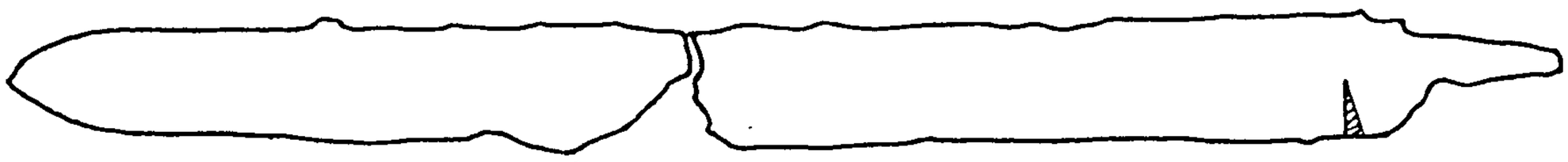

S17

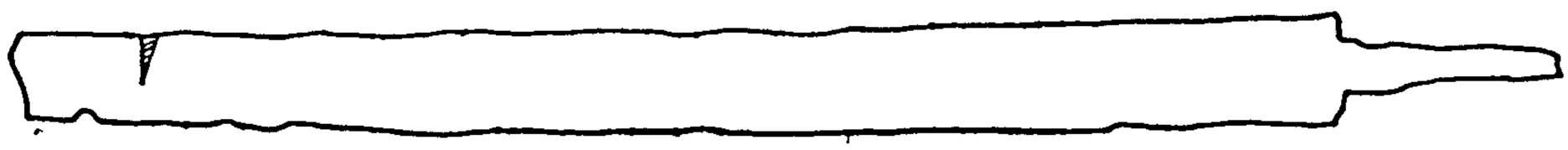

S18

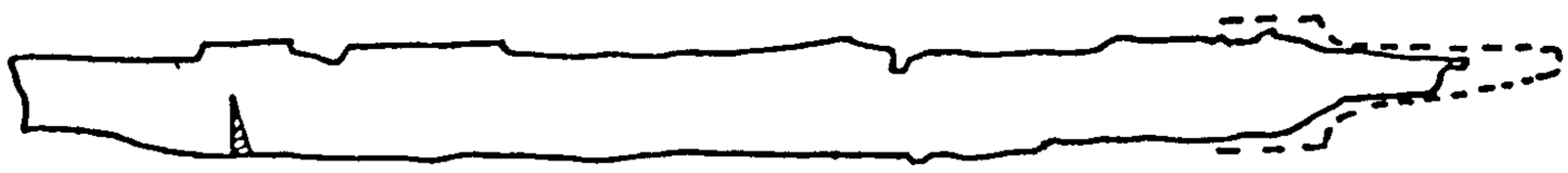

S19

S20

S23

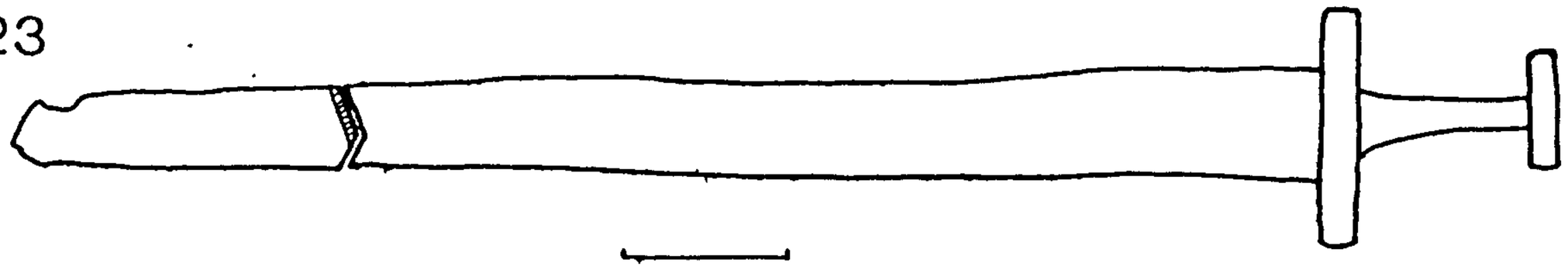

S24

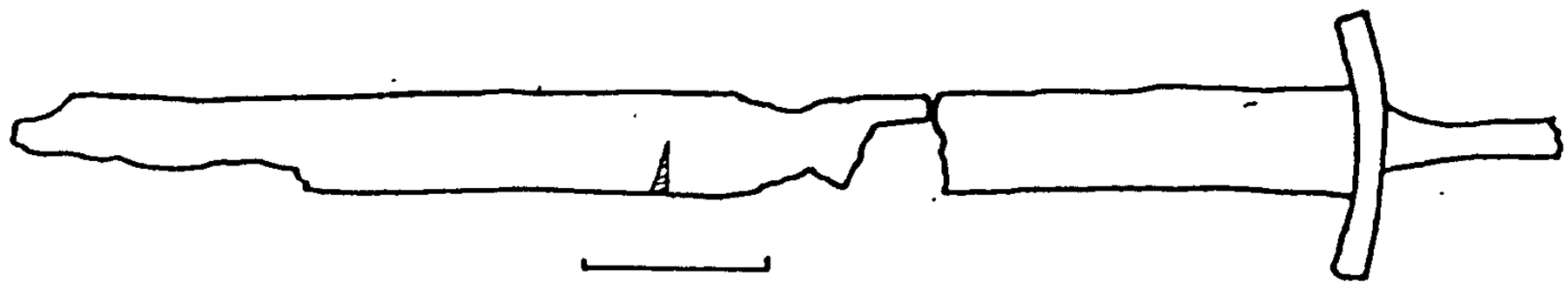

Fig 10 (continued)

S25

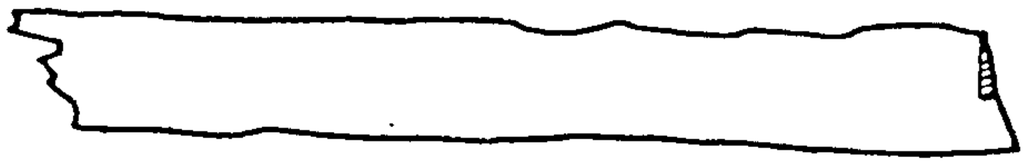

S26

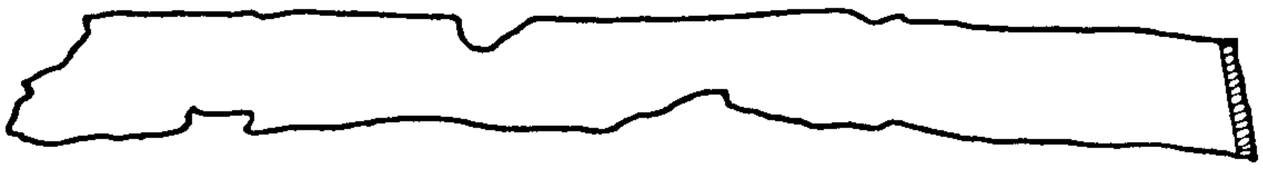

S27

S28

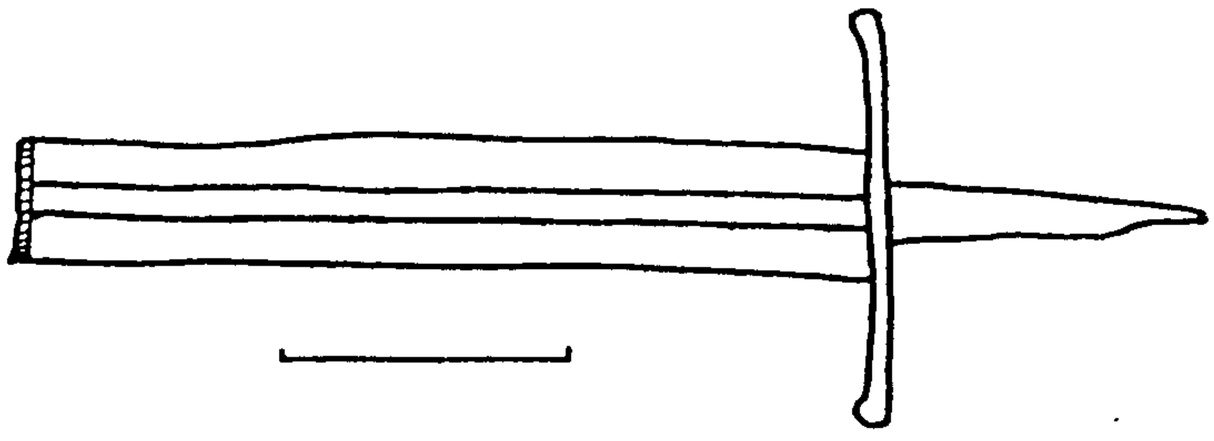

S29

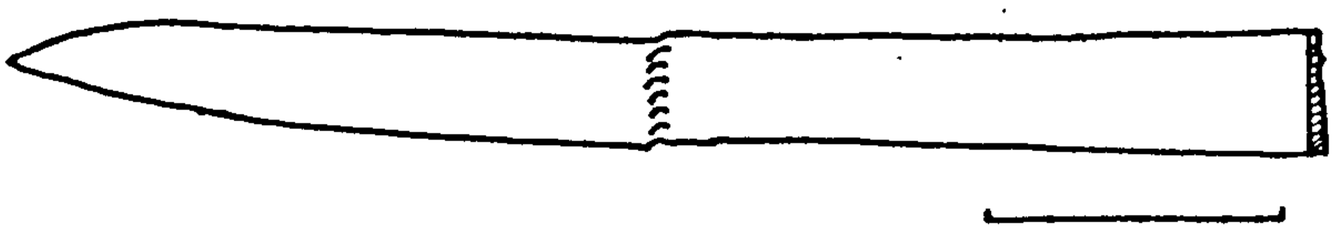

S30

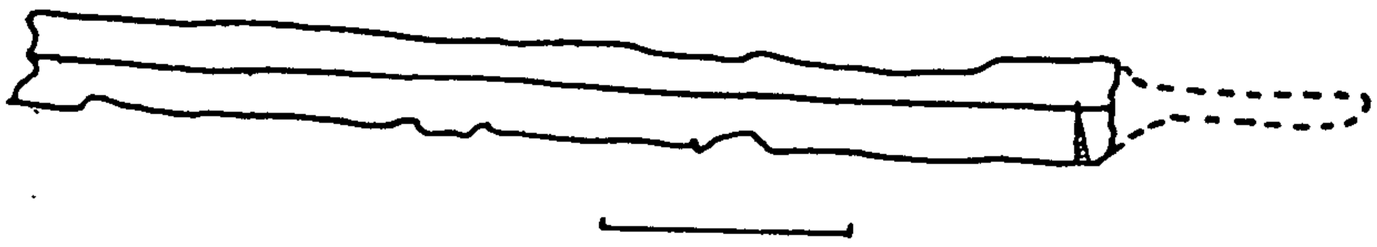

S31

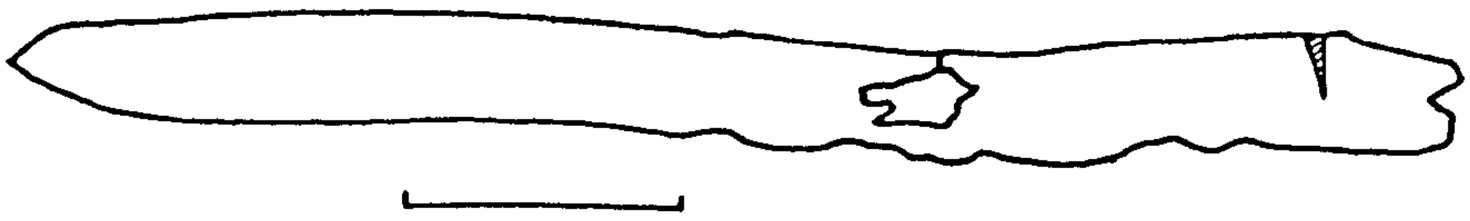

S32

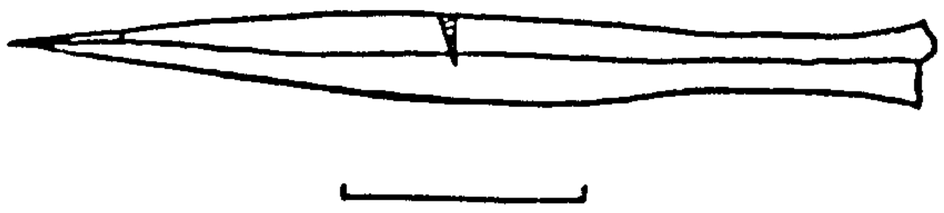

Fig 10 (continued)

S39

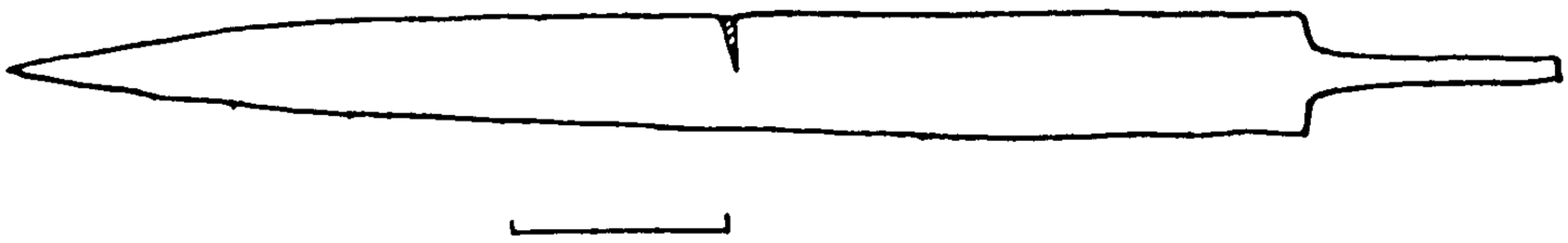

S40

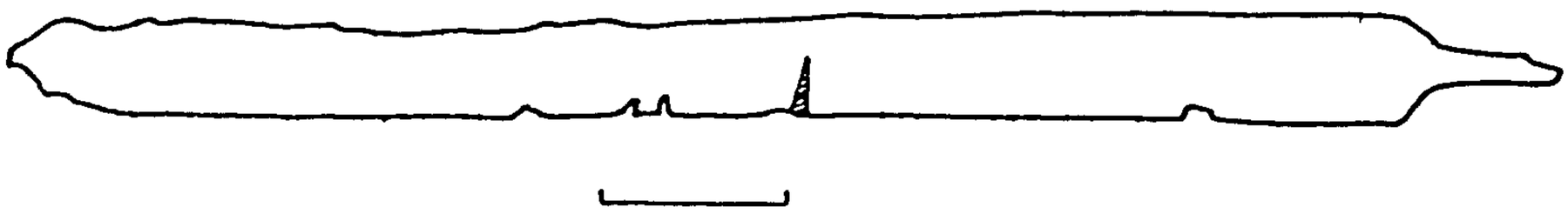

S41

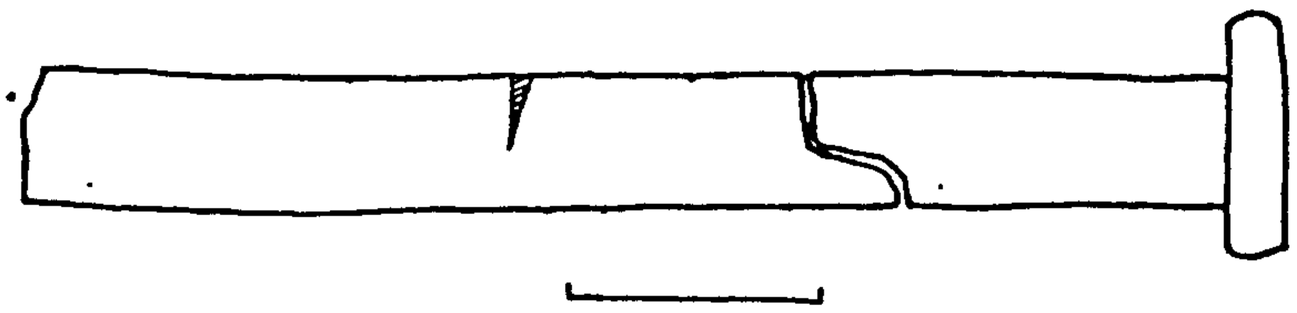

S43

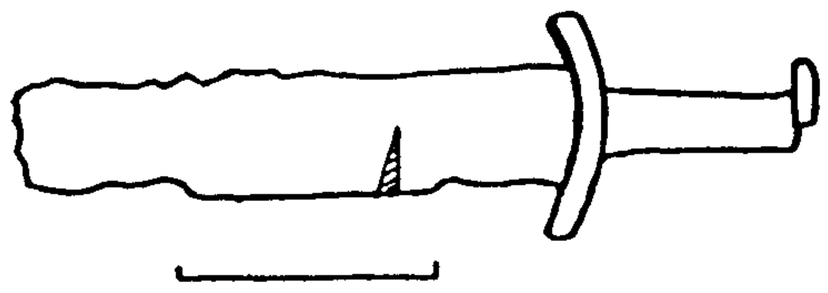

S44:

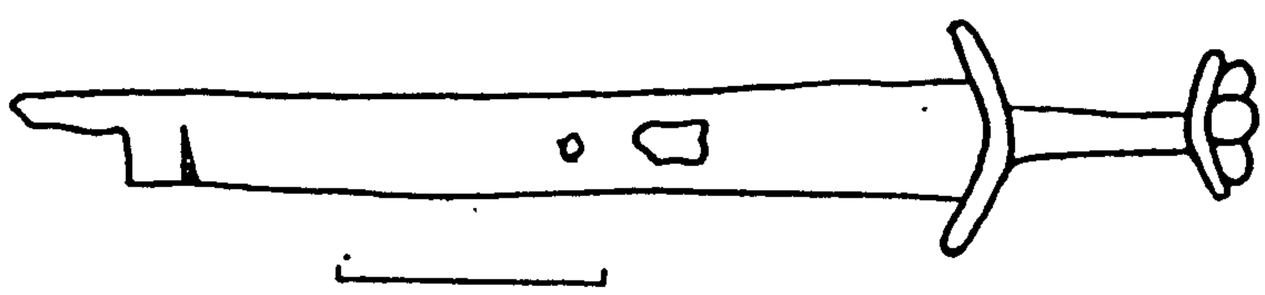

S45

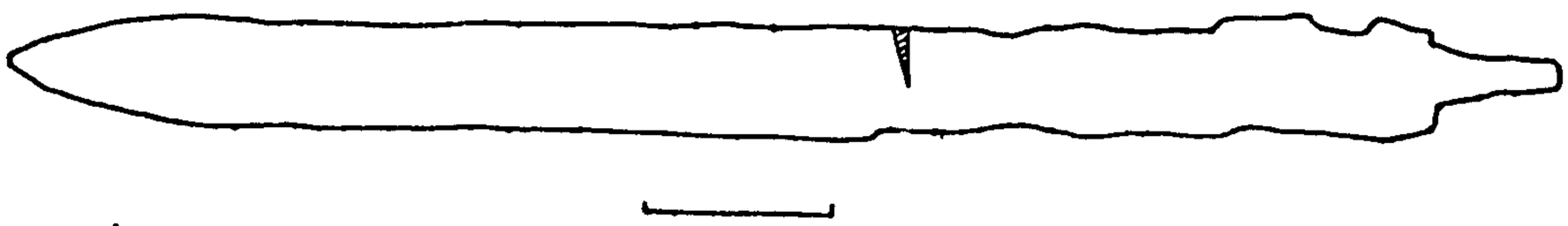

S46

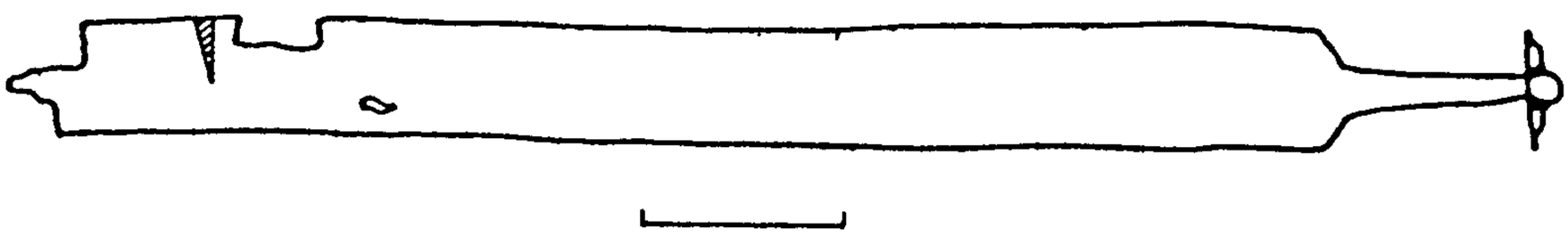

S47

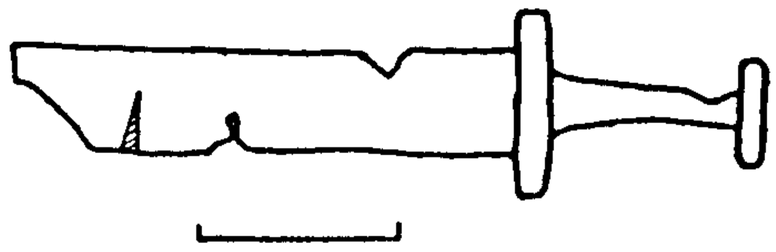

Fig 10 (continued)

S48

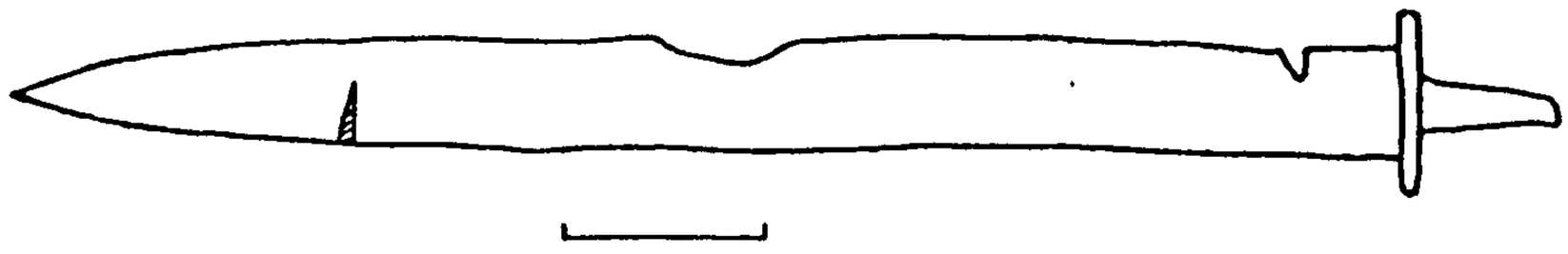

S49

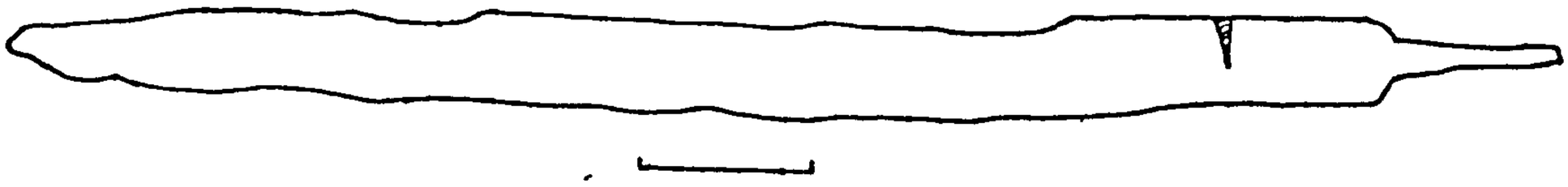

S51

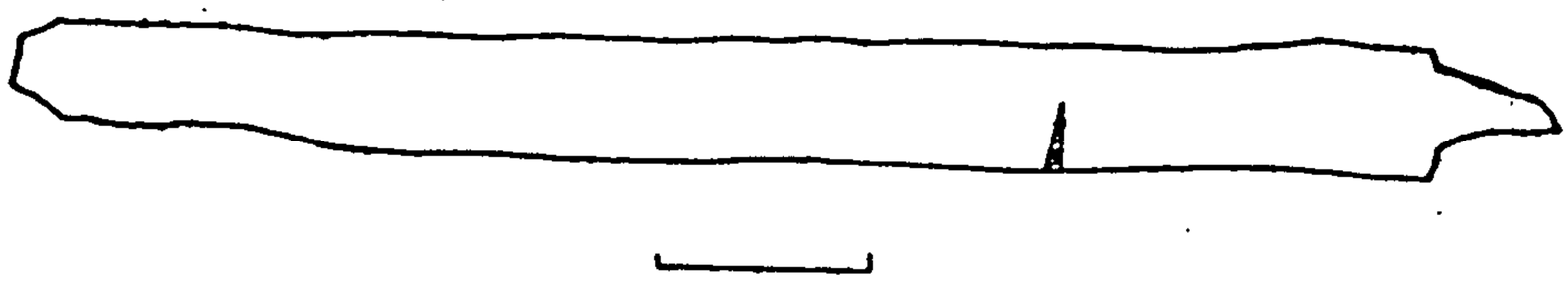

S52

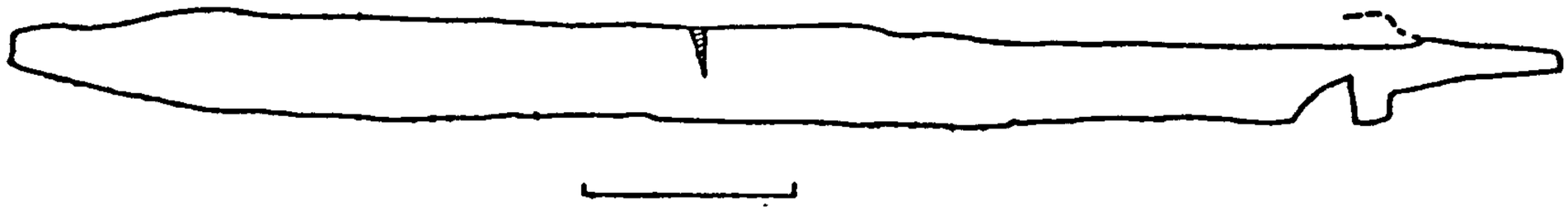

S53

S54

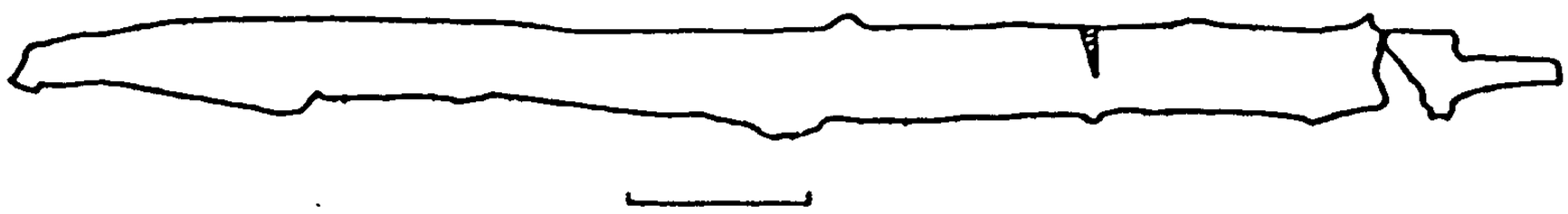

S55

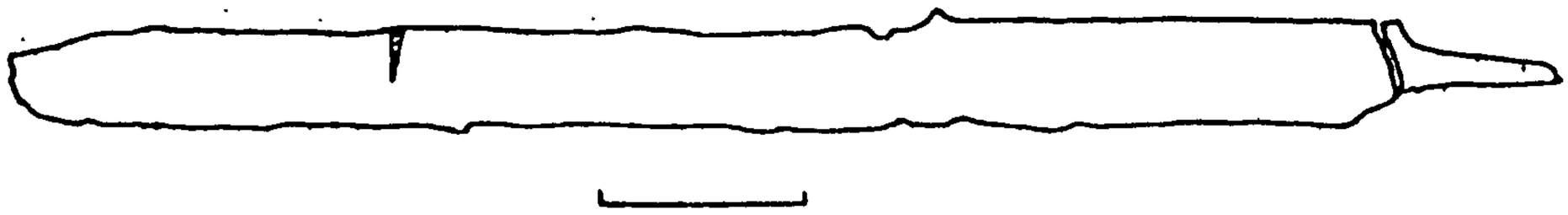

S56

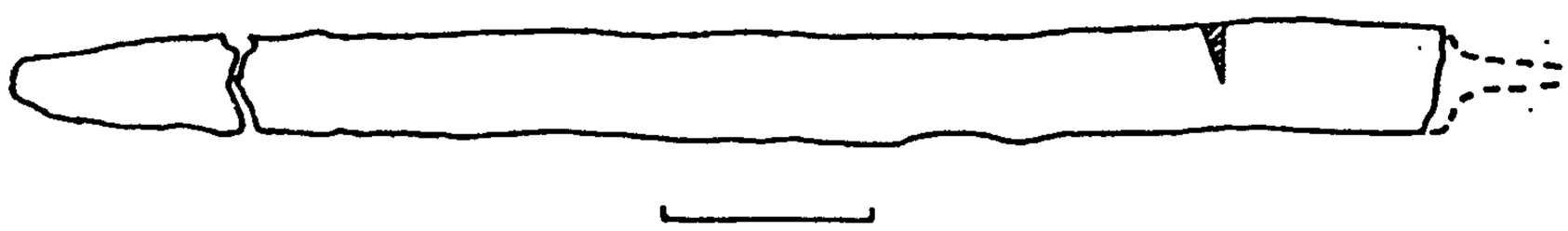

Fig 10 (continued)

Positions of sections scale bars 10cm

S4

S9

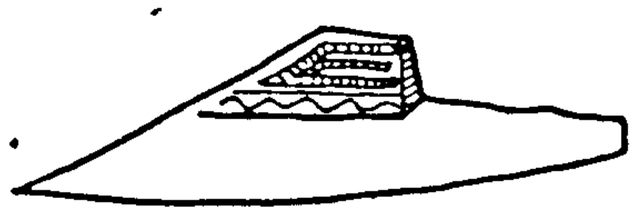

S22

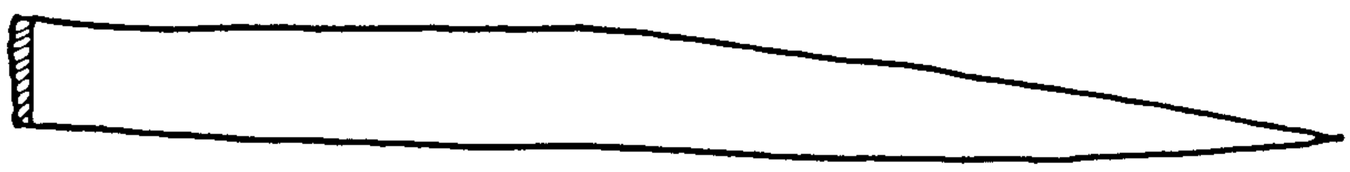

S34

S37

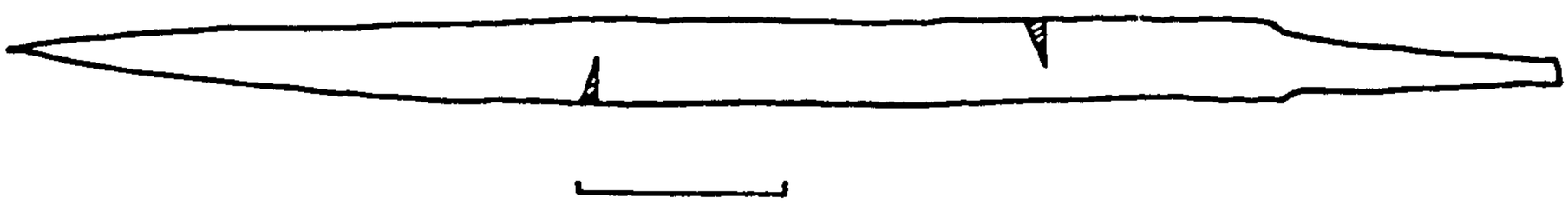

S42

S50

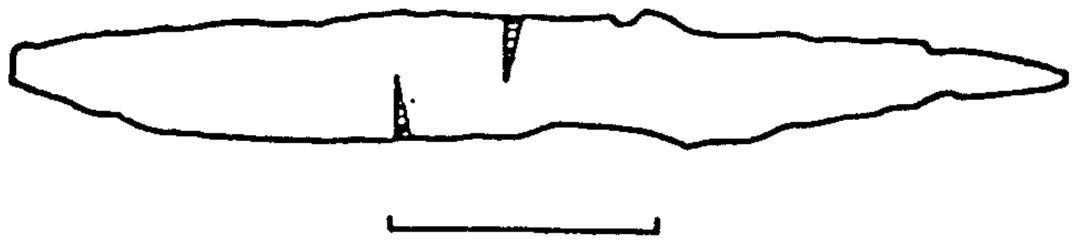

Fig 11 Outlines of scramasaxes with positions of sections (Chapter 6)

Positions of sections scale bars 10cm

S57

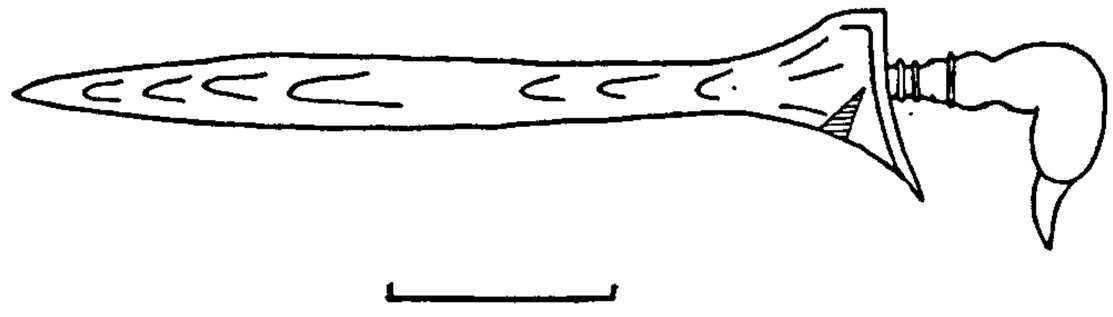

S35

S38

S33

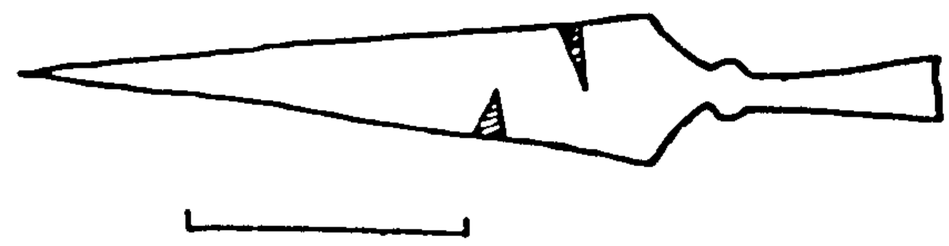

S36

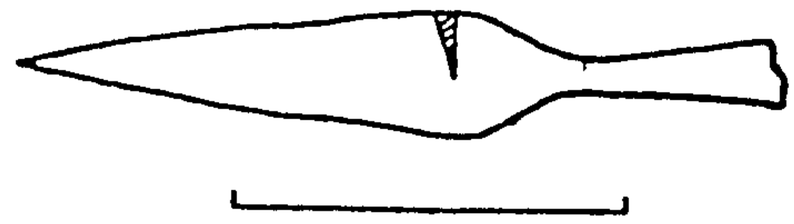

Positions of sections scale bars 10cm

Fig 13 Outline of spearheads with position of sections (Chapter 6)

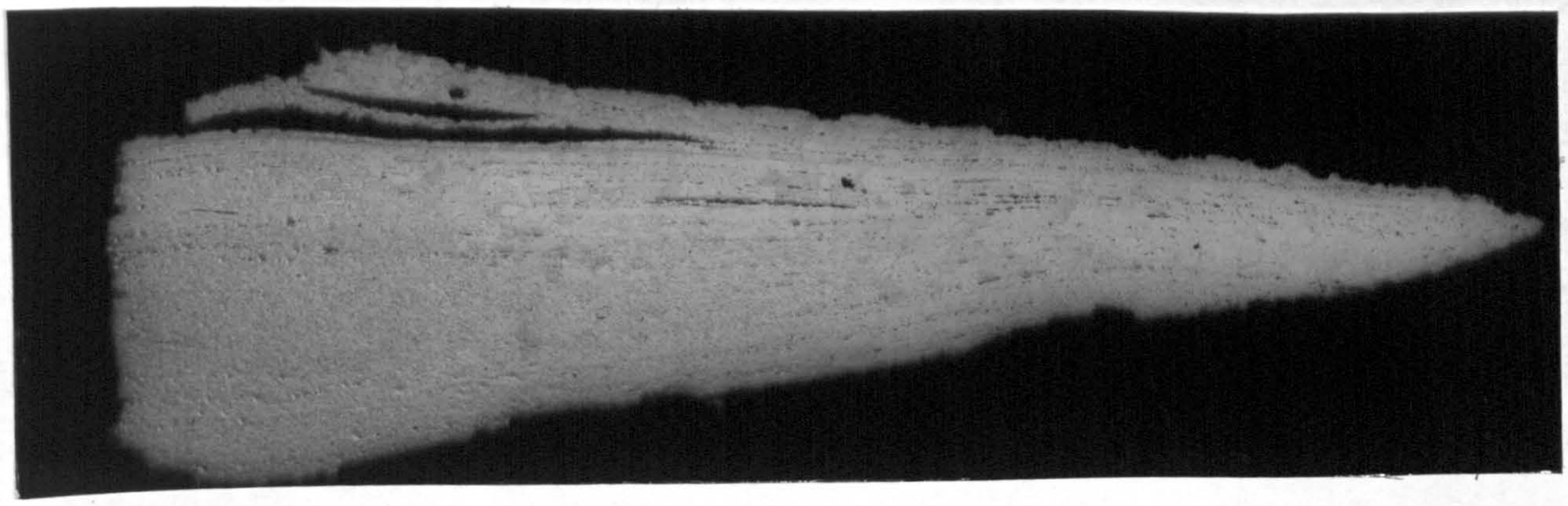

(a)

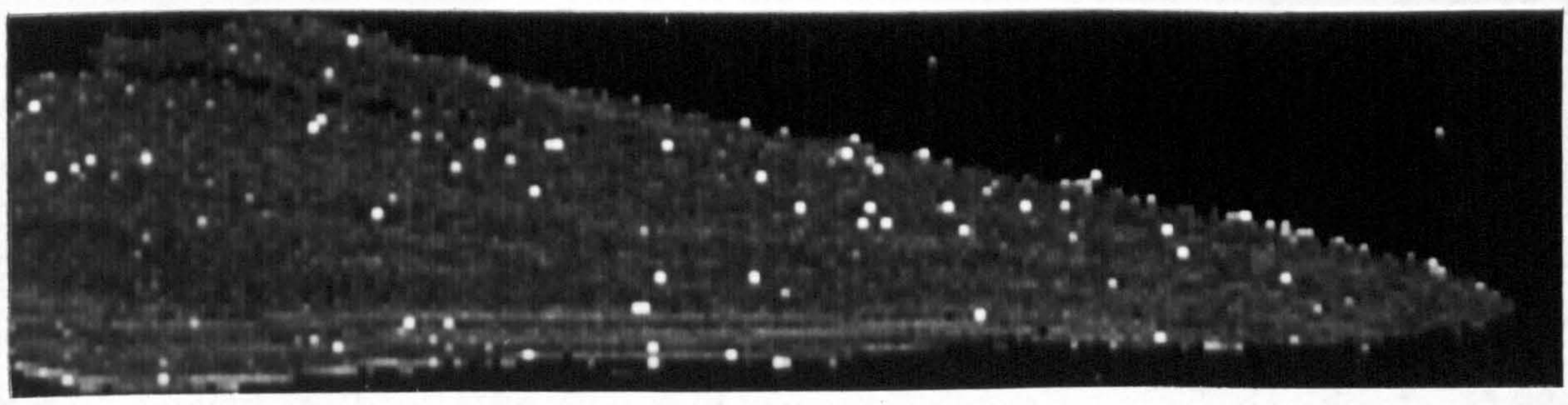

(b)

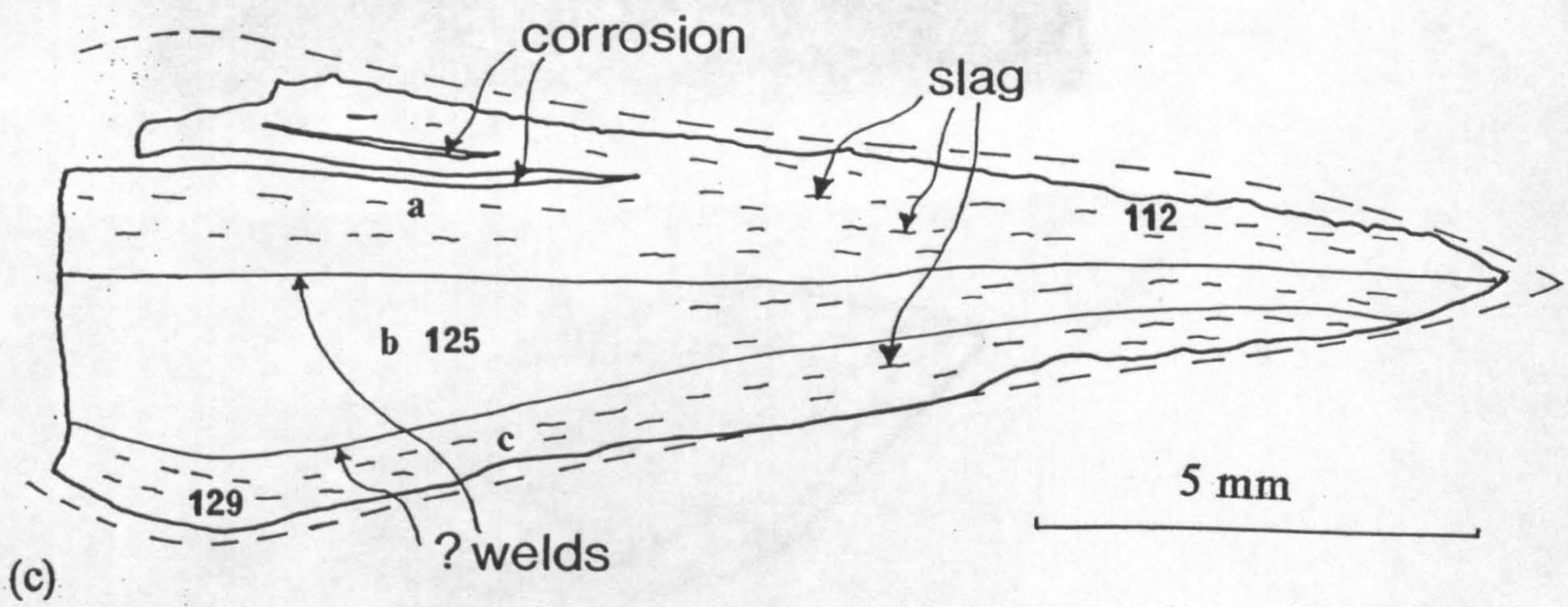

(c)

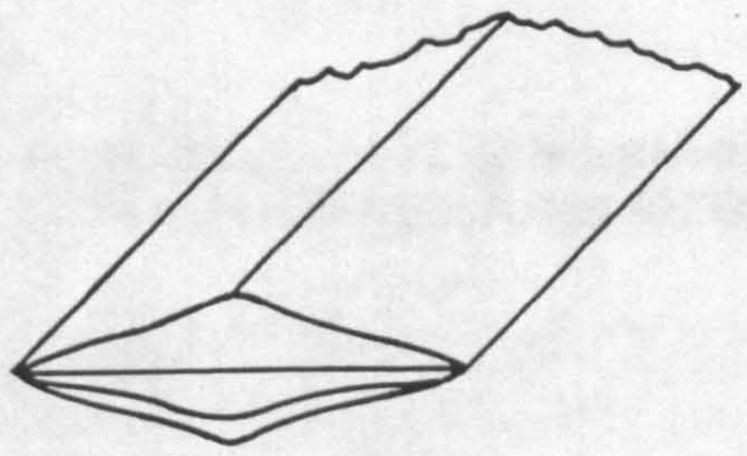

(d)

Fig 14 Sword blade S32, from Reading Museum (a) photomacrograph; (b) EPMA phosphorus map; (c) sketch of section; and (d) three-dimensional reconstruction

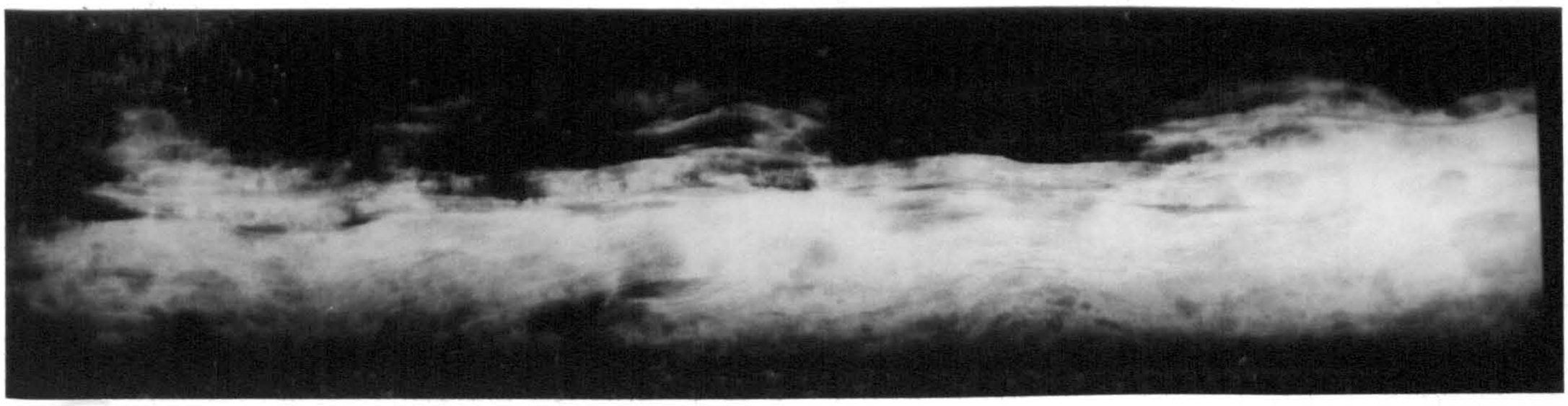

(a)

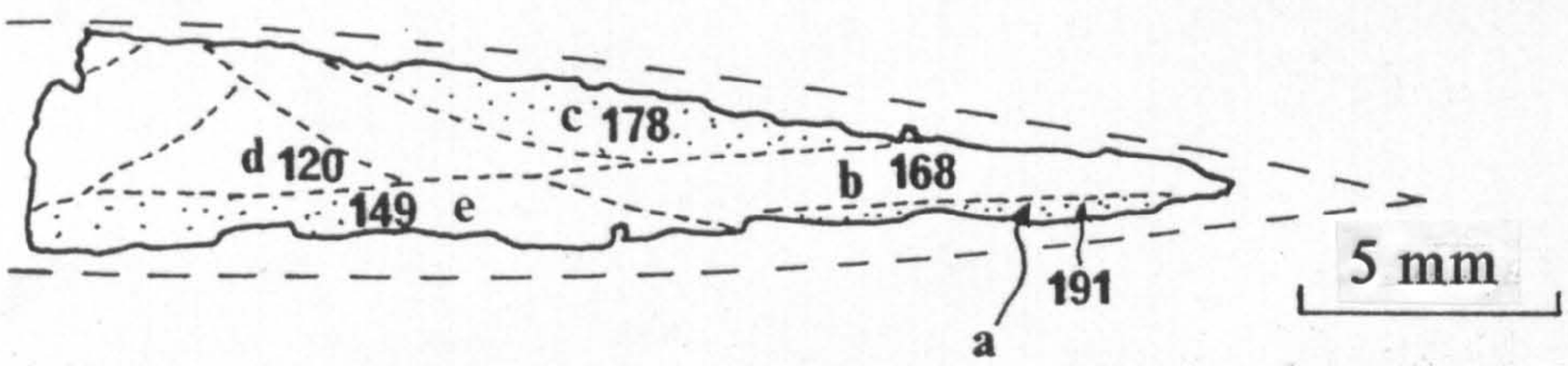

(b)

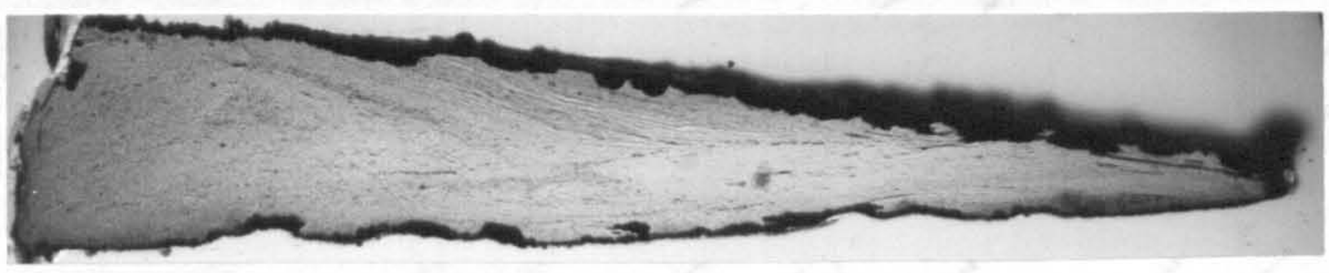

(c)

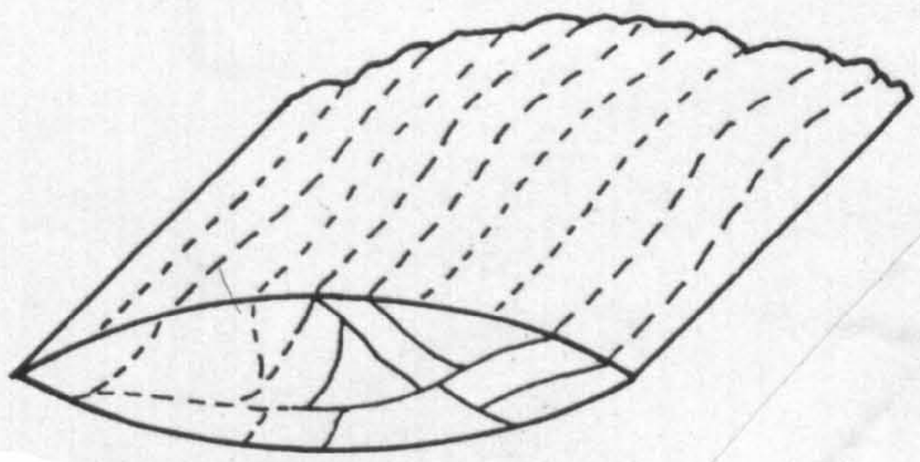

(d)

Fig 15

Sword blade S27, from the Thames at Little Wittenham: (a) x-radiograph of blade; (b) sketch of section, (c) photomacrograph, and (d) three-dimensional reconstruction

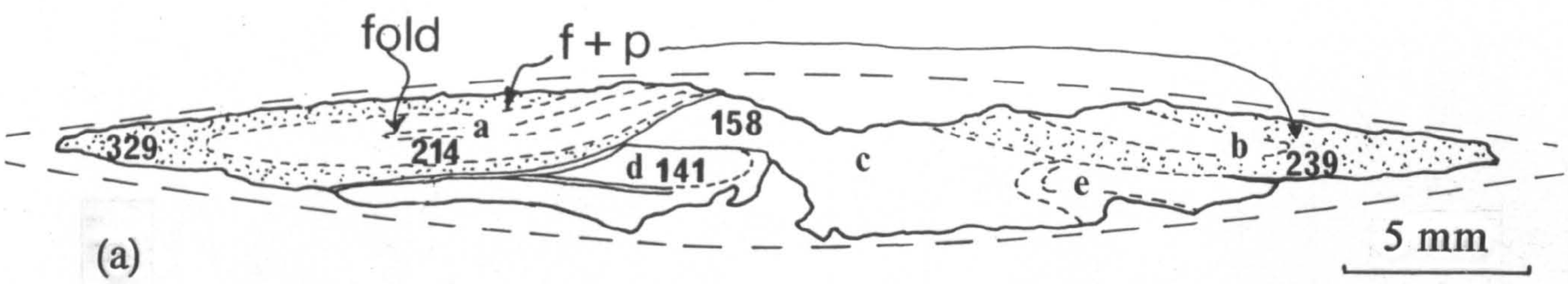

(b)

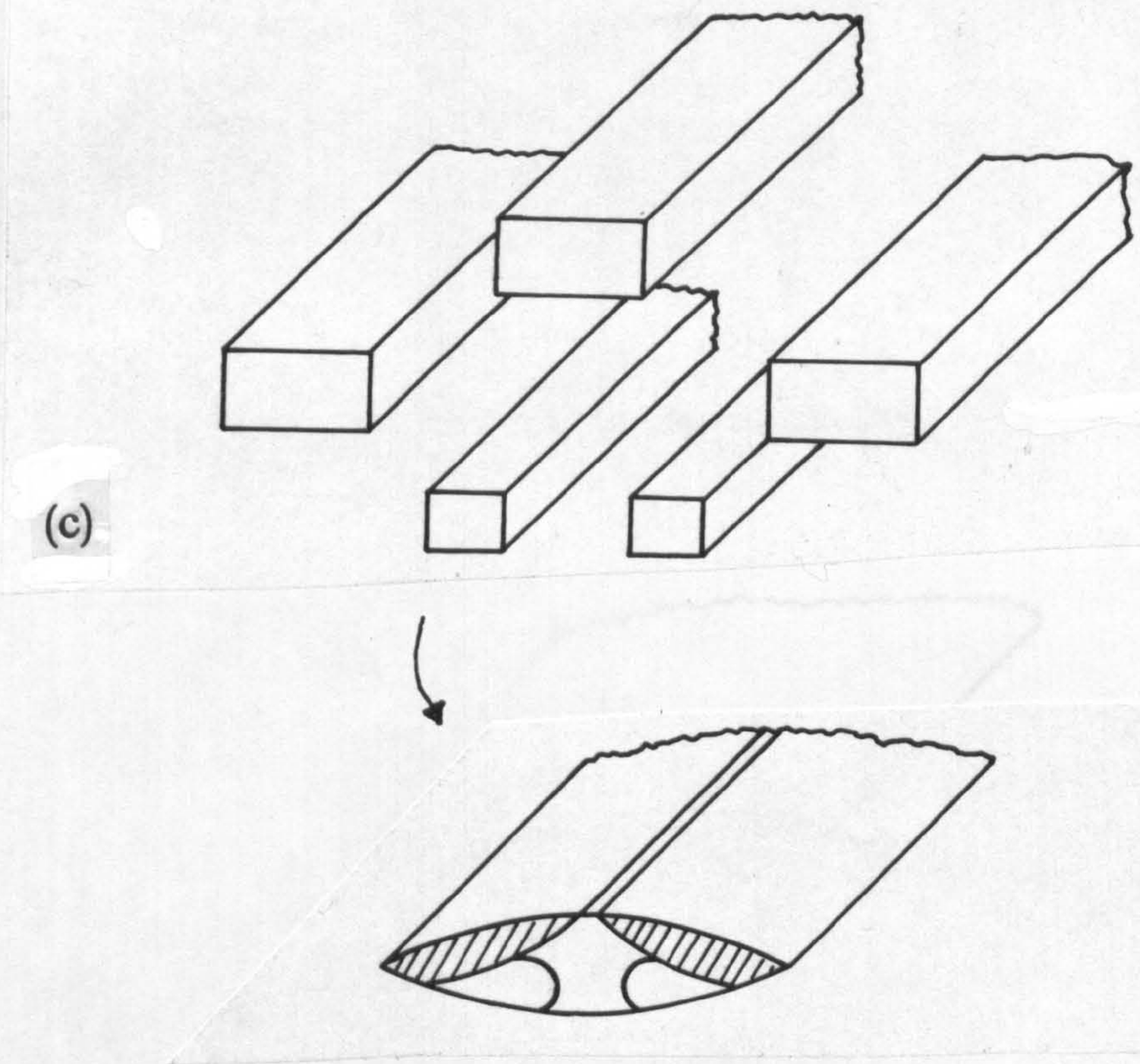

Fig 16 Sword blade S29, from the Thames at Little Wittenham: (a) sketch of section, (b) photomacrograph, and (c) three-dimensional reconstruction

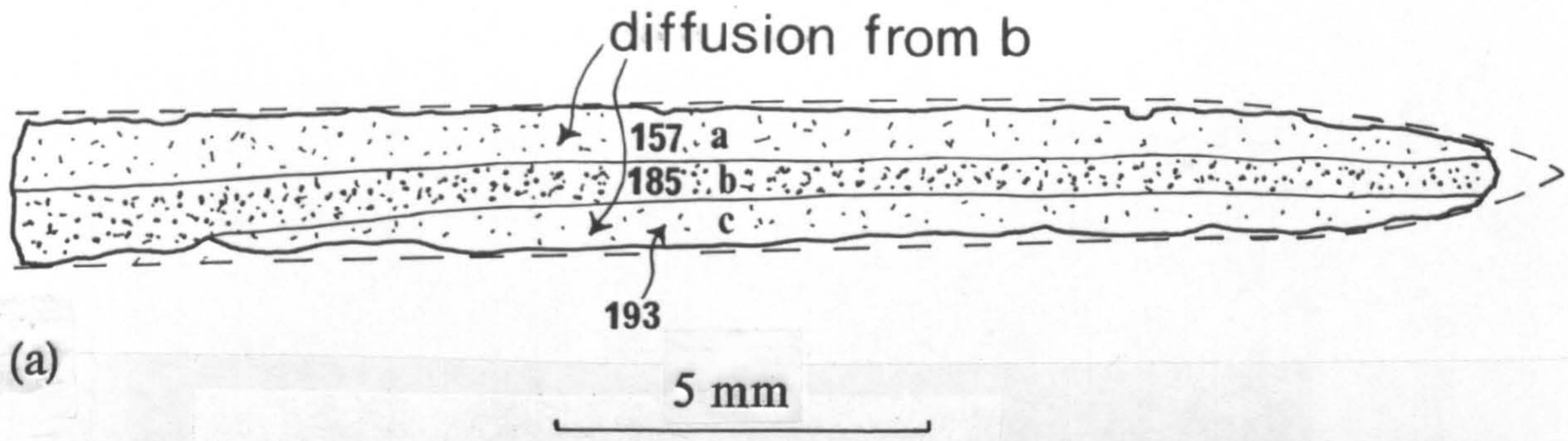

Fig 17 Sword blade S39, from Whittlesey : (a) sketch of section, (b) photomacrograph; (c) photomacrograph; (d) and (e) photomicrographs near edge and centre respectively; (f) photomicrograph across full thickness of blade

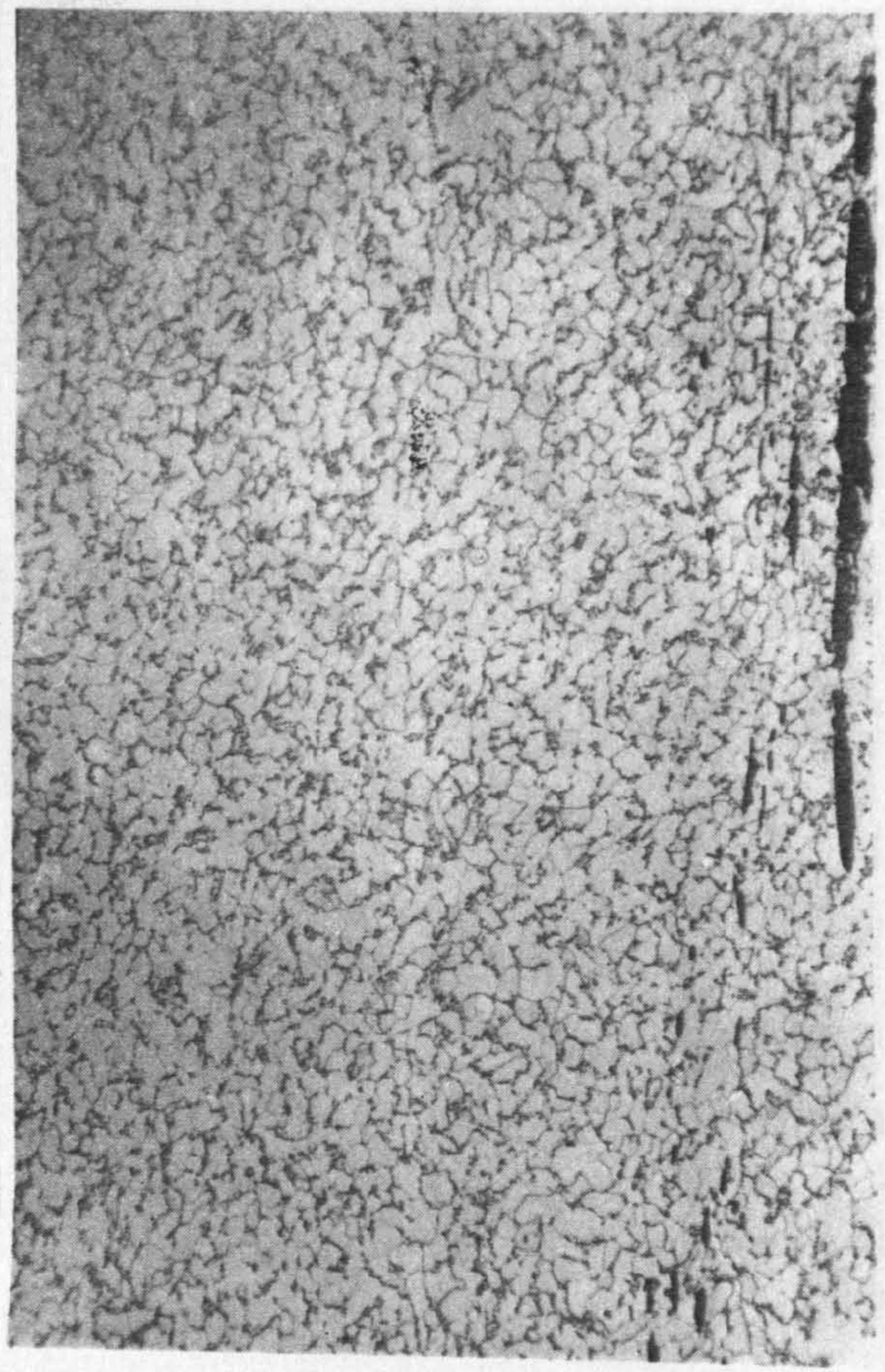

10 μm

(d)

10 μm

(e)

1 mm

(f)

Fig 17(continued)

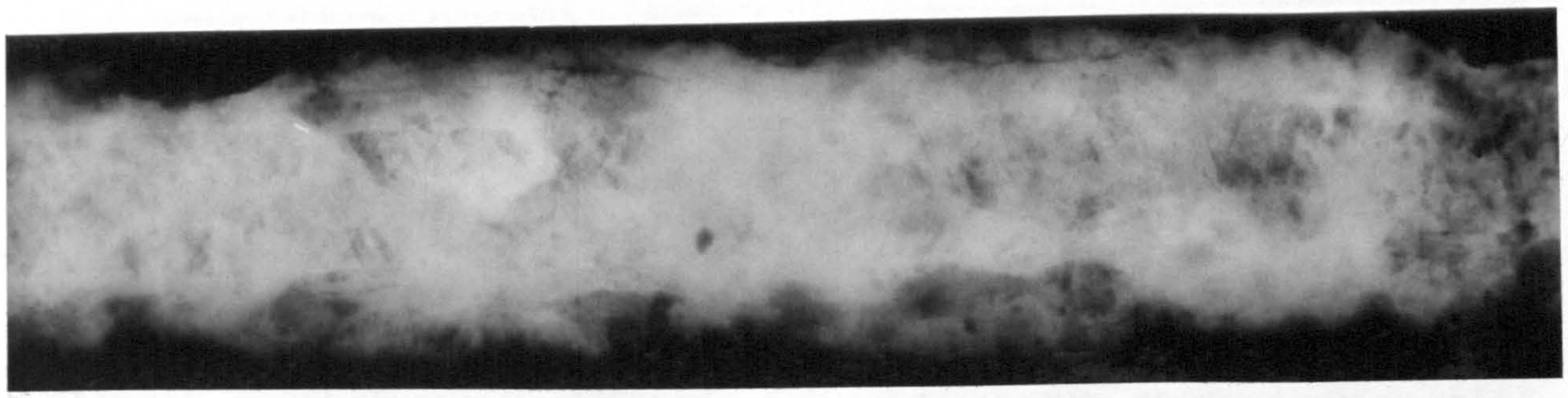

(a)

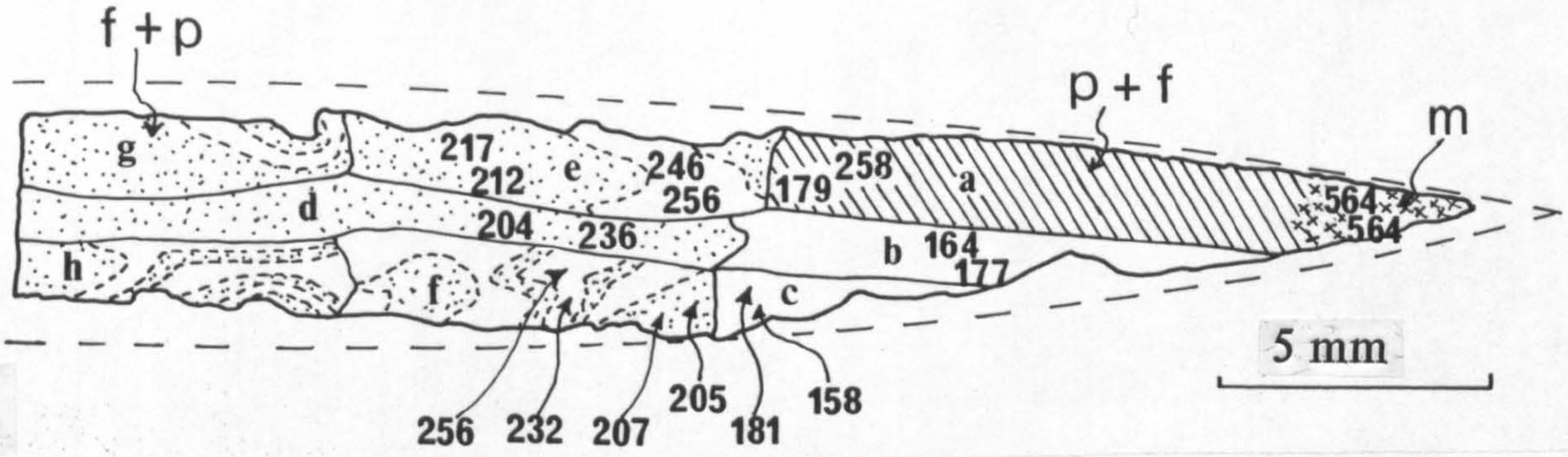

(b)

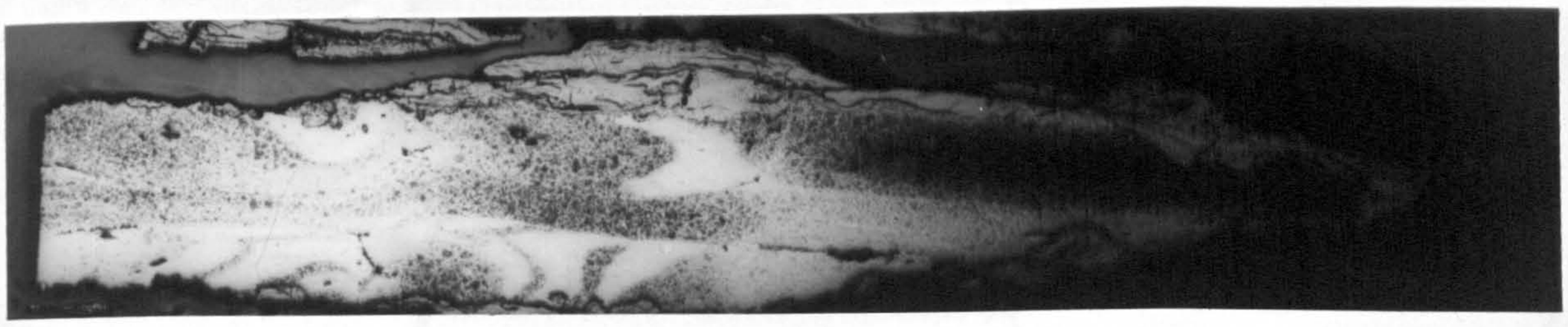

(c)

Fig 18 Sword blade S17, from Sarre: (a) x-radiograph; (b) sketch of section; (c) photomacrograph; (d) photomicrograph of higher carbon area of the central core piece d, showing Widmanstatten structure; (e) photomicrograph near tip of cutting edge showing martensite + radial pearlite (nodular troostite); (f) three-dimensional view.

(d)

(e)

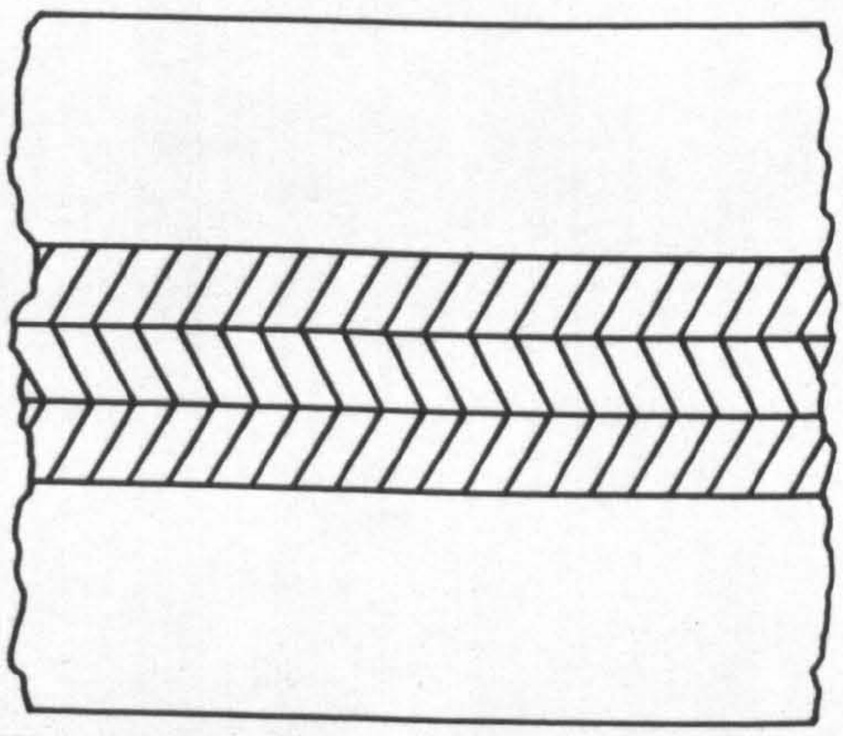

(f)

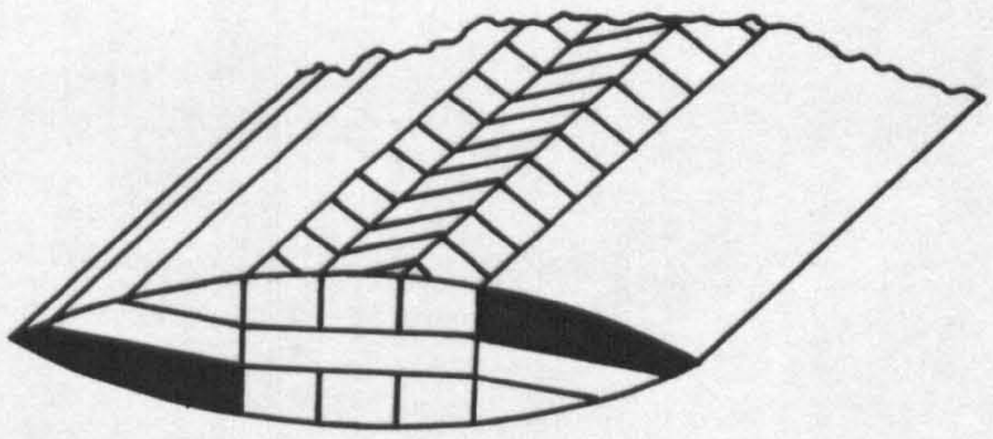

Fig 18 (continued)

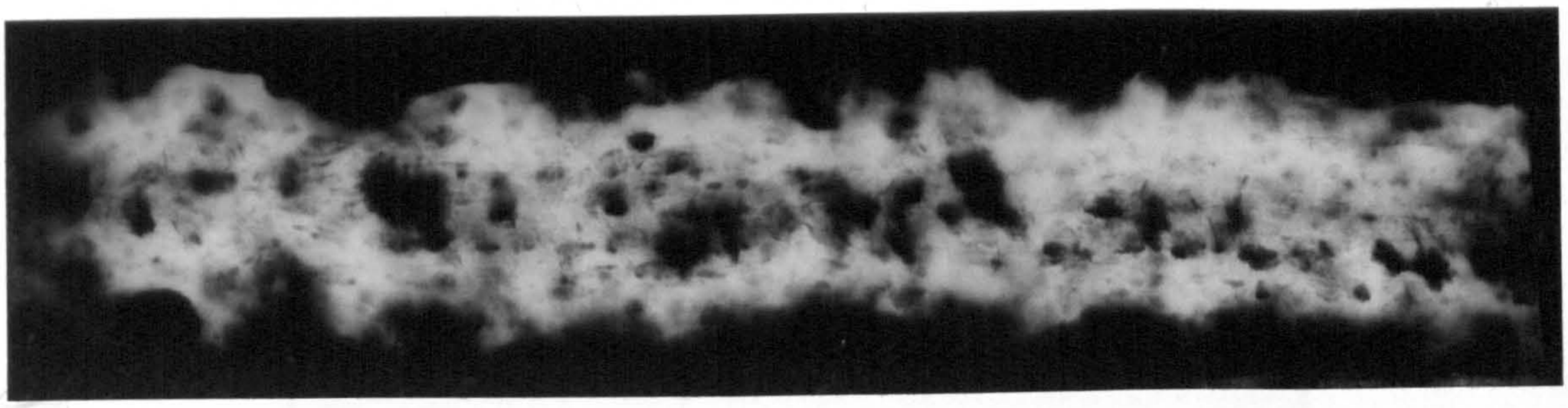

(a)

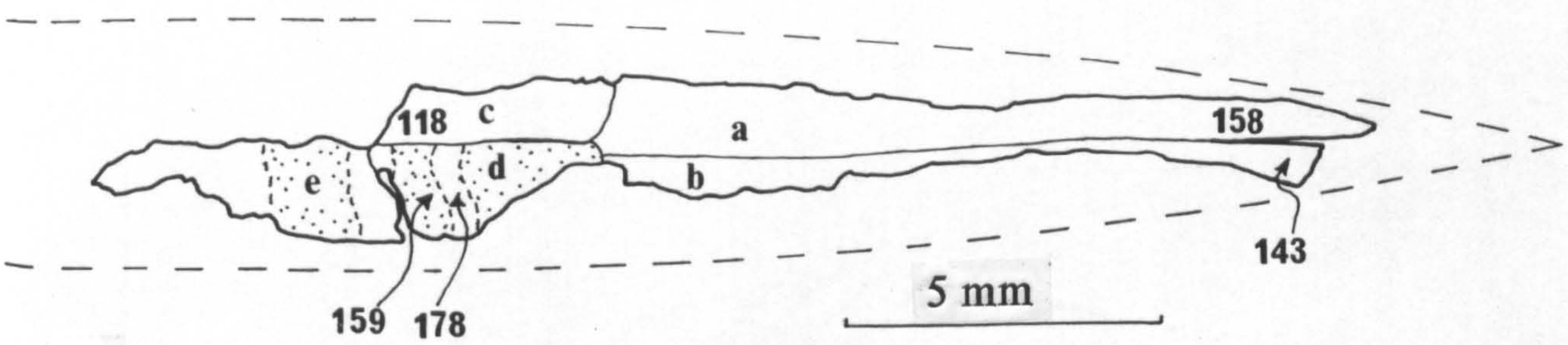

(b)

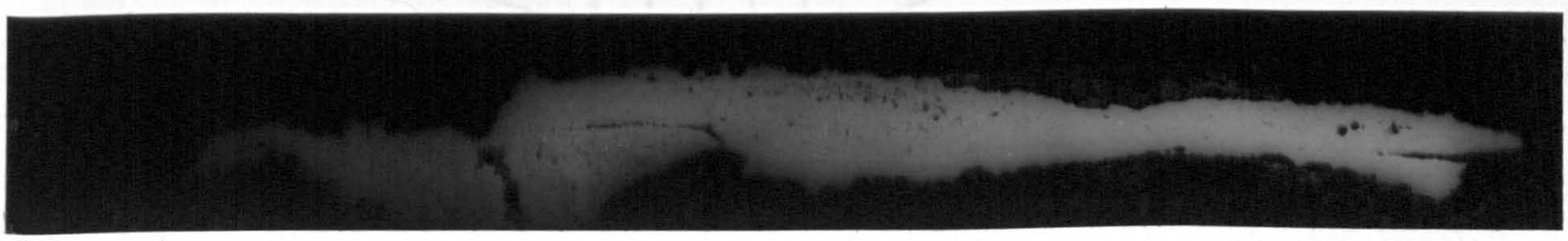

(c)

Fig 19 Sword blade S49, probably from Bifrons: (a) x-radiograph; (b) sketch of section; (c) photomacrograph; (d) surface detail and three-dimensional view

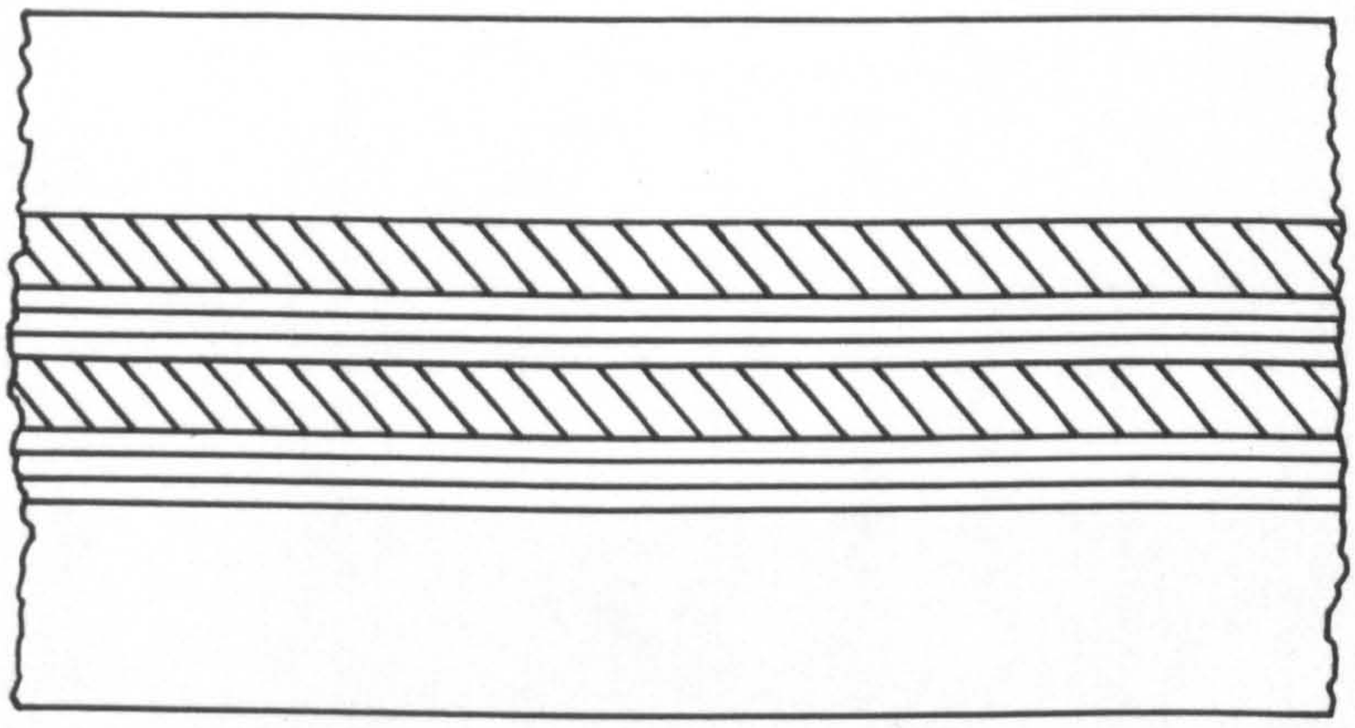

(d)

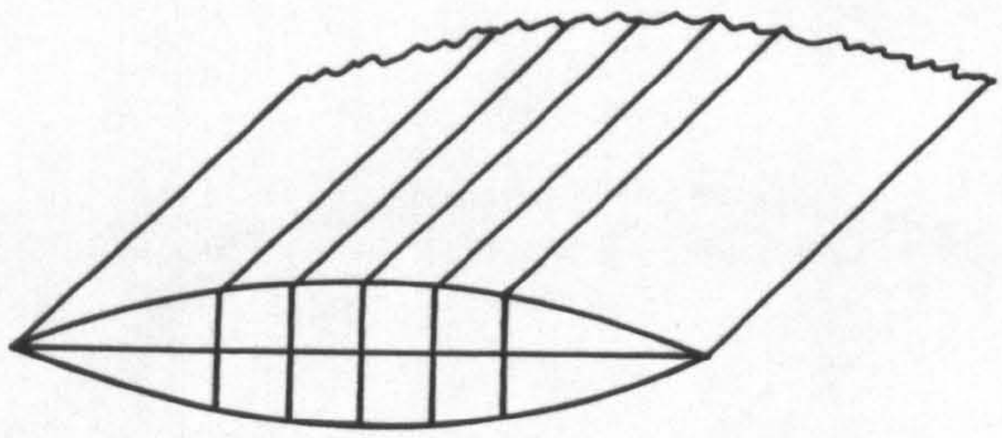

Fig 19 (continued)

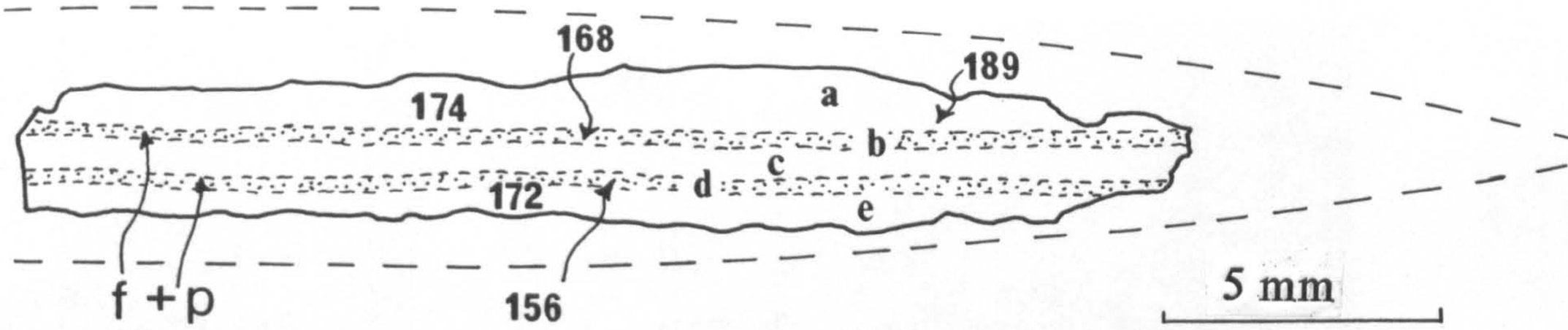

(a)

(b)

(c)

Fig 20 Sword blade S51, from Sarre : (a) sketch of section; (b) photomacrograph (c) three-dimensional view

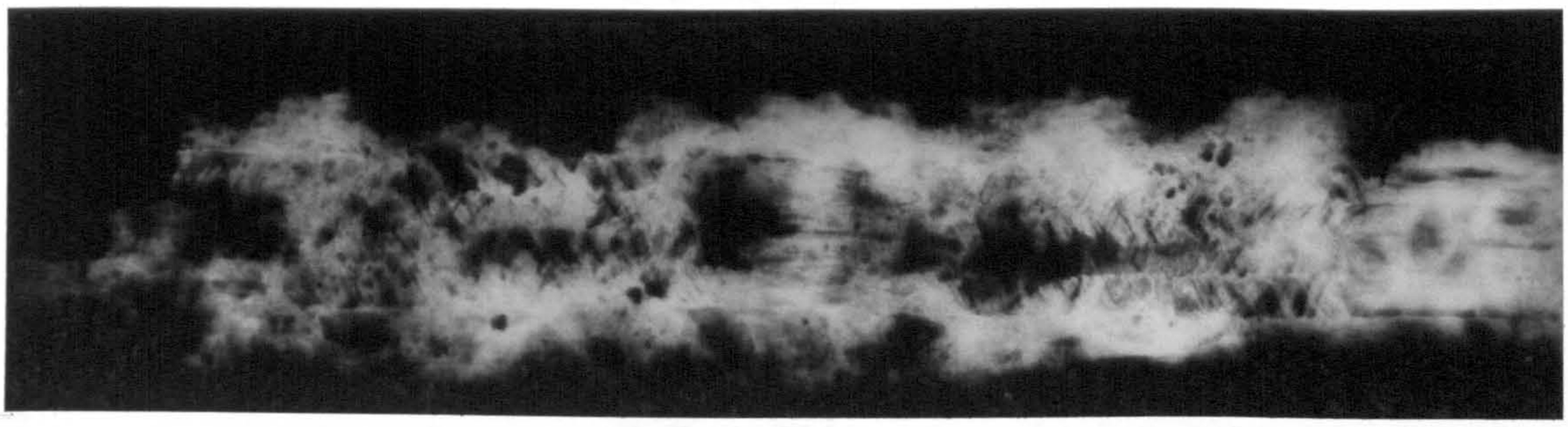

(a)

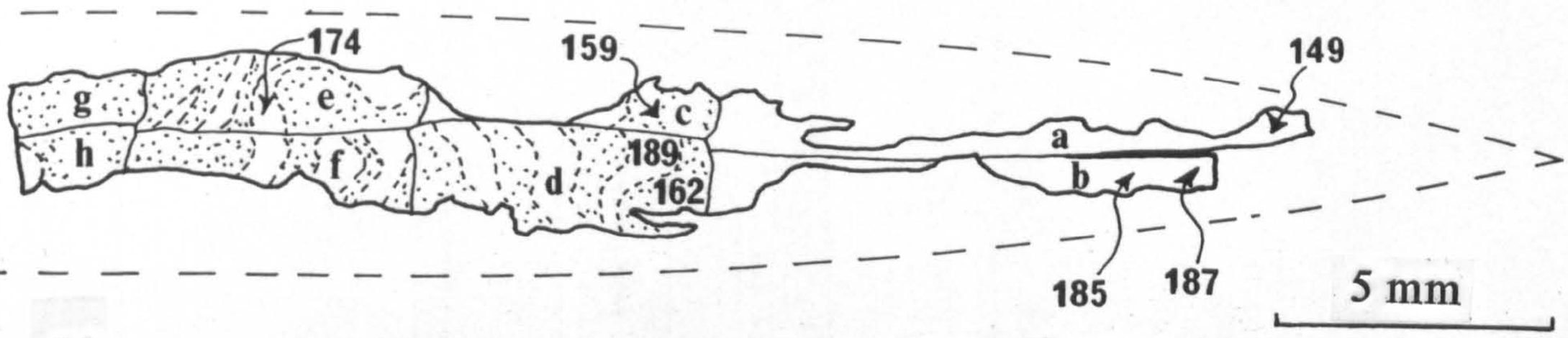

(b)

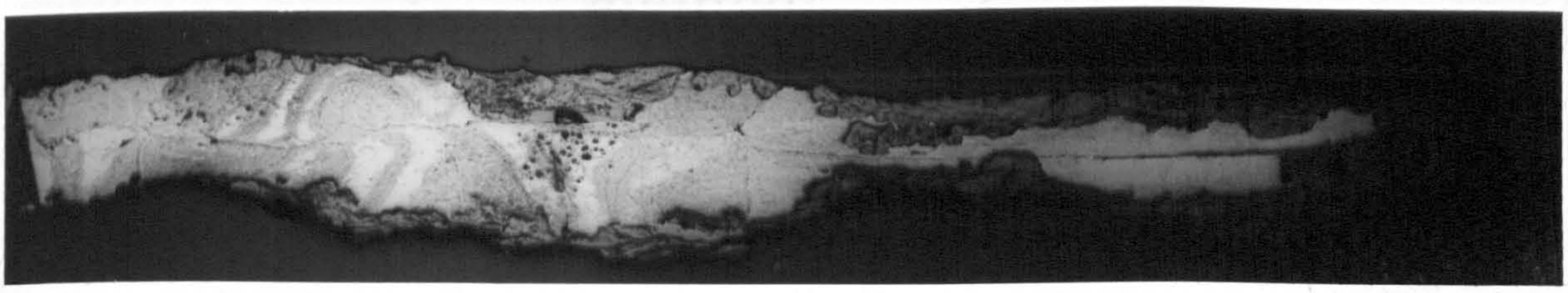

(c)

Fig 21 Sword blade S52, from Sarre: (a) x-radiograph; (b) sketch of section; (c) photomacrograph; (d) surface detail and three-dimensional view

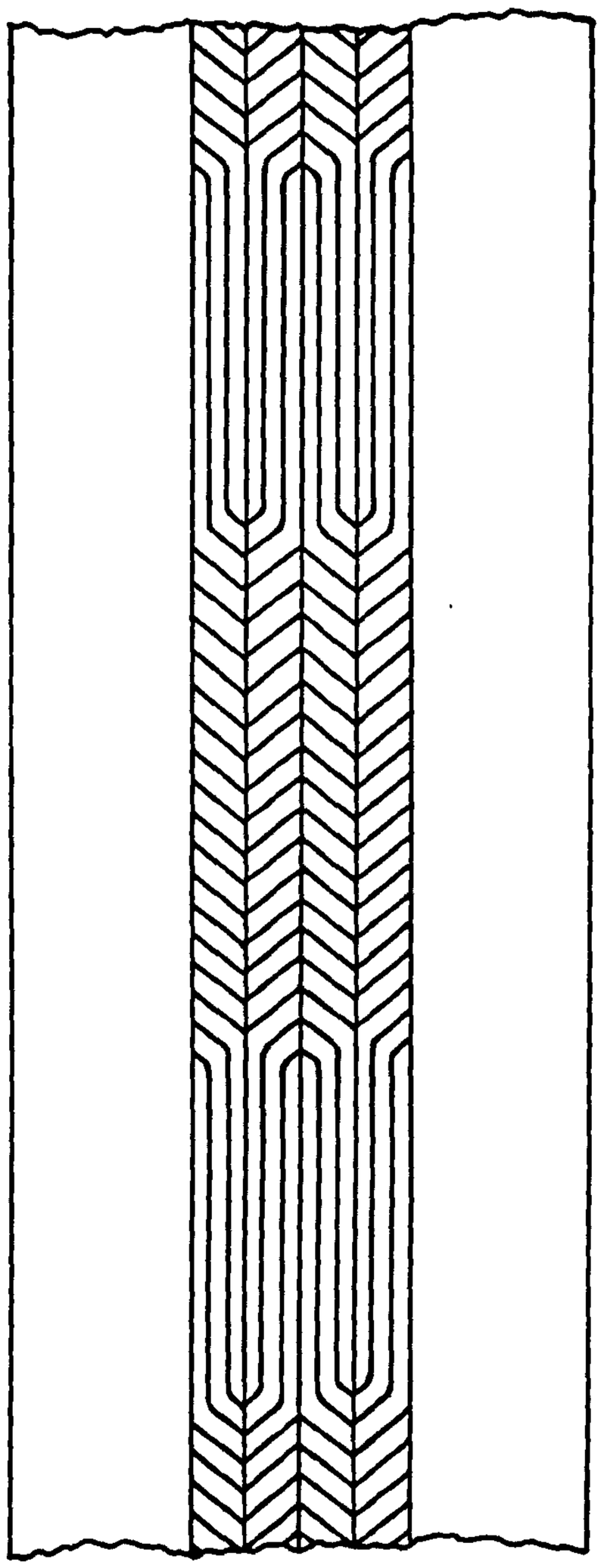

(d)

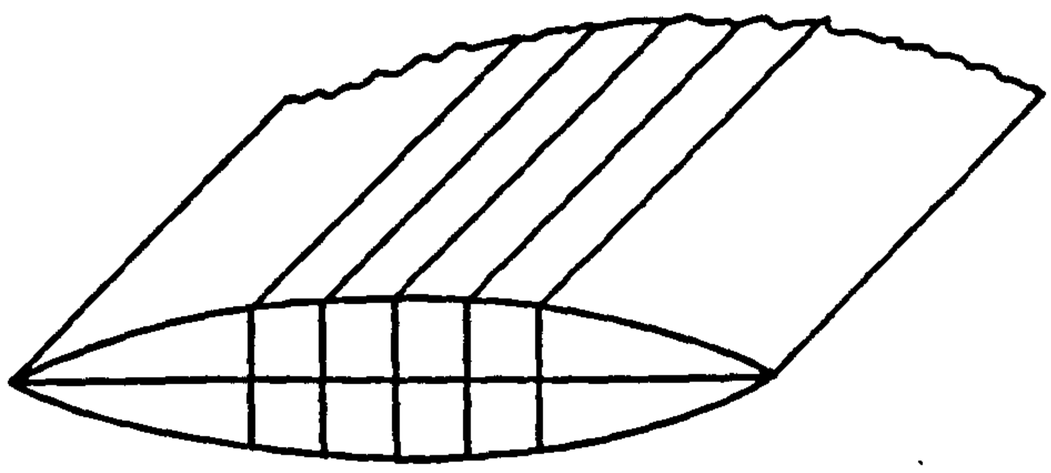

Fig 21 (continued)

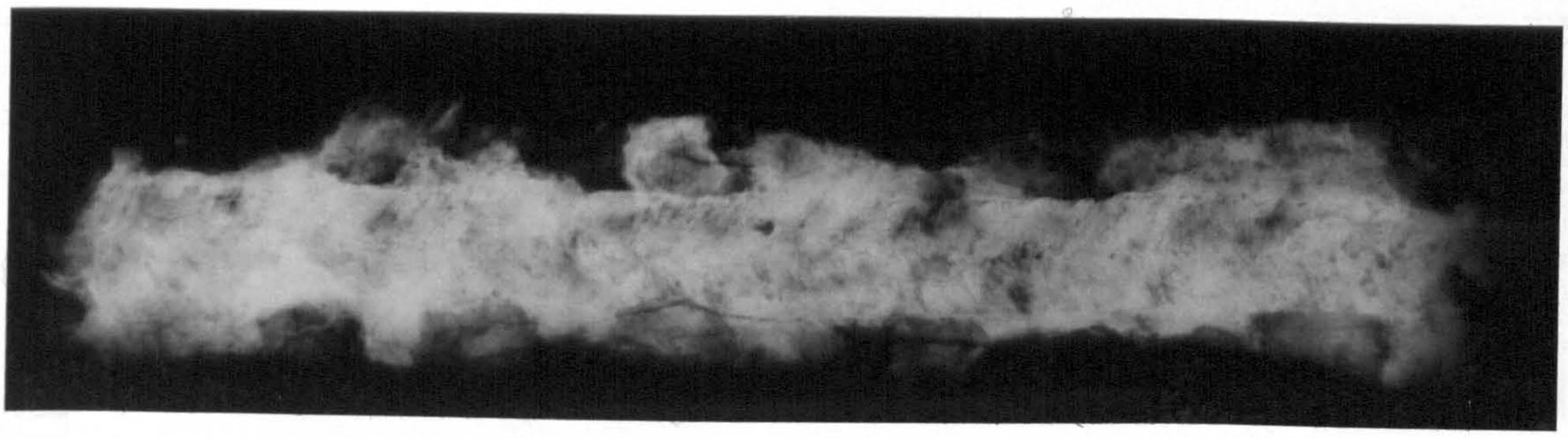

(a)

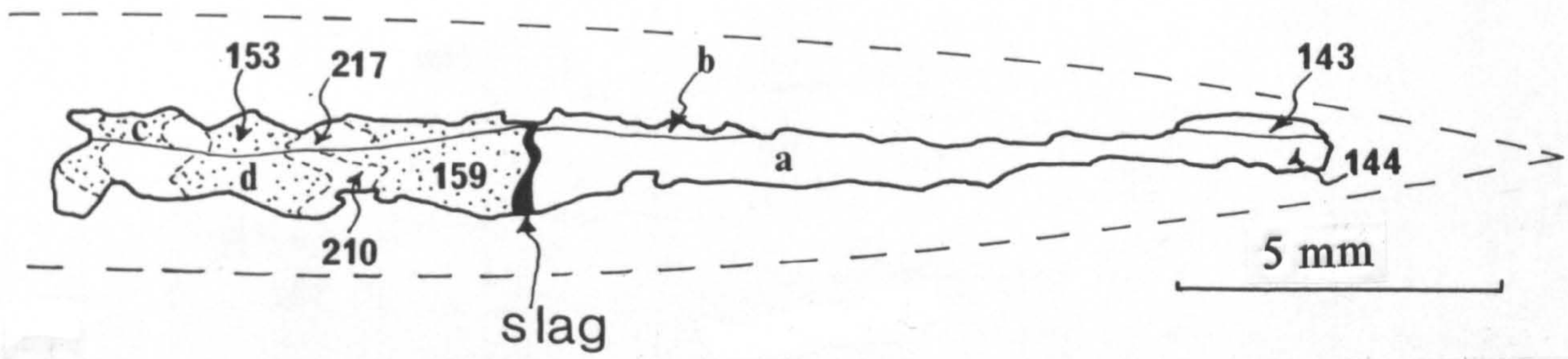

(b)

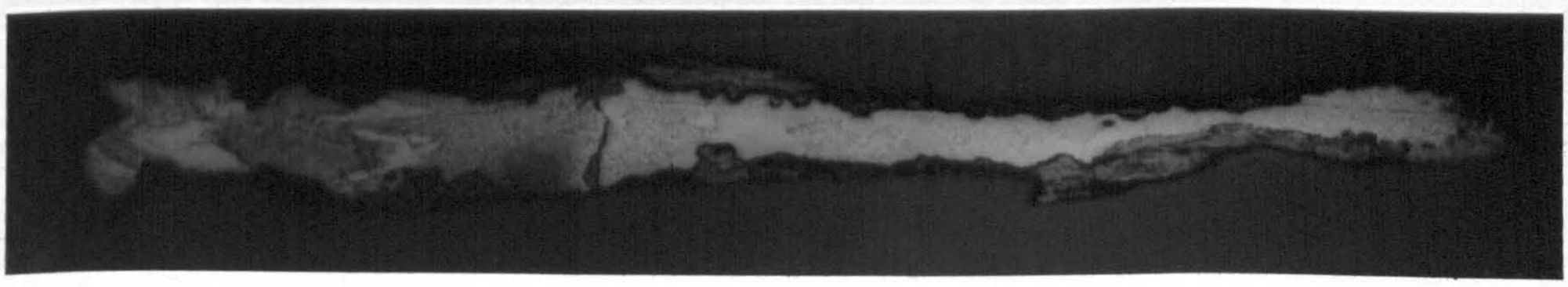

(c)

Fig 22 Sword blade S53, from Sarre: (a) x-radiograph; (b) sketch of section; (c) photomacrograph; (d) three-dimensional view

(a)

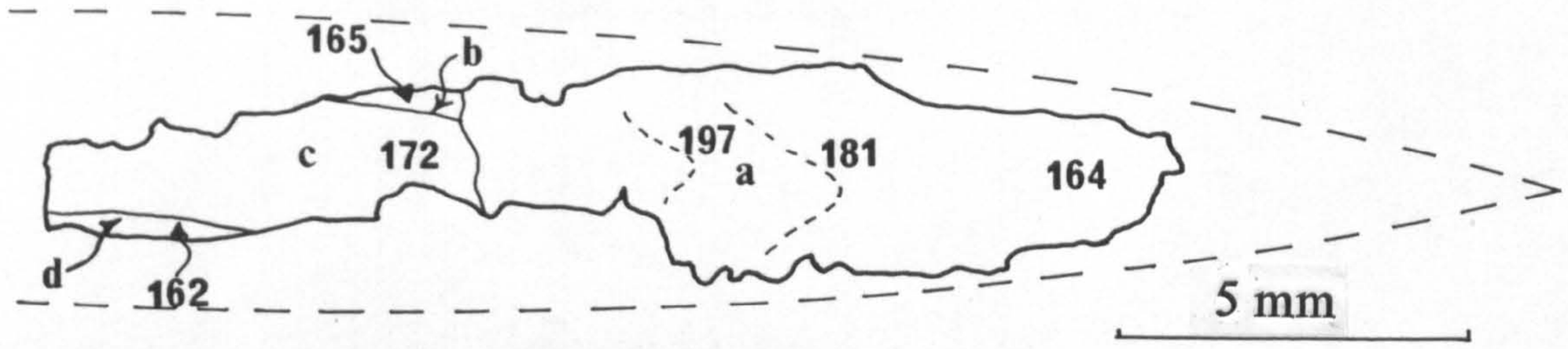

(b)

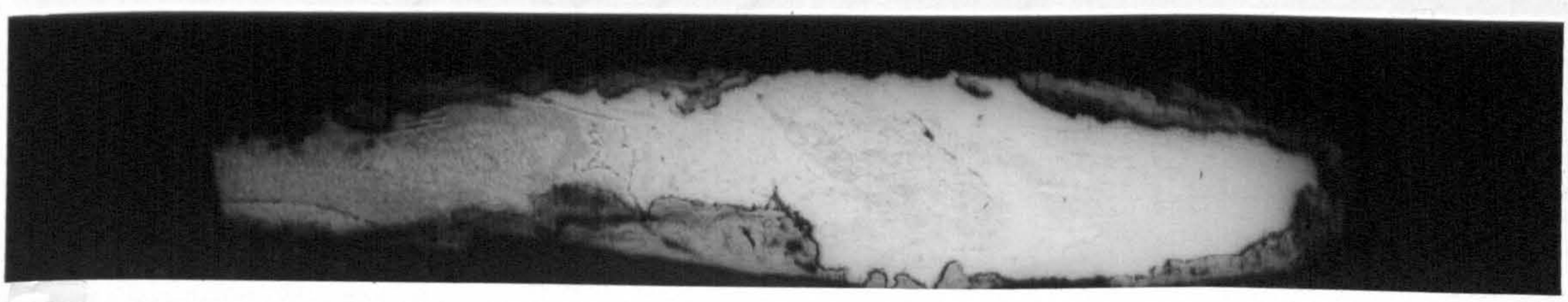

(c)

Fig 23 Sword blade S54, from Sarre or Bifrons: (a) x-radiograph; (b) sketch of section; (c) photomacrograph; (d) three-dimensional view

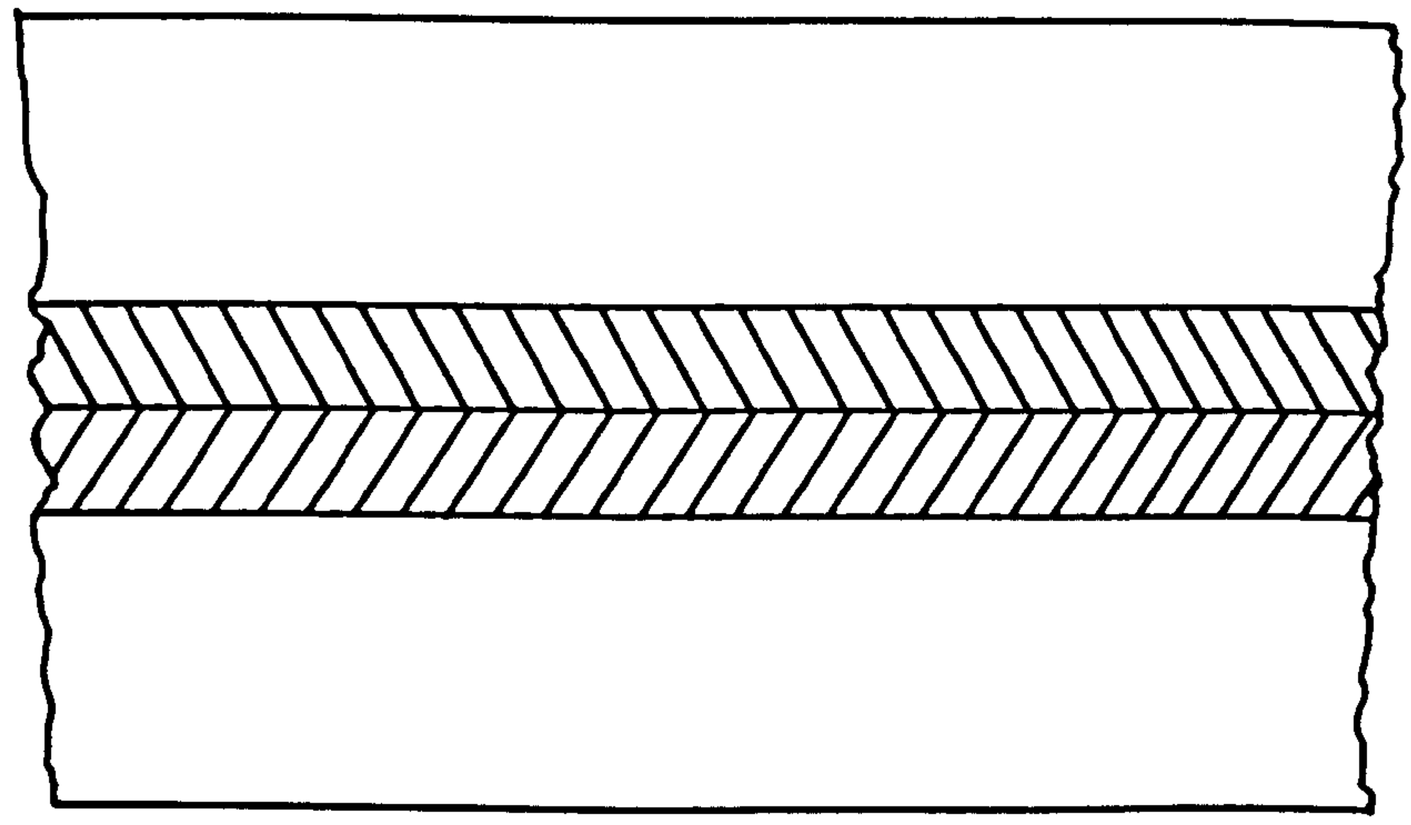

(d)

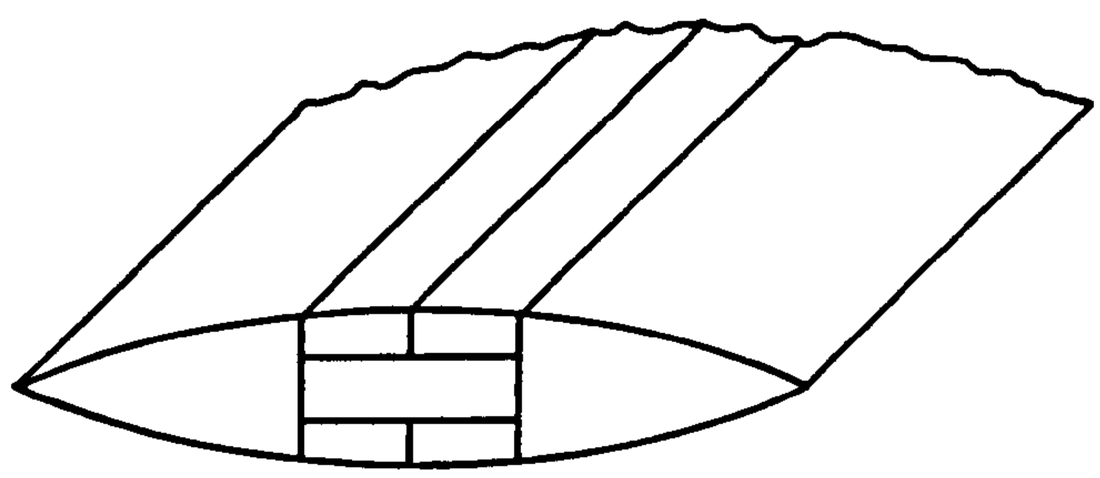

Fig 23 (continued)

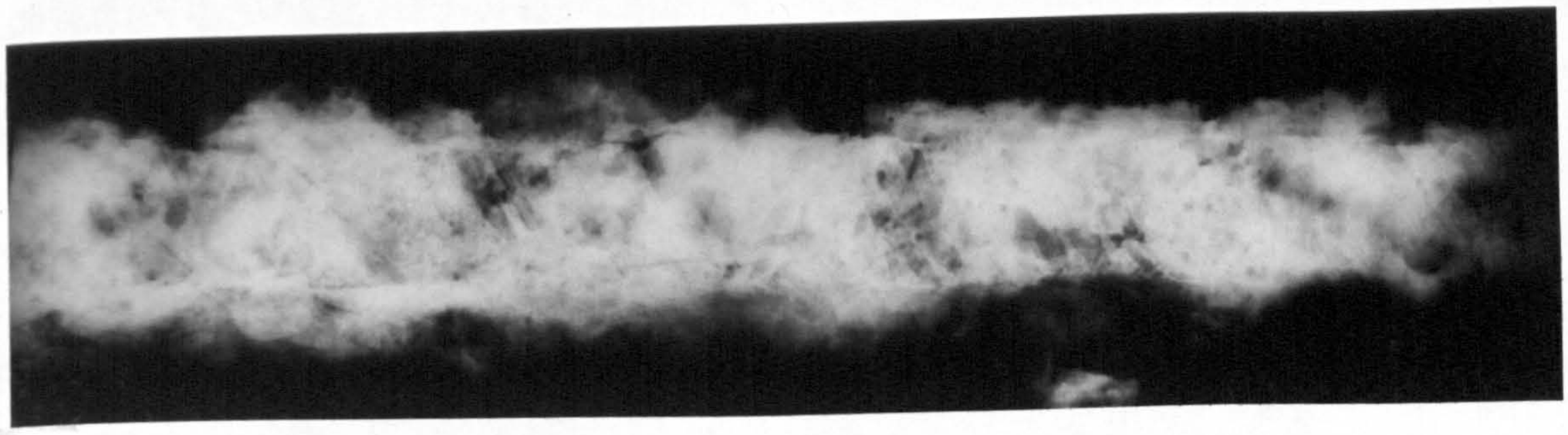

(a)

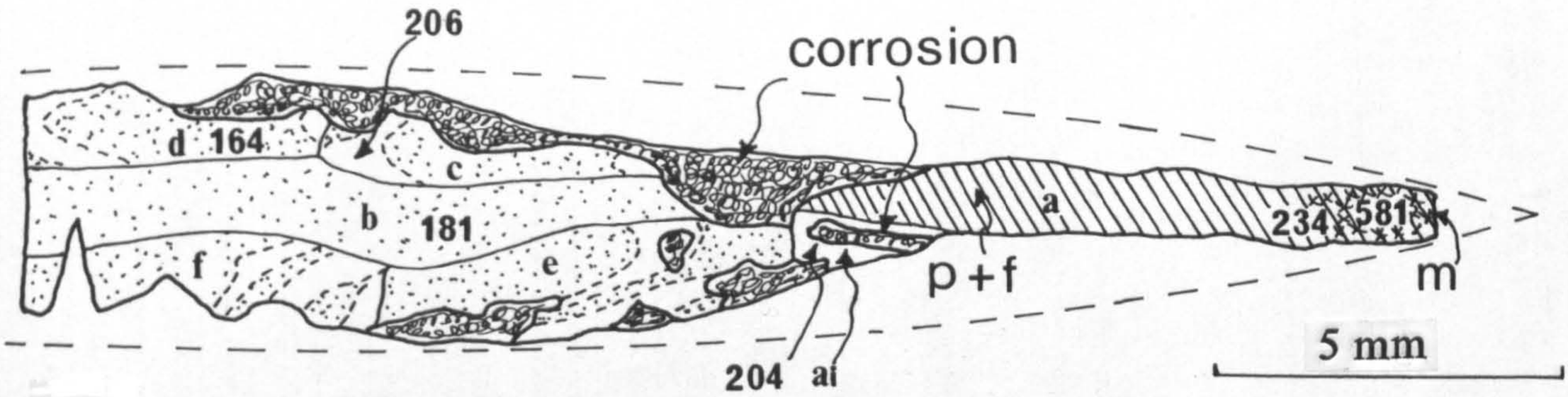

(b)

(c)

Fig 24 Sword blade S55, from Sarre or Bifrons: (a) x-radiograph; (b) sketch of section; (c) photomacrograph; (d) three-dimensional view

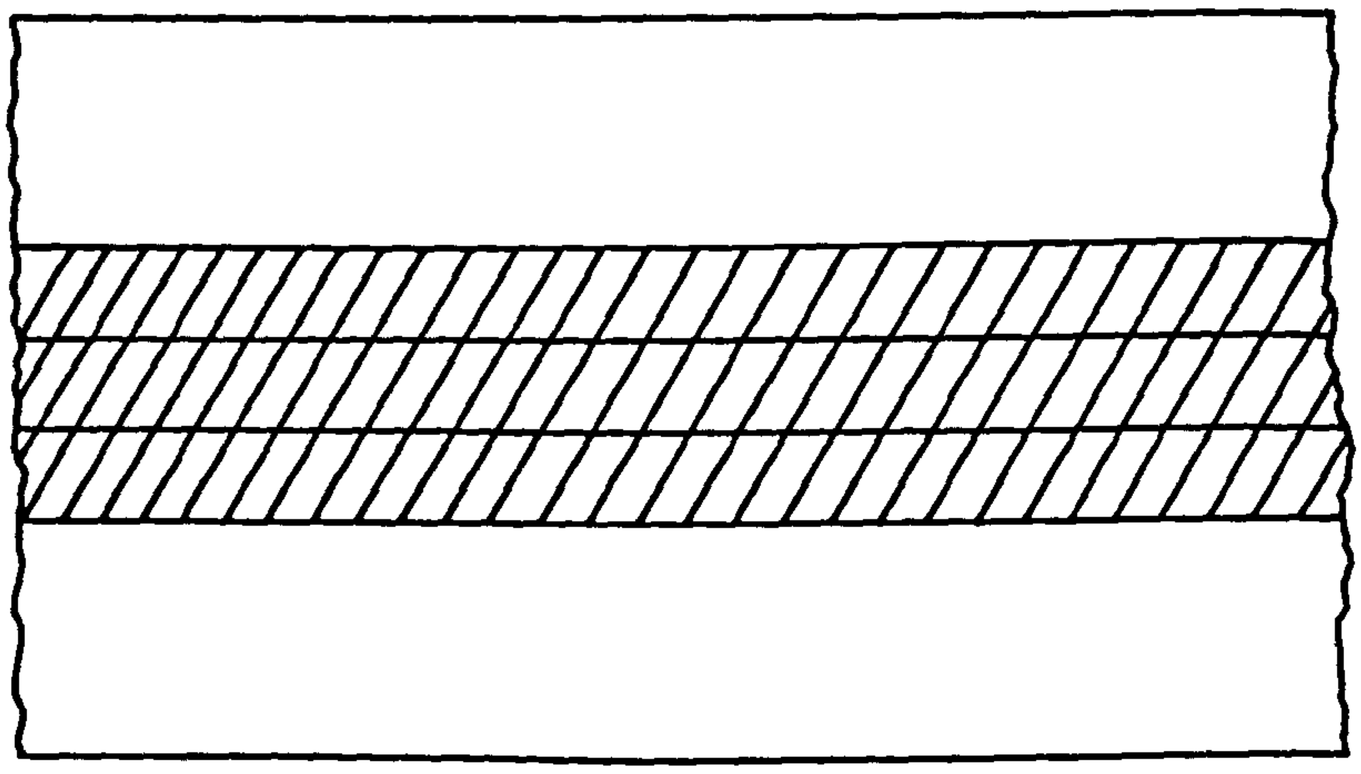

(d)

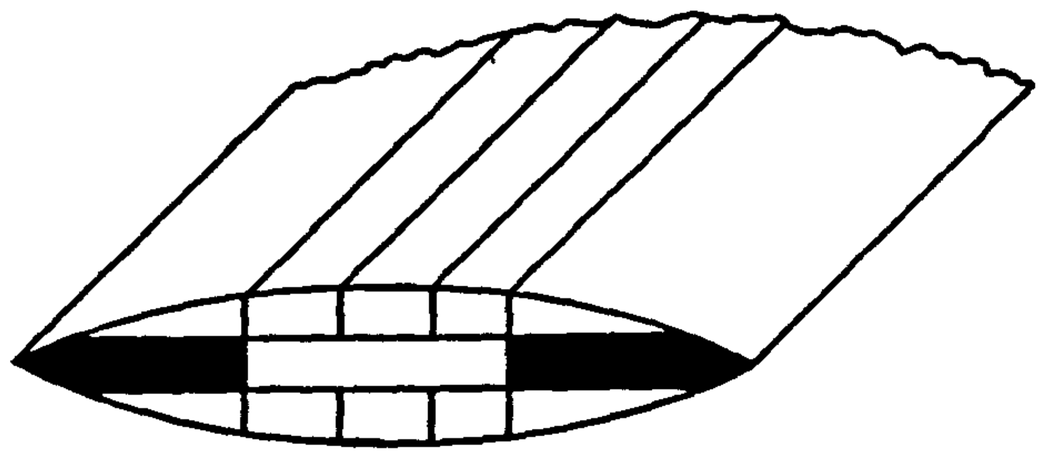

Fig 24 (continued)

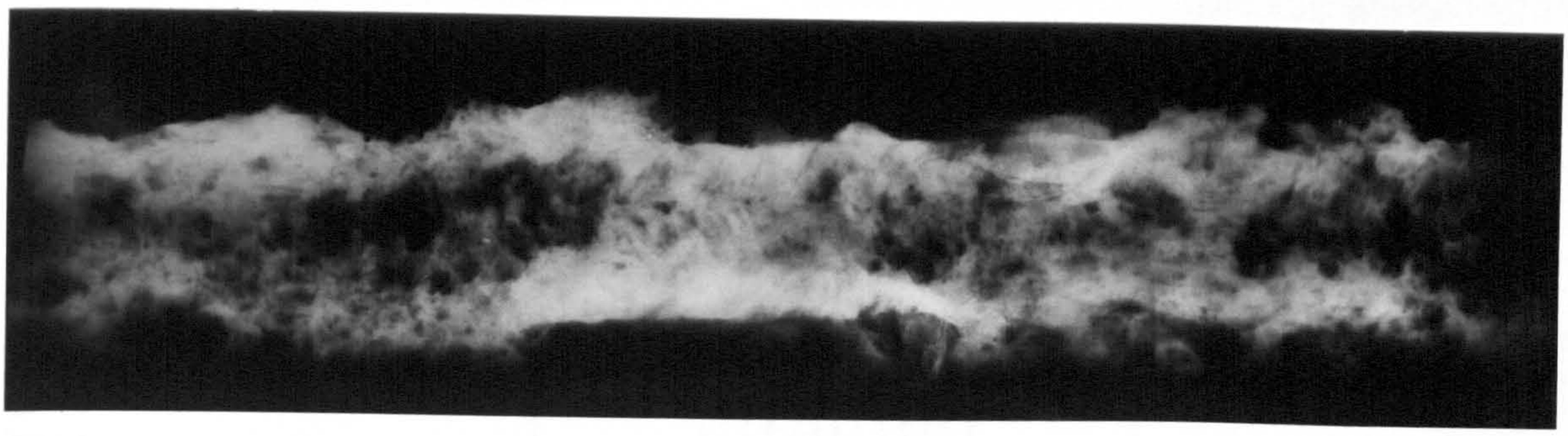

(a)

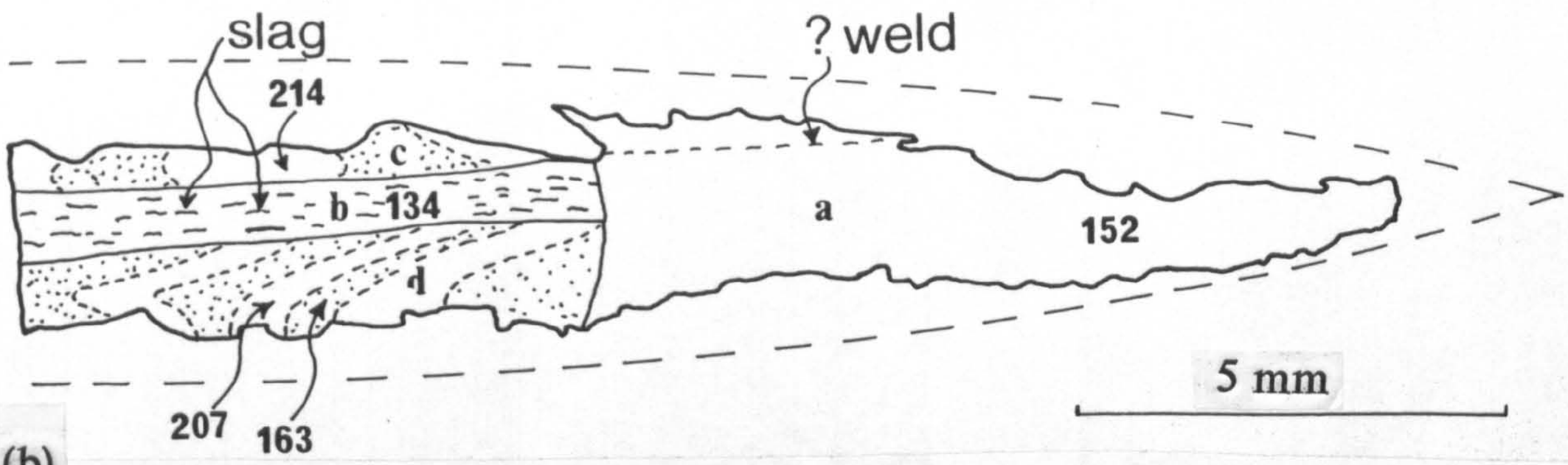

(b)

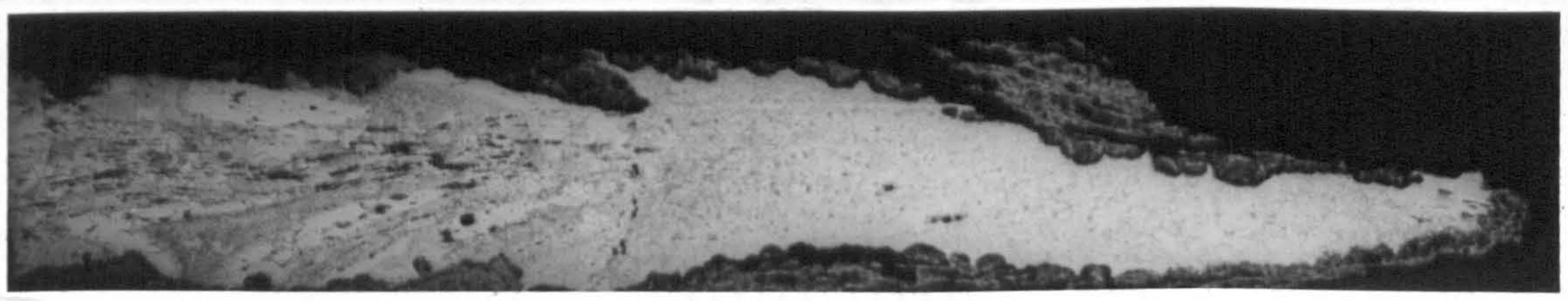

(c)

Fig 25 Sword blade S56, from Bifrons: (a) x-radiograph; (b) sketch of section; (c) photomacrograph; (d) three-dimensional view

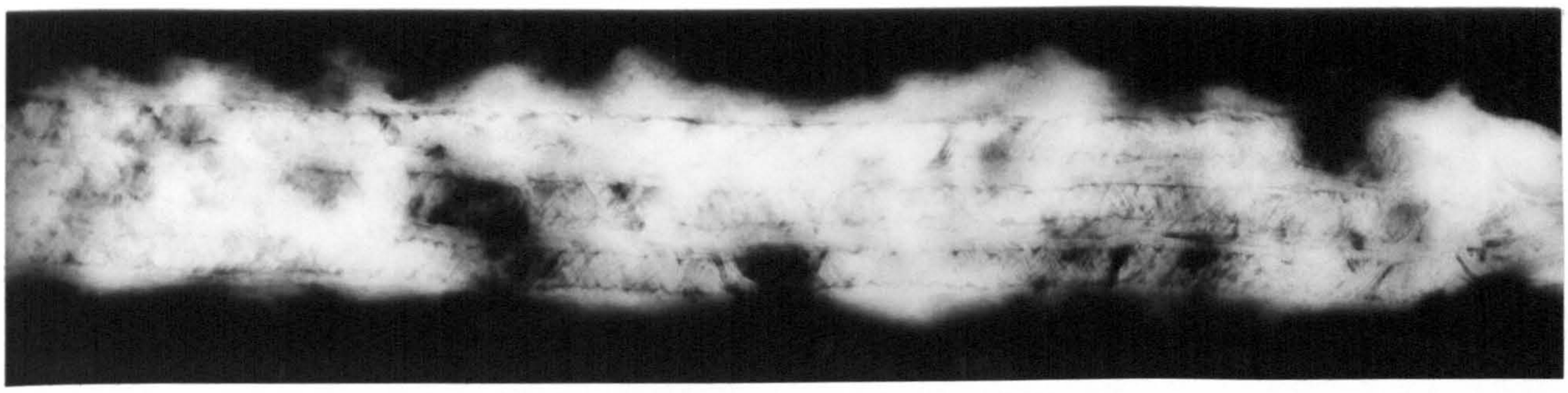

(a)

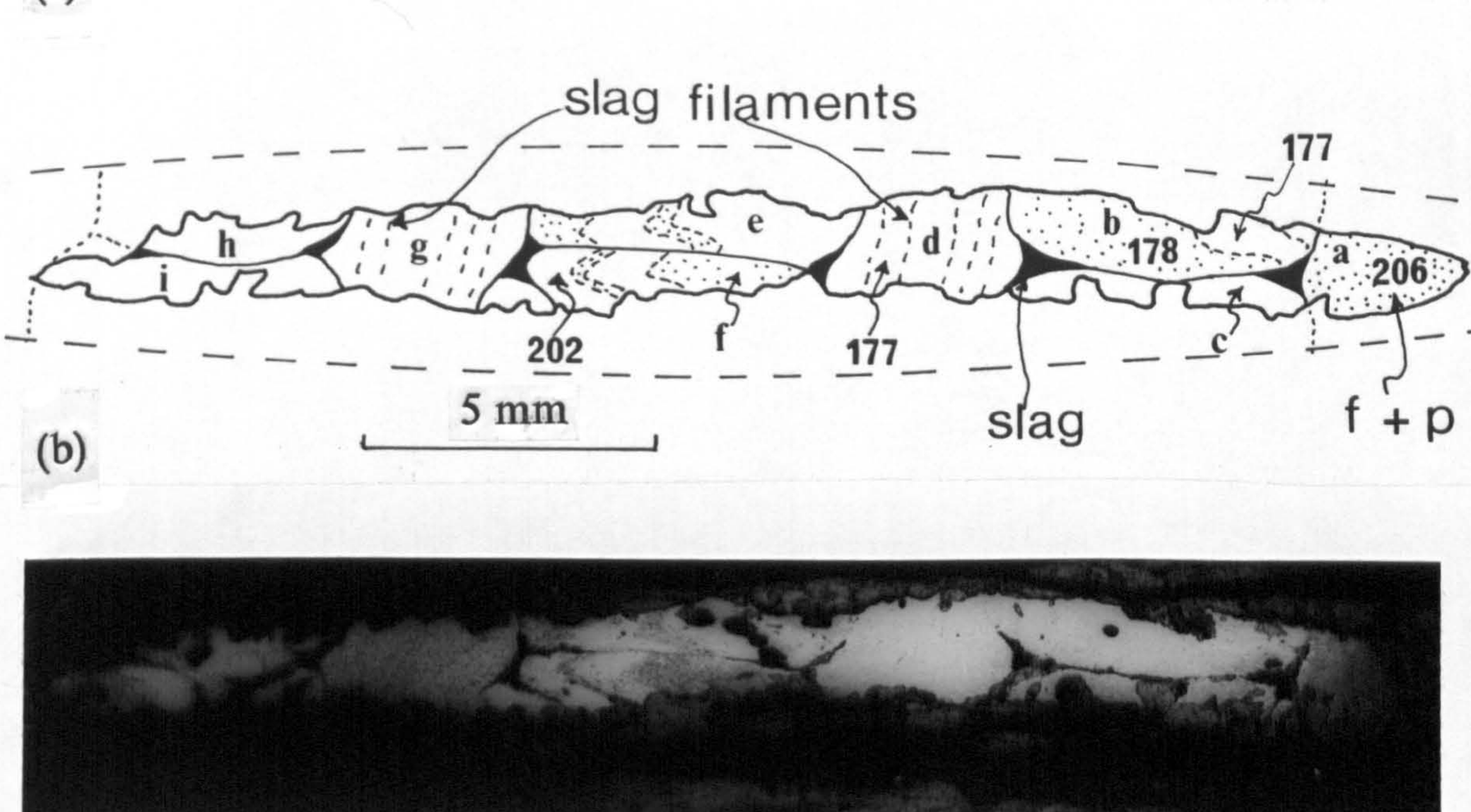

(b)

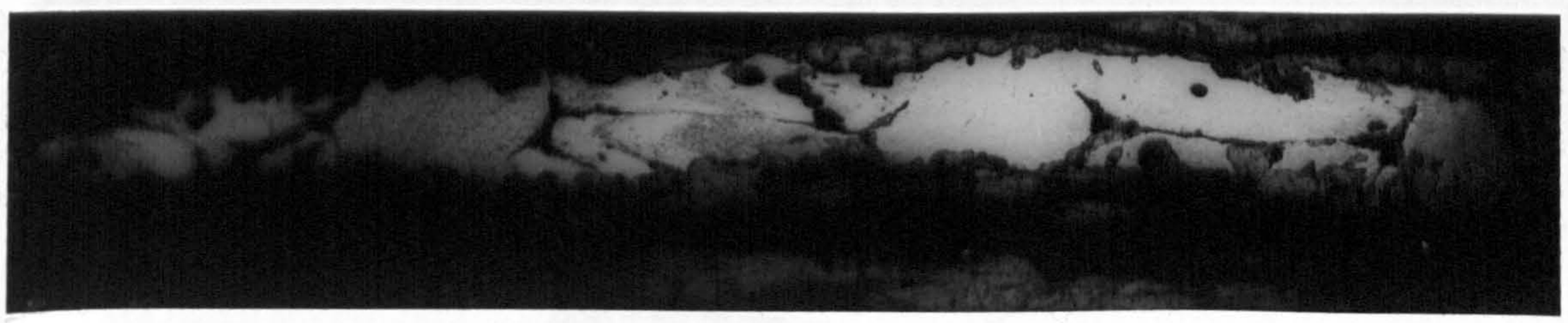

(c)

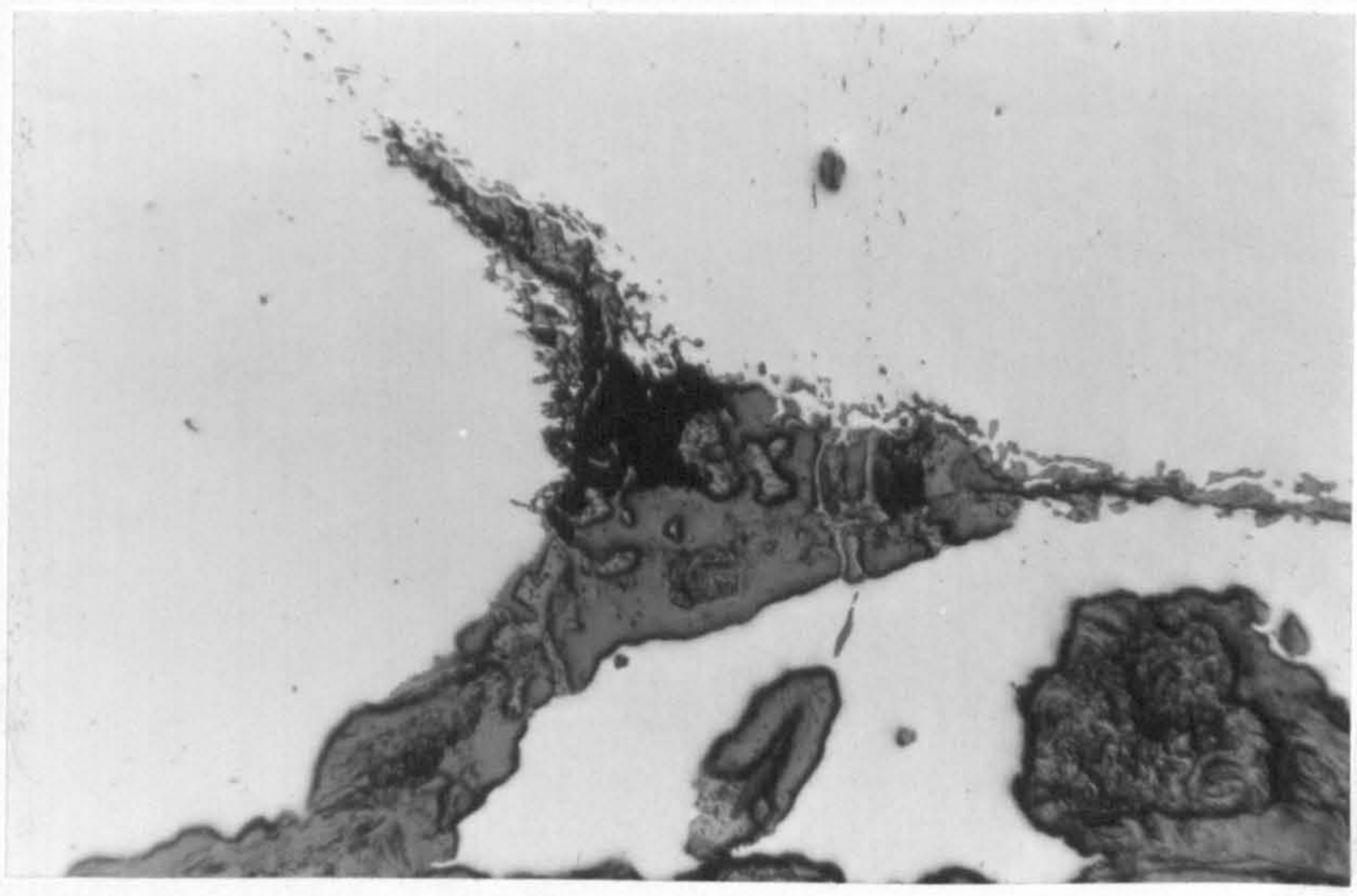

(d)

x50

Fig 26 Sword blade S12, from Wickhambreux: (a) x-radiograph; (b) sketch of section; (c) photomacrograph; (d) photomicrograph showing entrapped smithing slag and corrosion between the pattern-welded parts in the centre of the blade (unetched); (e) three-dimensional view

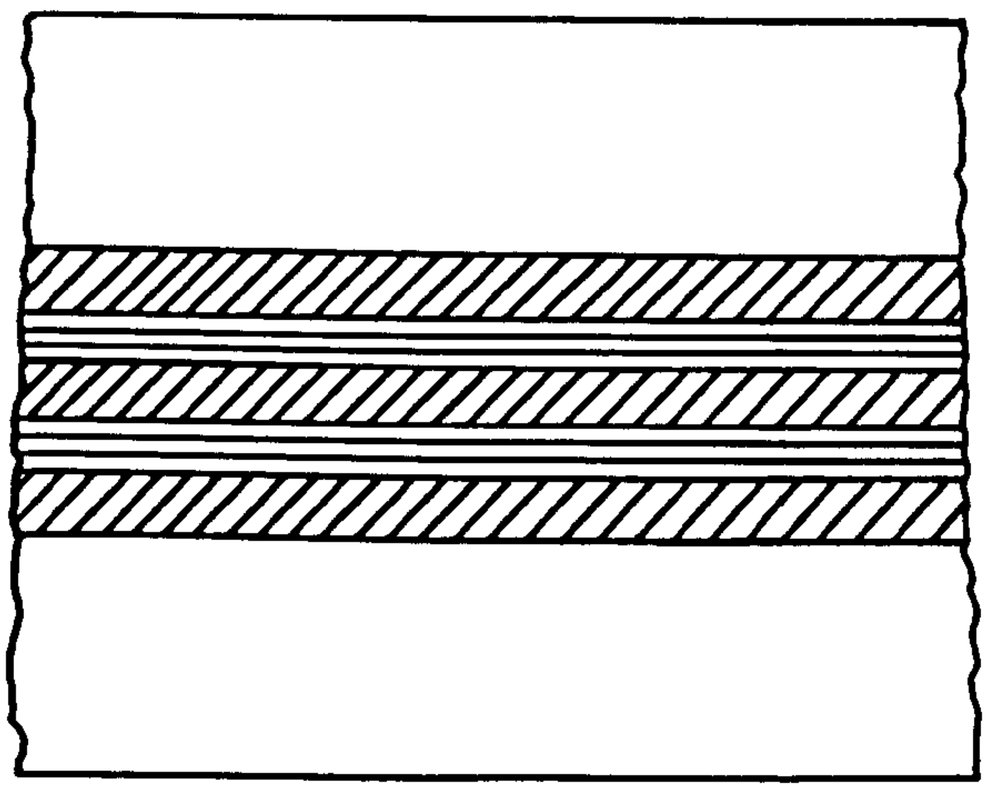

(e)

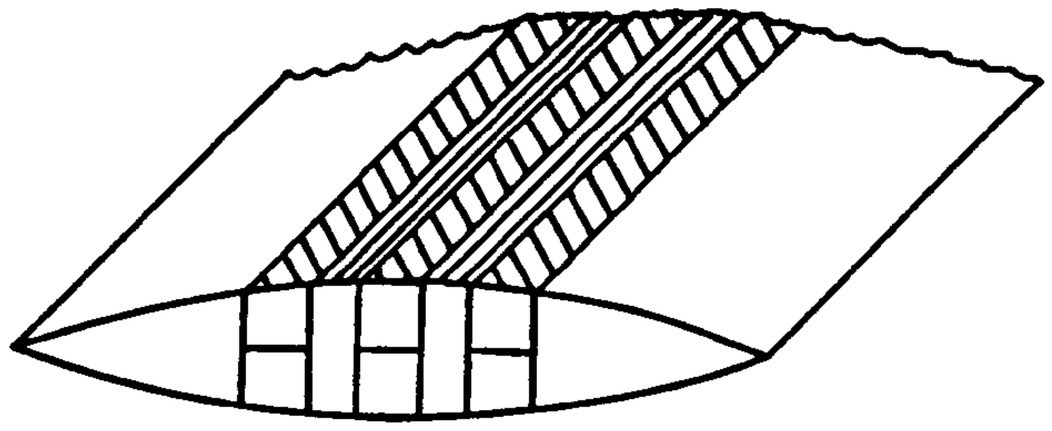

Fig 26 (continued)

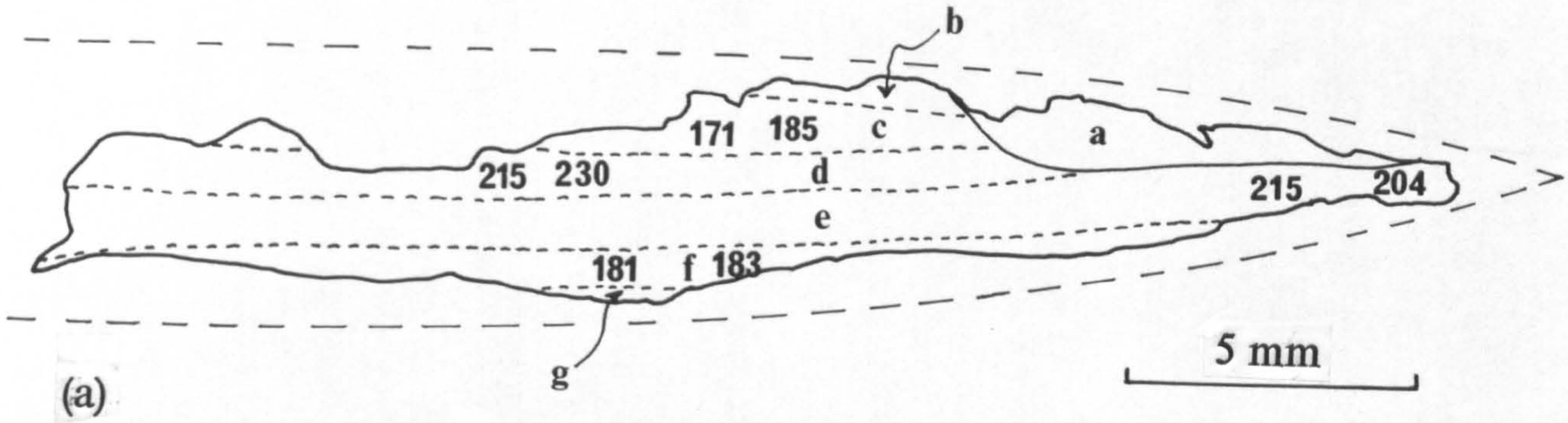

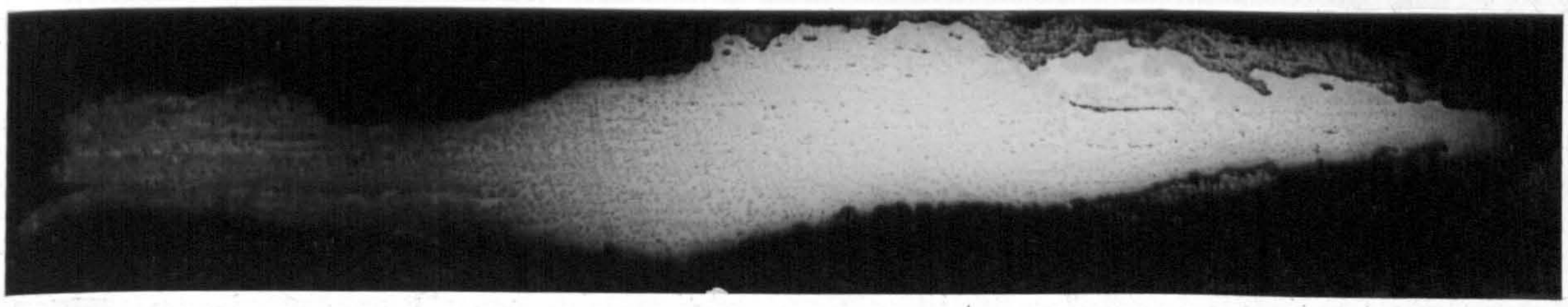

(b)

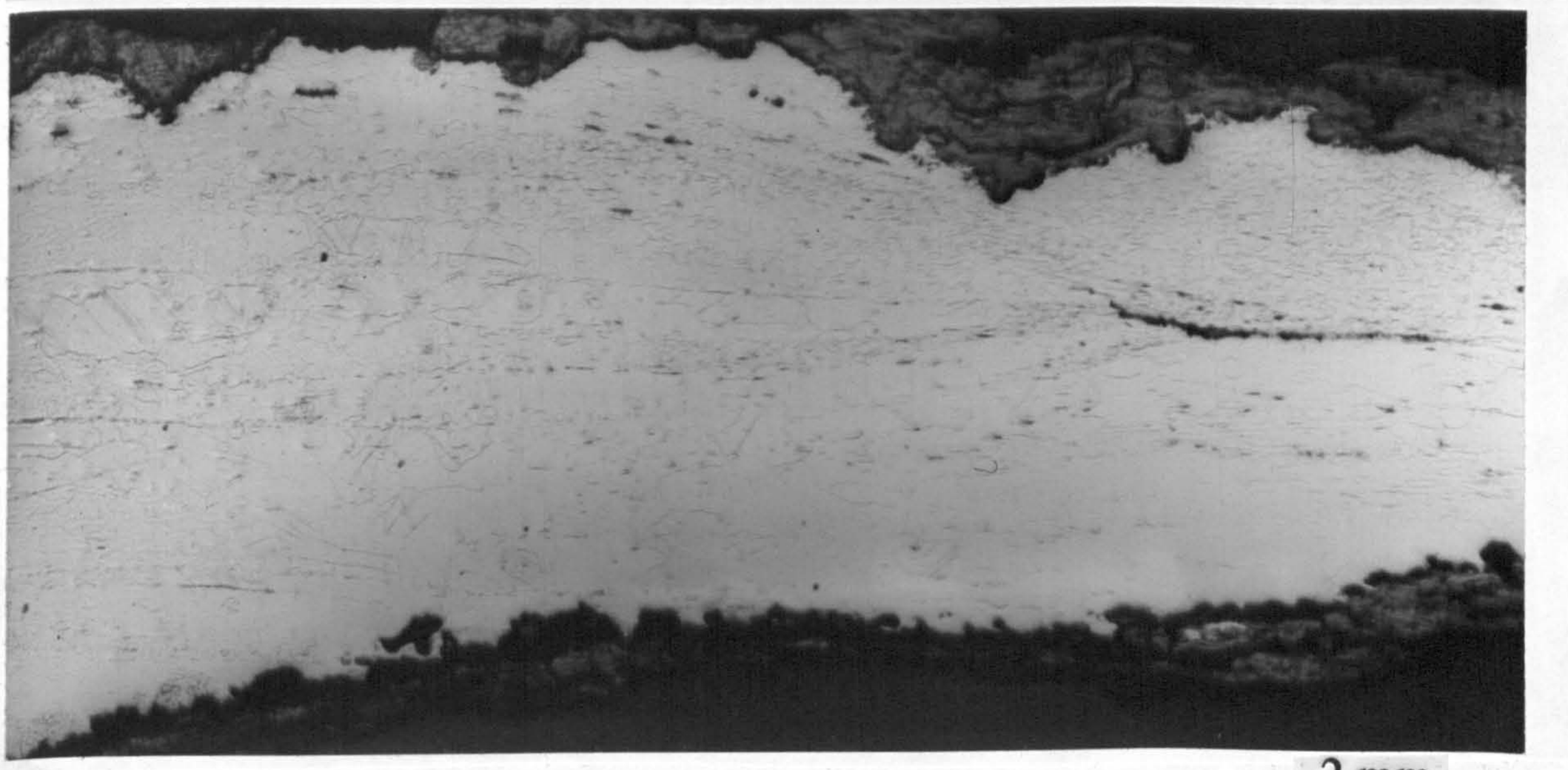

(c)

Fig 27 Sword blade S13, from Kent, possibly Bifrons: (a) x-radiograph; (b) photomacrograph; (c) three-dimensional view

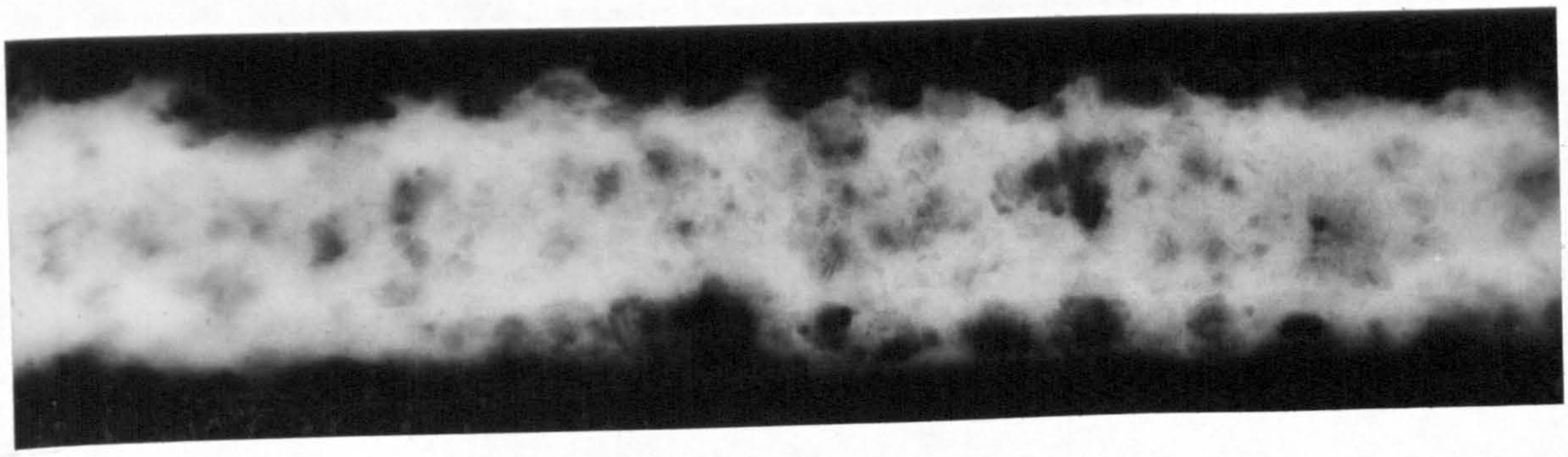

(a)

(b)

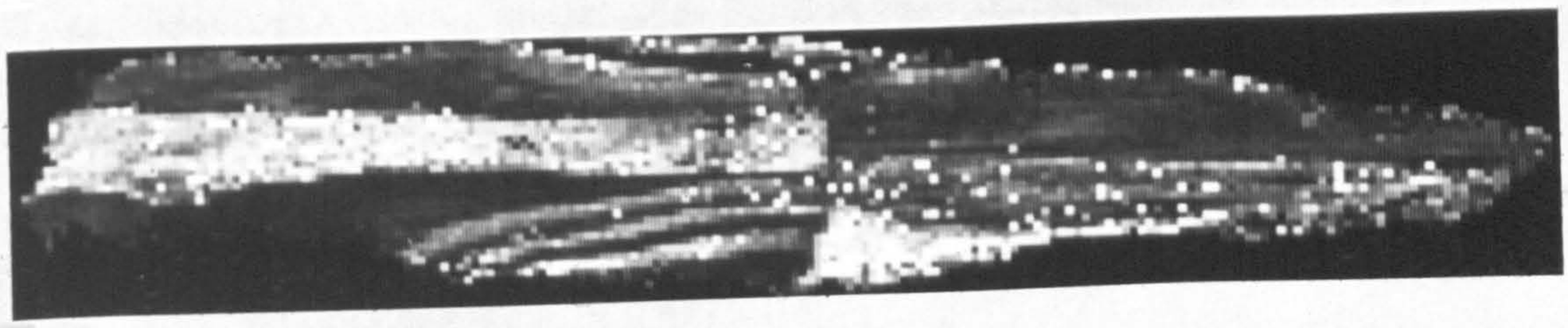

(c)

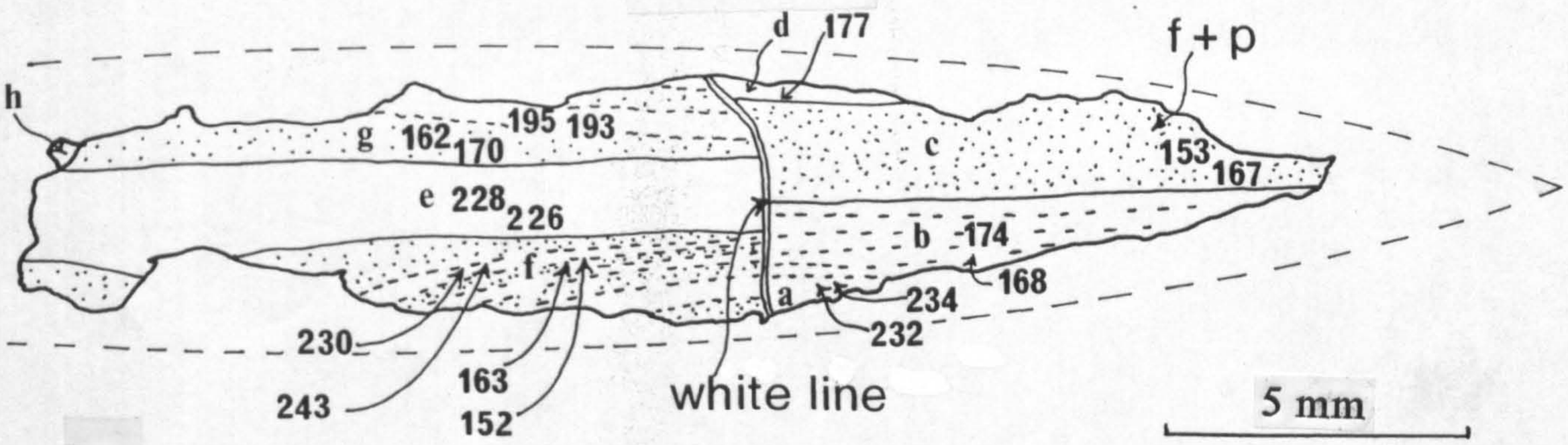

(d)

Fig 28 Sword blade S14, from Eastrey: (a) x-radiograph; (b) photomacrograph; (c) EPMA phosphorus map; (d) sketch of section; (e) photomicrograph showing finer grain, low carbon parts of the laminated pattern-welded low carbon pieces f and g on either side of the large grain high phosphorus core piece + entrapped smelting slag; (f) three-dimensional view

(e)

x50

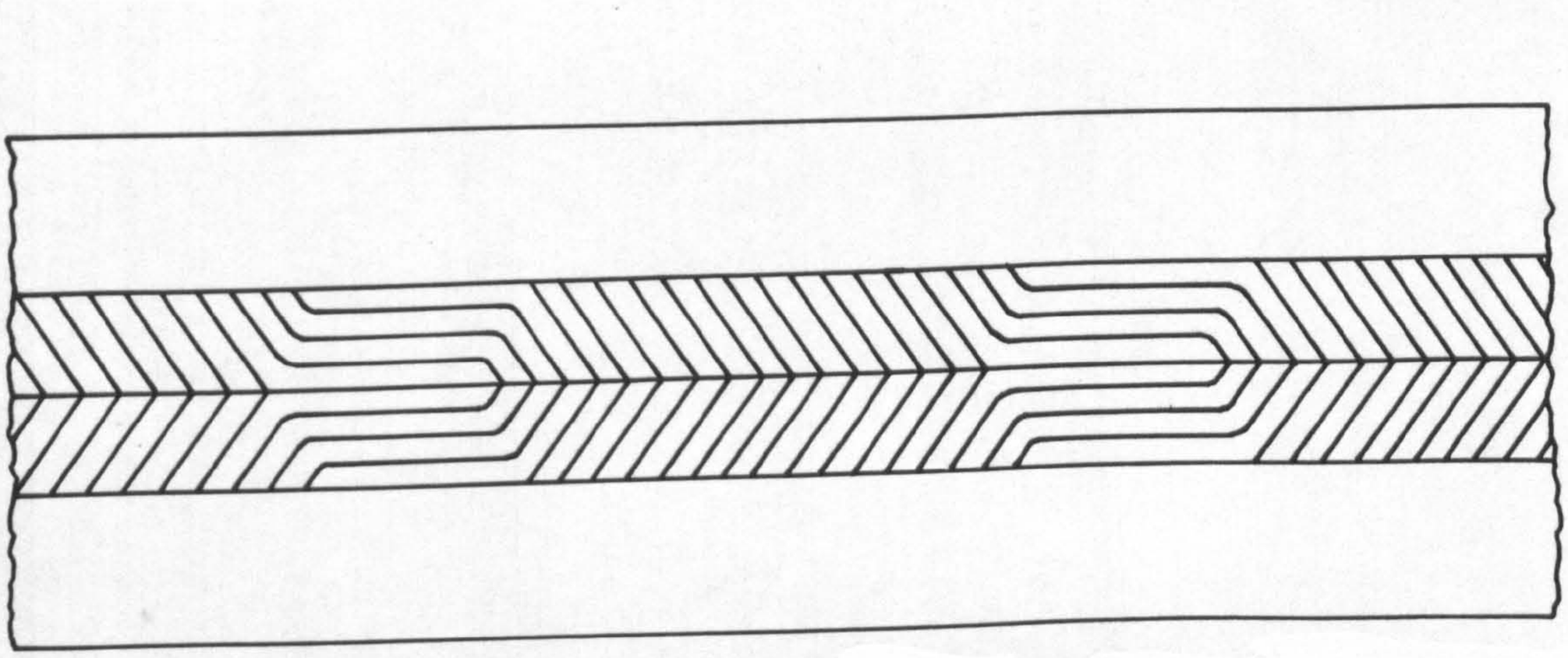

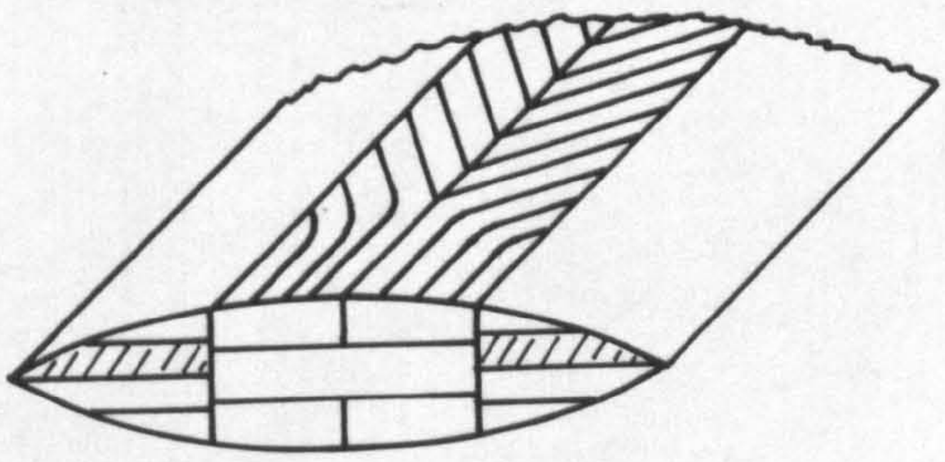

(f)

Fig 28 (continued)

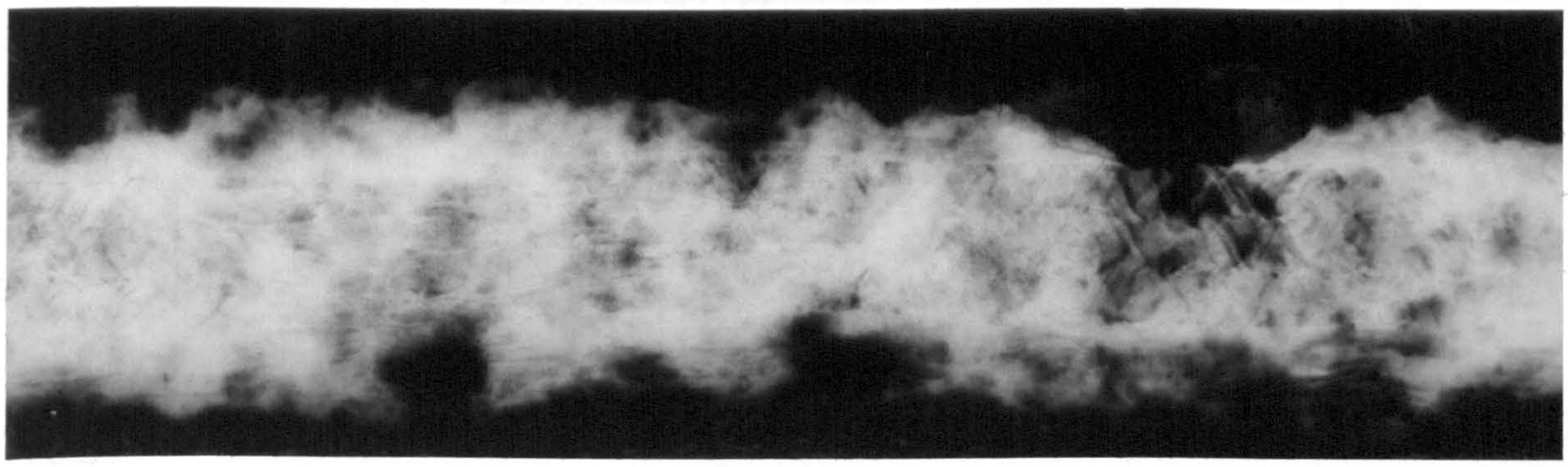

(a)

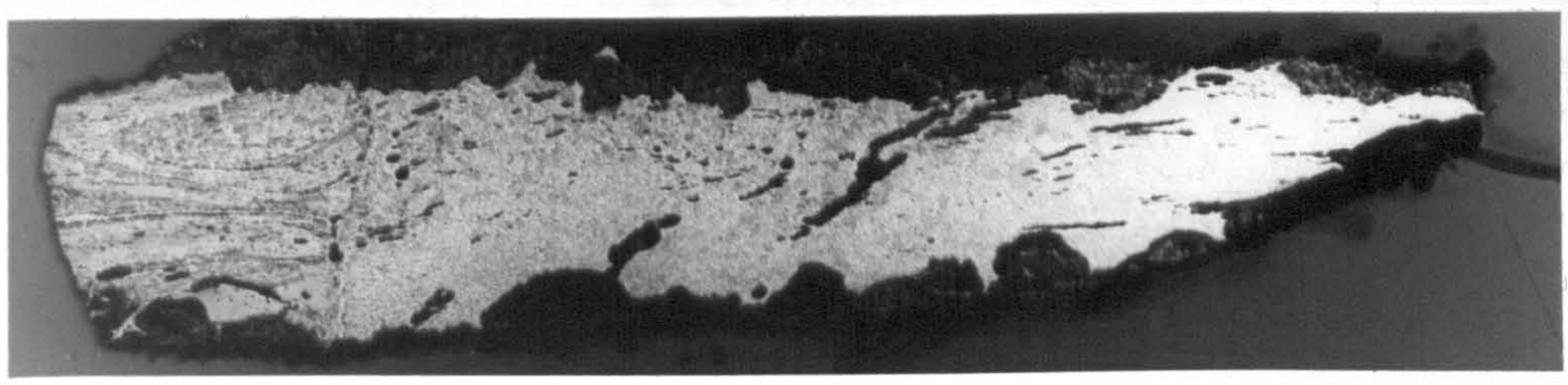

(b)

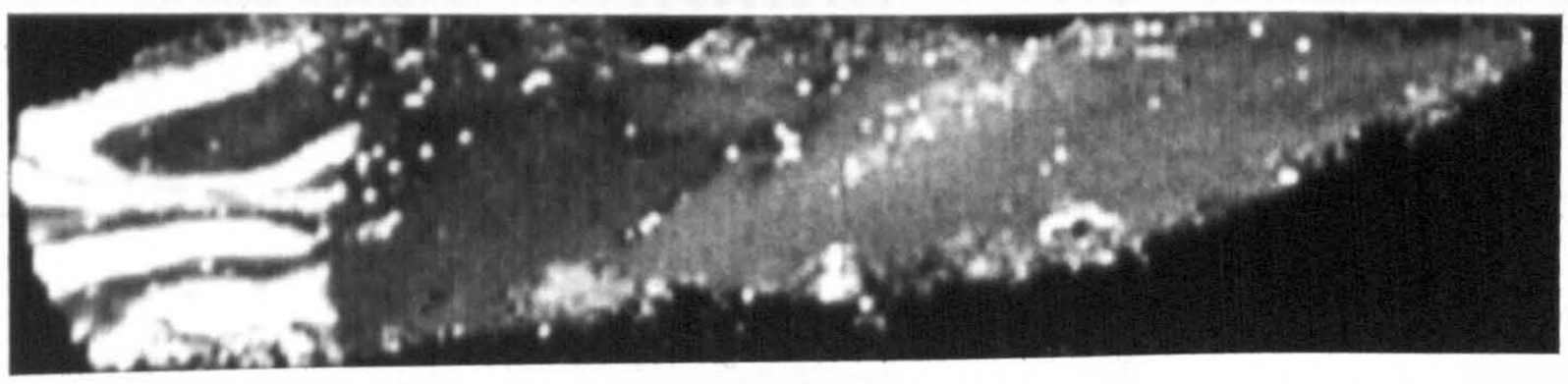

(c)

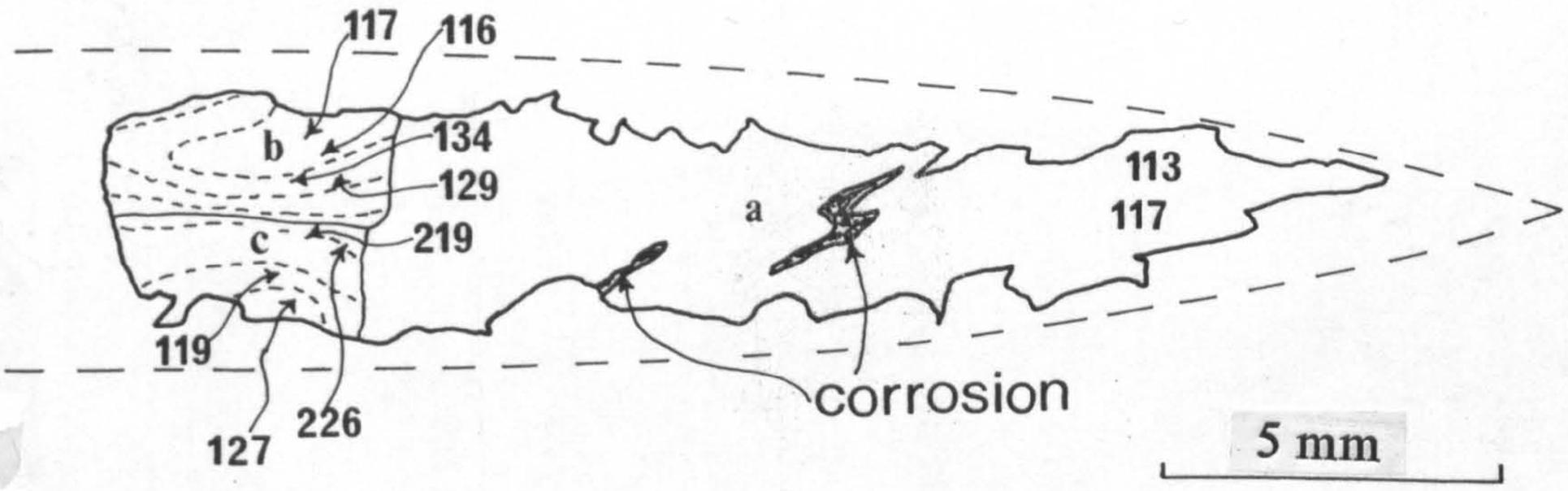

(d)

Fig 29 Sword blade S15, from Holborough: (a) x-radiograph; (b) photomacrograph; (c) EPMA phosphorus map; (d) sketch of section; (e) surface detail and three-dimensional view

(e)

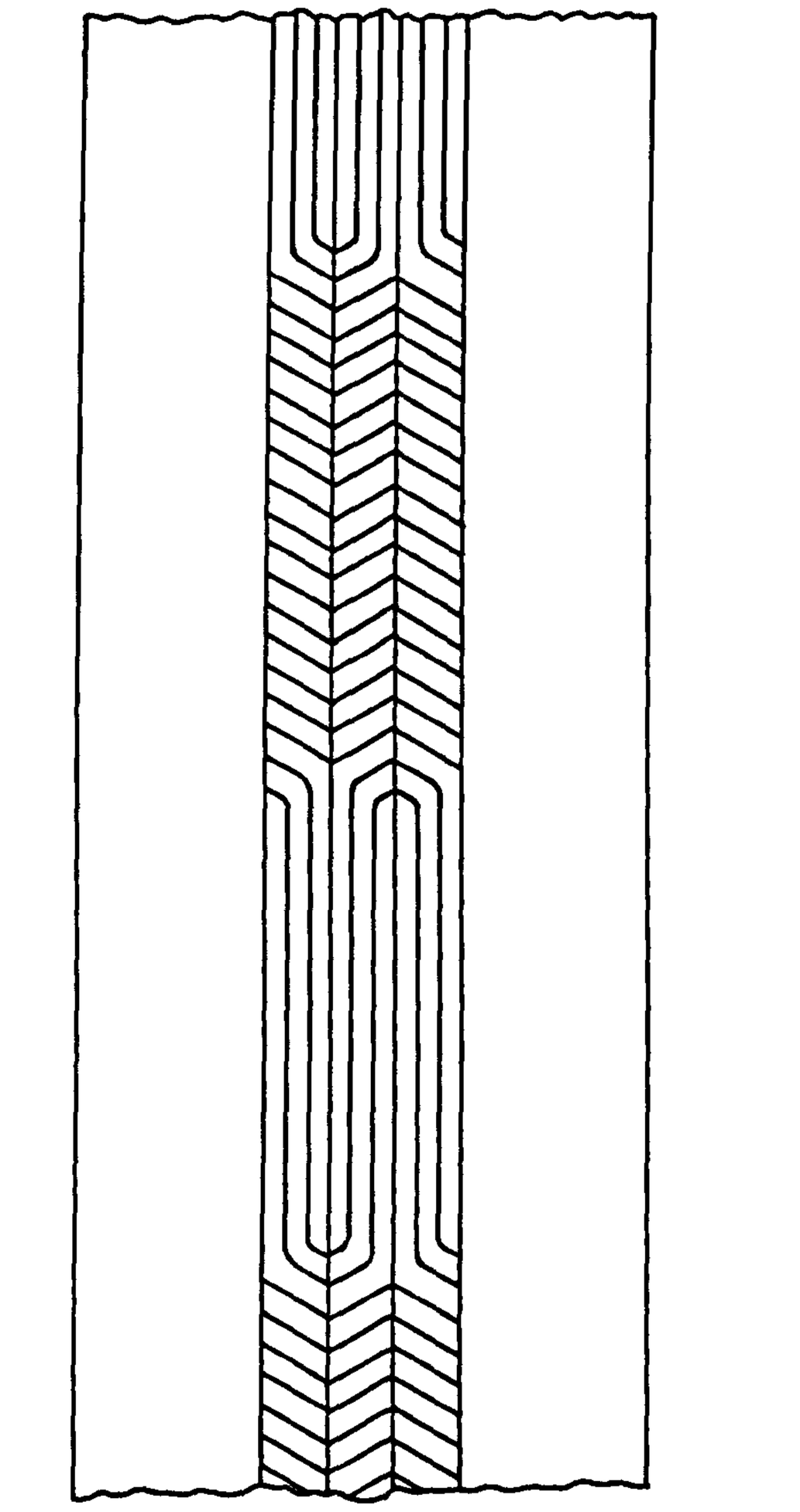

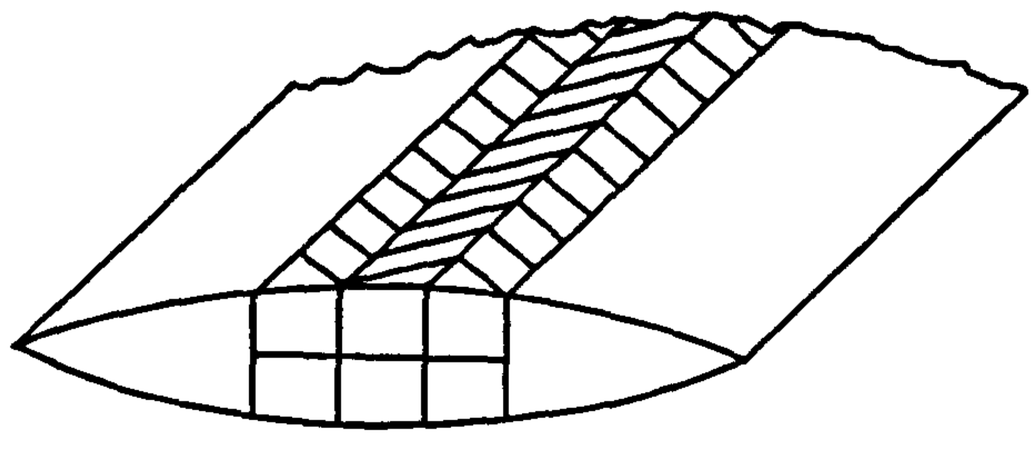

Fig 29 (continued)

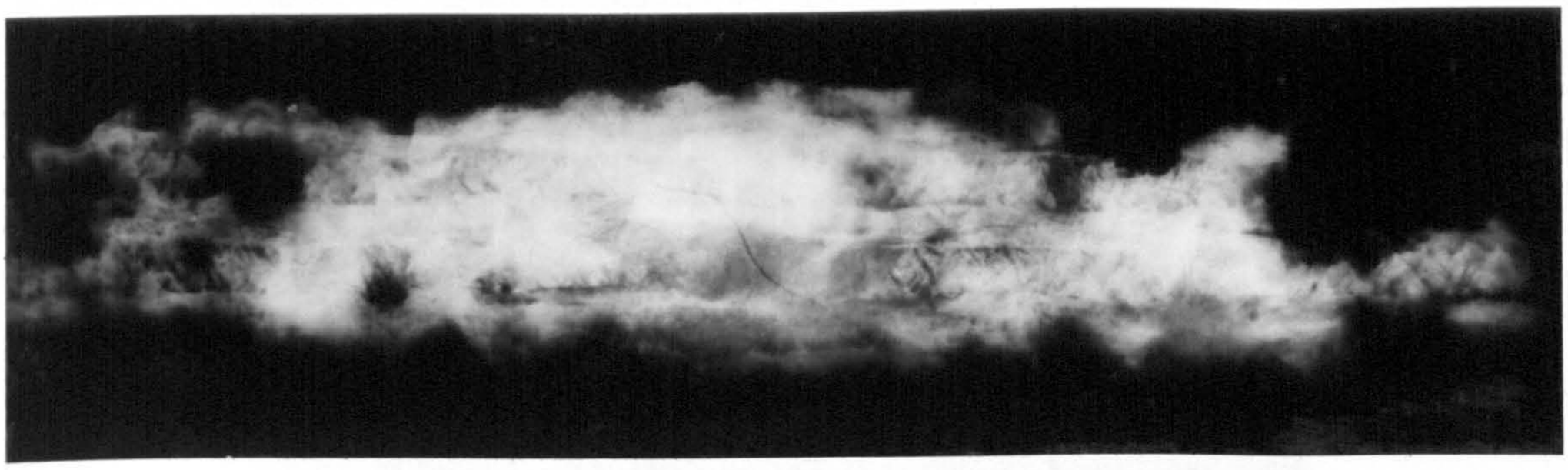

(a)

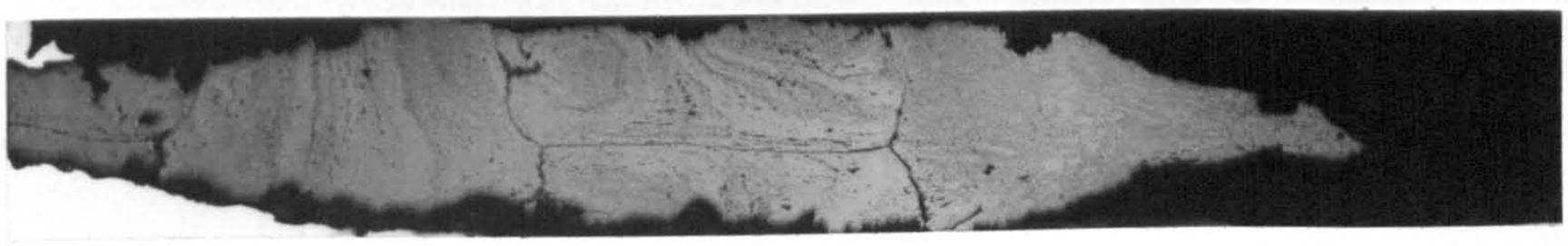

(b)

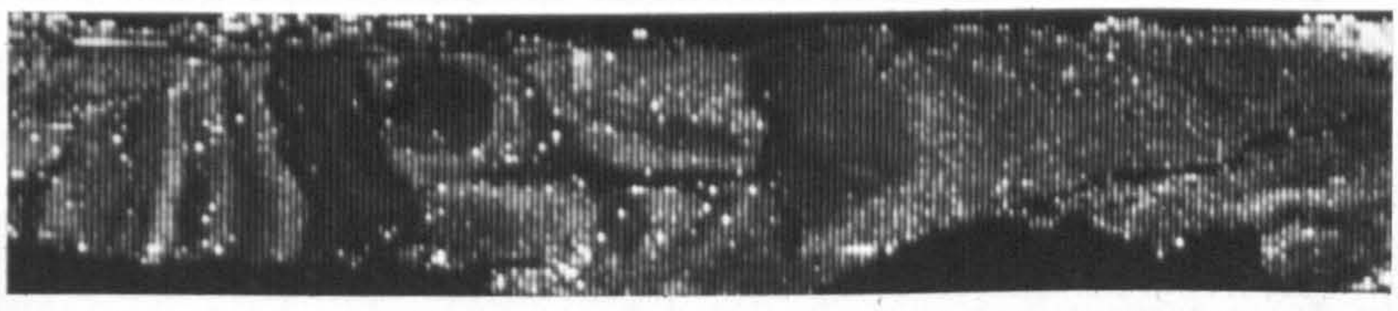

(c)

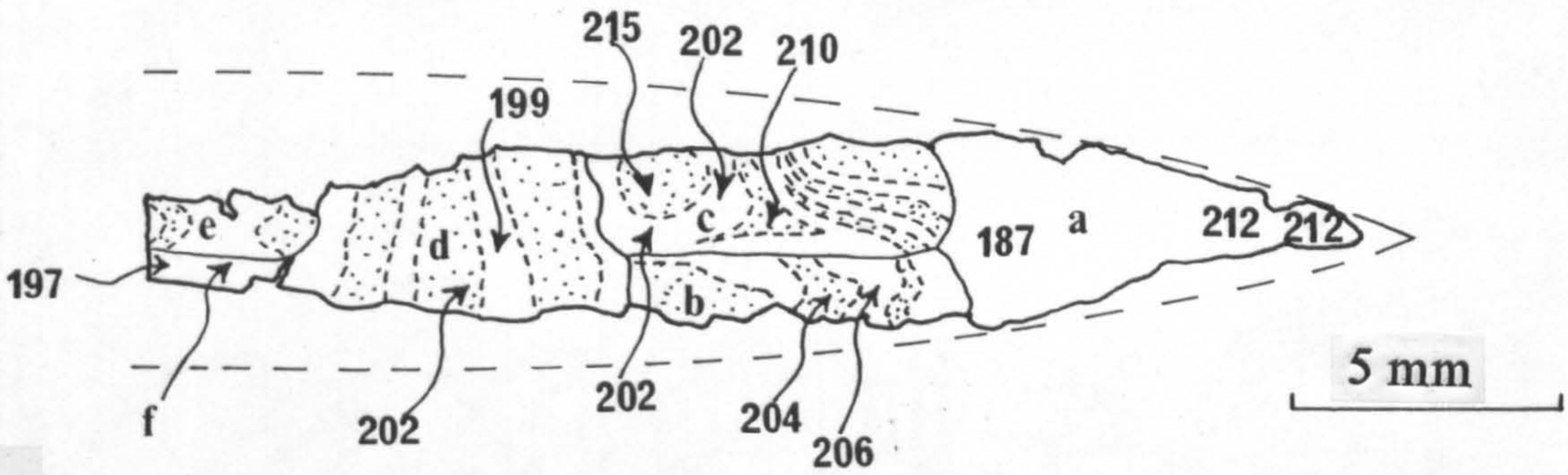

(d)

Fig 30 Sword blade S18, from Aylesford: (a) x-radiograph; (b) photomacrograph; (c) EPMA phosphorus map; (d) sketch of section (e) photomicrograph showing a line of pearlite and small two-phase inclusions of smithing slag along the central weld line between pattern-welded components b and c; (f) three-dimensional view

(e)

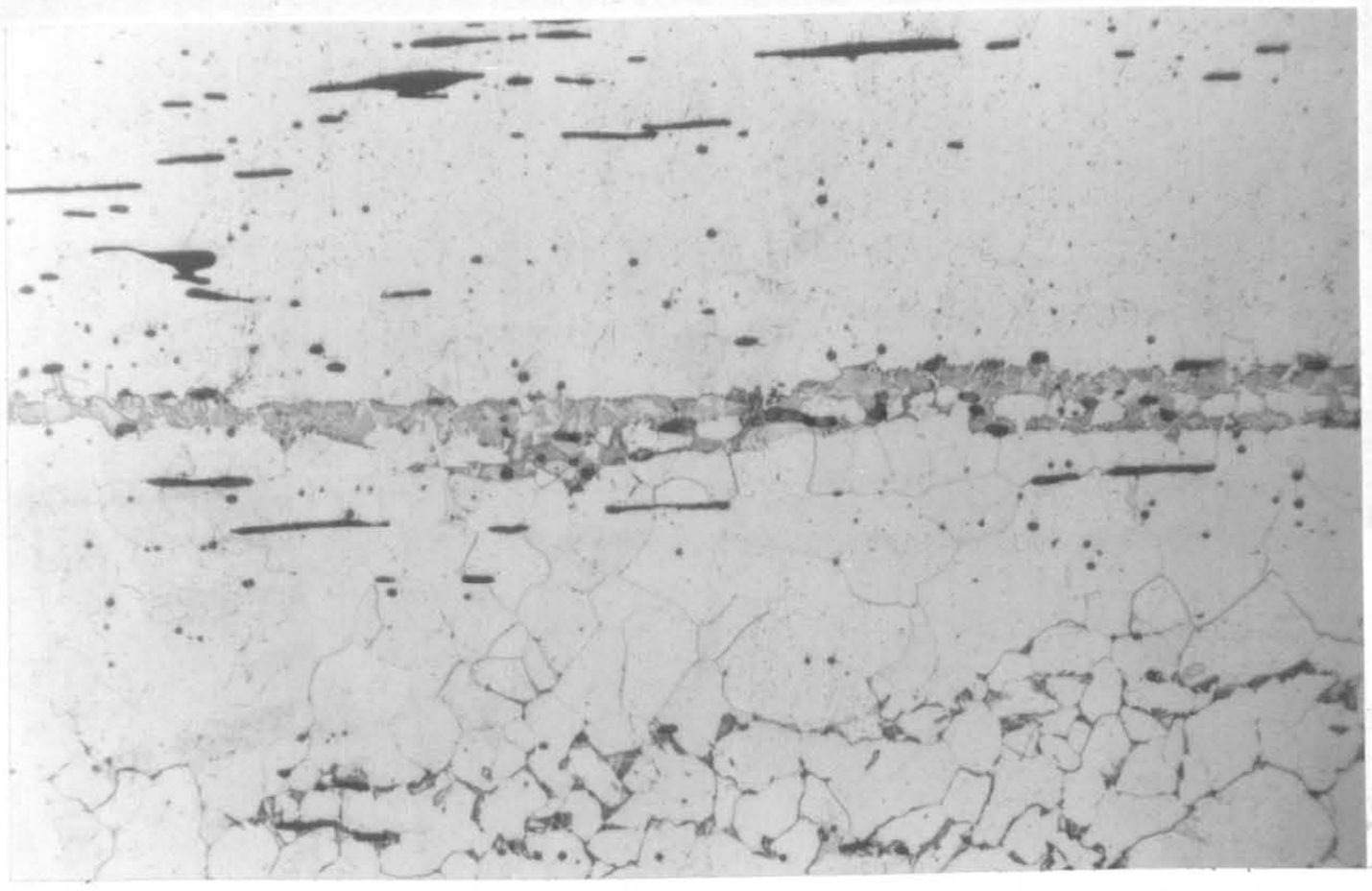

x200

(f)

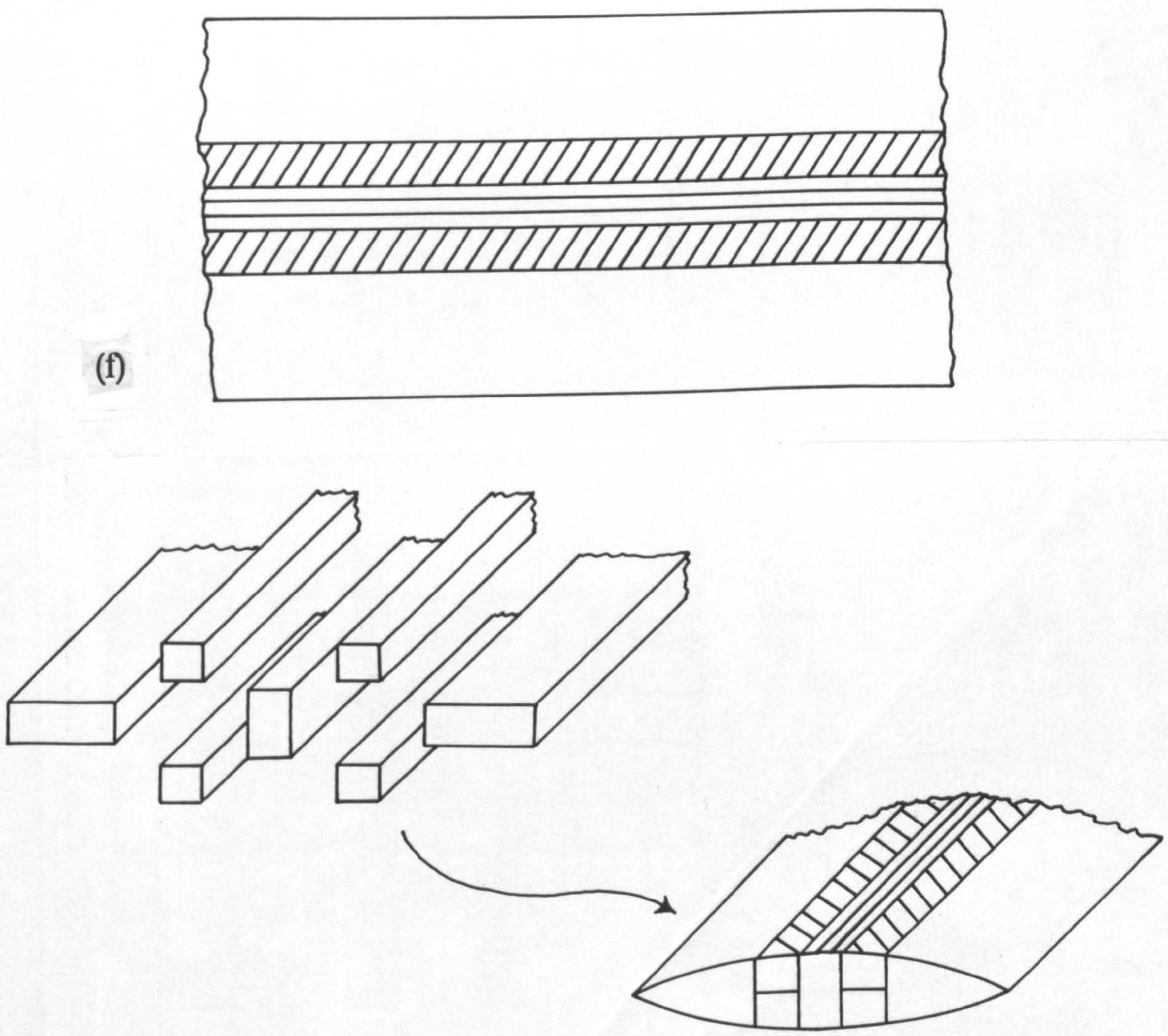

Fig 30 (continued)

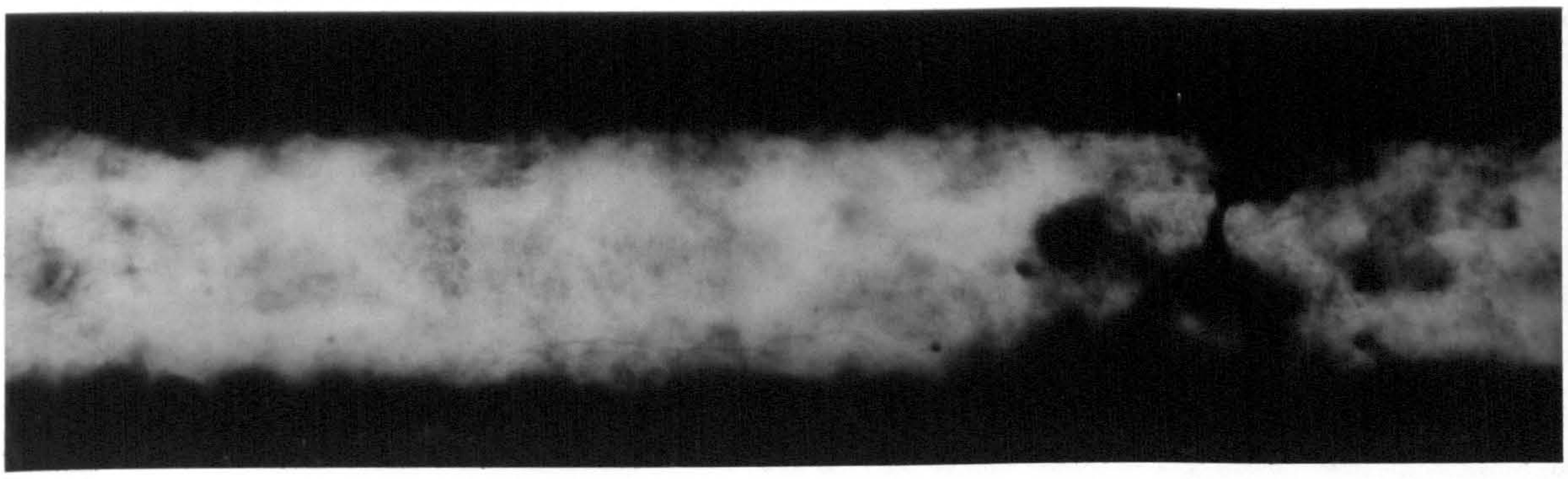

(a)

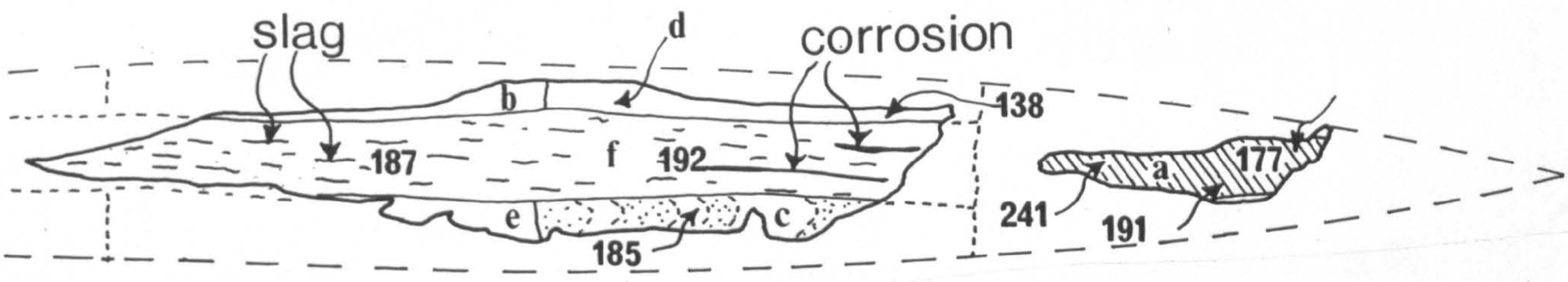

(b)

5 mm

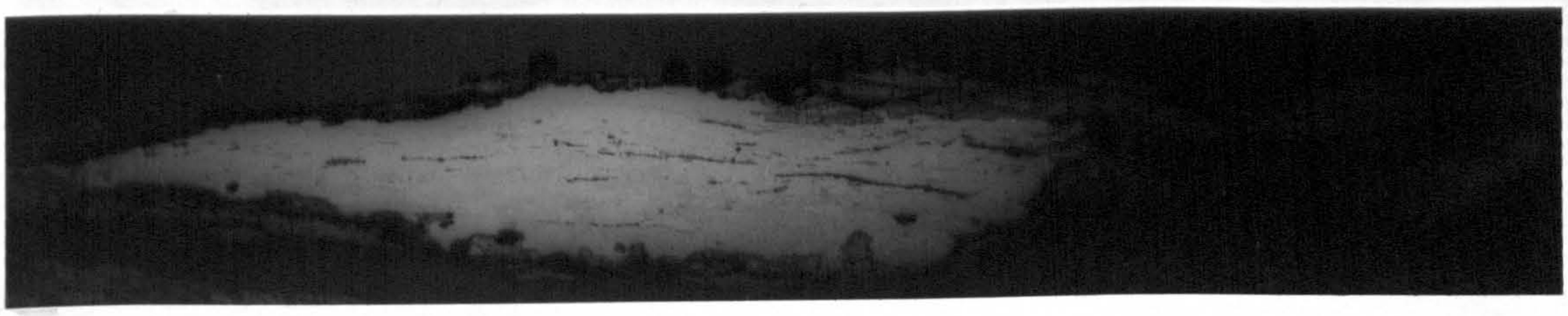

(c)

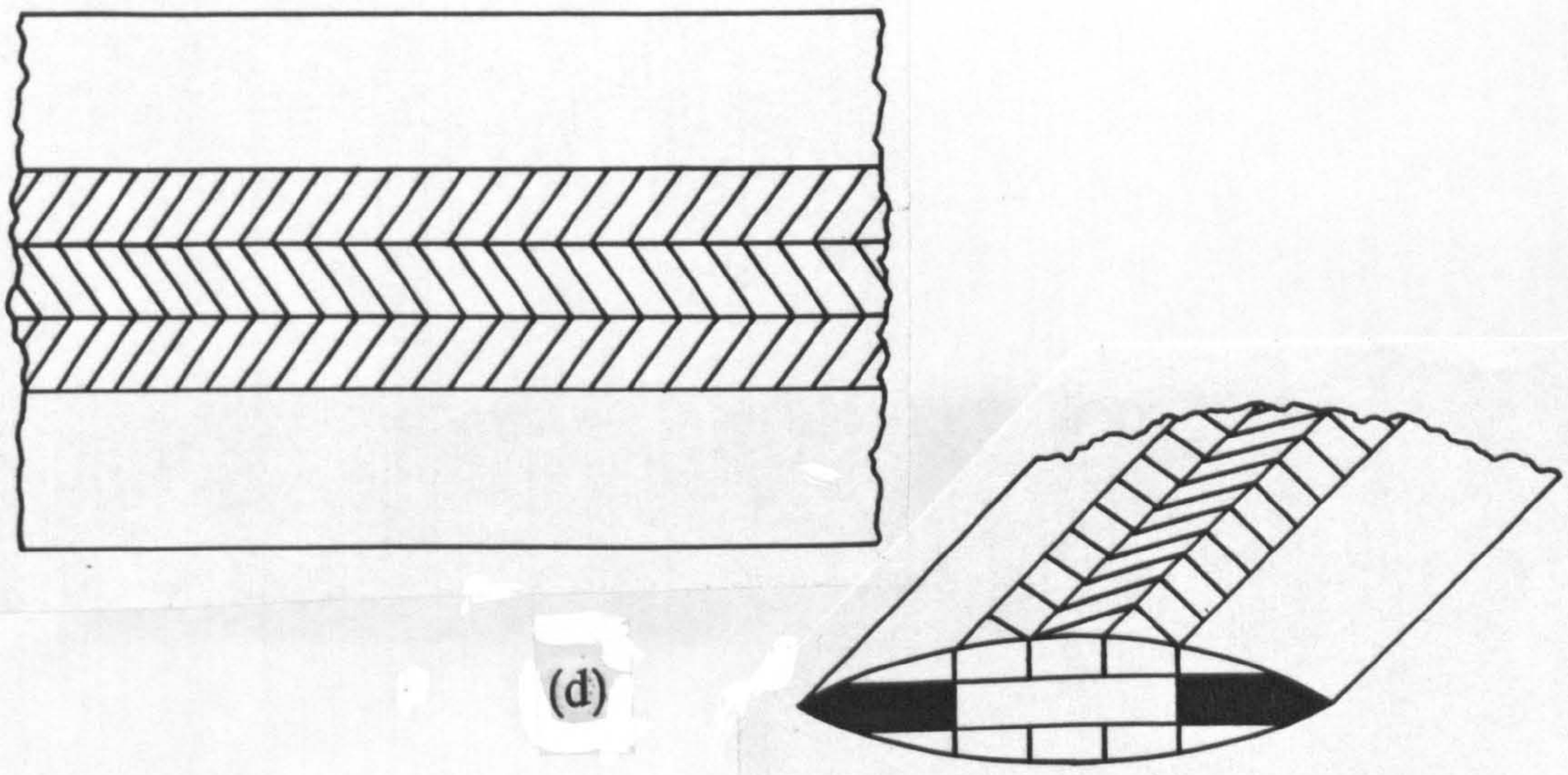

(d)

Fig 31 Sword blade S19, from Wickhambreux: (a) x-radiograph; (b) sketch of section; (c) photomacrograph; (d) three-dimensional view

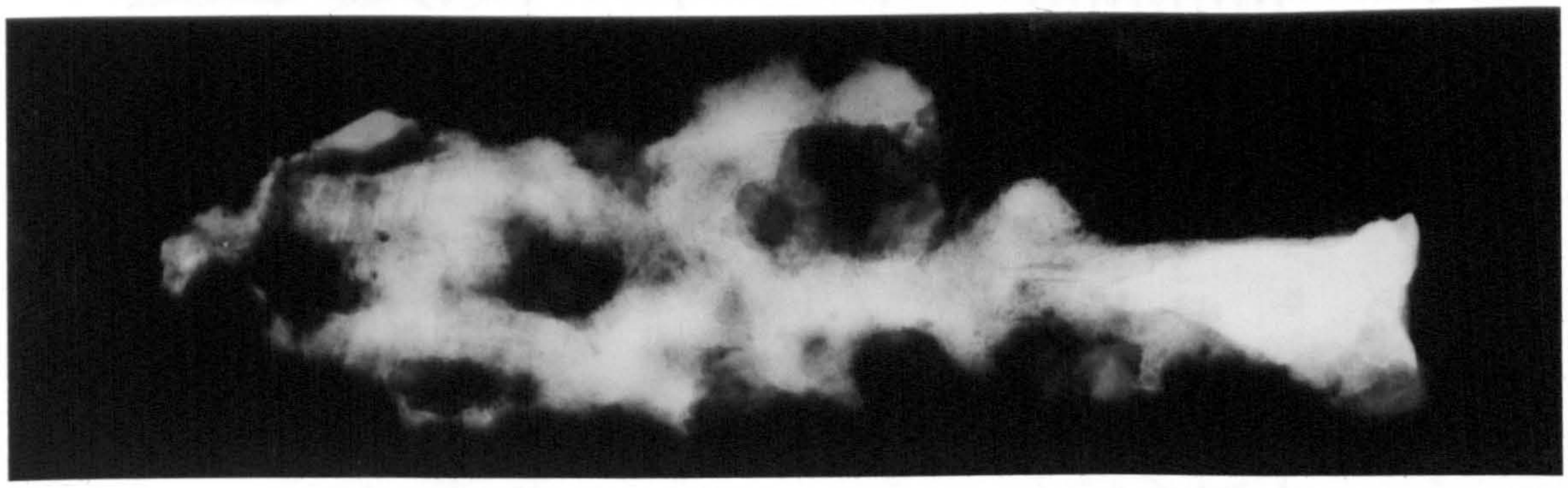

(a)

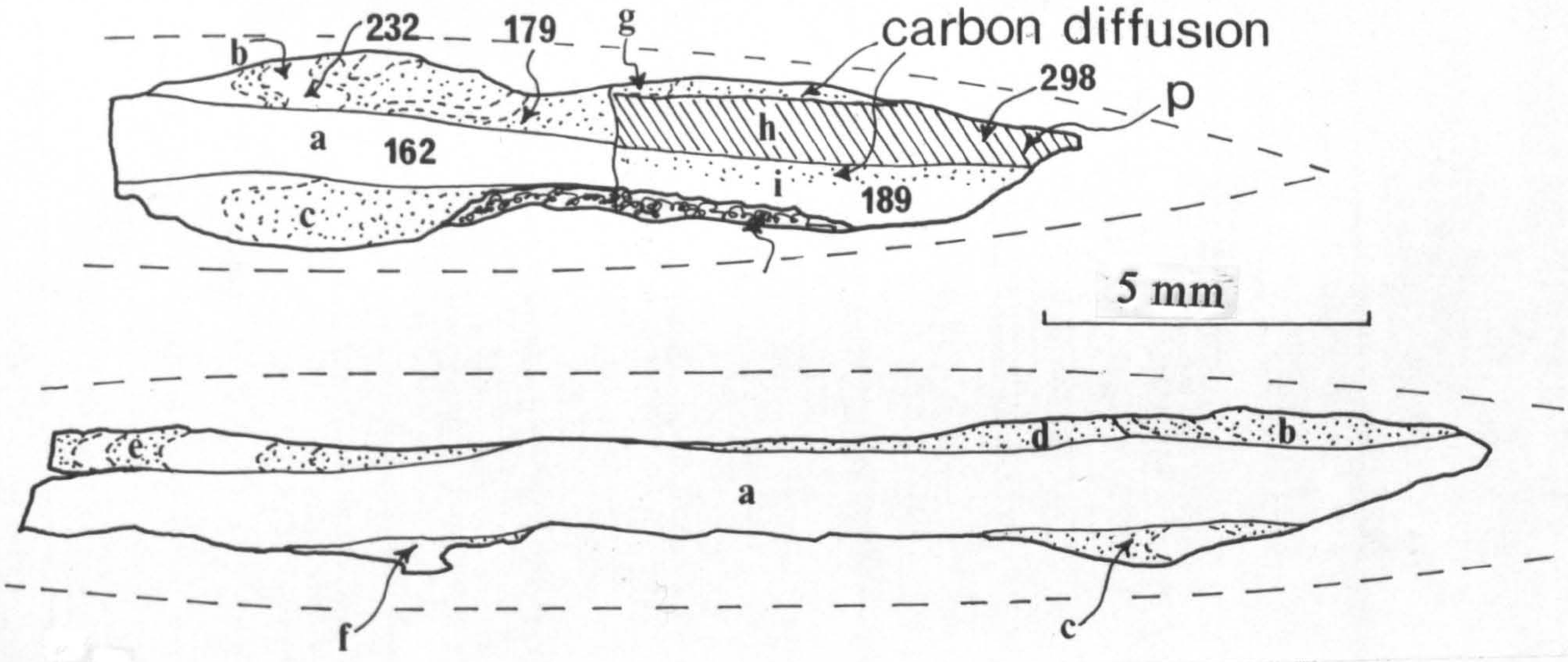

(b)

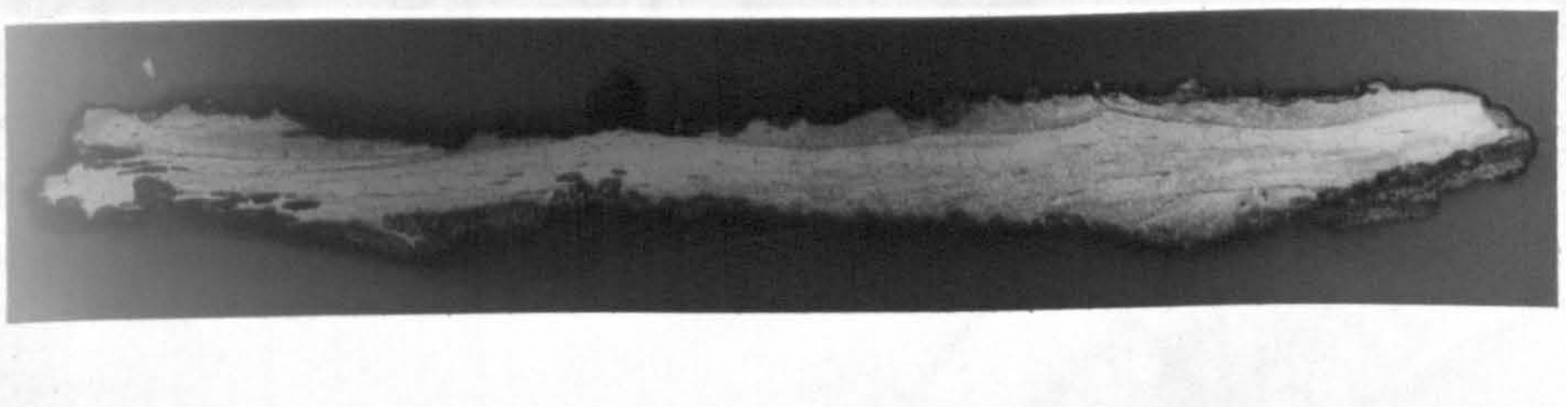

(c)

Fig 32 Sword blade S20, from Lenham: (a) x-radiograph; (b) sketch of section; (c) photomacrograph; (d) surface detail (both sides) and three-dimensional view

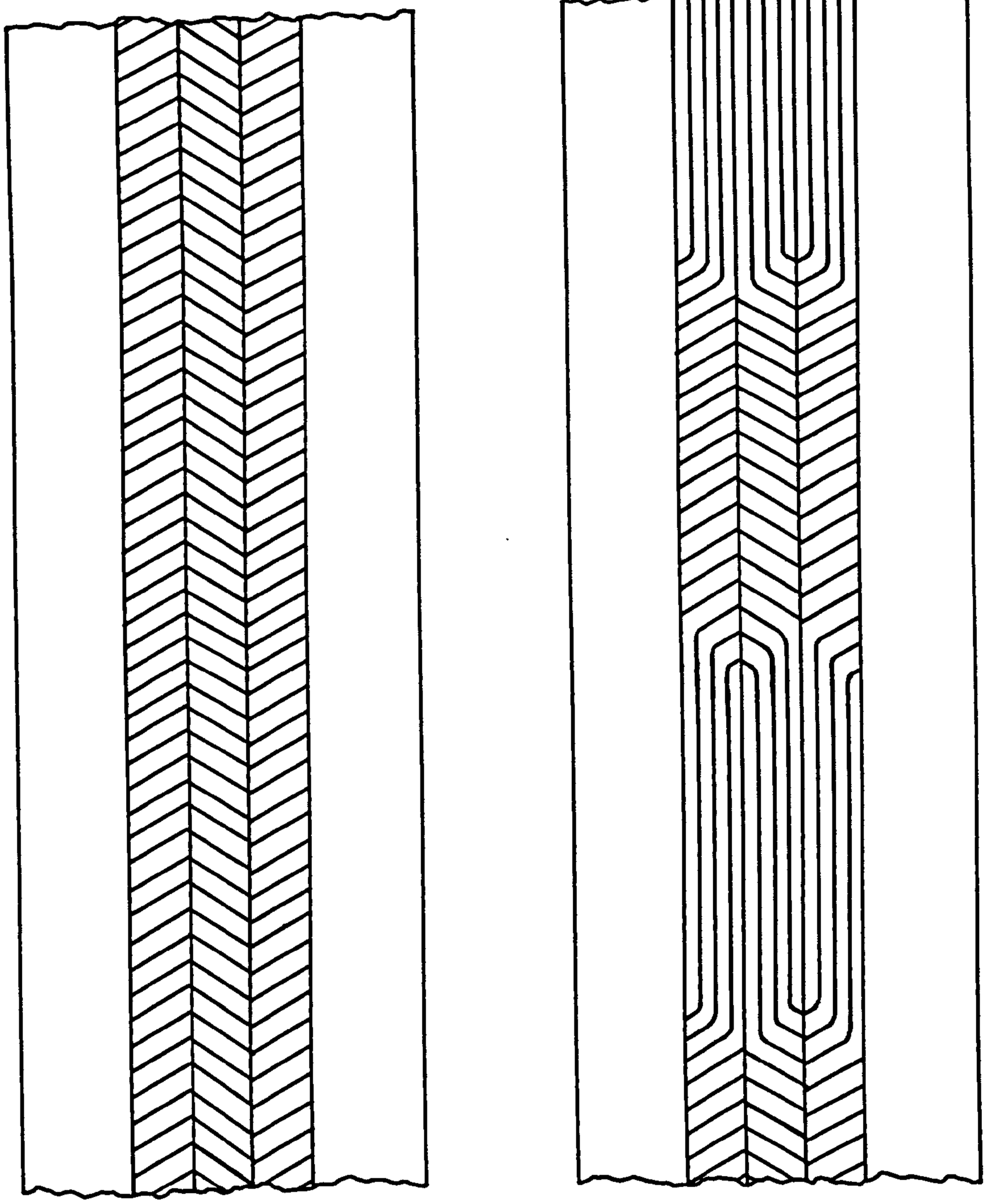

(d)

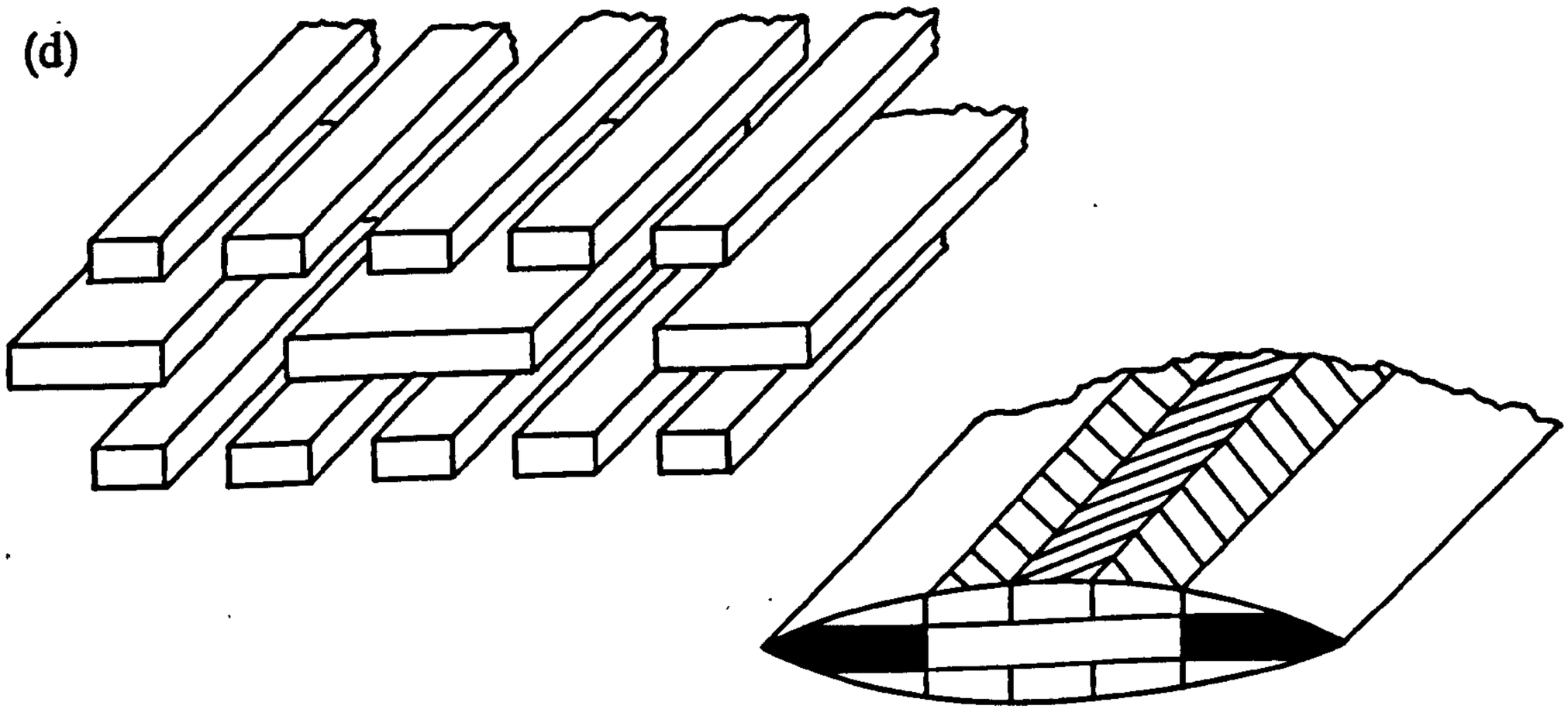

Fig 32 (continued)

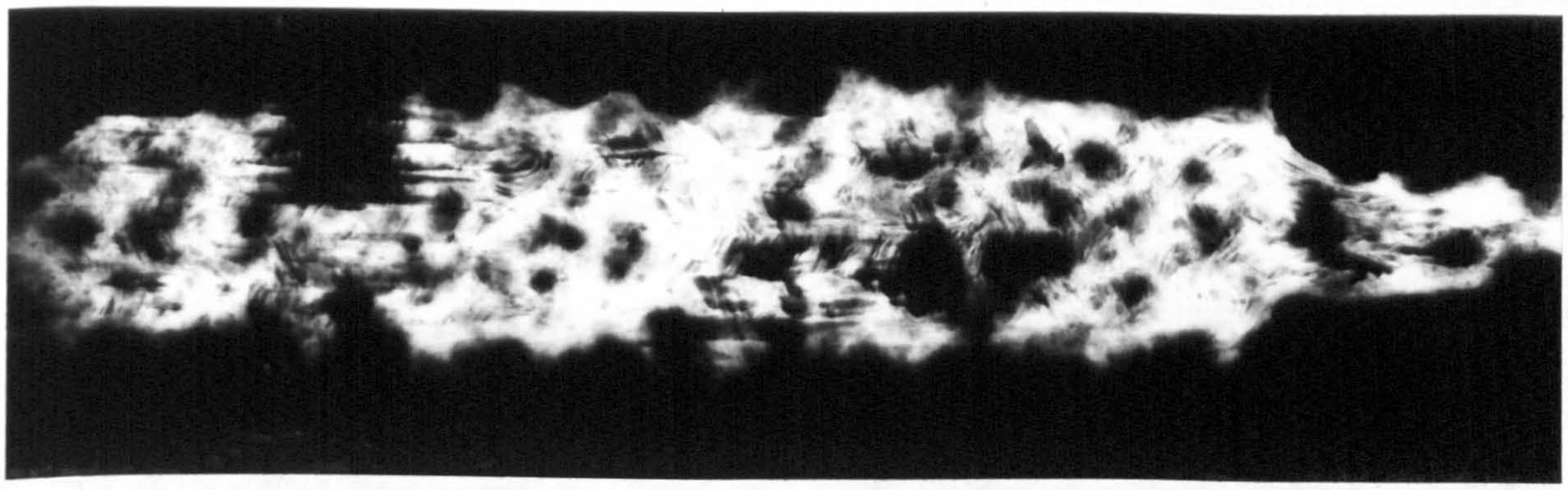

(a)

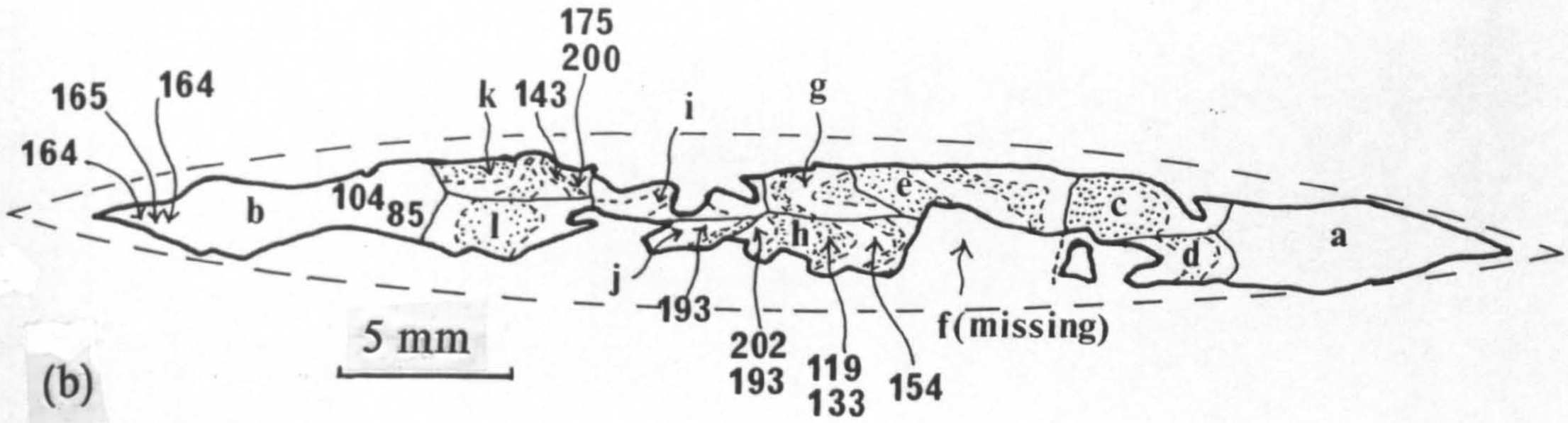

(b)

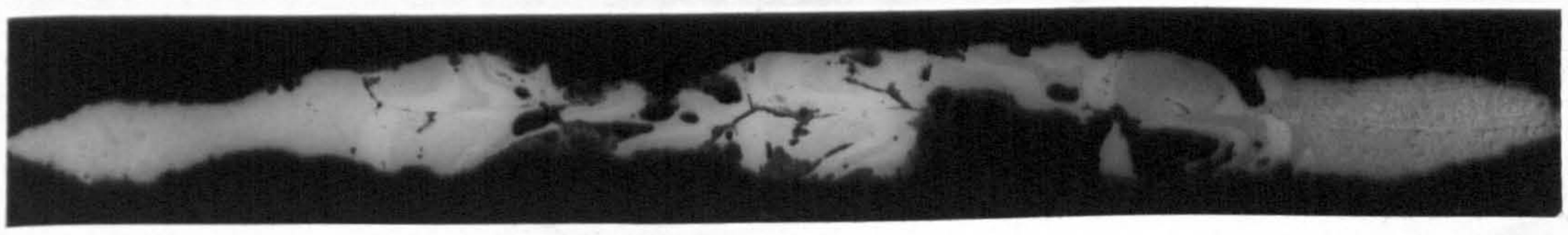

(c)

Fig 33 Sword blade S1, from Lovedon Hill: (a) x-radiograph; (b) sketch of section; (c) photomicrograph; (d) photomicrograph showing central pattern-welded part of blade; (e) surface appearance and three-dimensional view

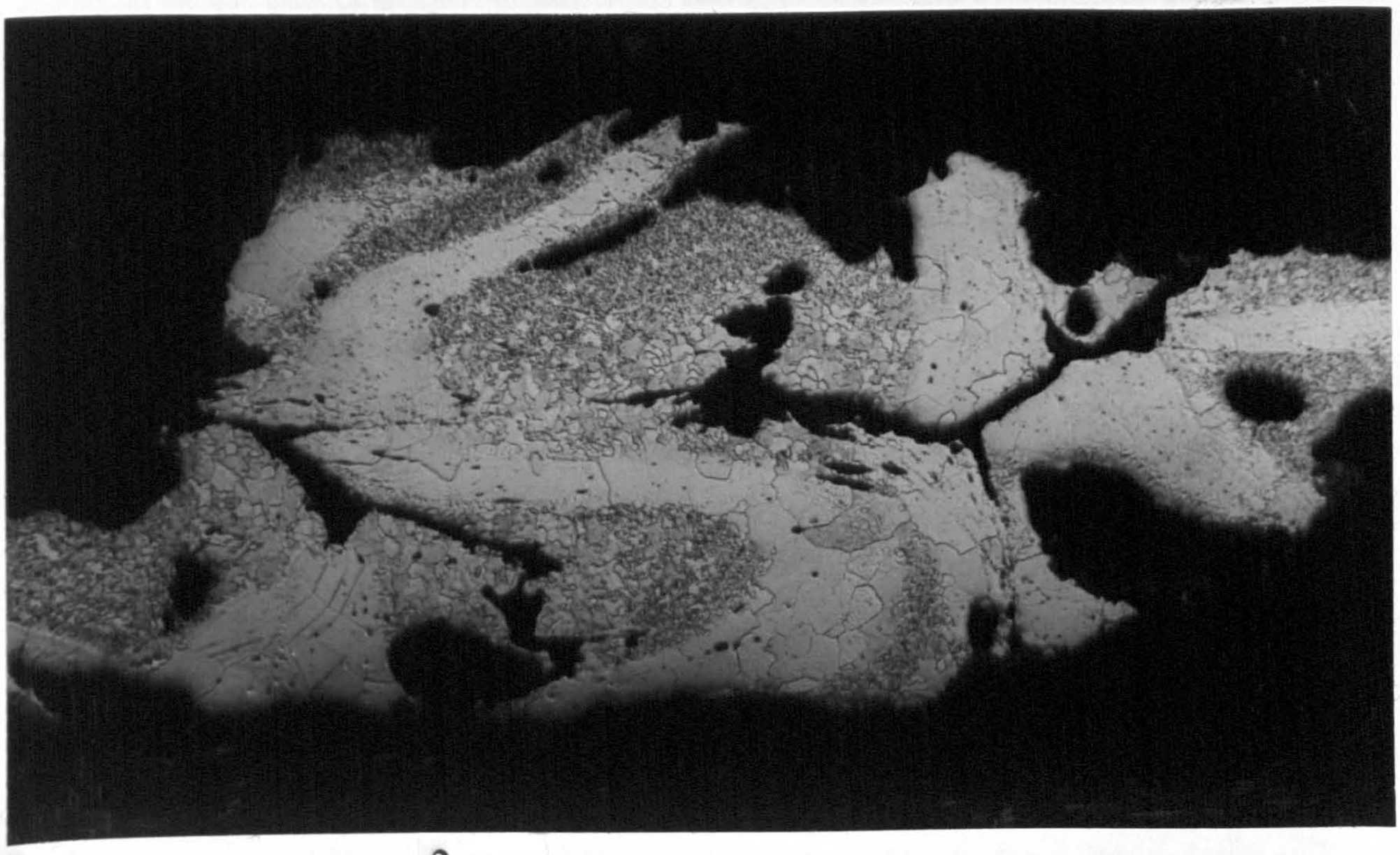

2 mm

(d)

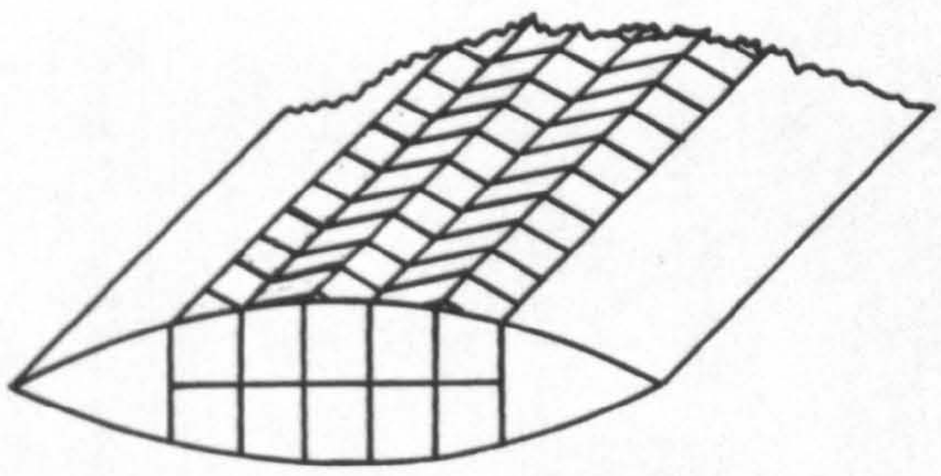

(e)

Fig 33 (continued)

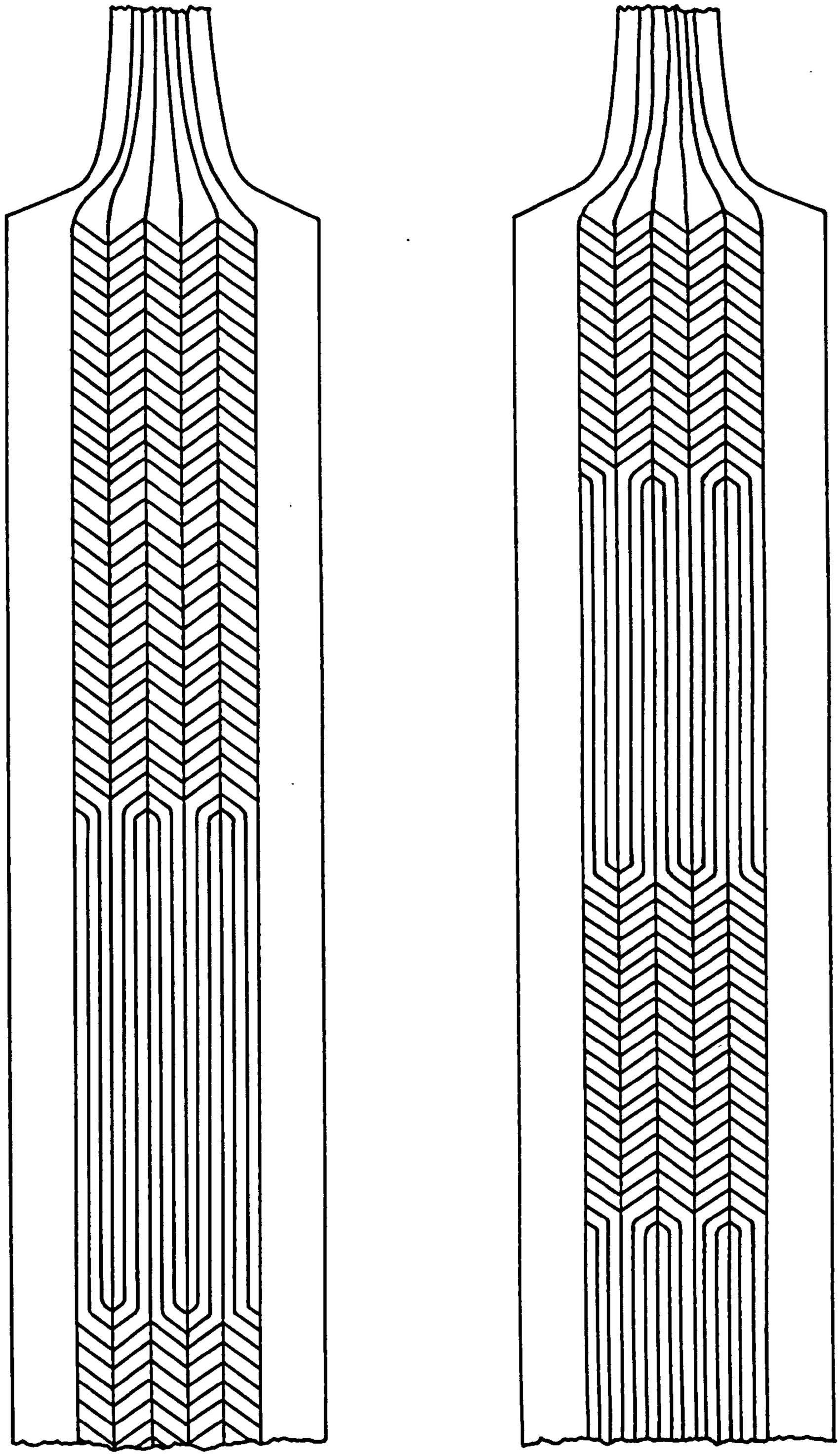

(e)

Fig 33 (continued)

(a)

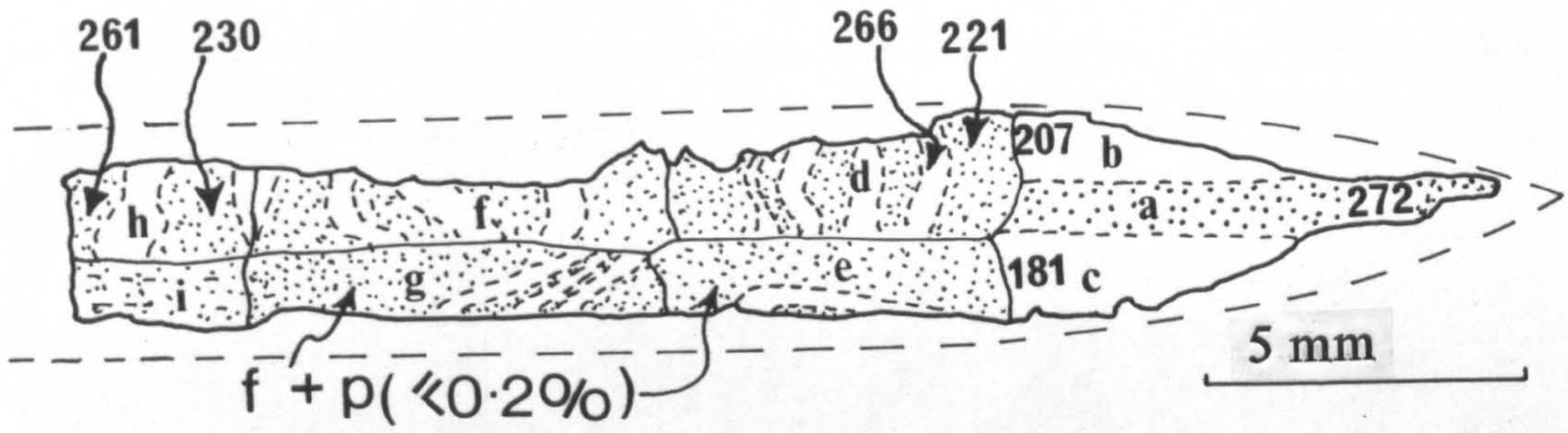

(b)

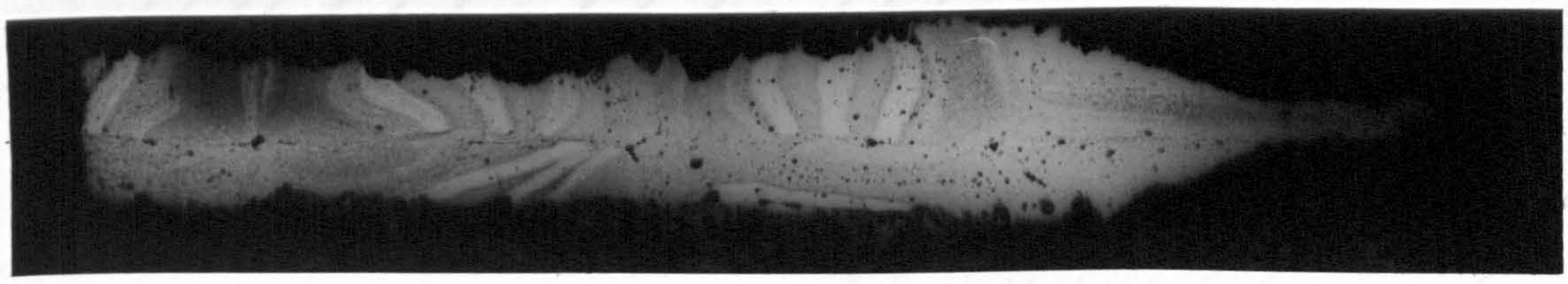

(c)

Fig 34 Sword blade S40, from Chesterton: (a) x-radiograph; (b) sketch of section; (c) photomacrograph; (d) surface detail and three-dimensional view

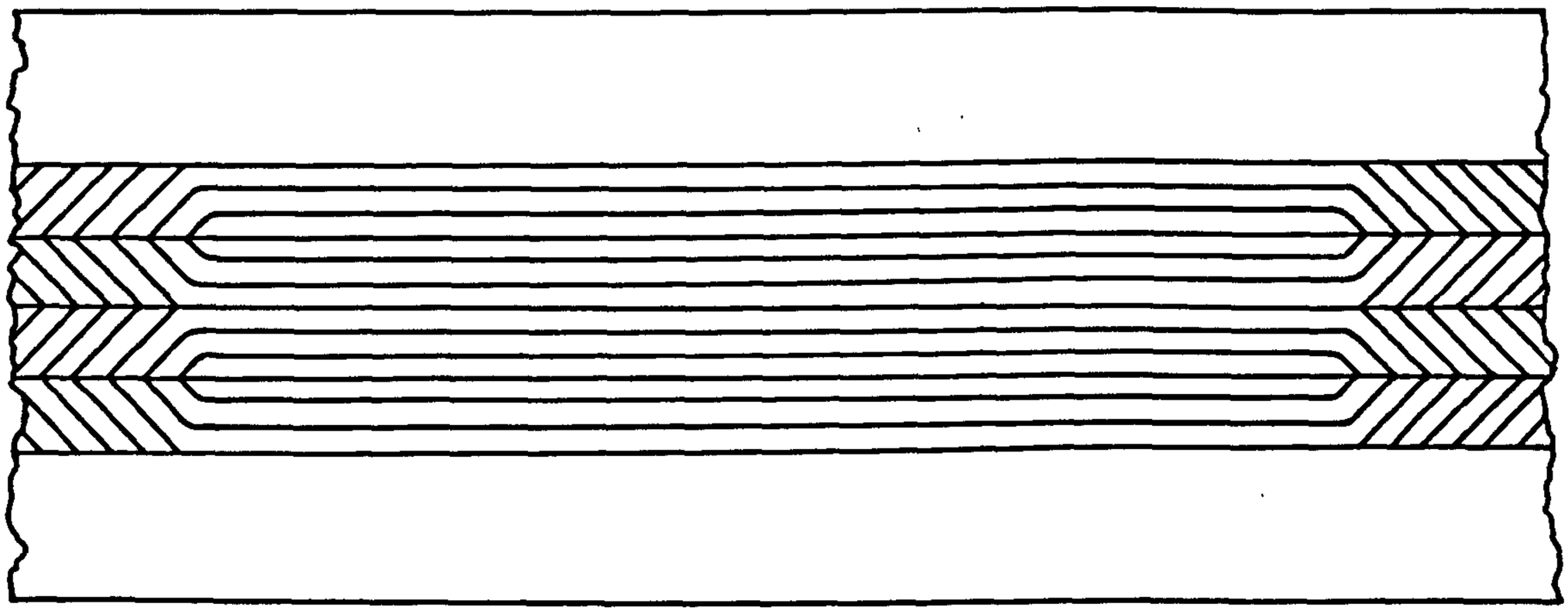

(d)

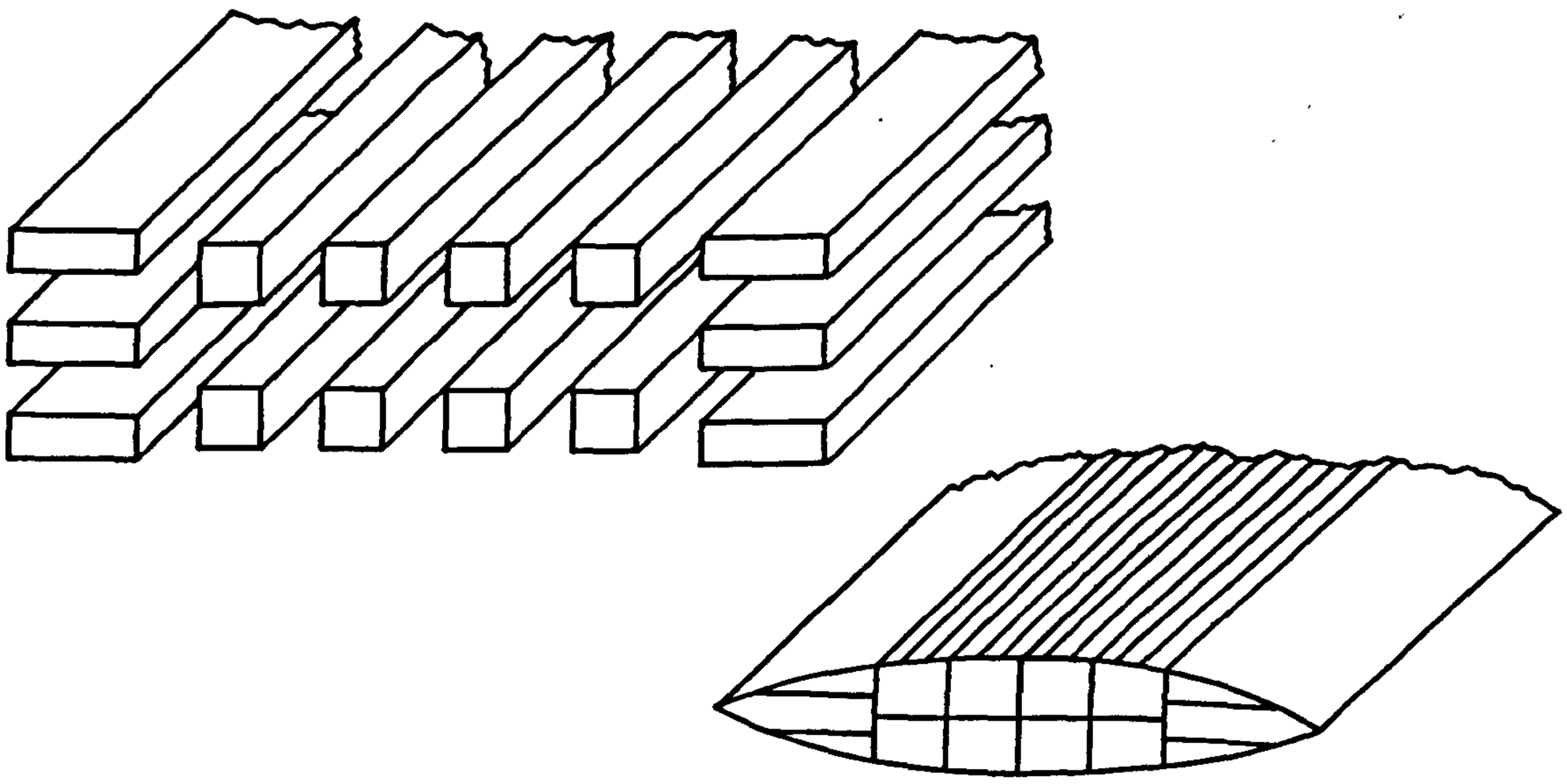

Fig 34 (continued)

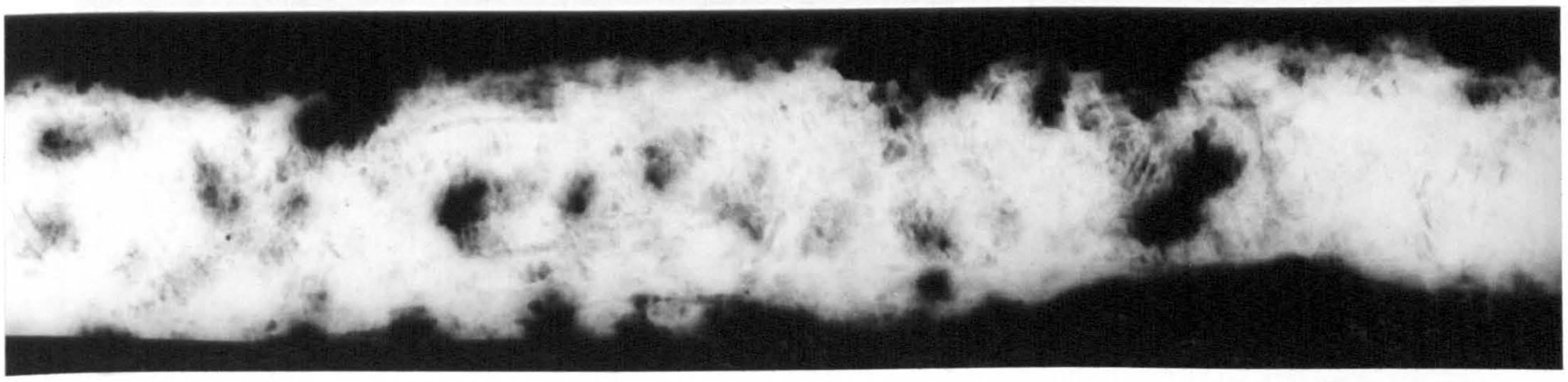

(a)

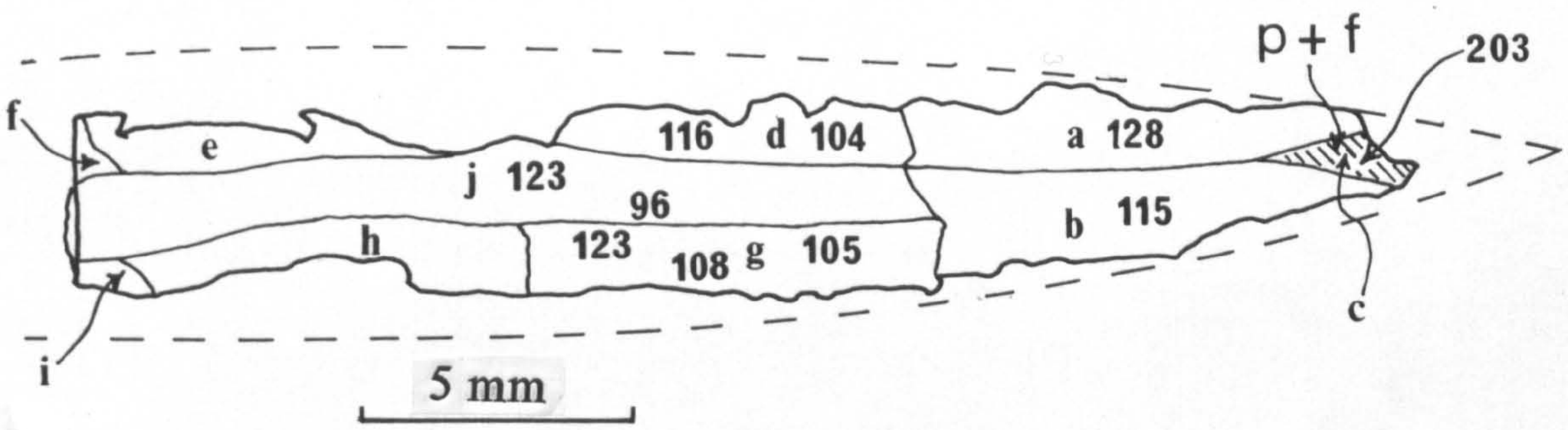

(b)

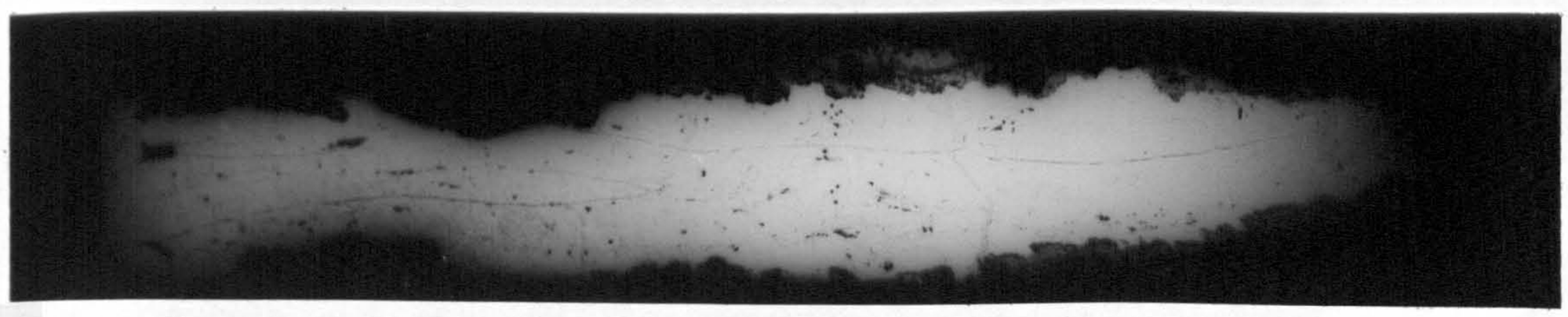

(c)

Fig 35 Sword blade S10, from Mitcham: (a) x-radiograph; (b) sketch of section; (c) photomacrograph; (d) photomicrograph showing weld junctions between the cutting edge and the central pattern-welded parts; (e) photomicrograph showing the mainly pearlitic tip of the cutting edge part c and carbon diffusion into parts a and b; (f) three-dimensional view

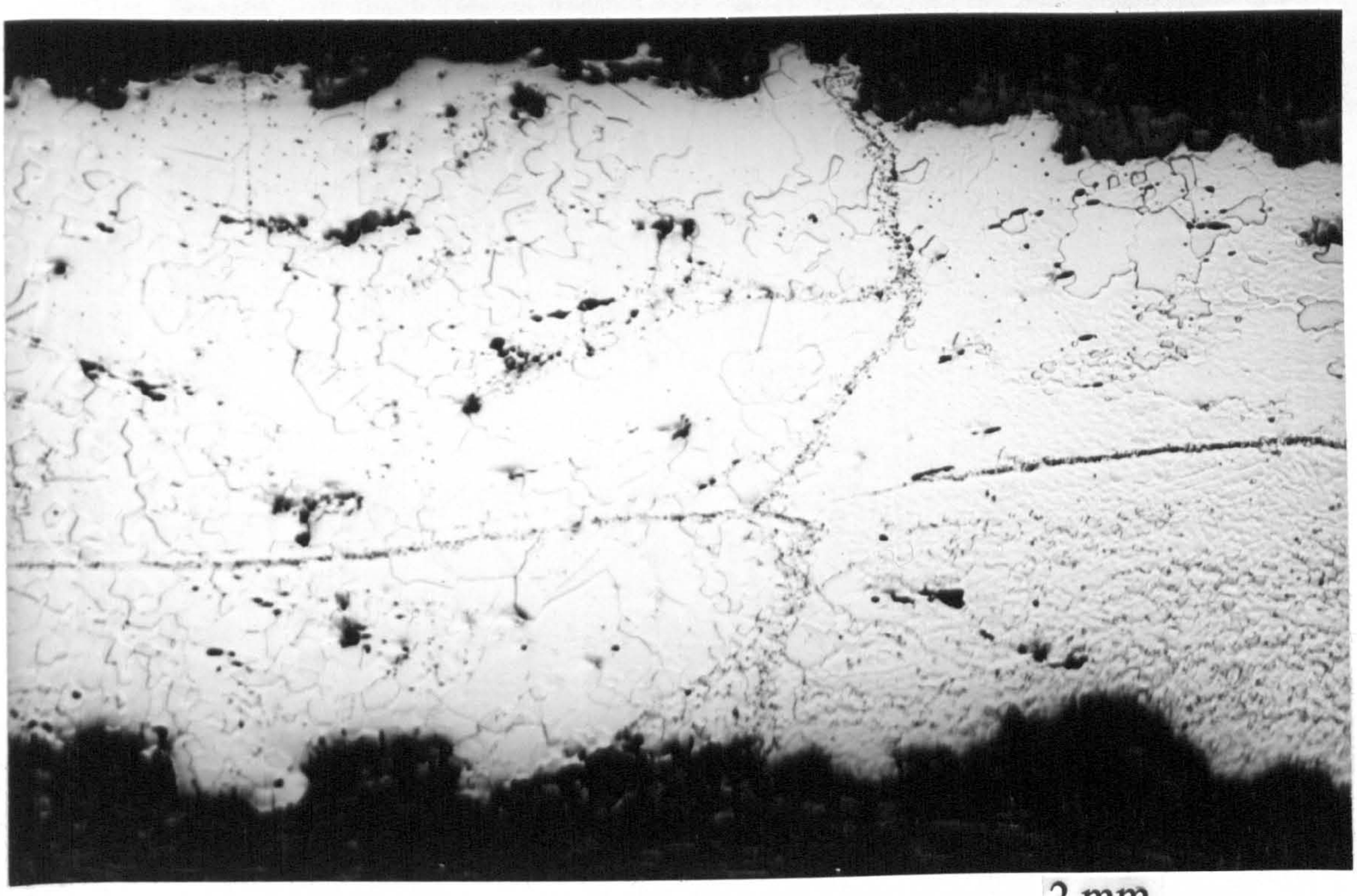

(d)

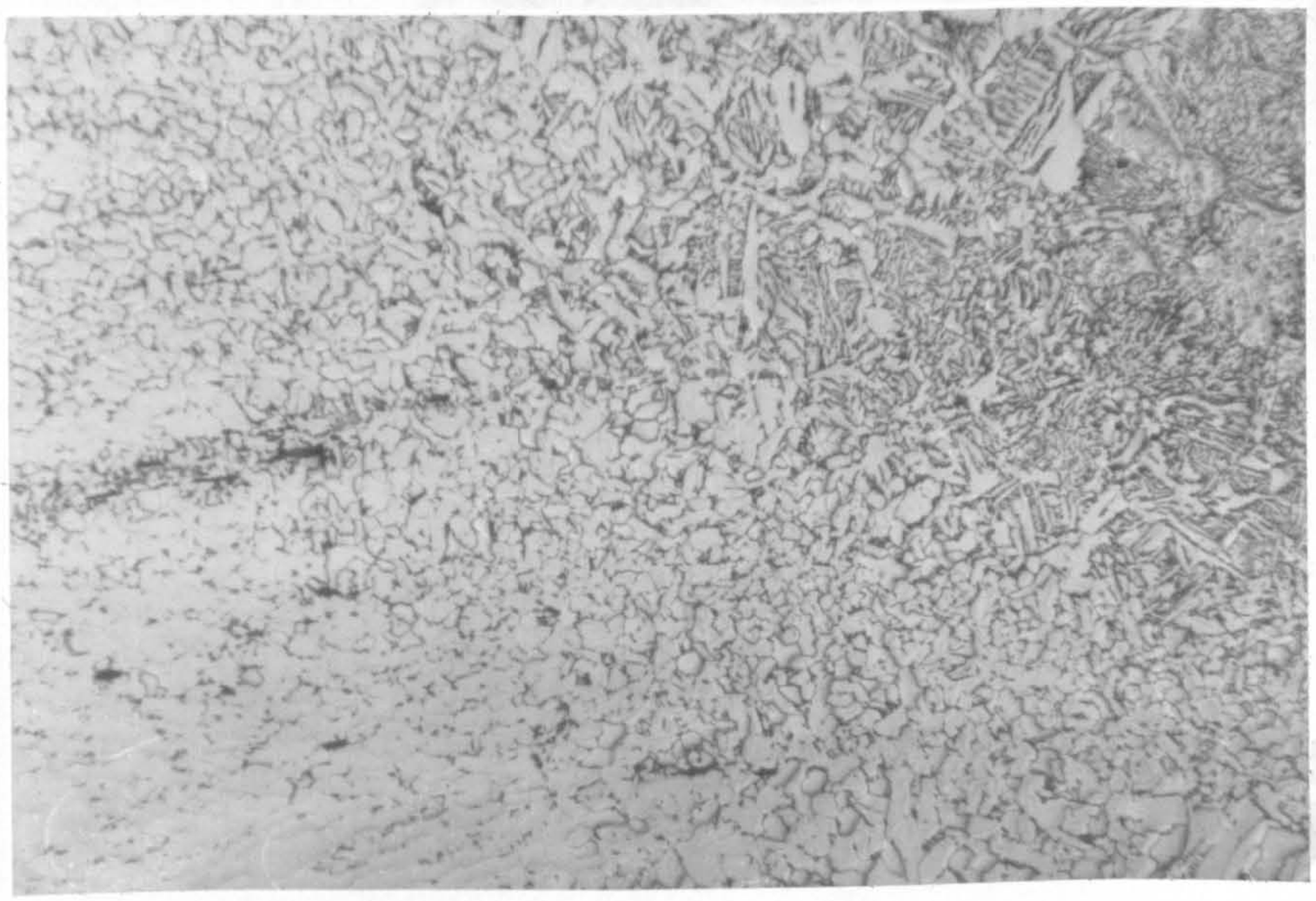

(e)

Fig 35 (continued)

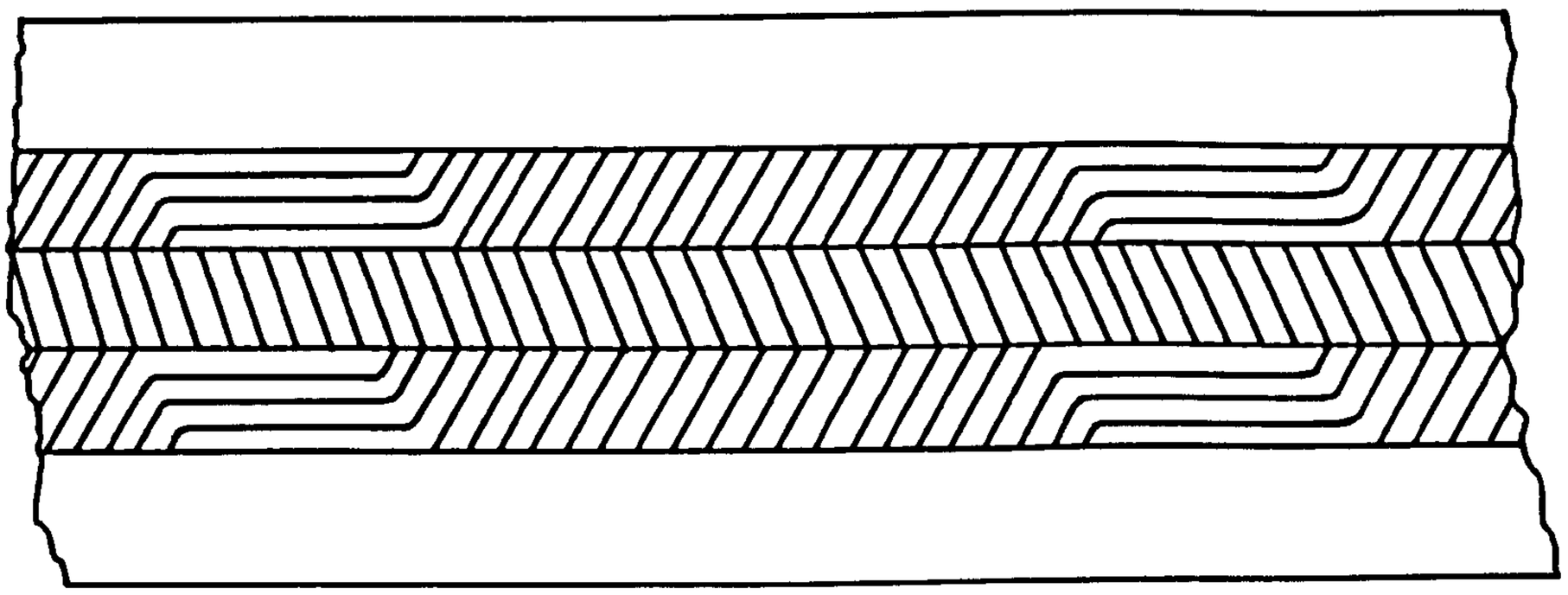

(f)

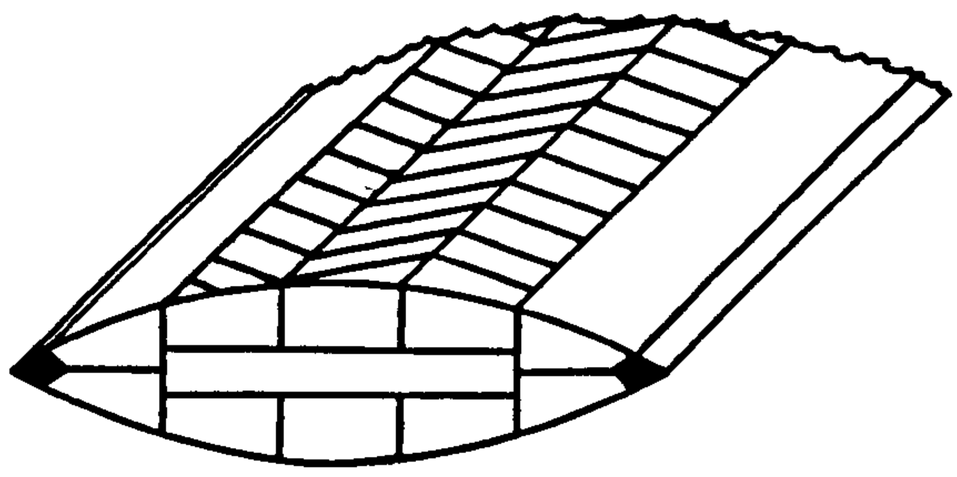

Fig 35 (continued)

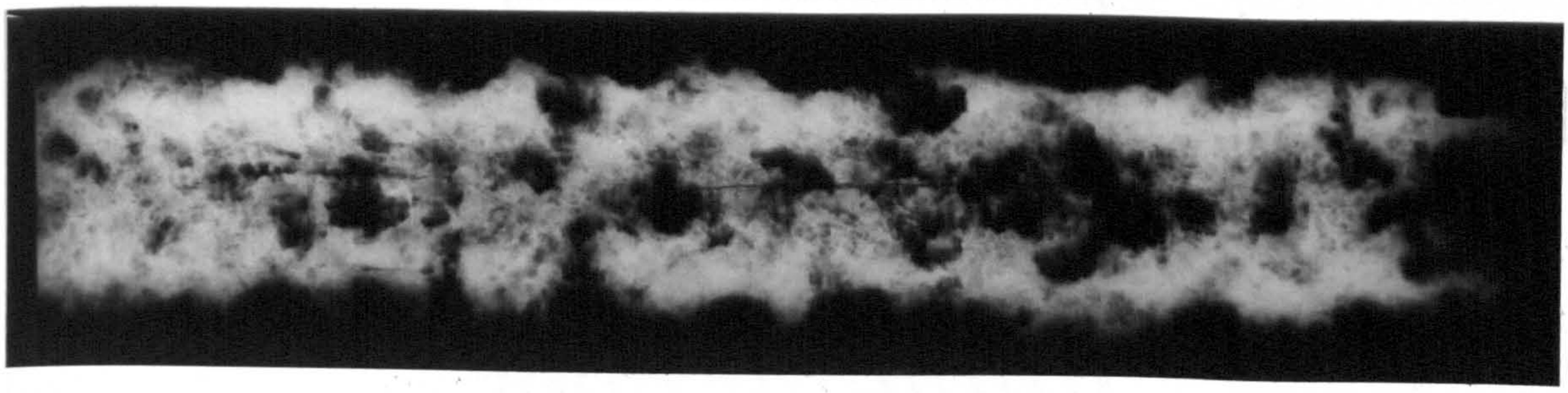

(a)

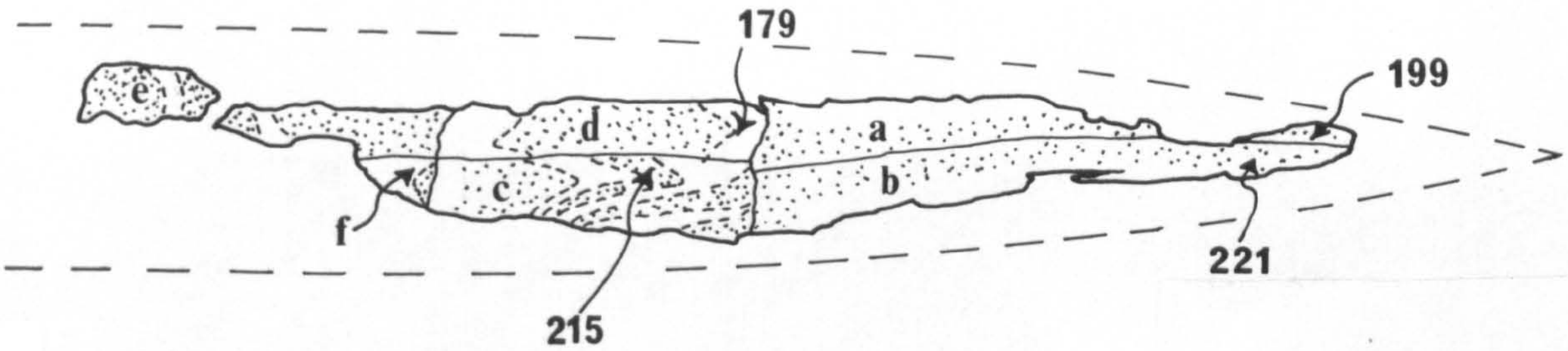

(b)

5 mm

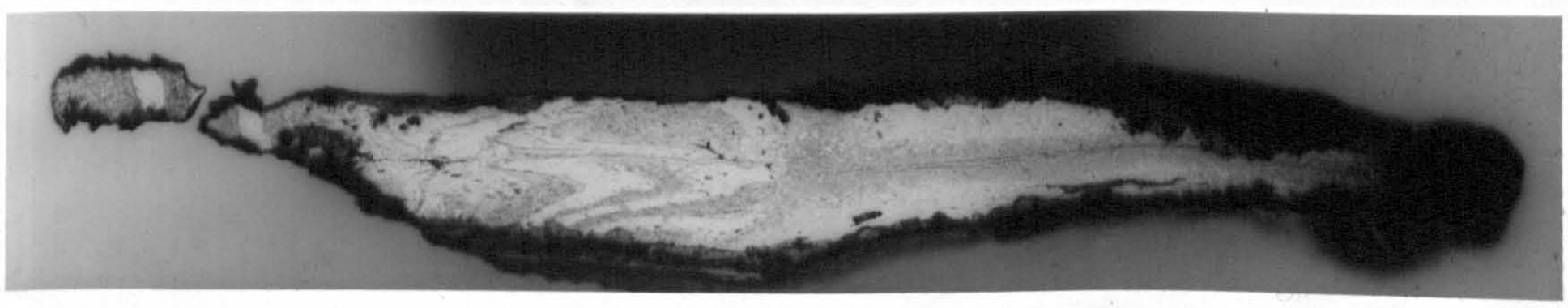

(c)

Fig 36 Sword blade S45, from Mitcham: (a) x-radiograph; (b) sketch of section; (c) photomacrograph; (d) surface detail and three-dimensional reconstruction

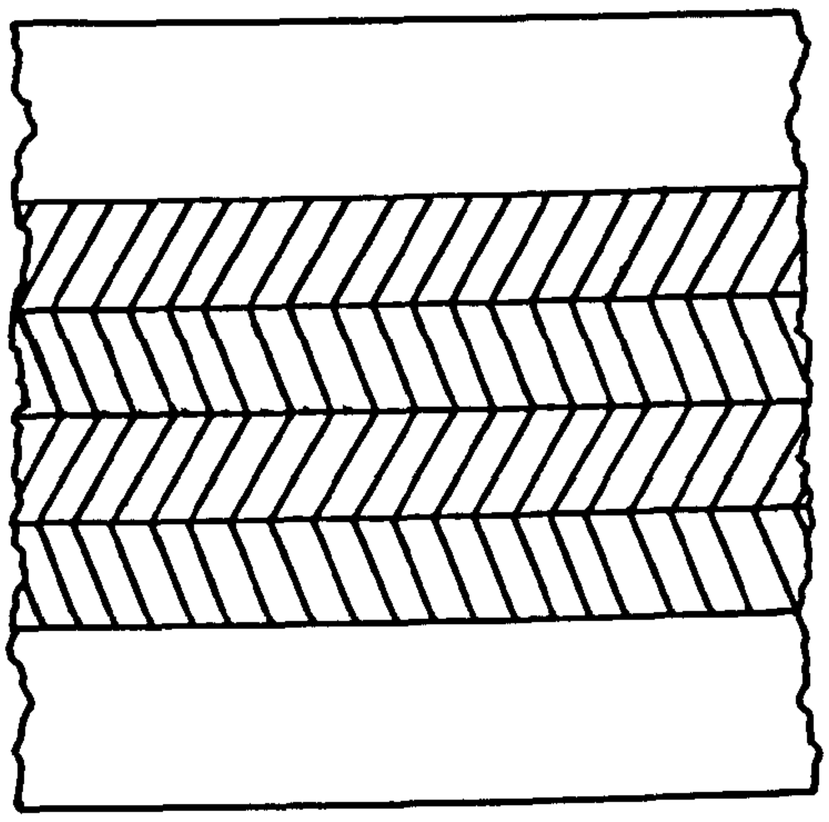

(d)

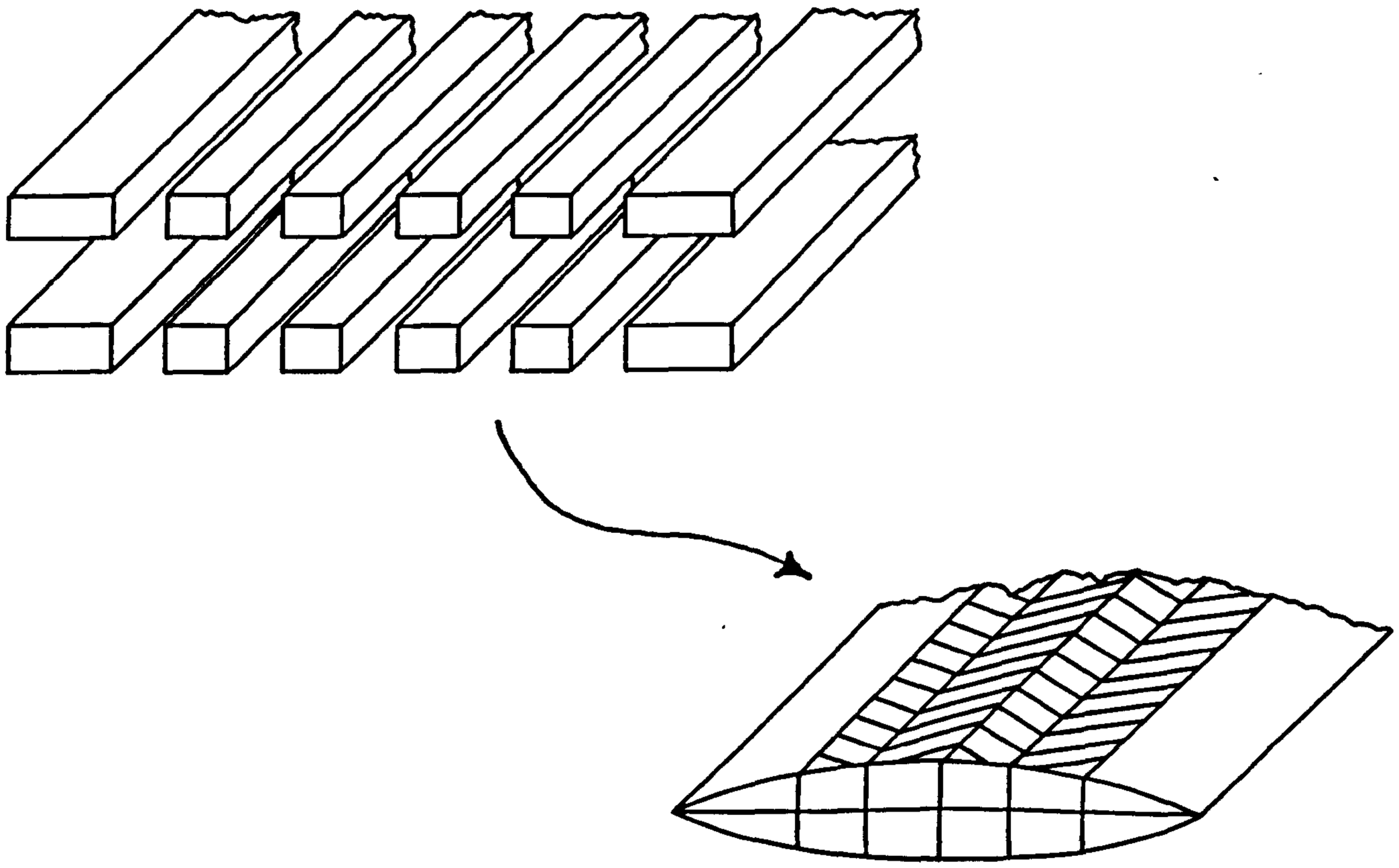

Fig 36 (continued)

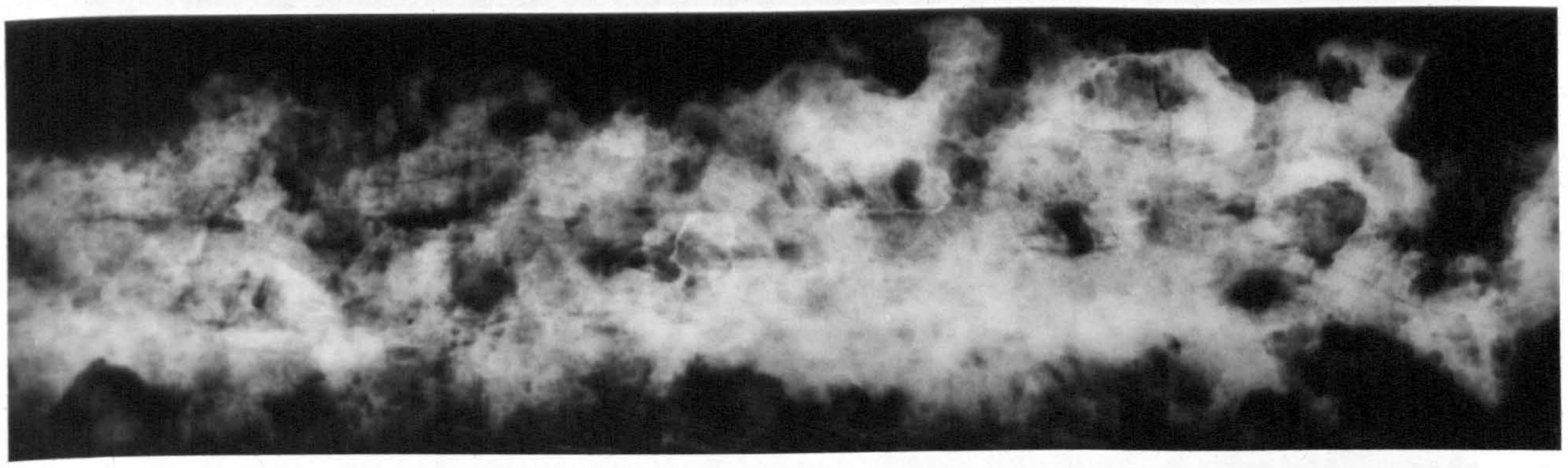

(a)

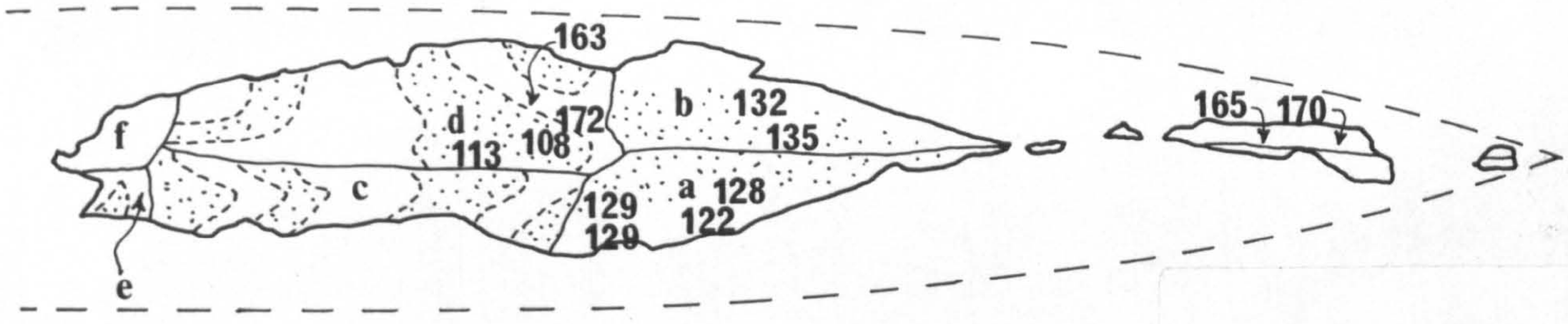

(b)

5 mm

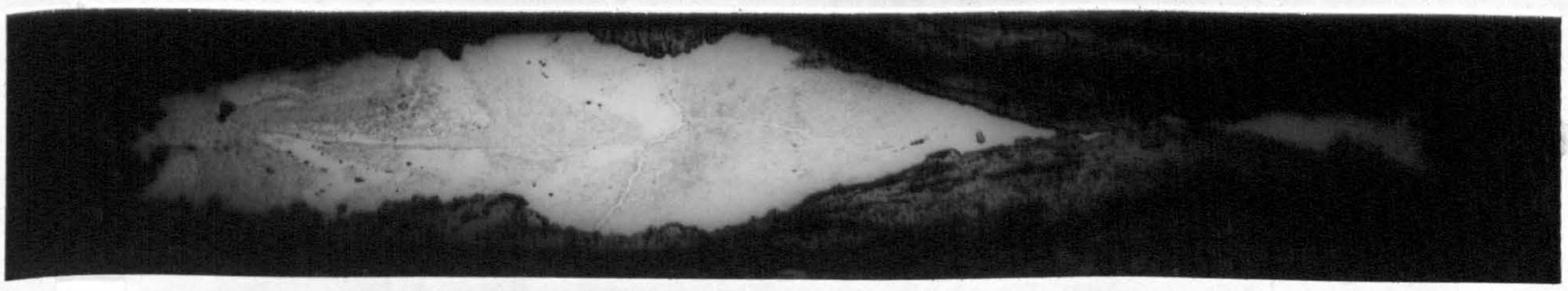

(c)

Fig 37 Sword blade S16, from Sarre: (a) x-radiograph; (b) sketch of section; (c) photomacrograph; (d) photomicrograph showing parts of the cutting edge pieces a and b, and pattern-welded pieces c and d; (e) photomicrograph showing carbide or nitride needles in a large grain ferritic part of the pattern-welded piece d; (f) three-dimensional view

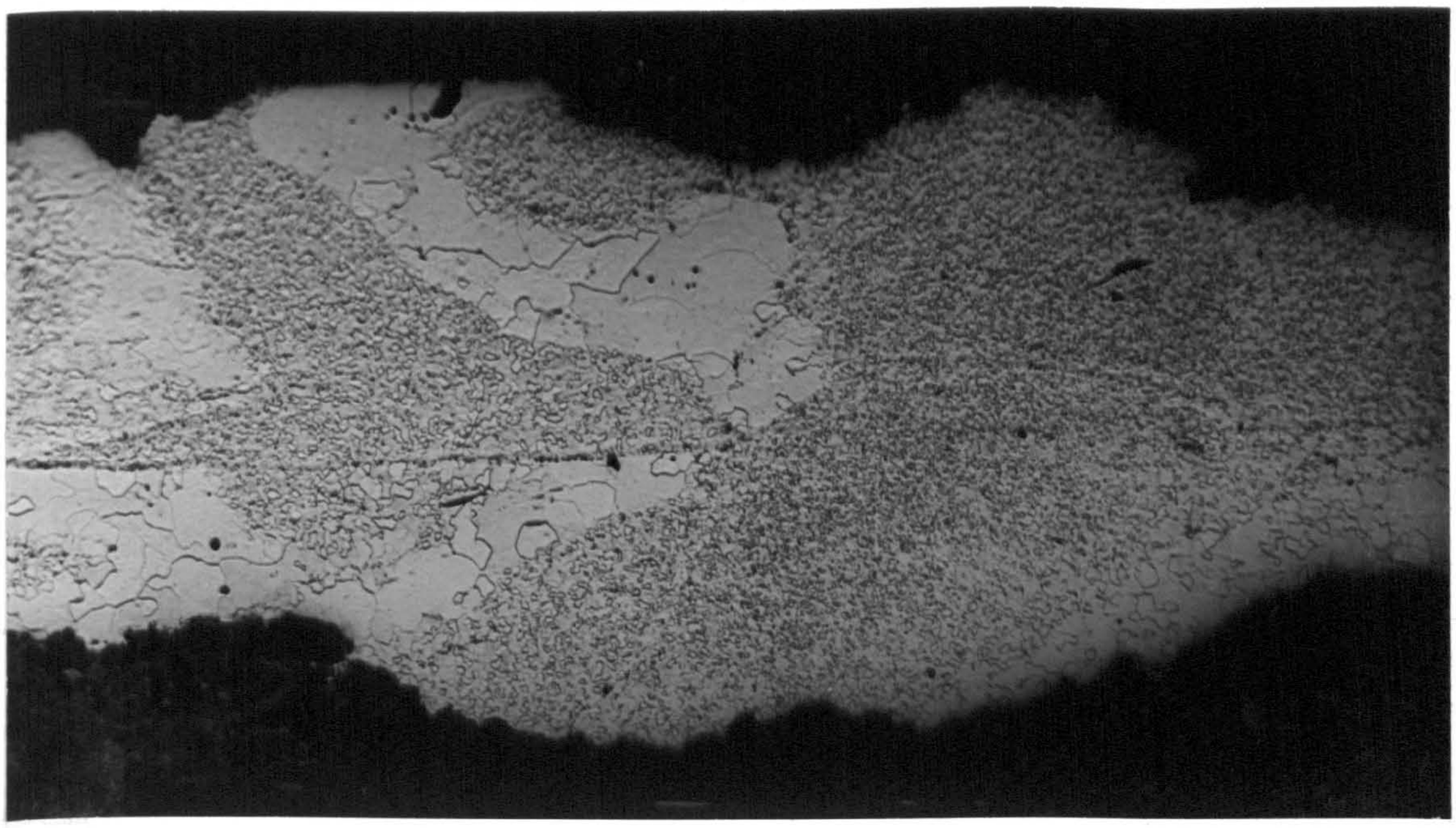

(d)

2 mm

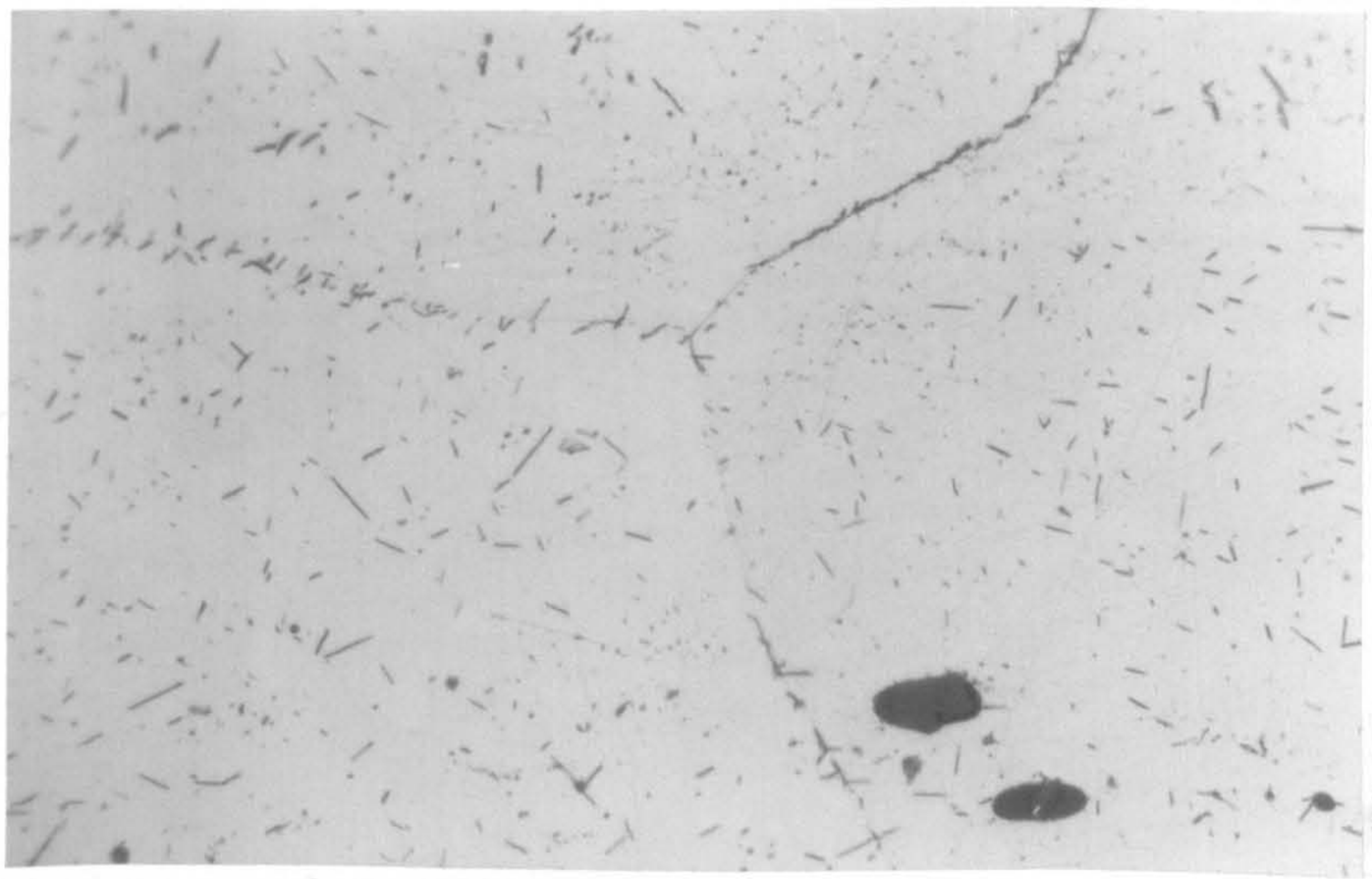

(e)

x400

Fig 37 (continued)

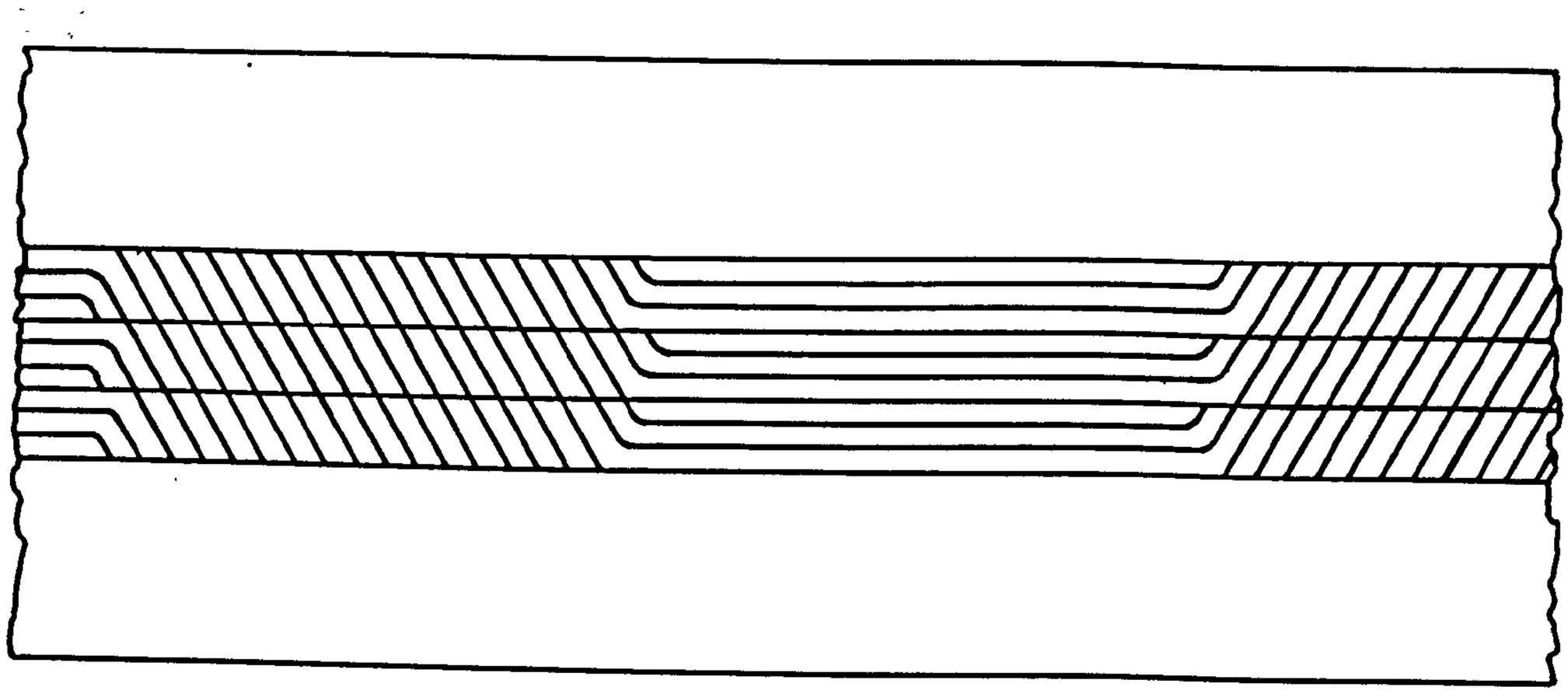

(f)

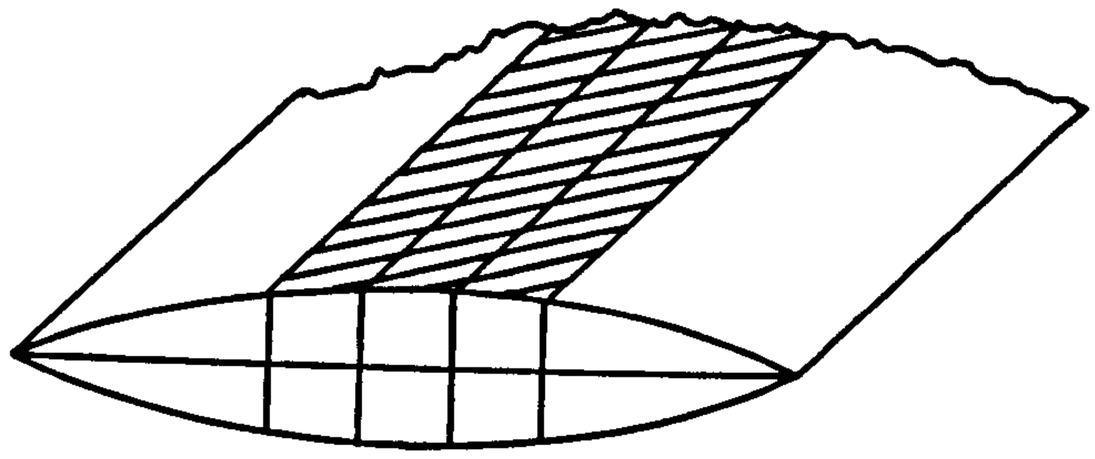

Fig 37 (continued)

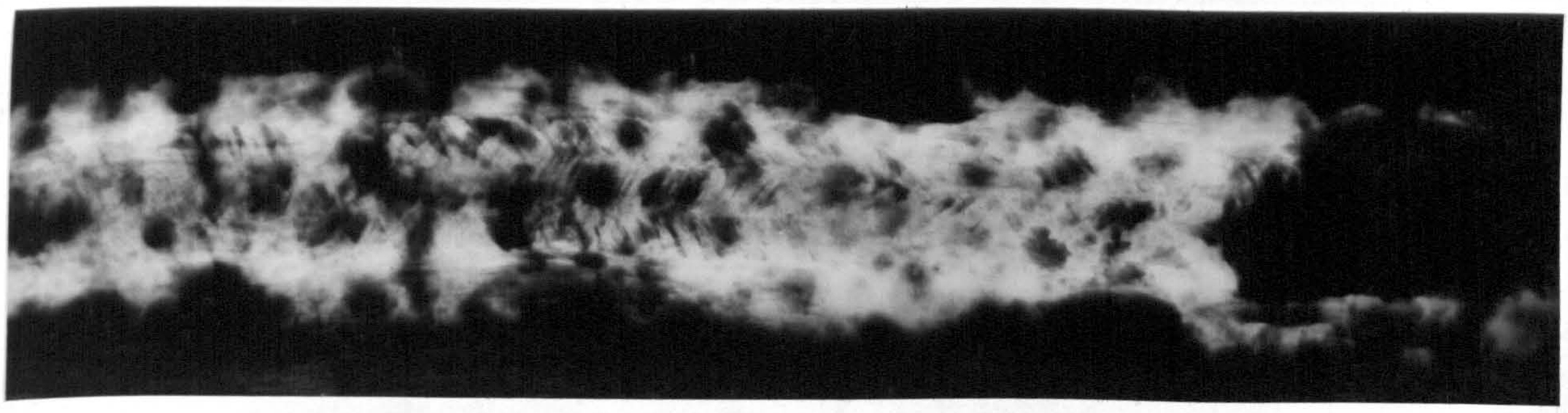

(a)

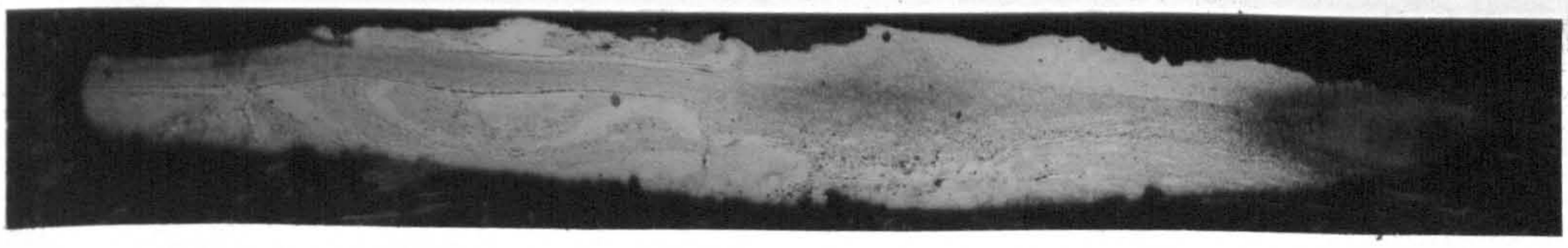

(b)

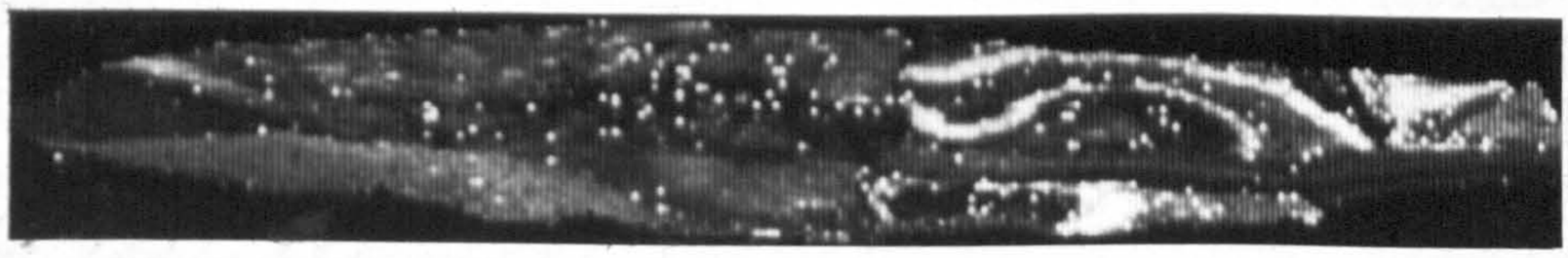

(c)

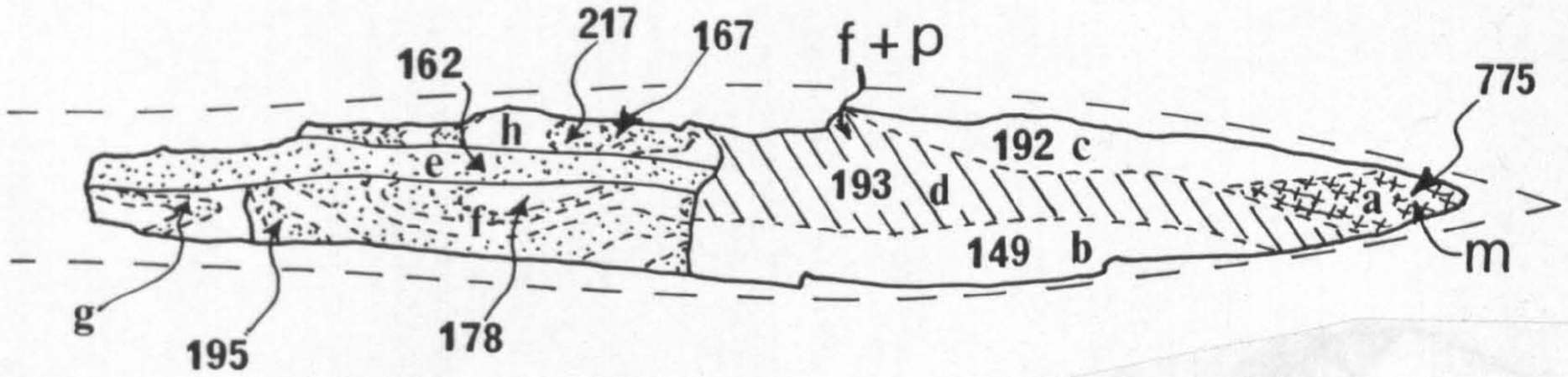

(d)

5 mm

Fig 38 Sword blade S31, from Caversham: (a) x-radiograph; (b) photomacrograph; (c) EPMA phosphorus map; (d) sketch of section; (e) photomicrograph showing pearlite and slag inclusions along welds between the core piece e and the pattern-welded pieces f and g, also the neumann bands in the large grain ferritic parts of the pattern-welded piece f; (f) surface appearance and three-dimensional view

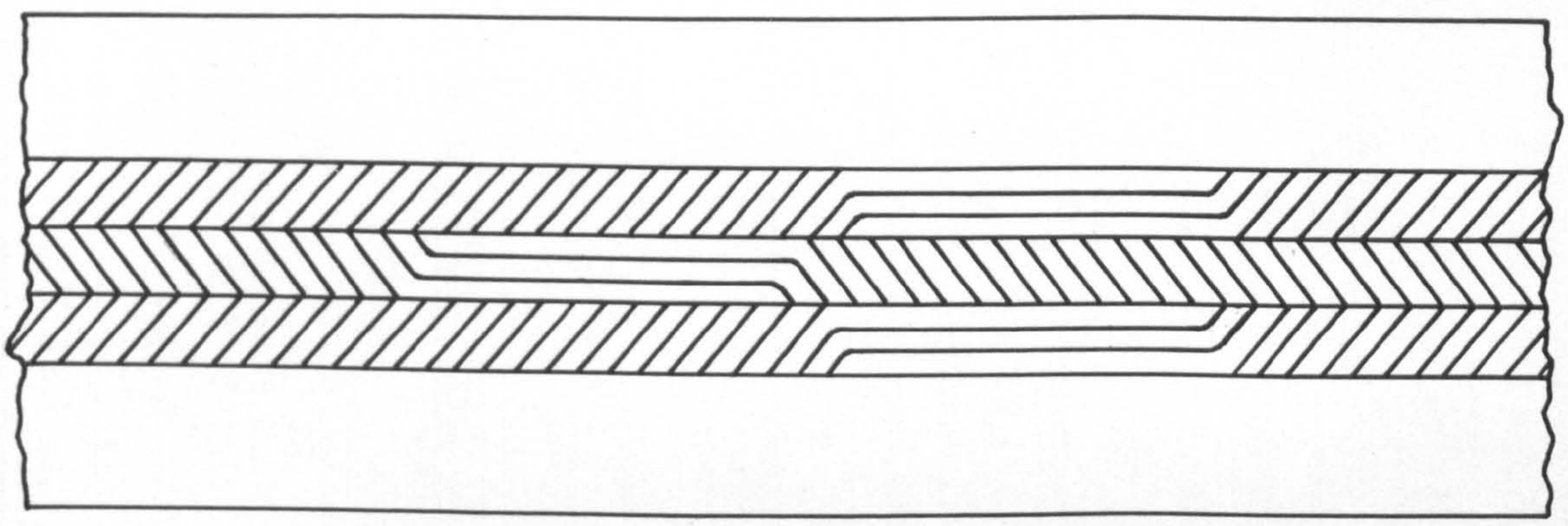

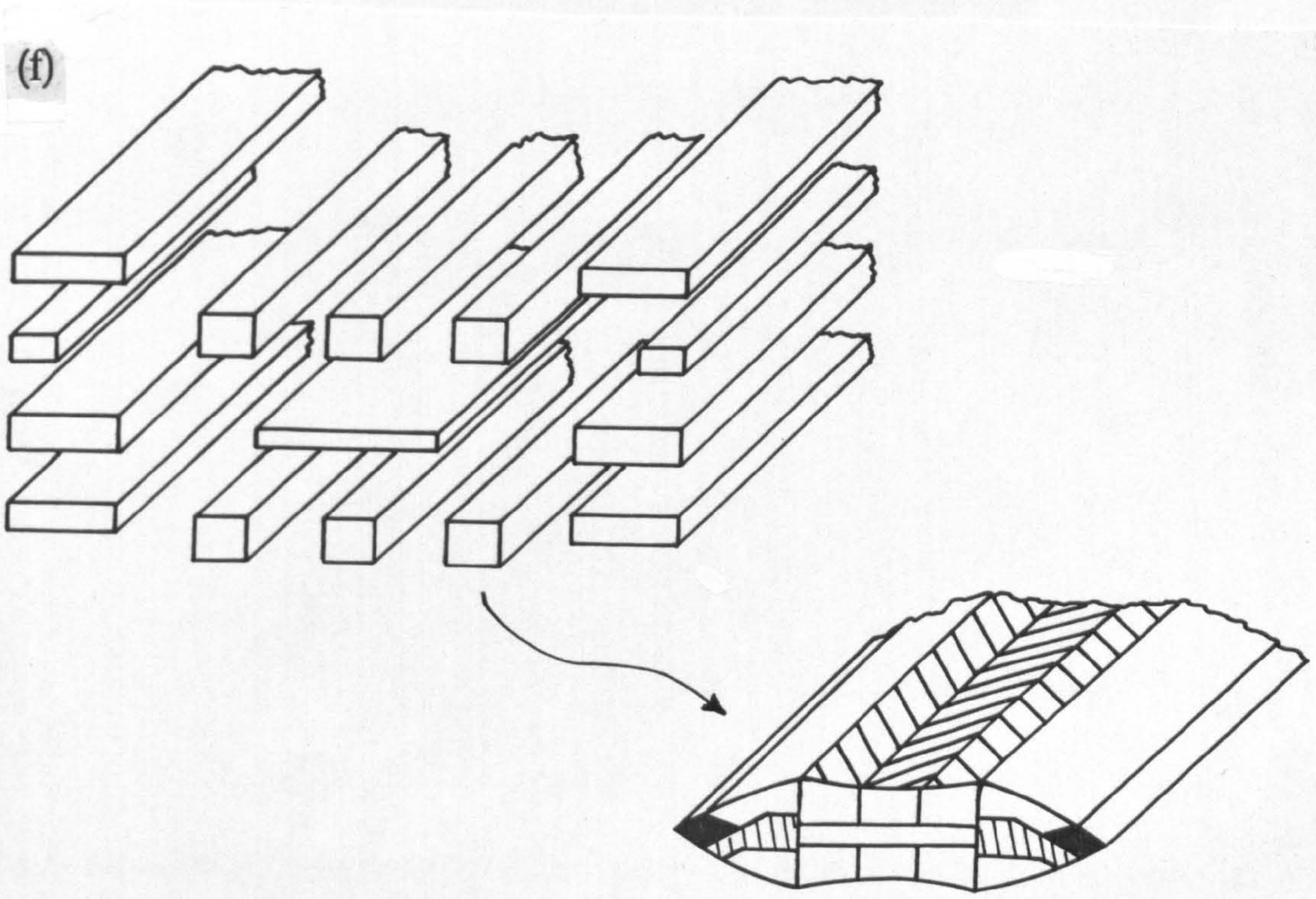

Fig 38 (continued)

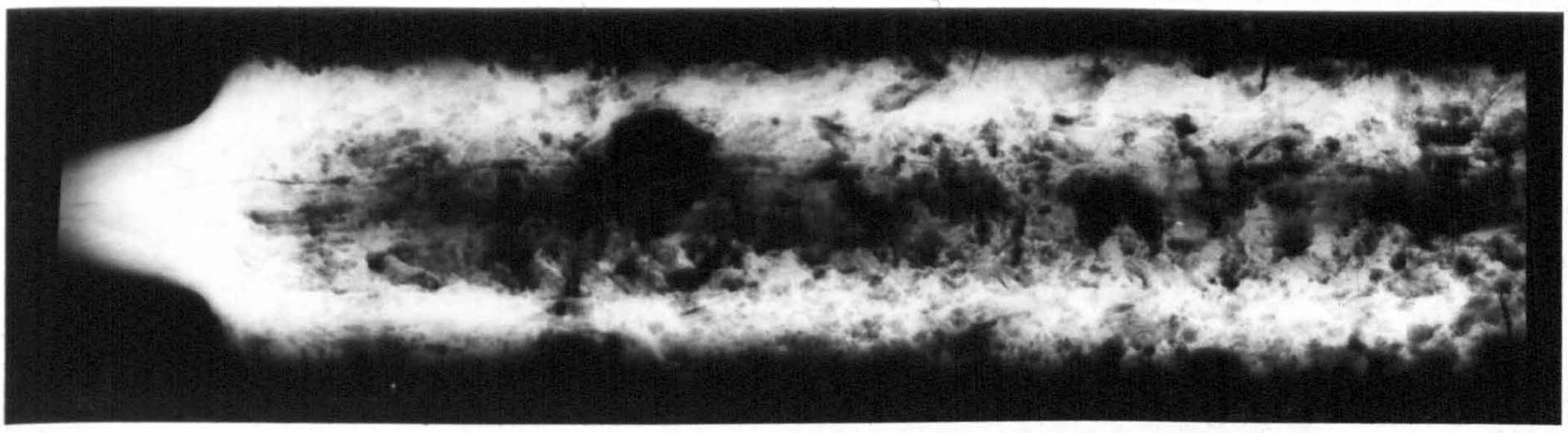

(a)

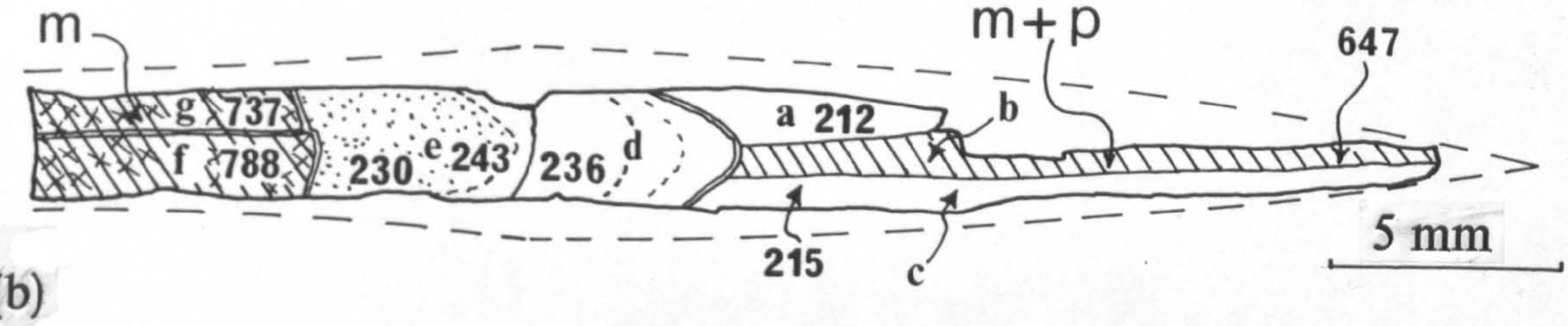

(b)

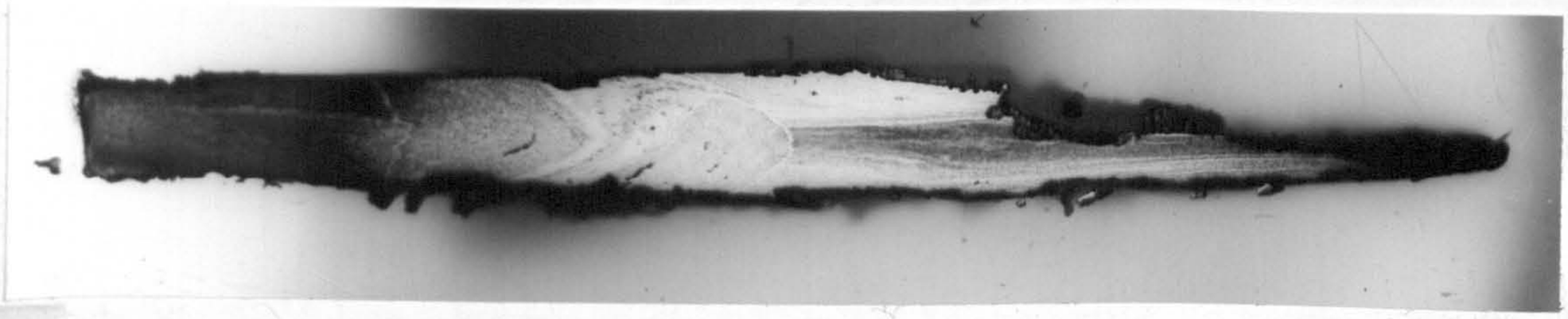

(c)

Fig 39 Sword blade S46, from Brentford: (a) x-radiograph; (b) sketch of section; (c) photomacrograph; (d) surface detail and three-dimensional view

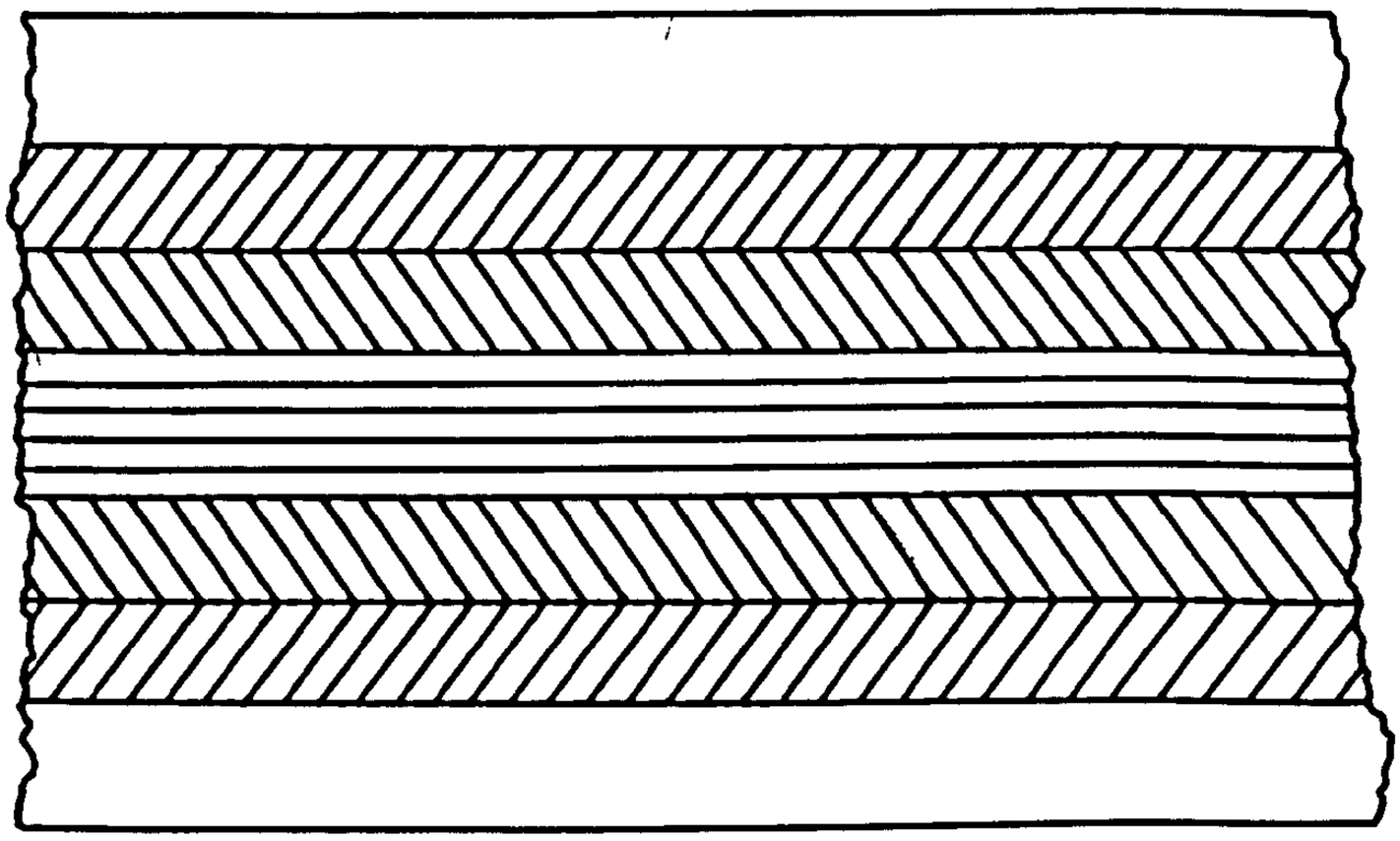

(d)

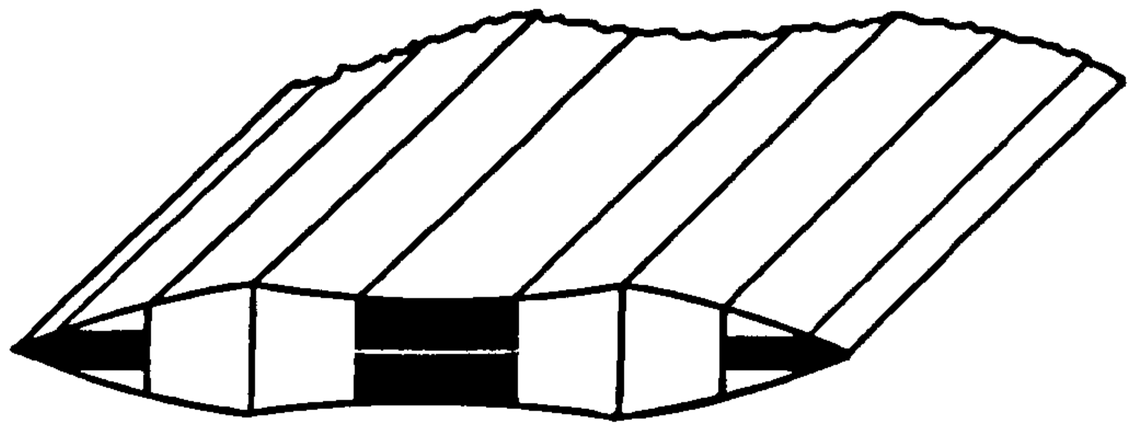

Fig 39 (continued)

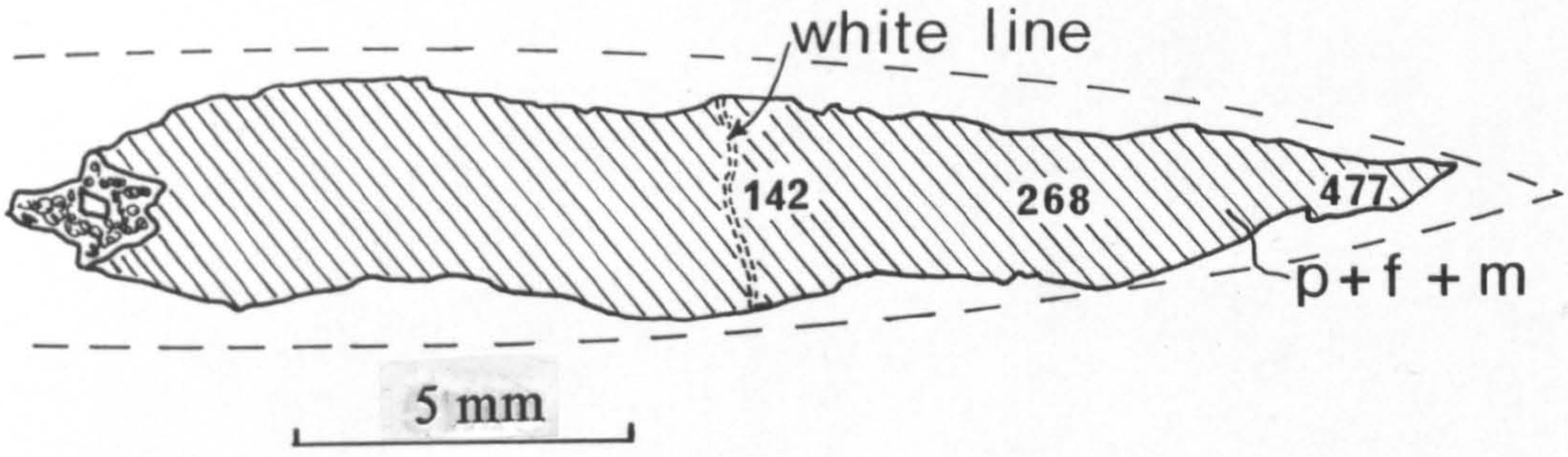

(a)

(b)

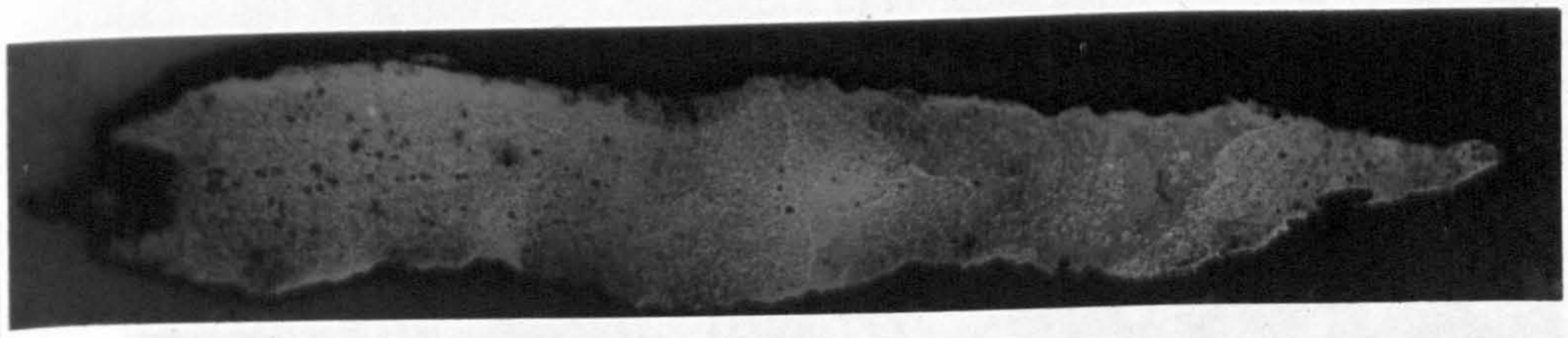

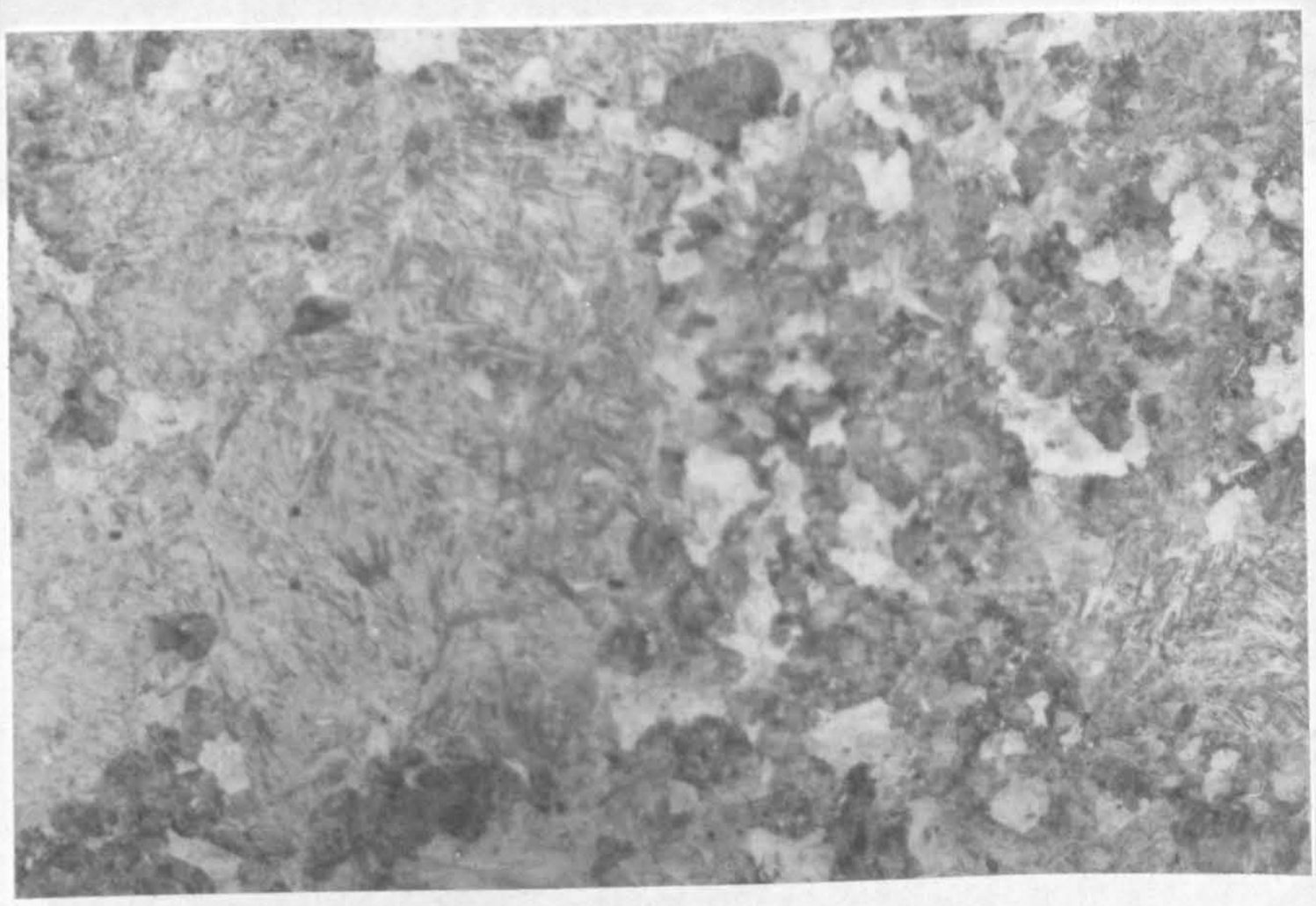

(c)

x450

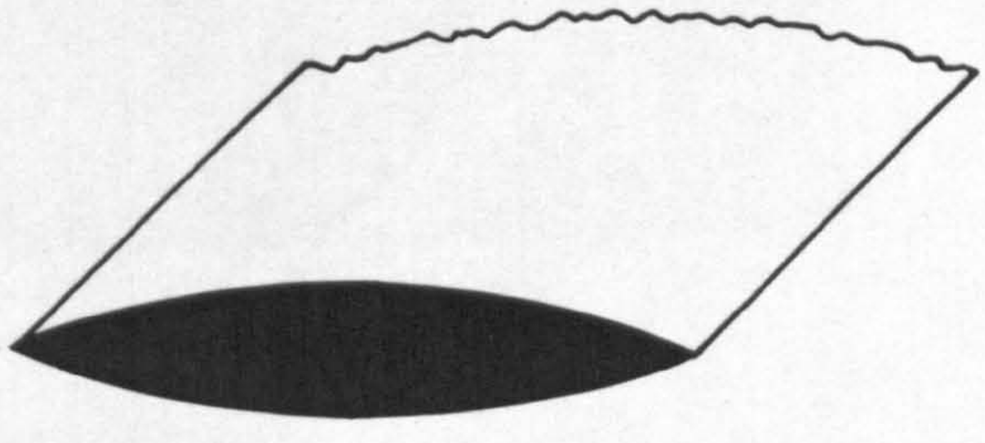

(d)

Fig 40 Sword blade S7, ? The Thames near London: (a) sketch of section; (b) photomacrograph; (c) photomicrograph showing martensite and radial pearlite near centre; (d) three-dimensional view

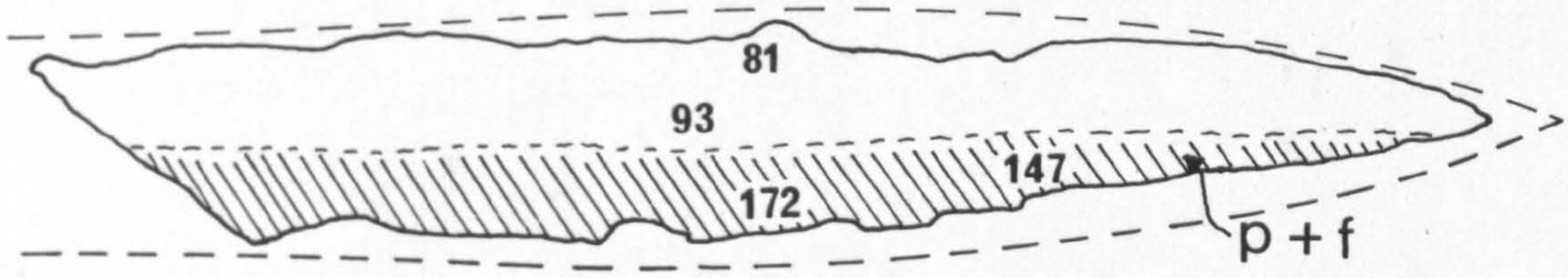

(a)

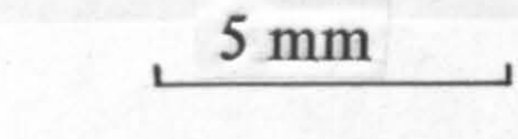

(b)

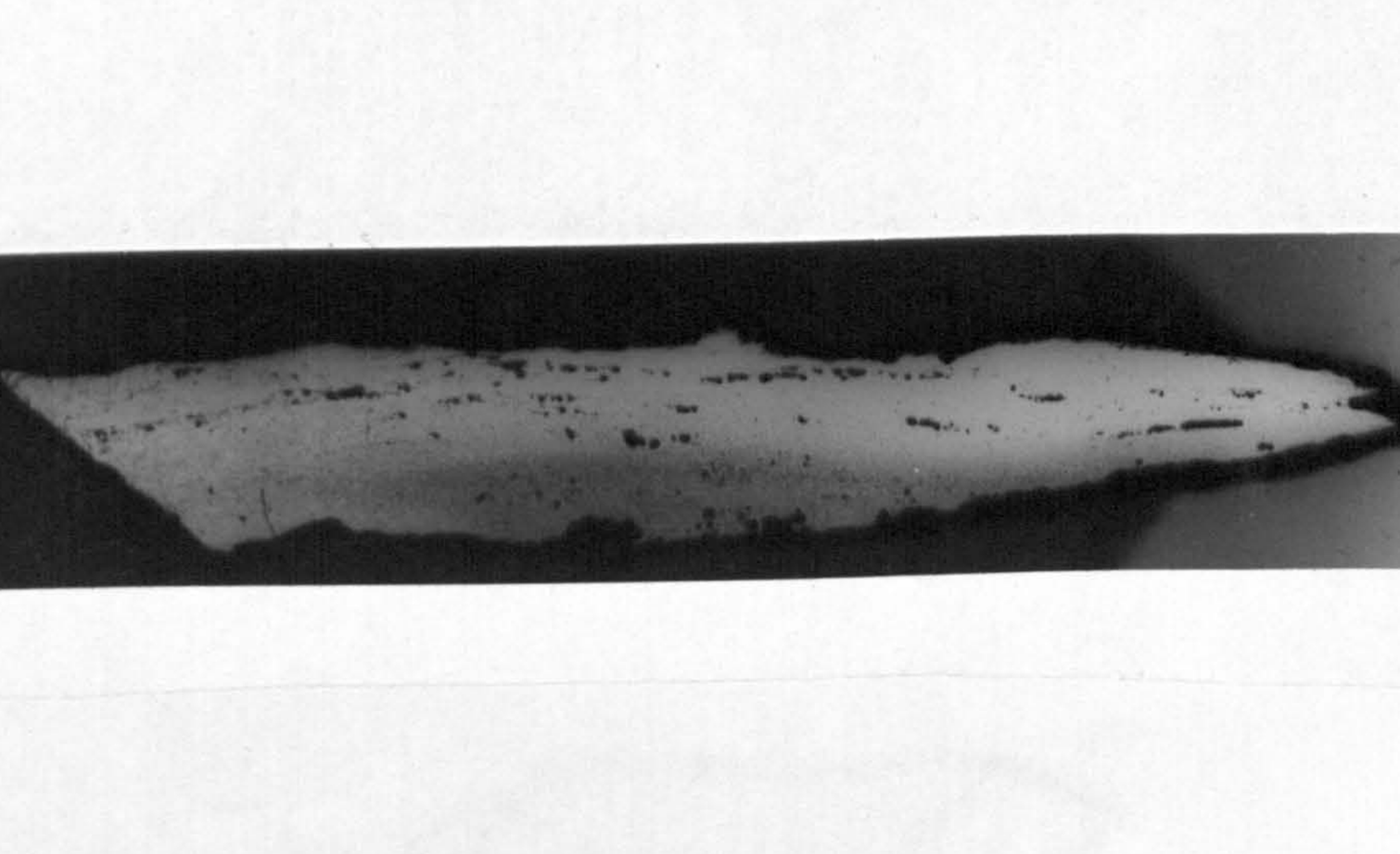

(d)

x450

Fig 41 Sword blade S8, from ? the Thames near London (a) sketch of section; (b) photomacrograph; (c) photomicrograph showing diffused carbon in weld zone between high carbon (pearlitic) half and the wrought iron (ferrite) half; (d) photomicrograph showing small surviving areas of spheroidised pearlite amongst remnant carbide in a corroded part of the section; (e) three-dimensional view

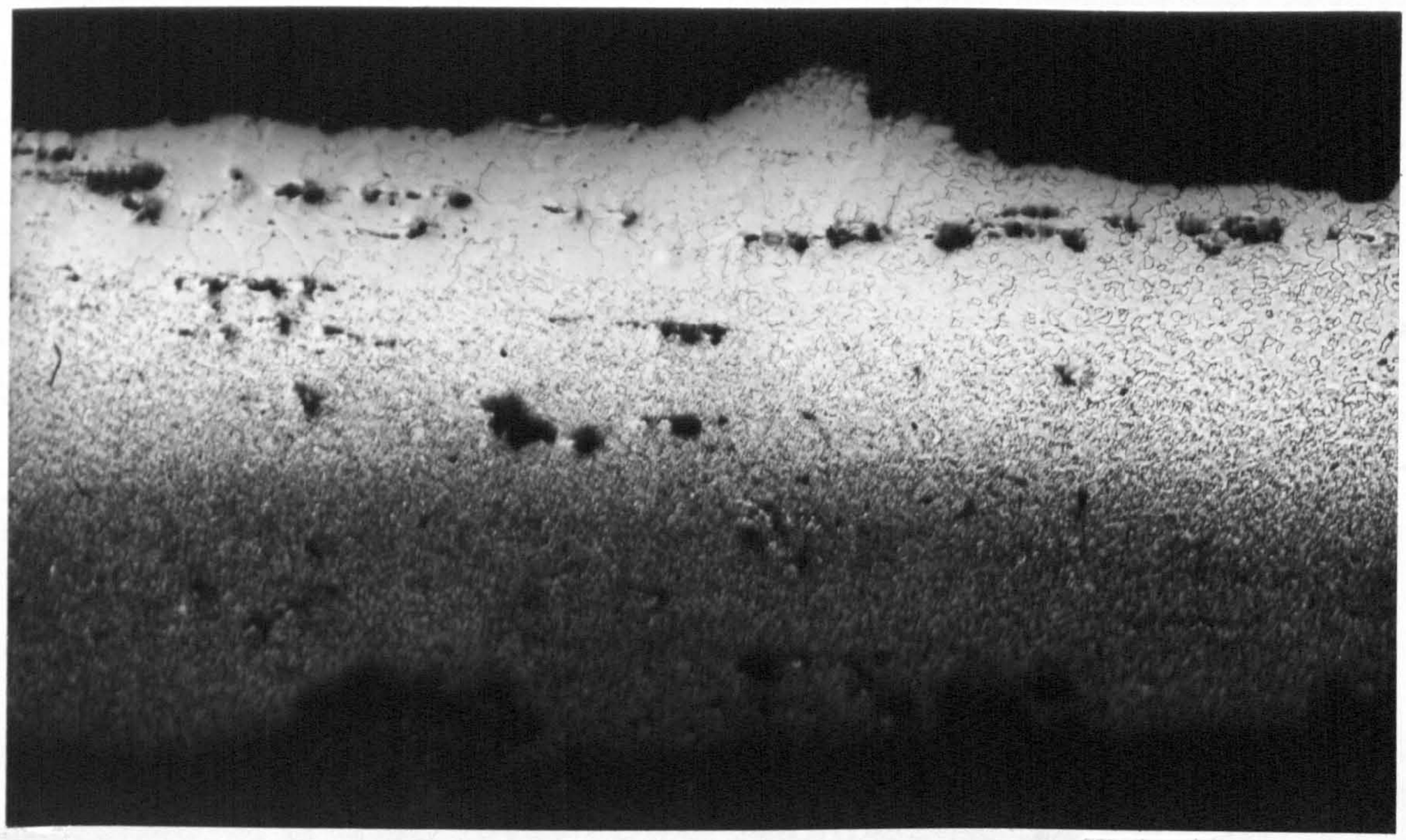

2 mm

(c)

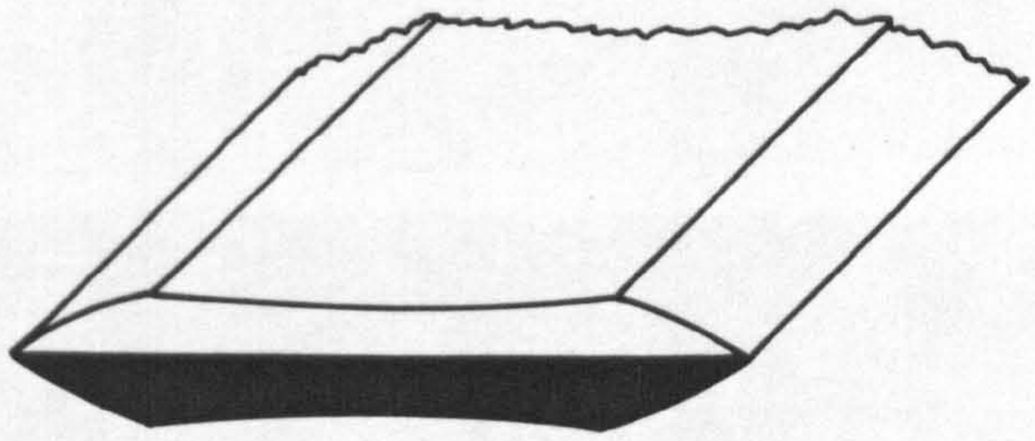

(e)

Fig 41 (continued)

(a)

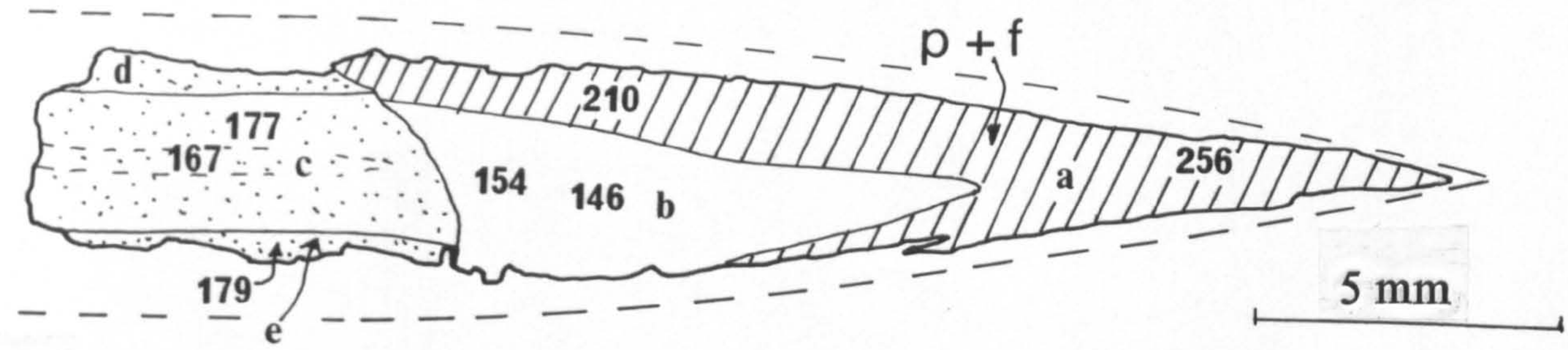

(b)

(c)

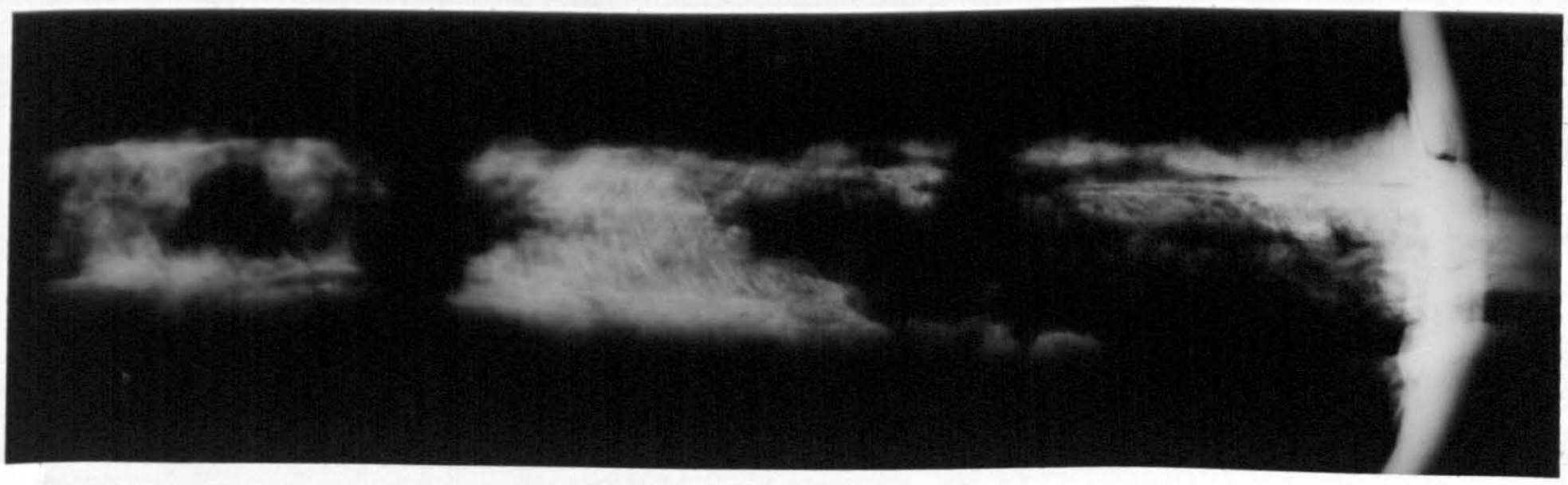

Fig 42 Sword blade S43, from the Thames: (a) sketch of section; (b) photomacrograph; (c) x-radiograph; (d) surface detail and three-dimensional view

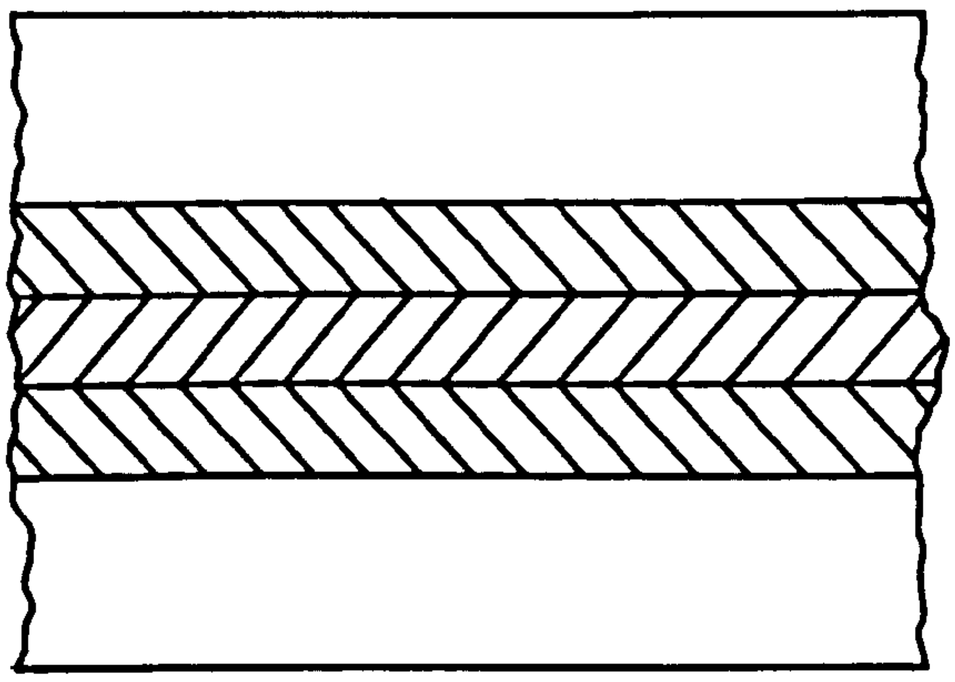

(d)

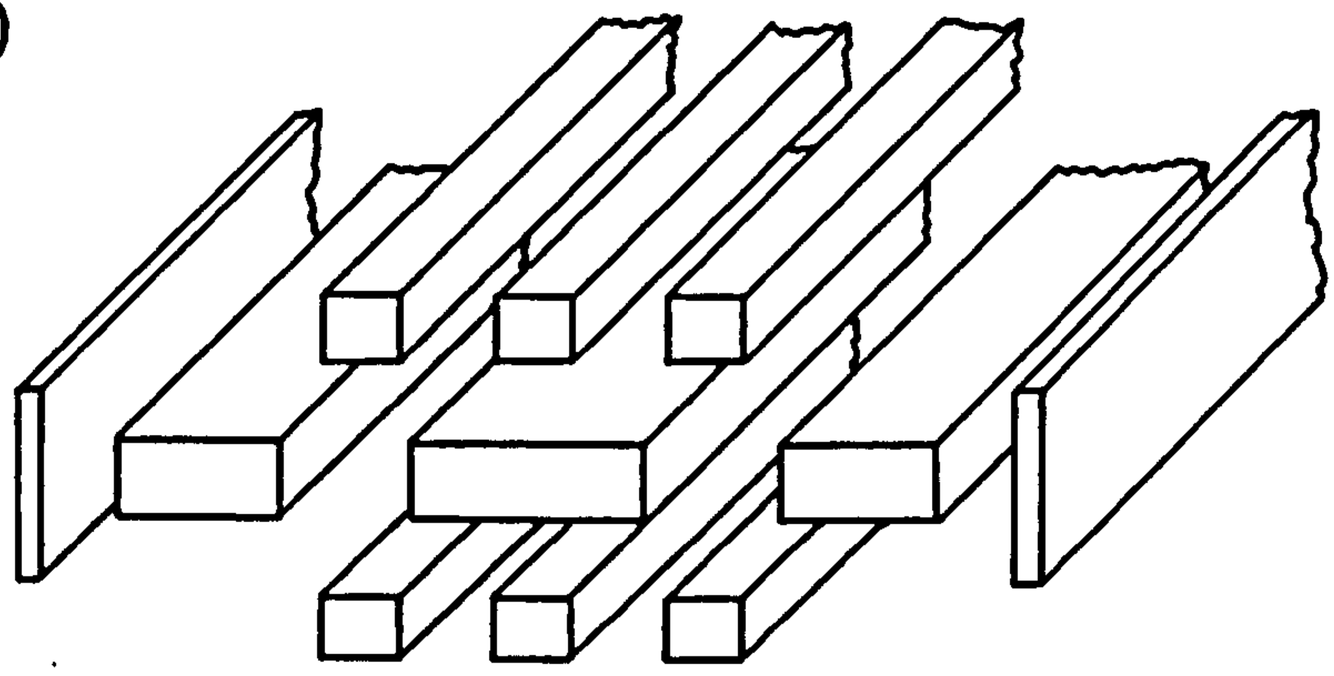

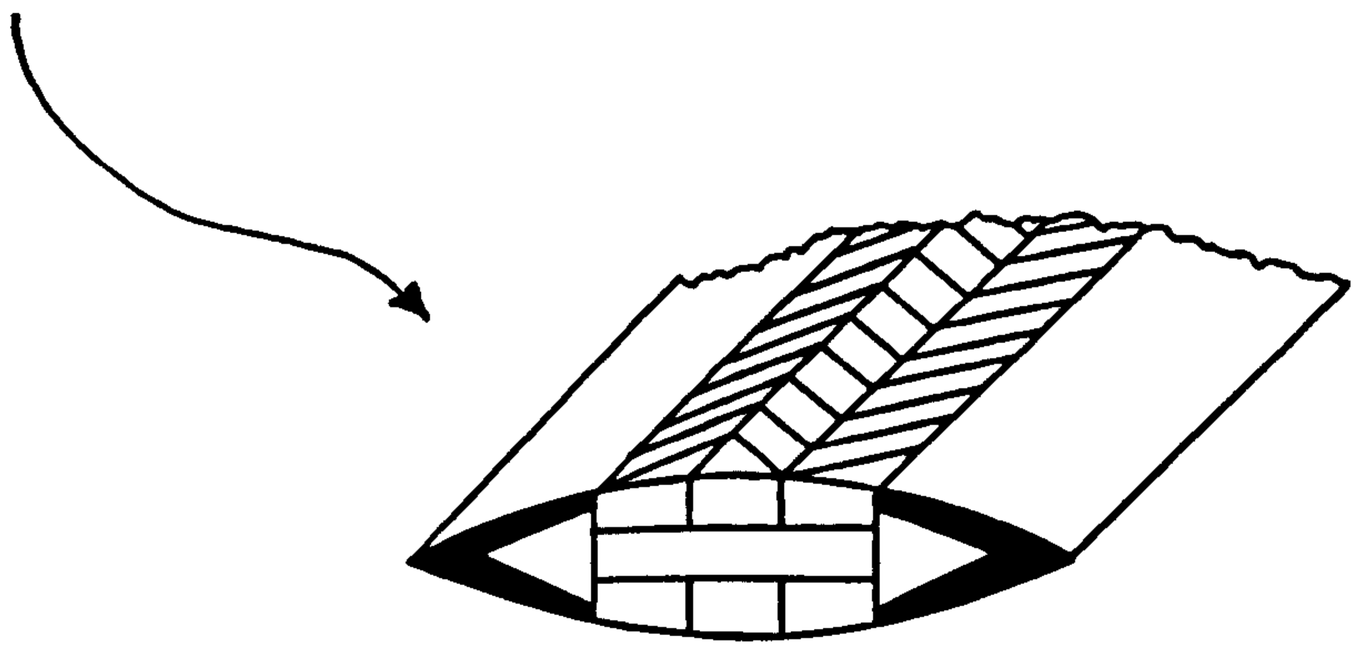

Fig 42 (continued)

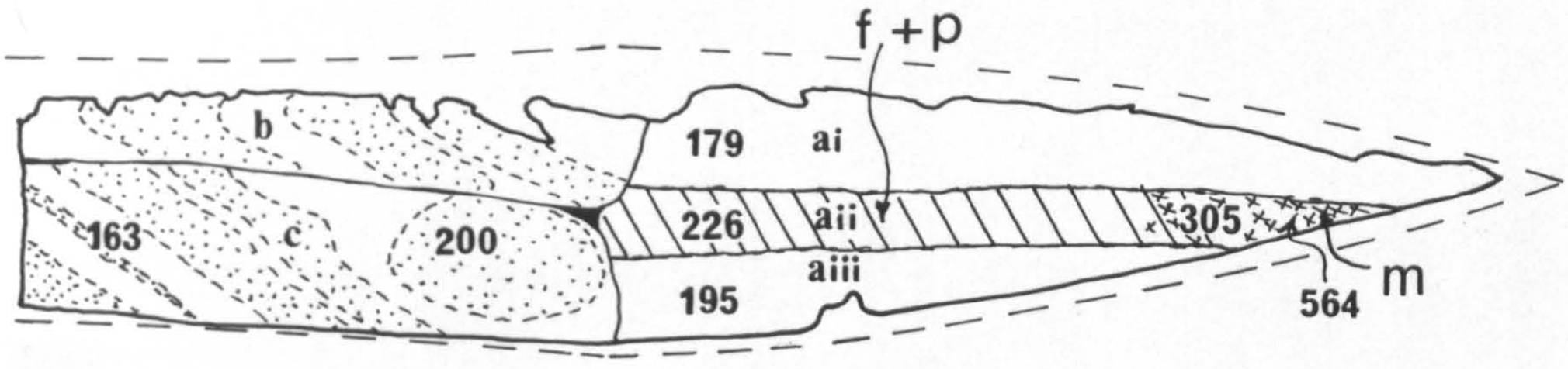

(a)

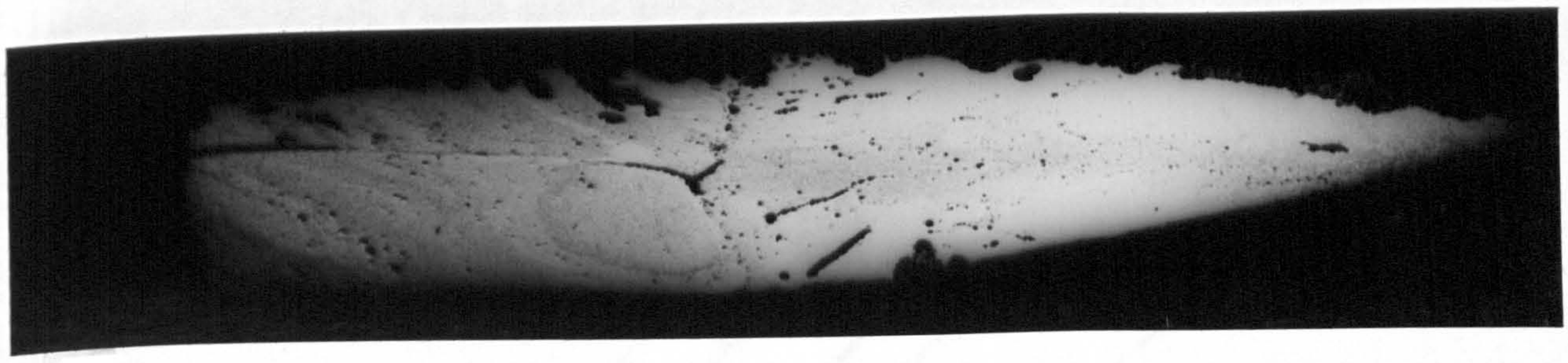

(b)

5 mm

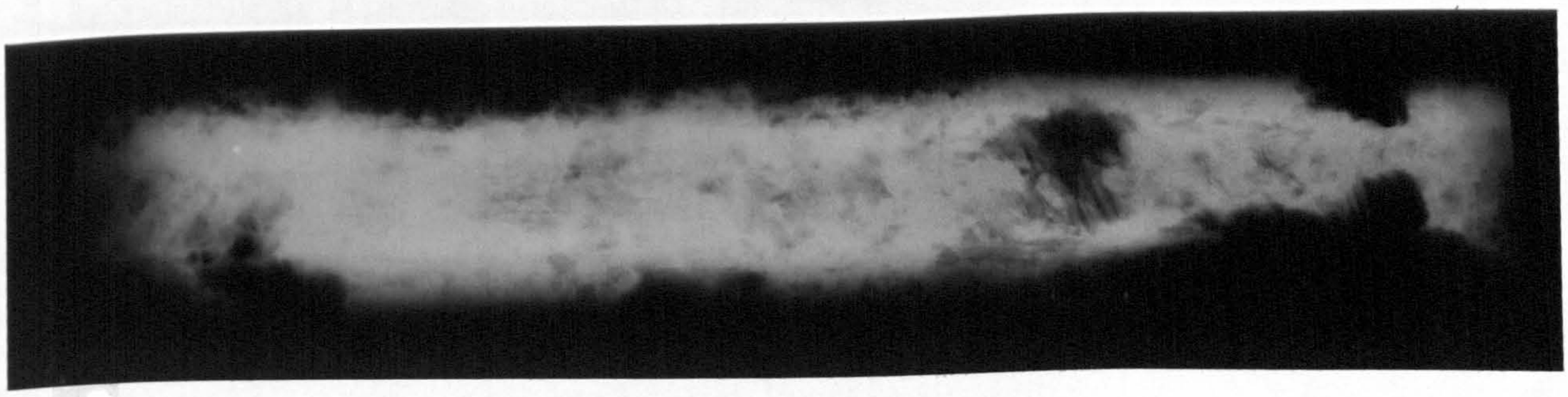

(c)

Fig 43 Sword blade S48, from Rochester: (a) sketch of section; (b) photomacrograph; (c) x-radiograph; (d) surface detail and three-dimensional view

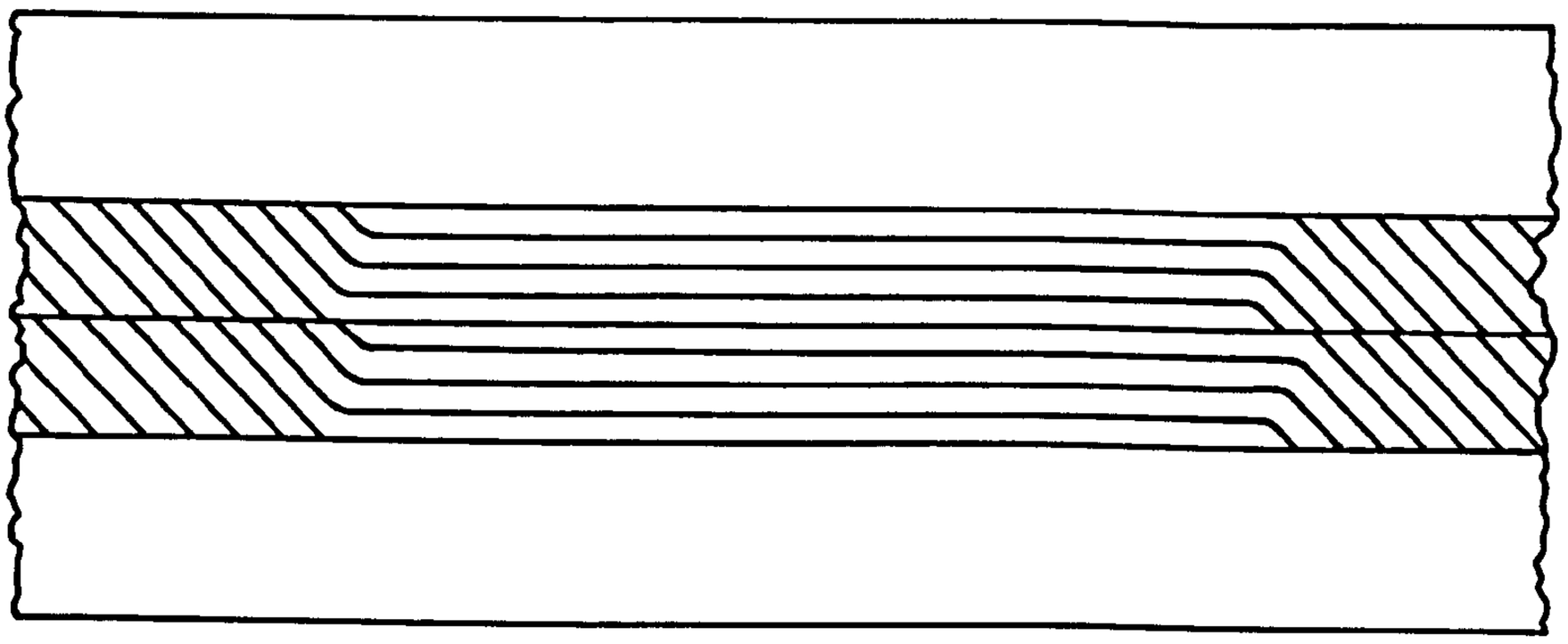

(d)

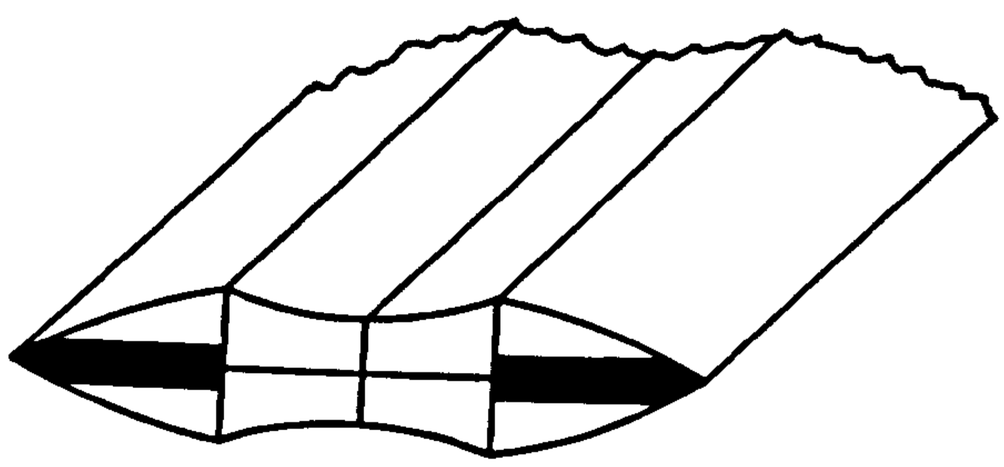

Fig 43 (continued)

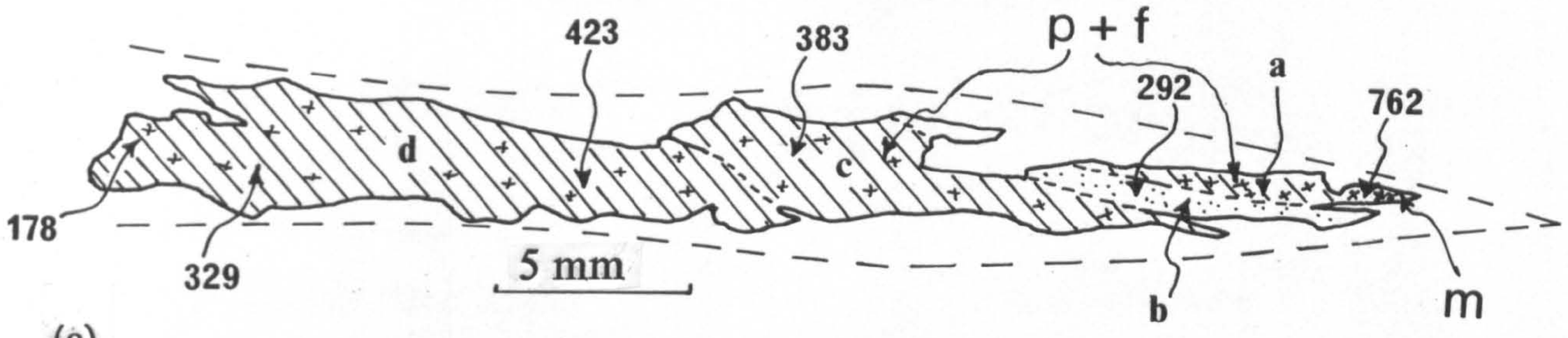

(a)

(b)

(c)

(d)

(f)

(e)

Fig 44 Sword blade S23, ? from Thames at Reading: (a) sketch of section; (b) photomacrograph; (c) x-radiograph; (d) three-dimensional view; (e) interpretation of inlaid design; (f) twisted inlaid piece

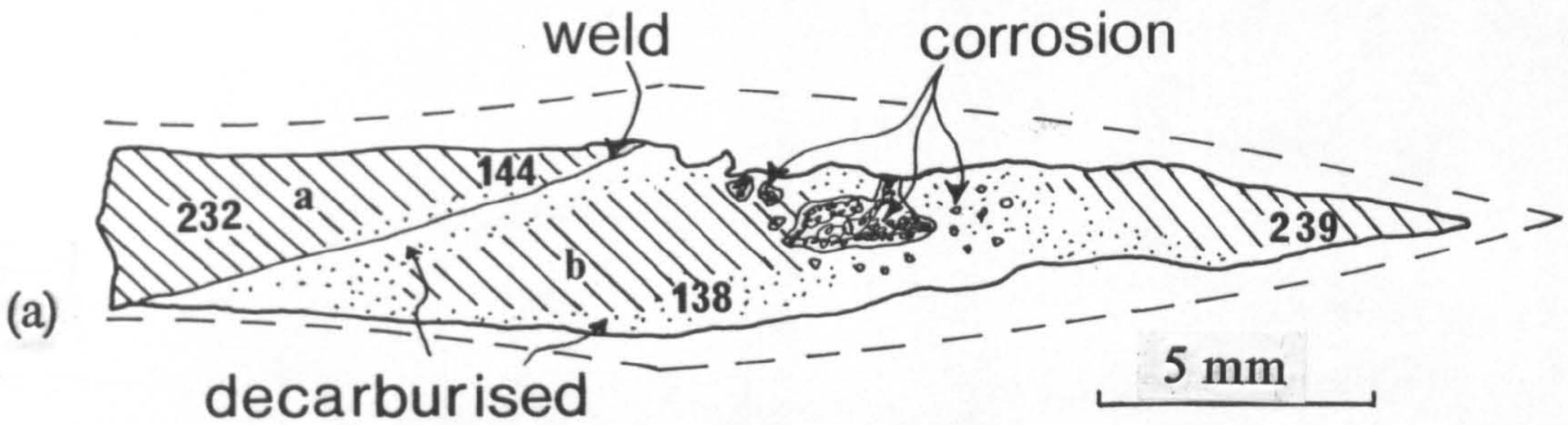

(a)

(b)

(c)

(d)

(e)

(f)

Fig 45 Sword blade S47, from the Thames at Waterloo Bridge: (a) sketch of section; (b) photomacrograph; (c) x-radiograph; (d) interpretation of inlaid design; (e) twisted inlaid piece (f) three-dimensional view

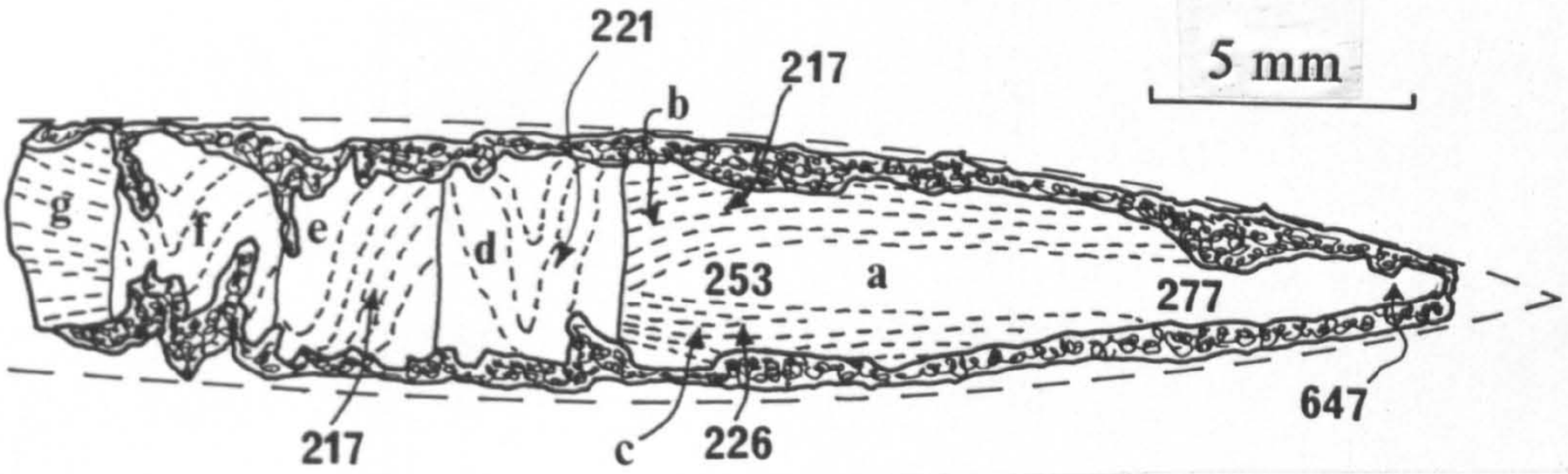

(a)

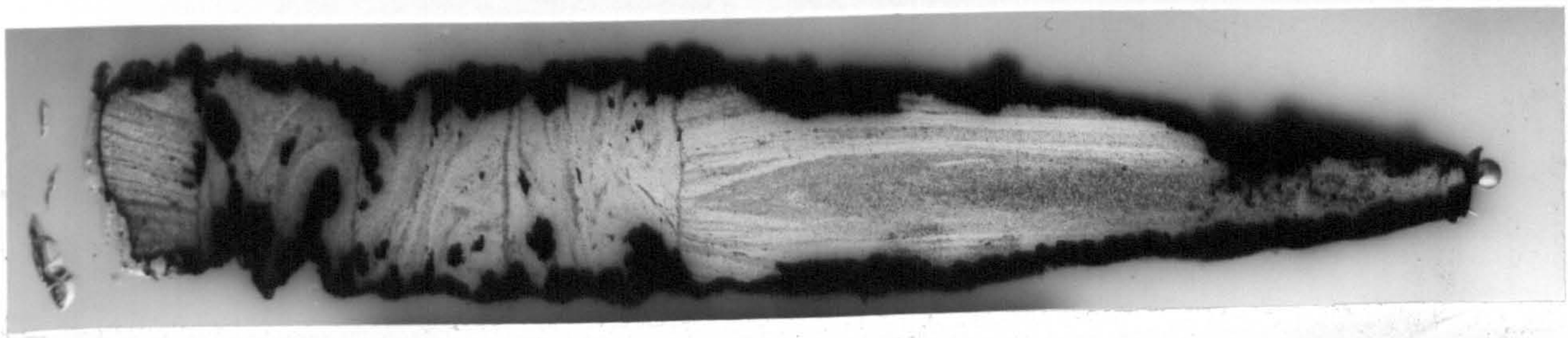

(b)

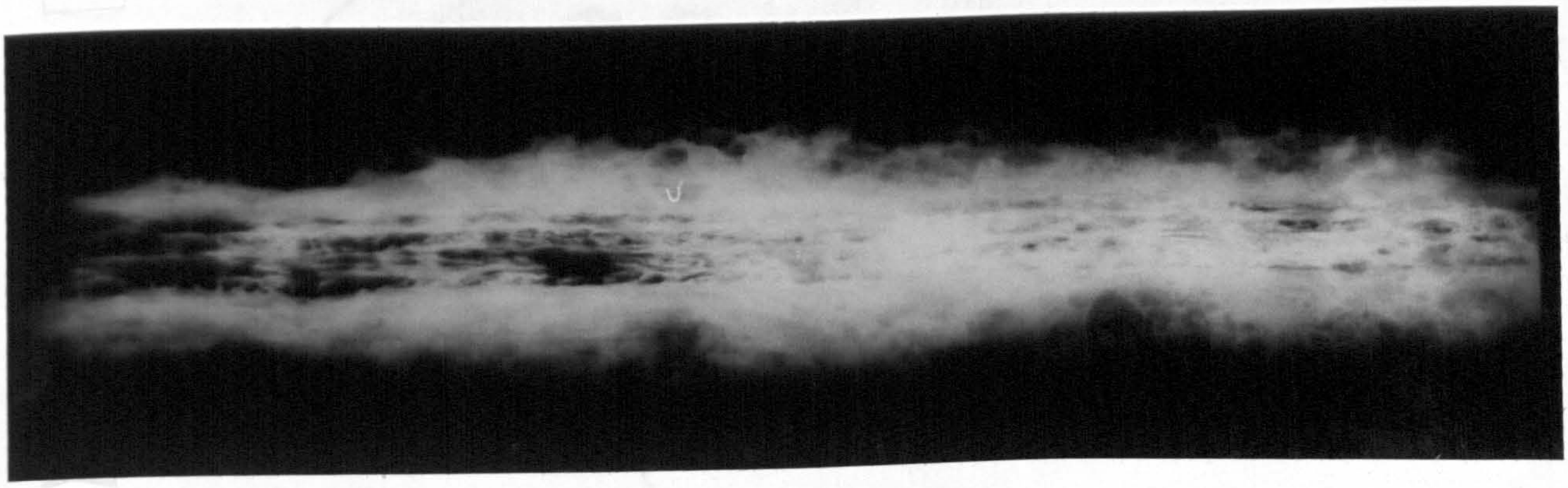

(c)

Fig 46 Sword blade S24, from the Thames at Cleeve: (a) sketch of section; (b) photomacrograph; (c) x-radiograph; (d) surface detail and three-dimensional reconstruction

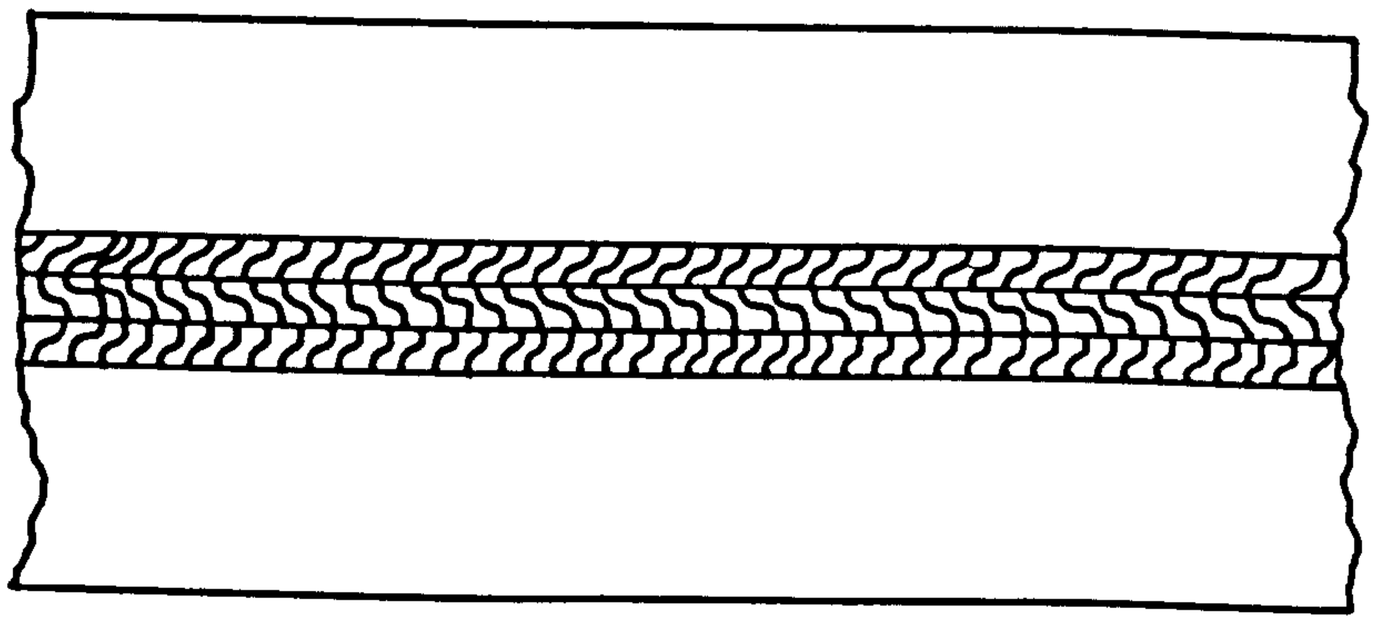

(d)

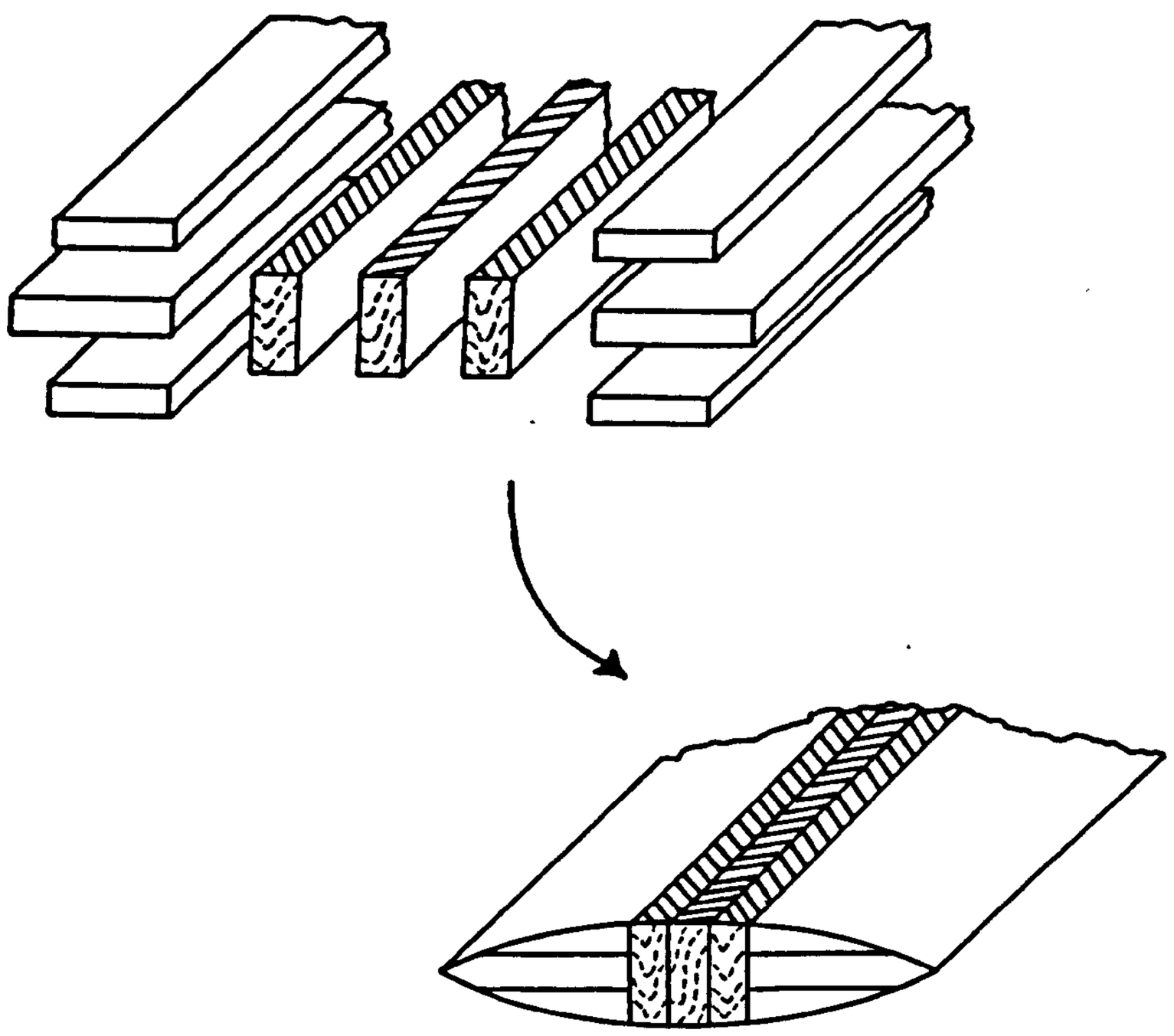

Fig 46 (continued)

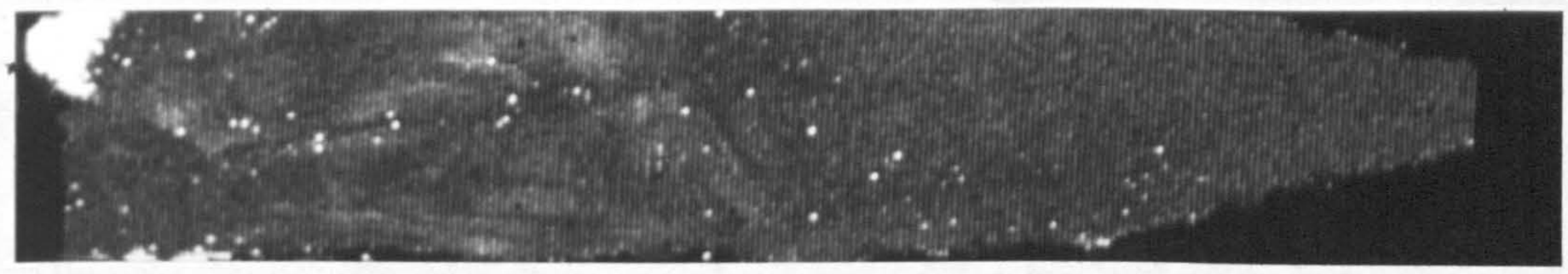

(a)

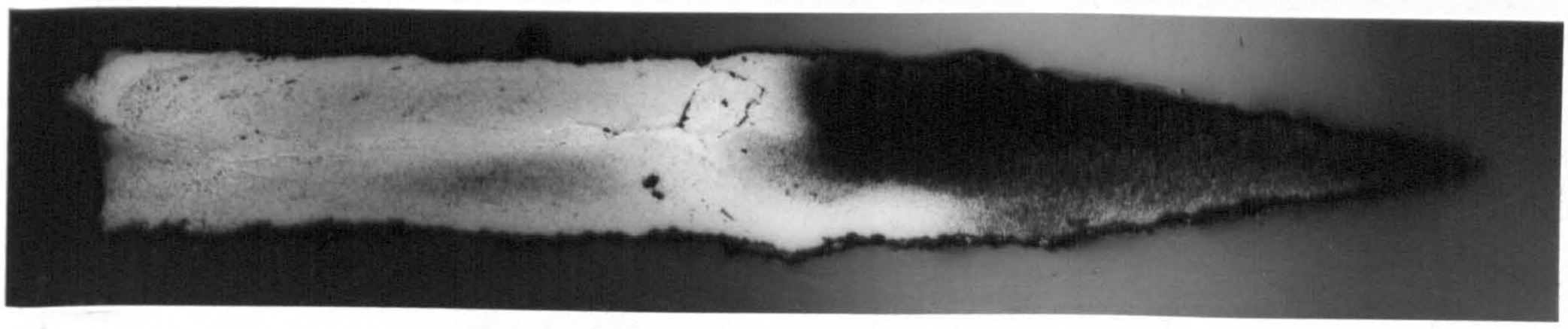

(b)

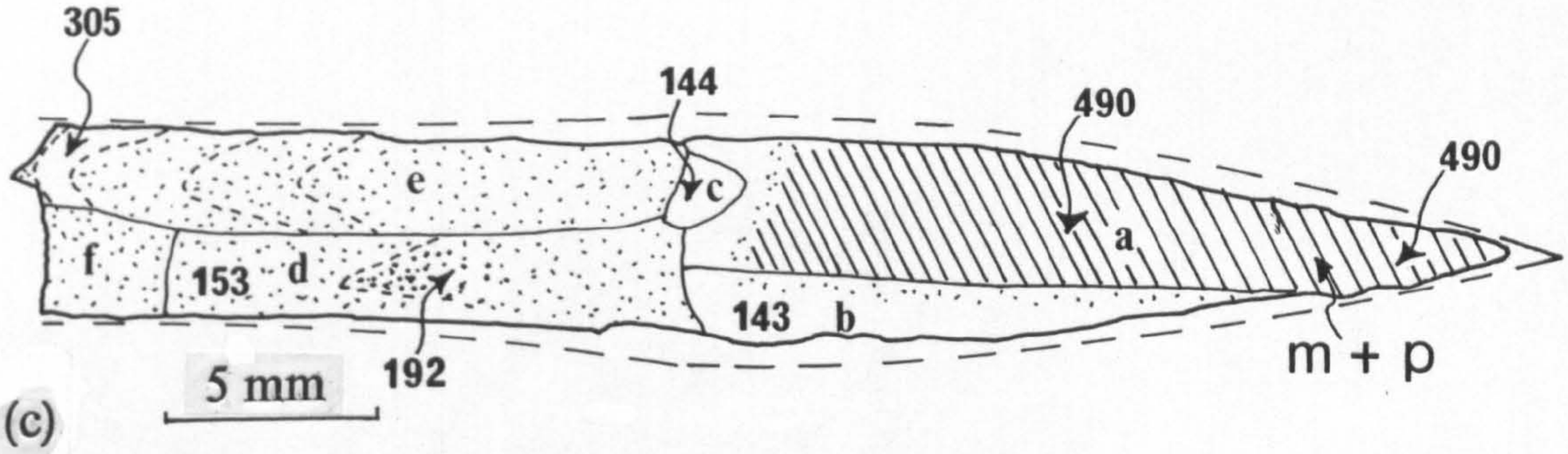

(c)

Fig 47

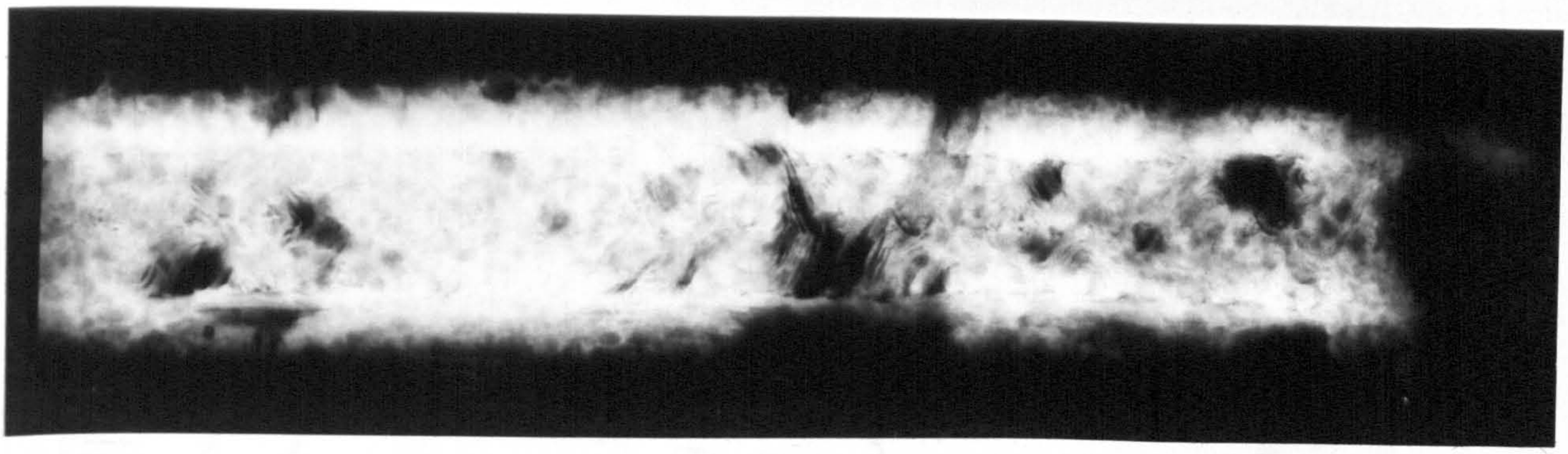

(d)

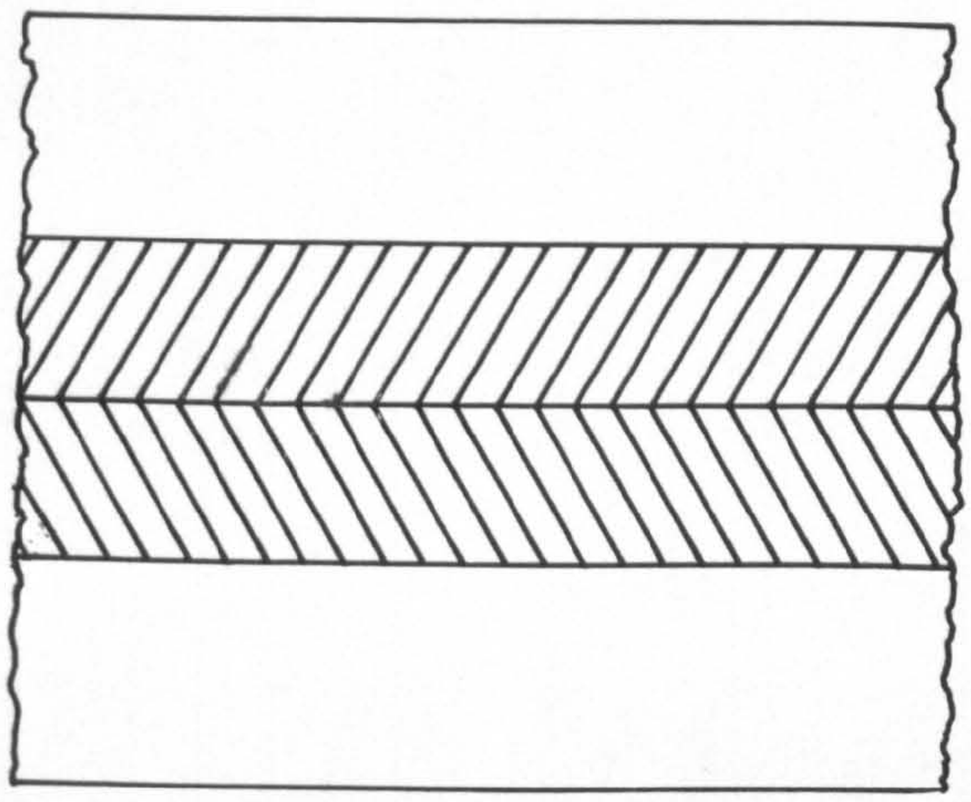

(e)

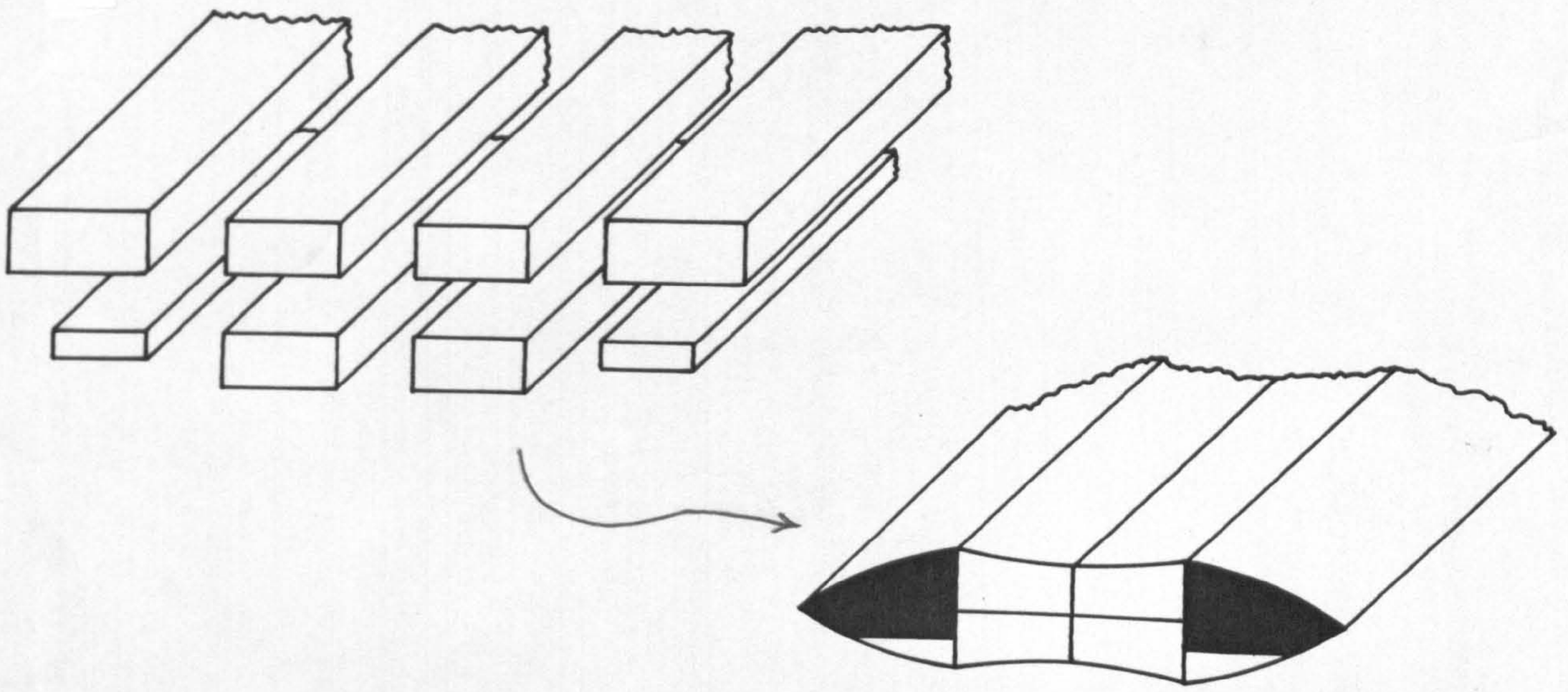

Fig 47 (continued)

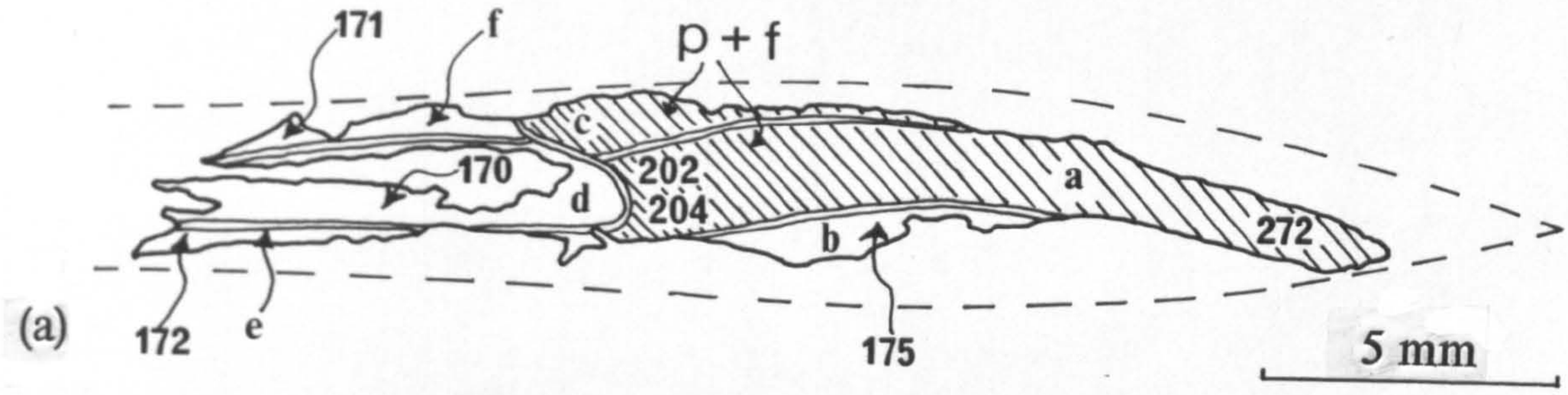

(a)

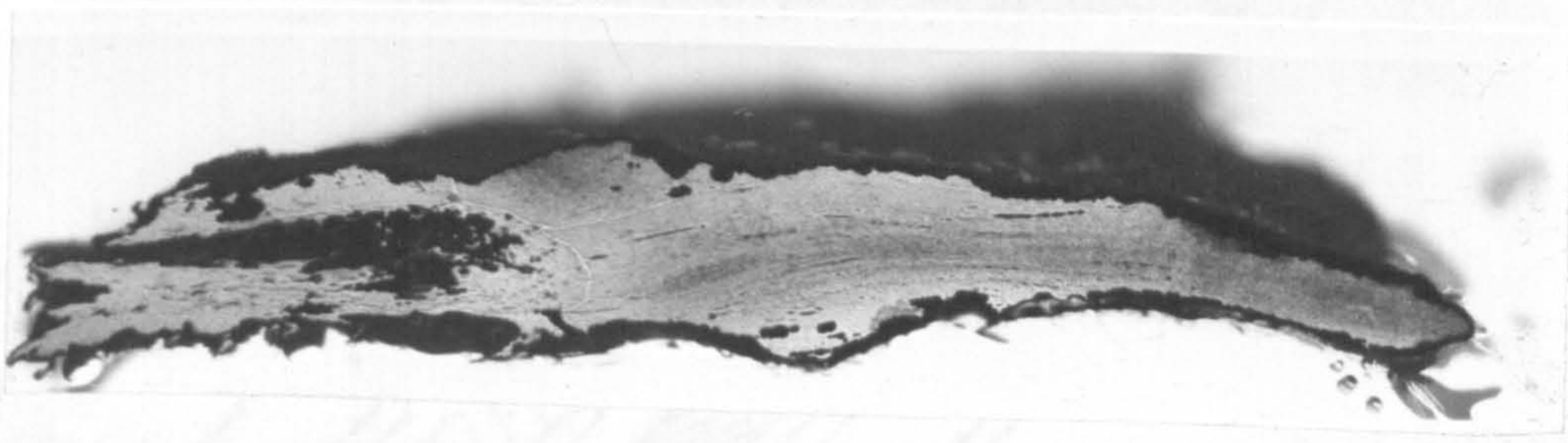

(b)

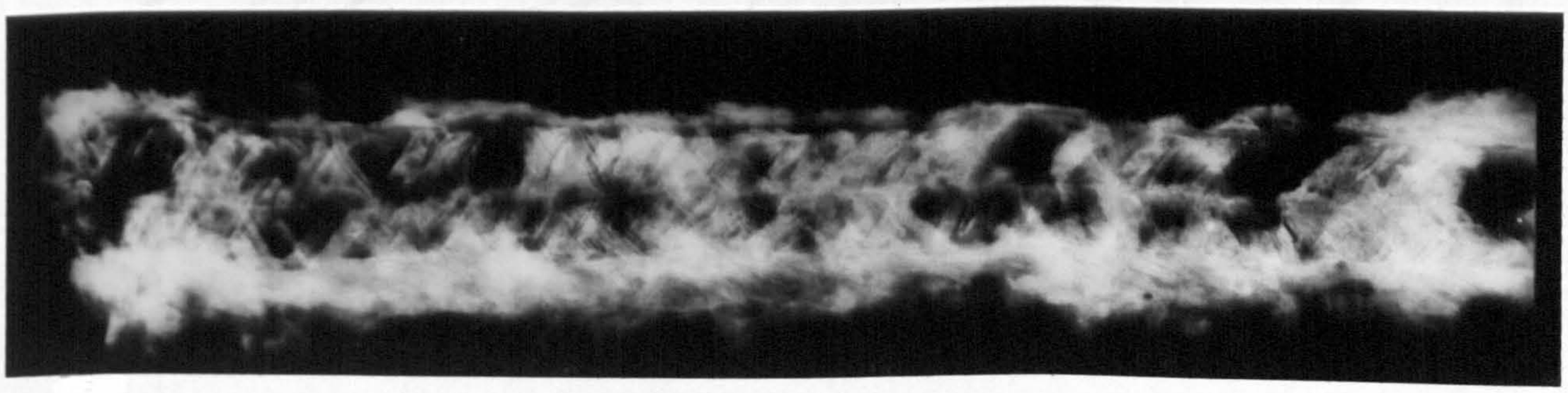

(c)

Fig 48 Sword blade S25, from Reading (? Thames): (a) sketch of section; (b) photomacrograph; (c) x-radiograph; (d) surface detail and three-dimensional reconstruction

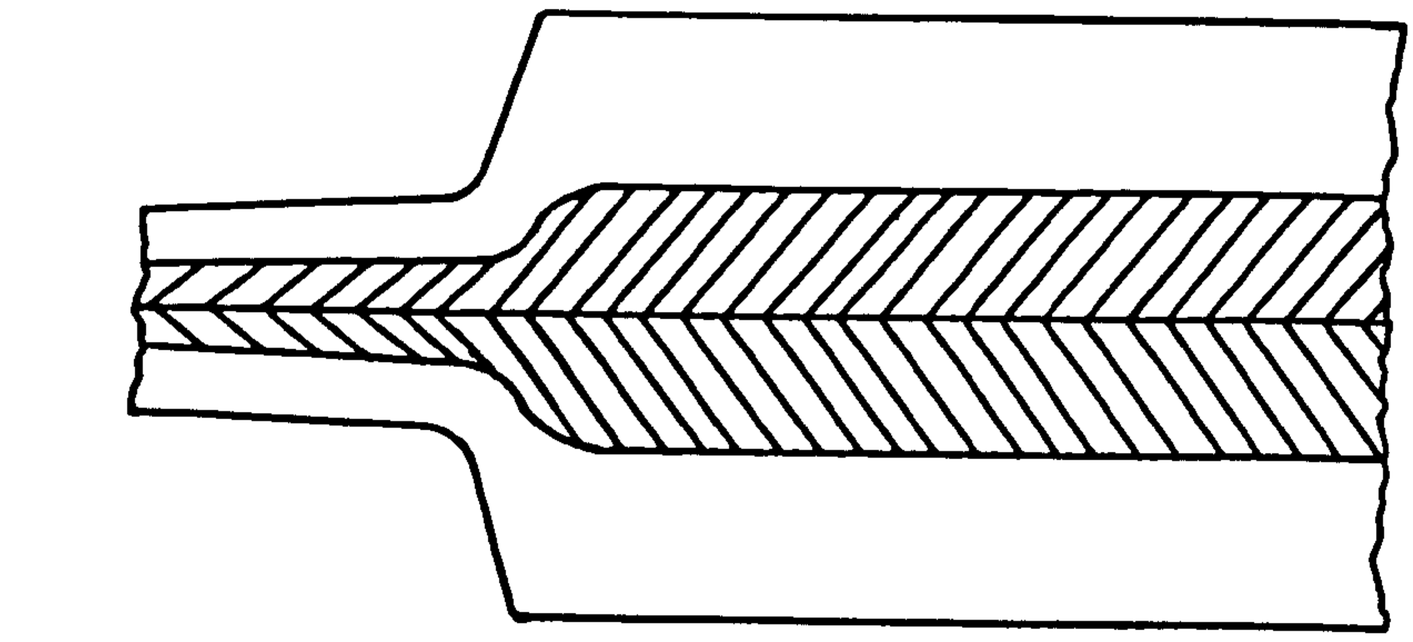

(d)

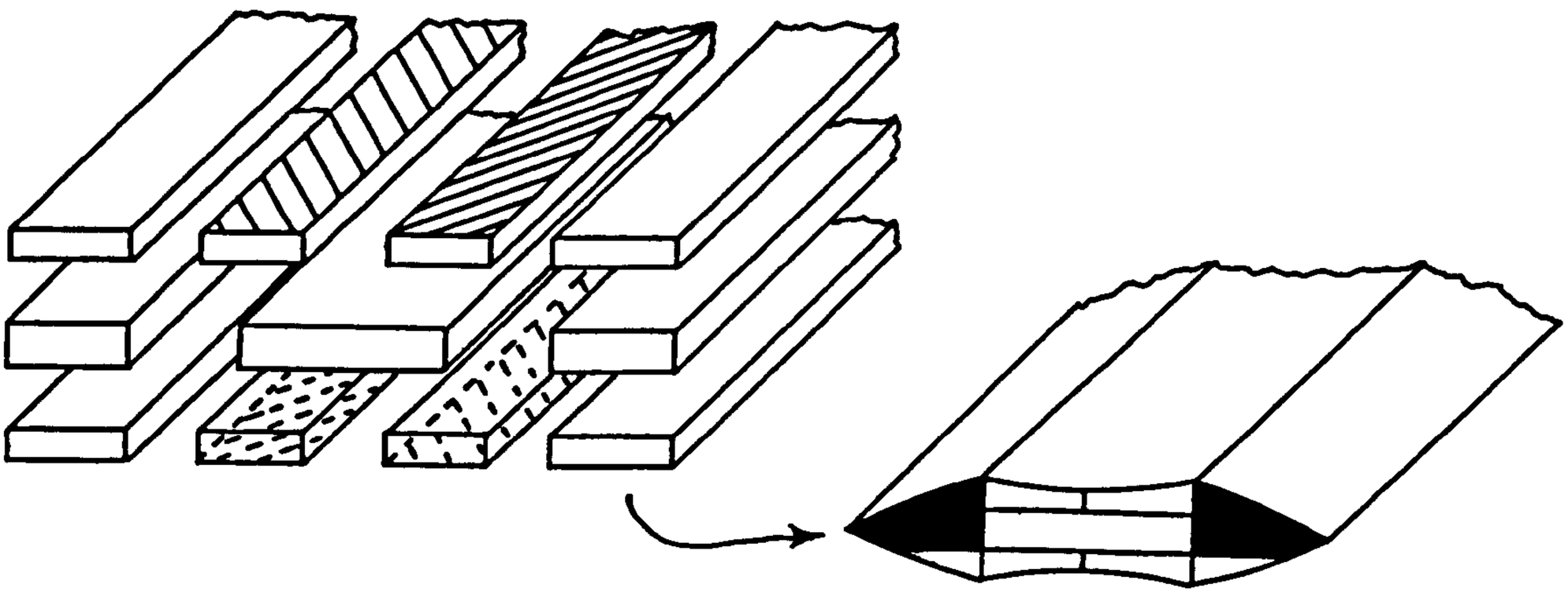

Fig 48 (continued)

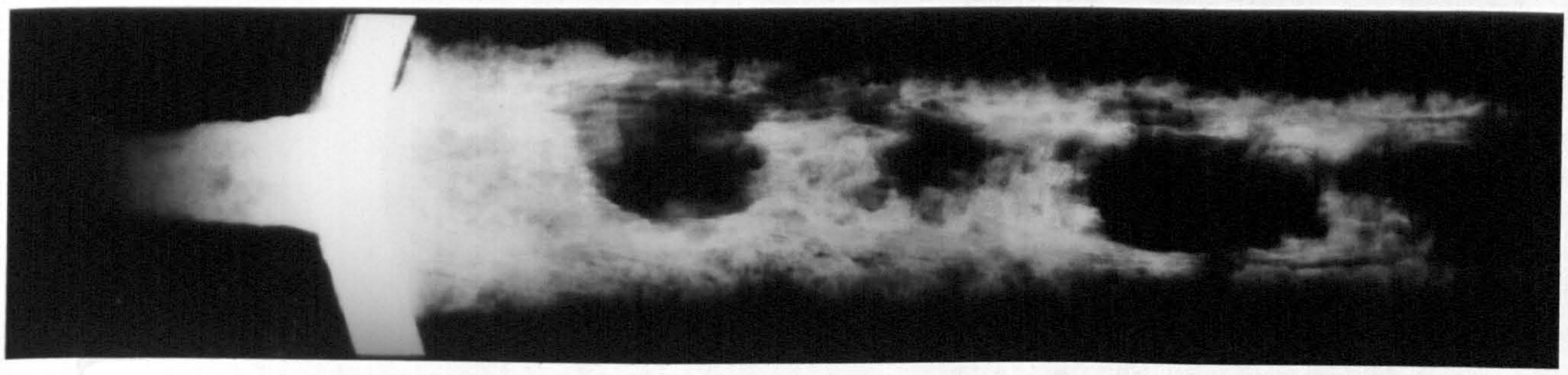

(d)

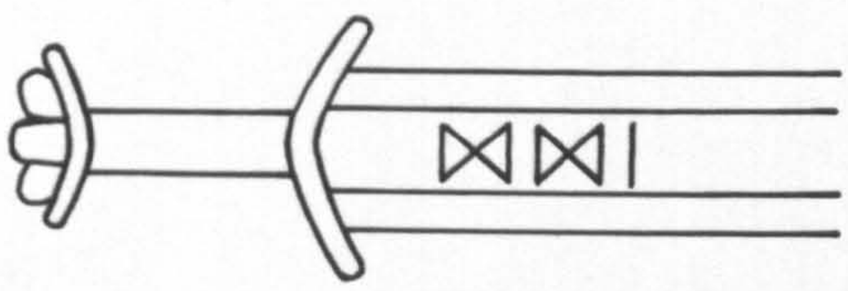

(f)

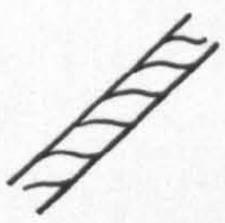

(e)

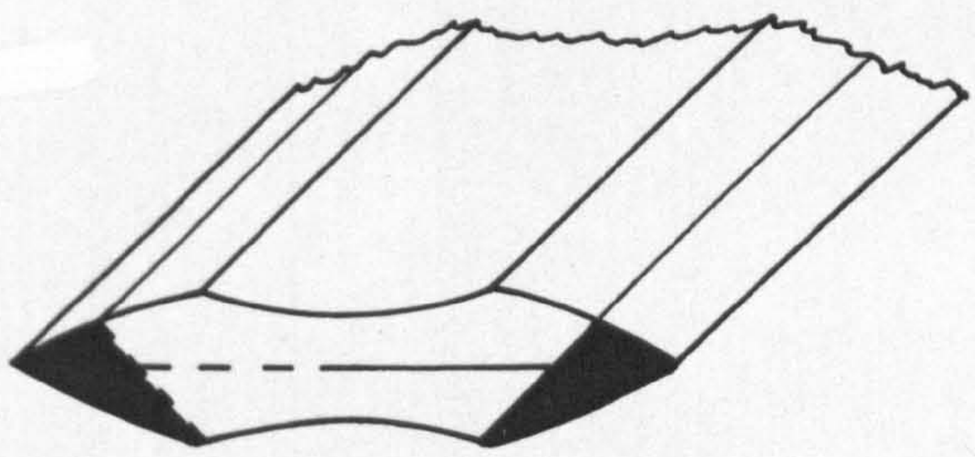

Fig 49 (continued)

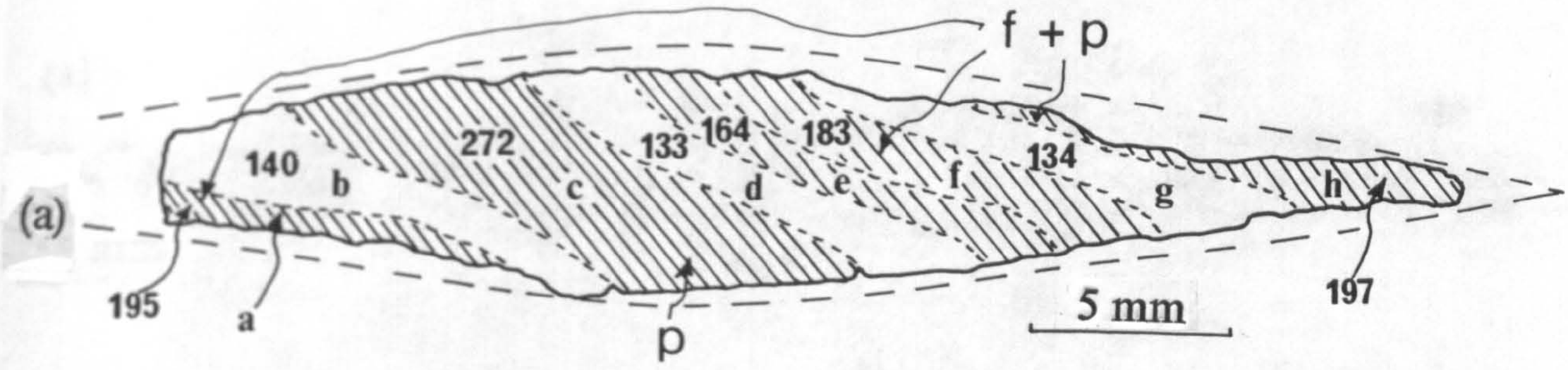

Fig 50 Sword blade S26, from the Thames at Wallingford Bridge:(a) sketch of section; (b) photomacrograph; (c) three-dimensional reconstruction; (d) likely effect of polishing and etching the surface.

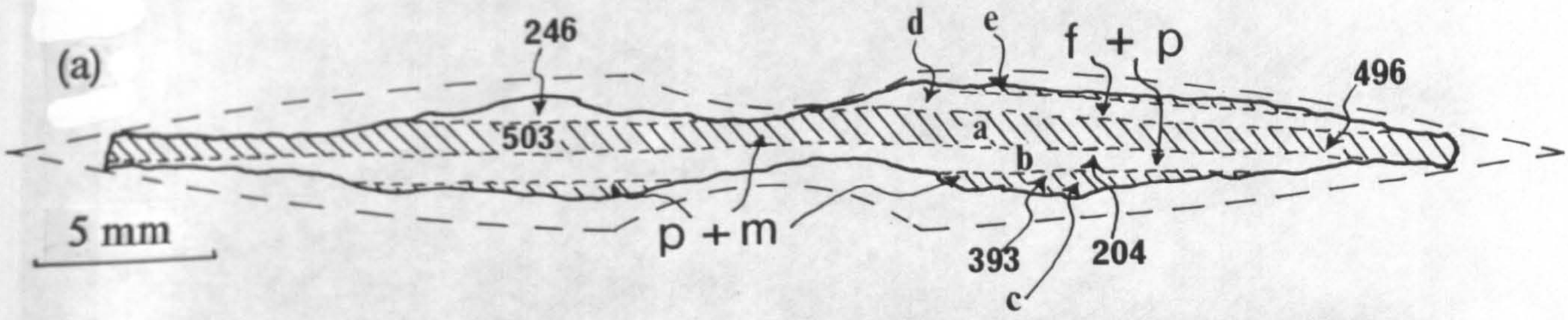

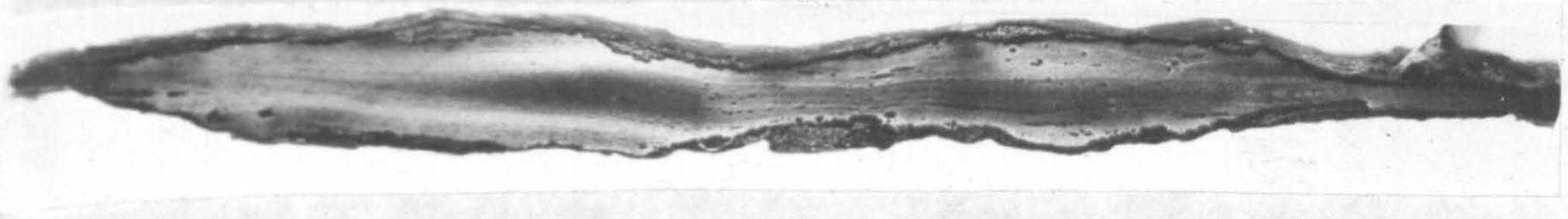

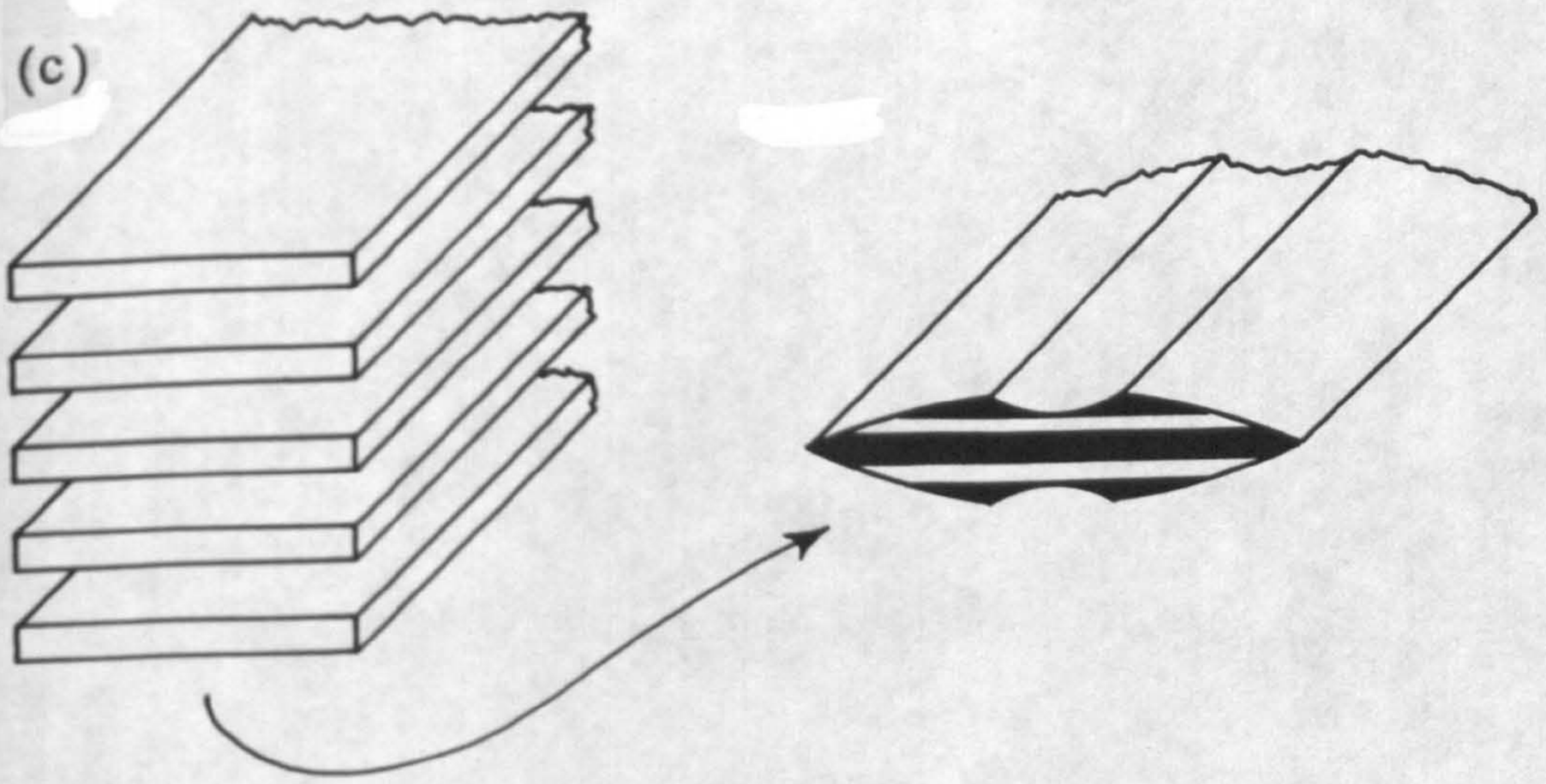

Fig 51 Sword blade S28, no provenance : (a) sketch of section; (b) photomacrograph; (c) three-dimensional reconstruction

(a)

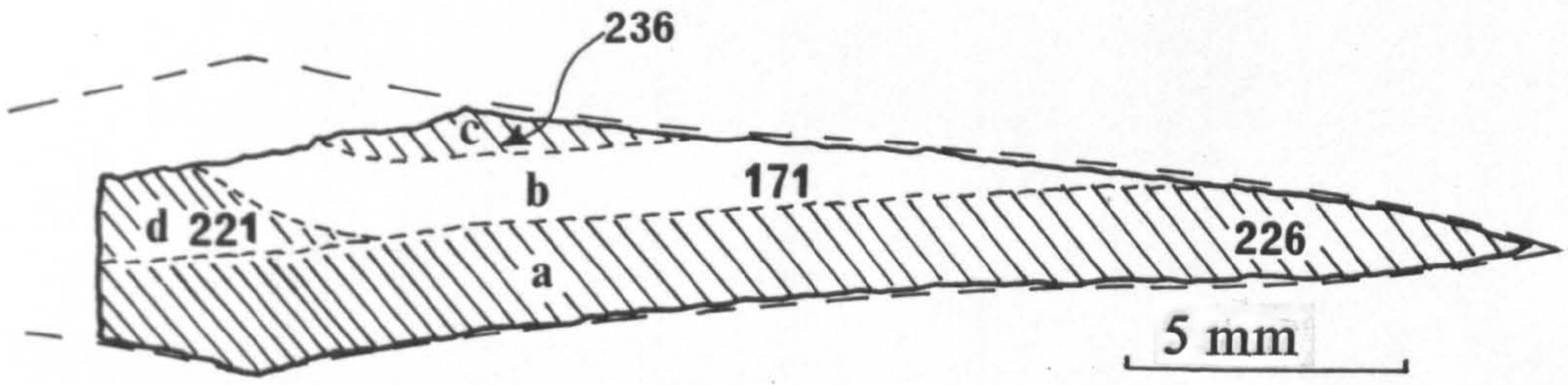

(b)

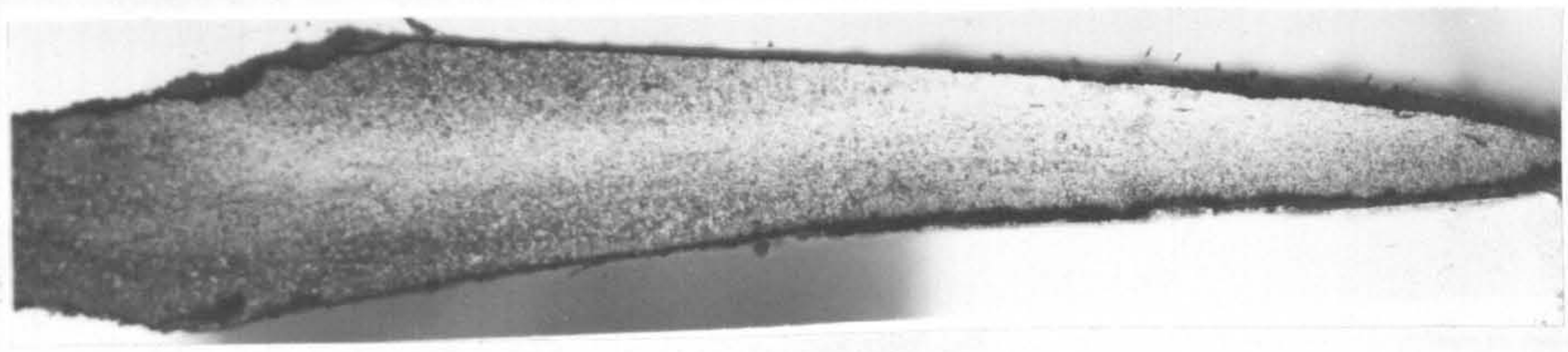

(c)

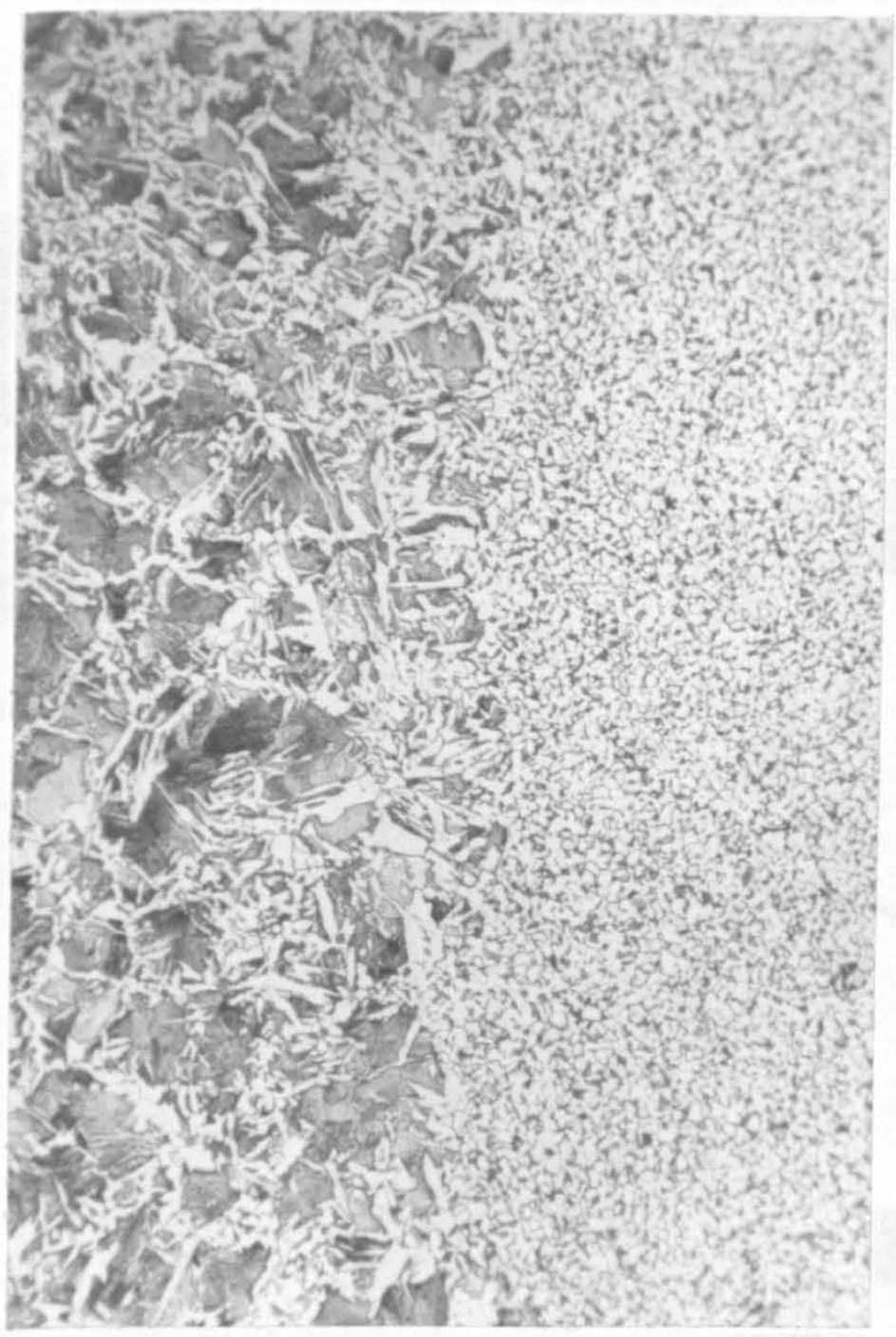

x100

x400

(d)

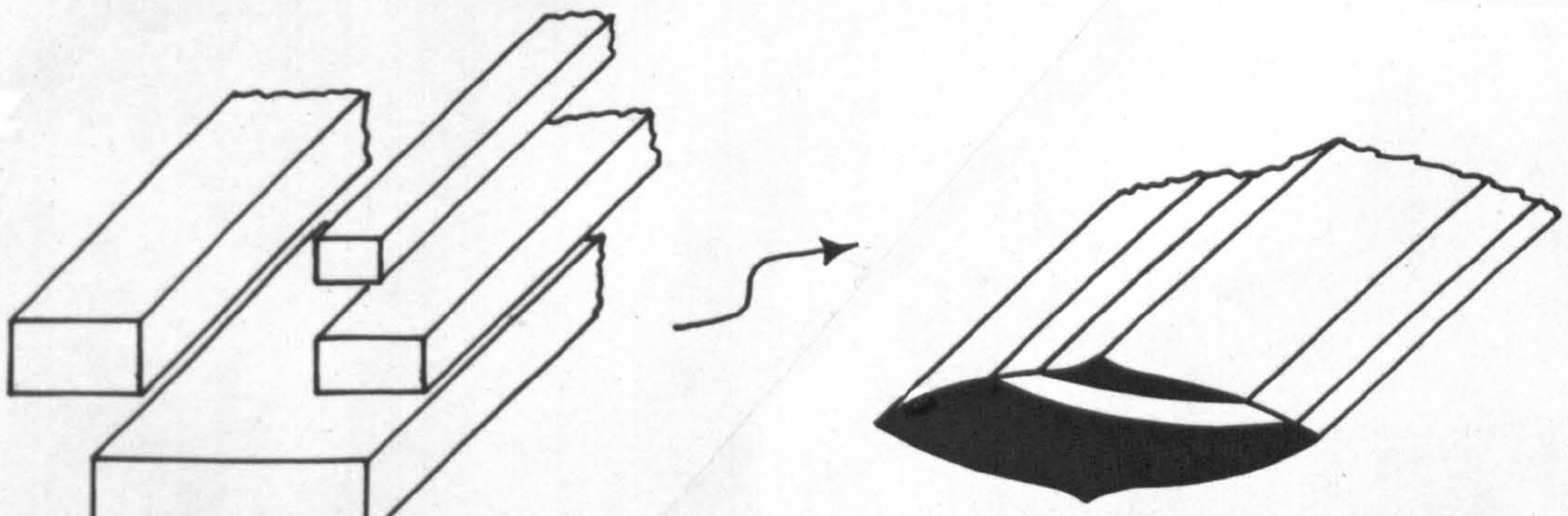

Fig 52 Sword blade S30, from Sunbury Weir Stream: (a) sketch of section; (b) photomacrograph; (c) photomicrograph showing the junction between the fine grain low carbon strip and the adjoining higher carbon, larger grained area which shows the Widmanstatten effect (d) photomicrograph showing predominantly pearlite of the main high (0.7 - 0.8%) carbon part of the blade

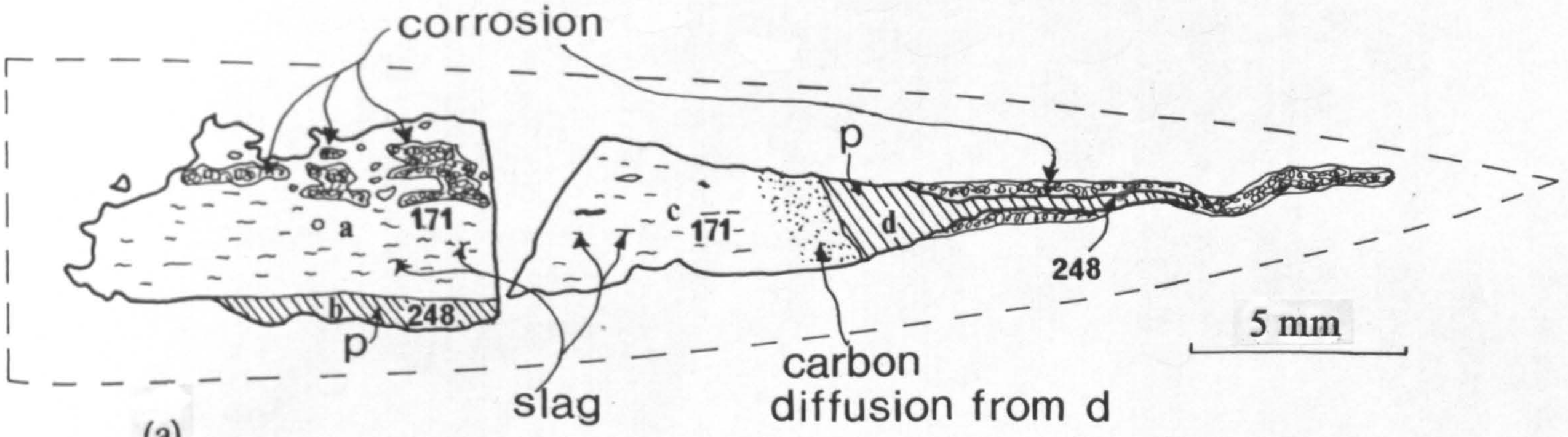

(a)

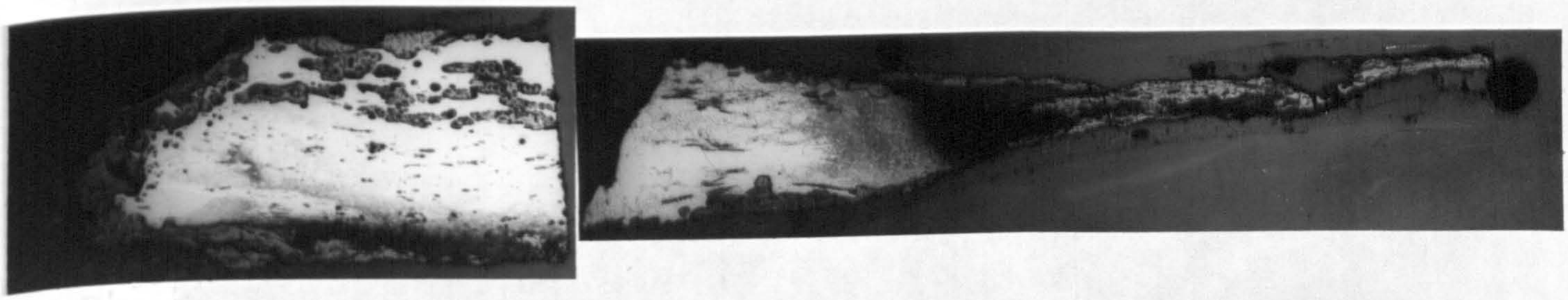

(b)

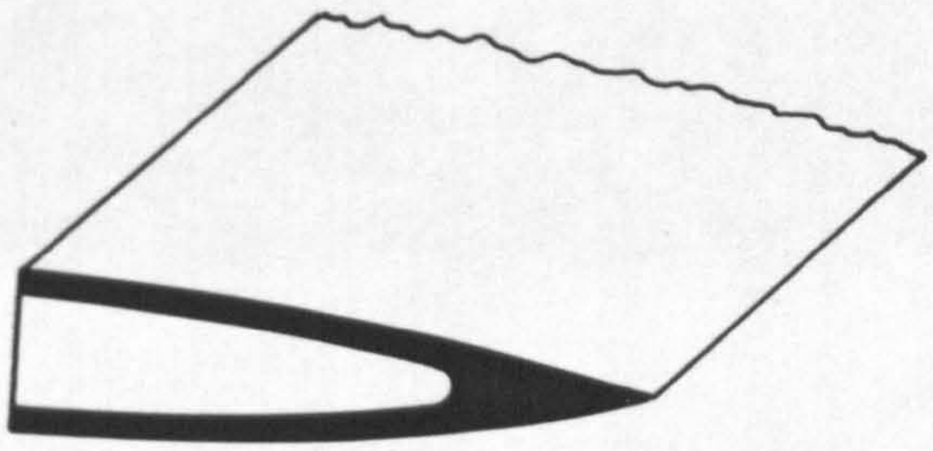

(c)

Fig 53 Sword blade S50, from Barham Down: (a) sketch of section; (b) photomacrograph; (c) three-dimensional view

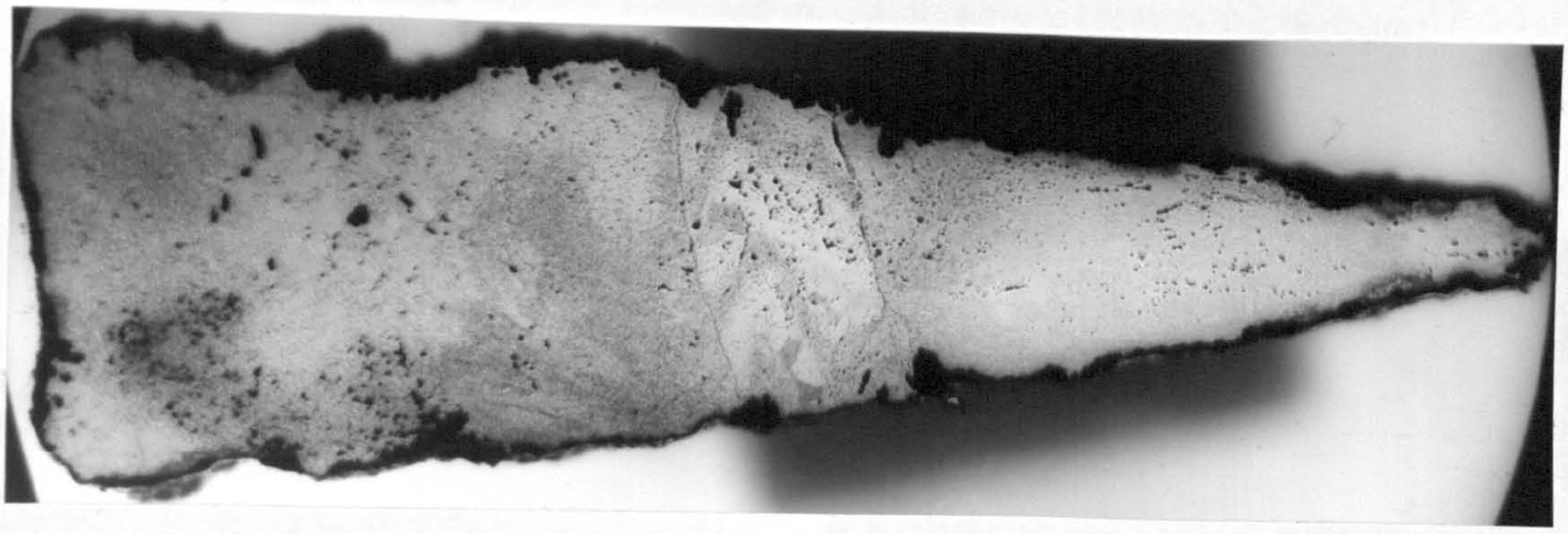

(a)

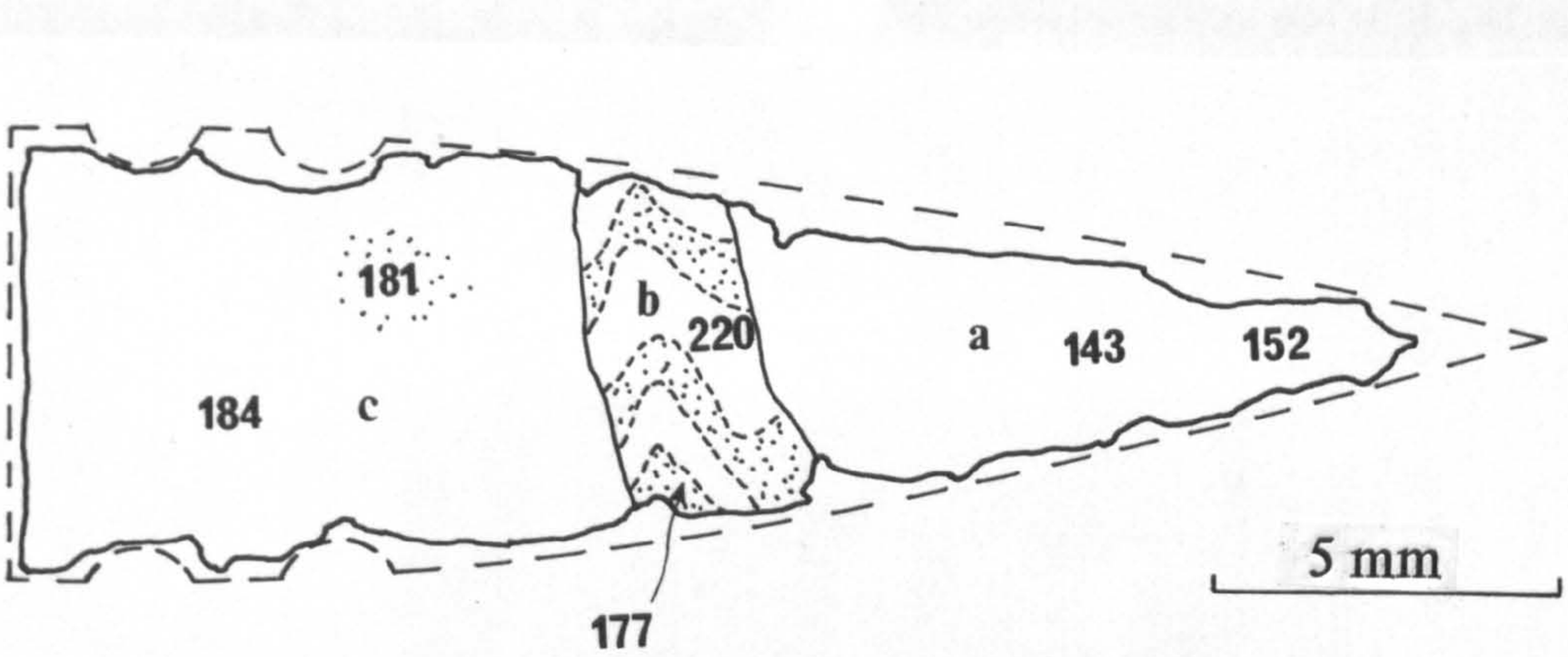

(b)

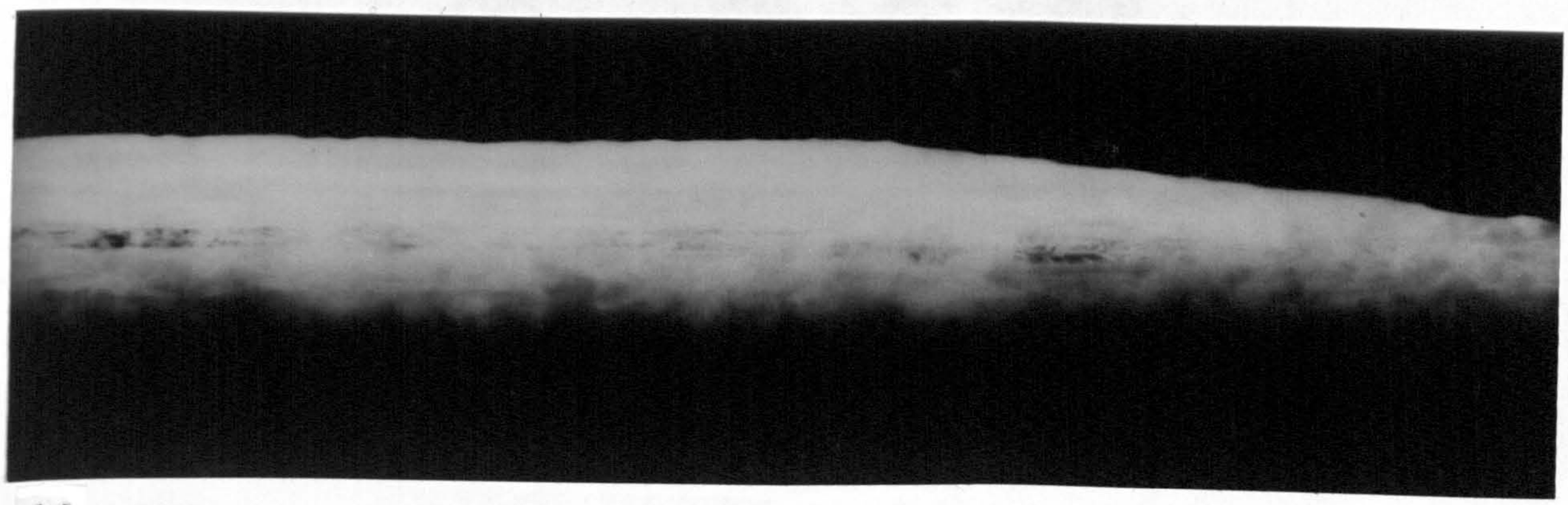

(c)

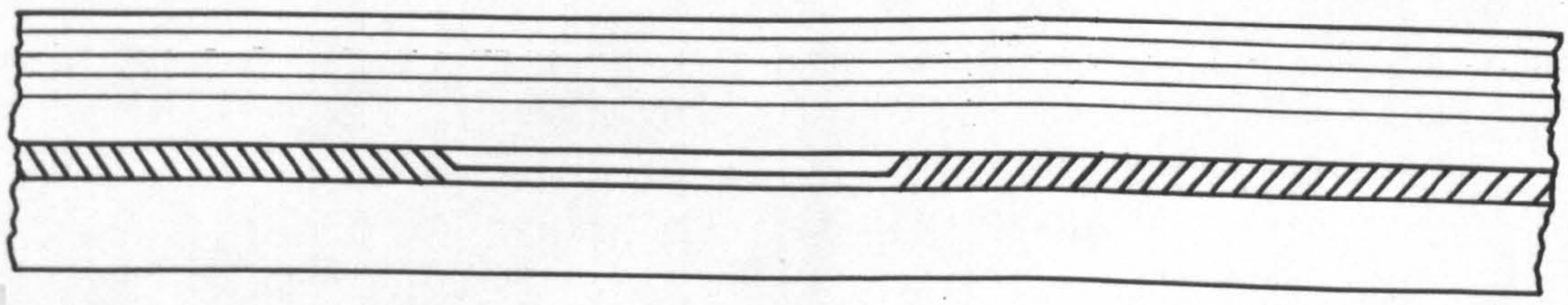

(d)

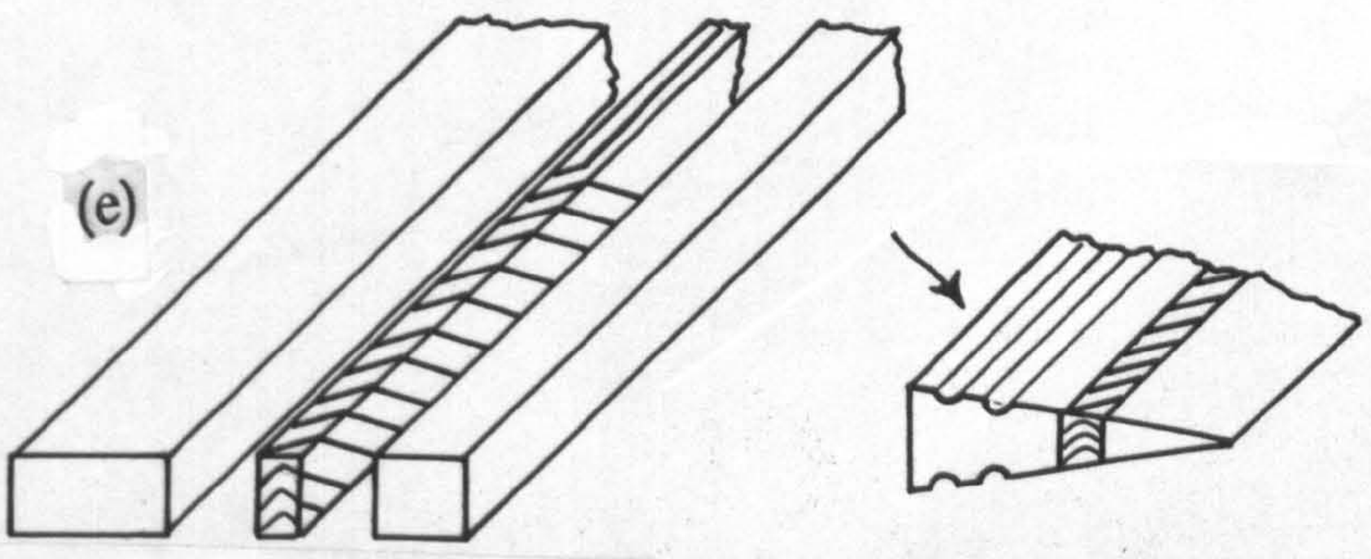

Fig 54 Scramasax S22, from the Thames at Reading: (a) photomacrograph; (b) sketch of section; (c) x-radiograph; (d) surface detail; (e) three-dimensional reconstruction

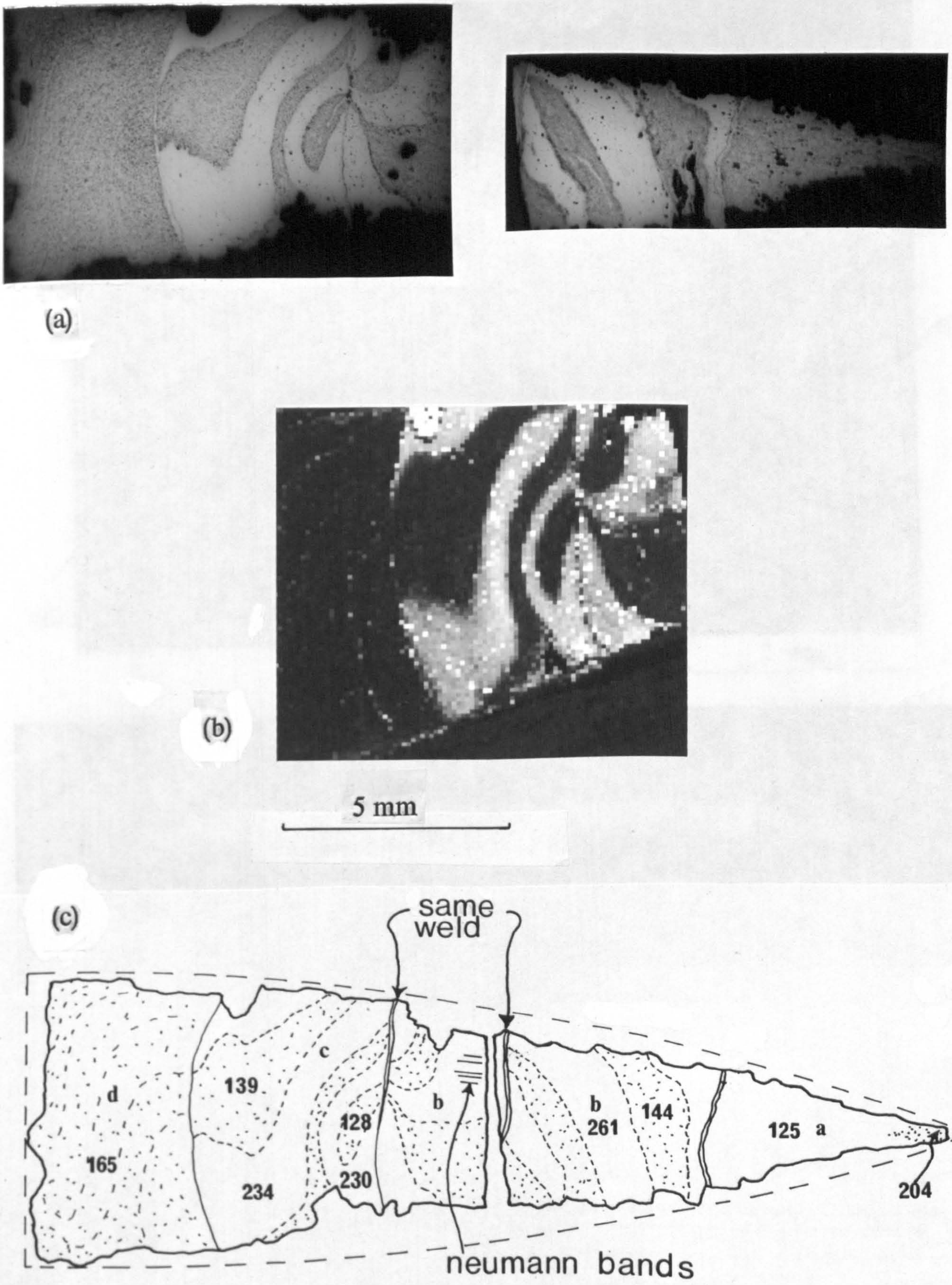

Fig 55 Scramasax S34, from Kempsford: (a) photomacrograph; (b) EPMA phosphorus map; (c) sketch of section; (d) photomicrograph showing fine grain (grey) low carbon and large grain (white) high phosphorus parts; (e) x-radiograph; (f) three-dimensional and surface views

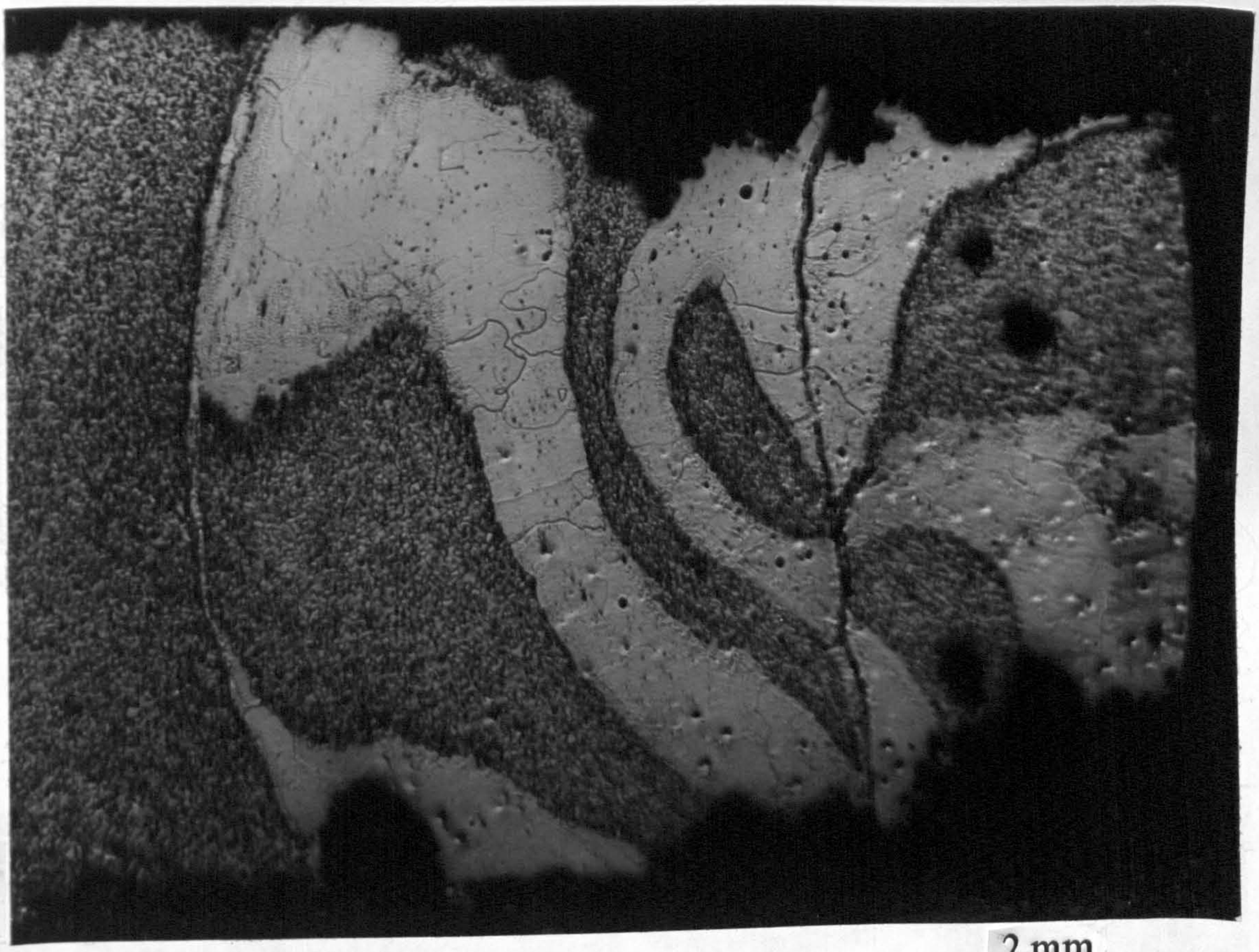

(d)

2 mm

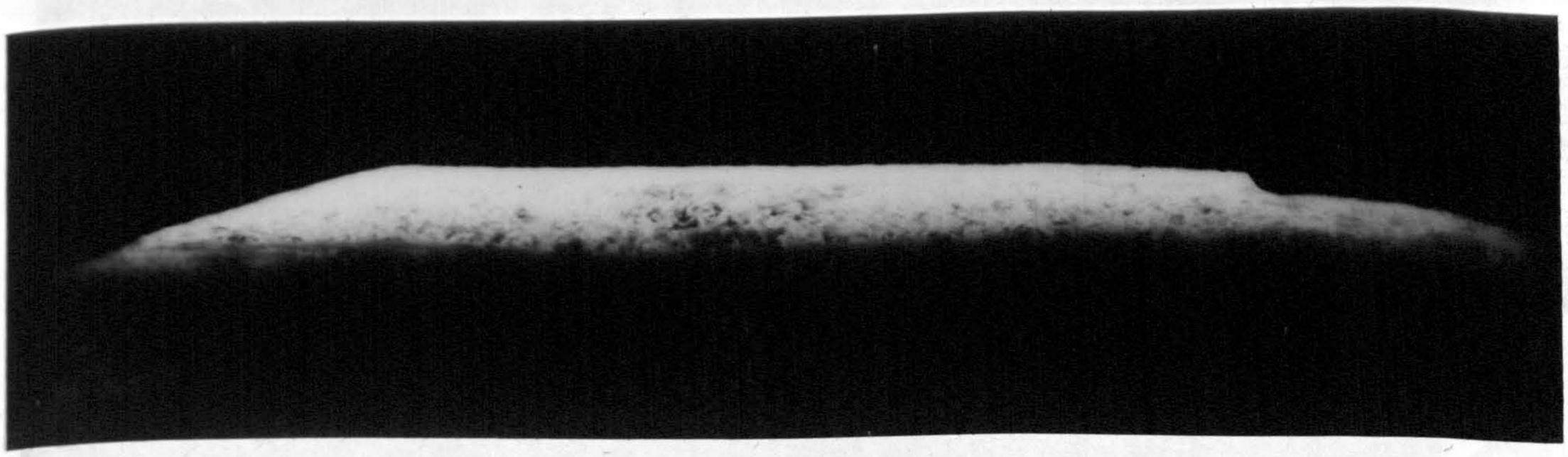

(e)

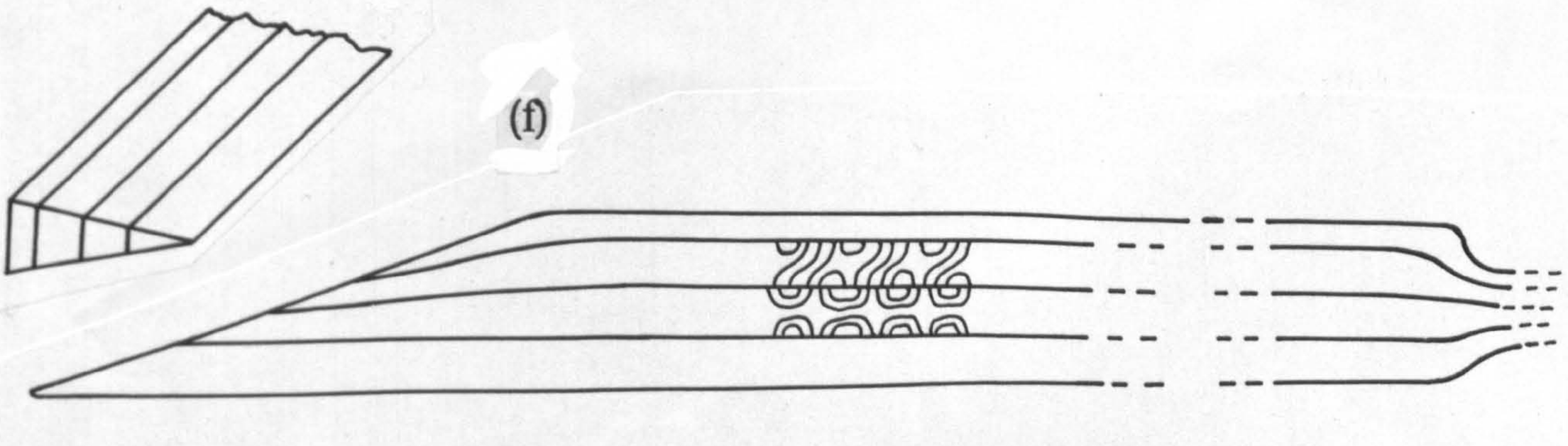

(f)

Fig 55 (continued)

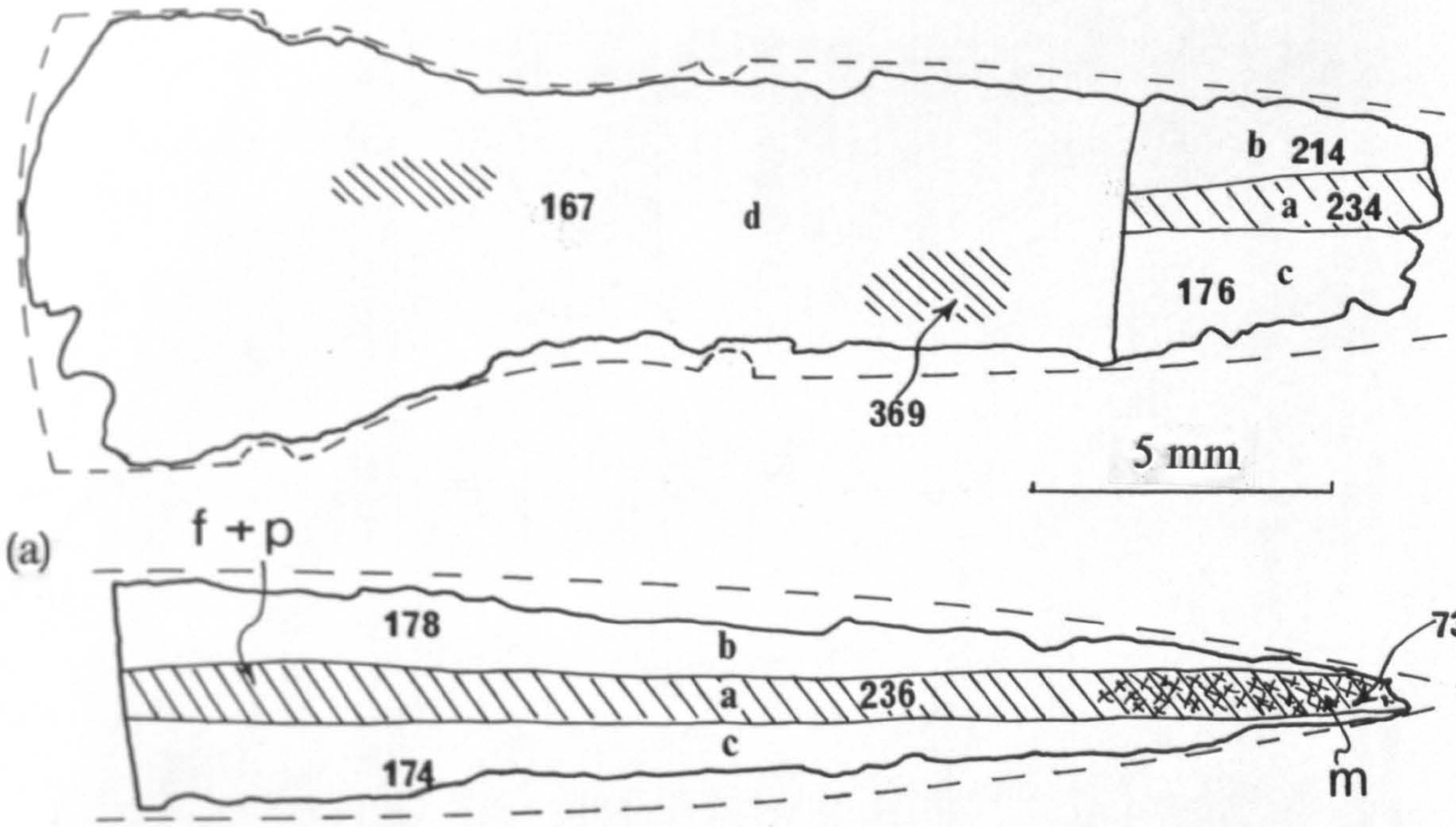

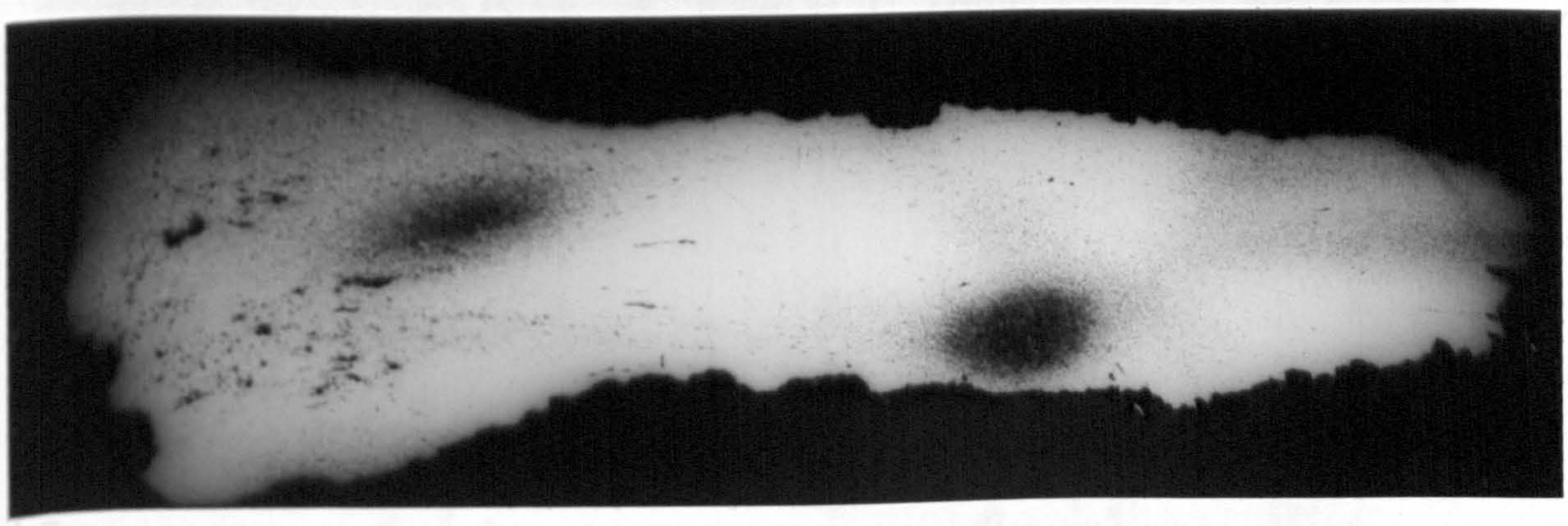

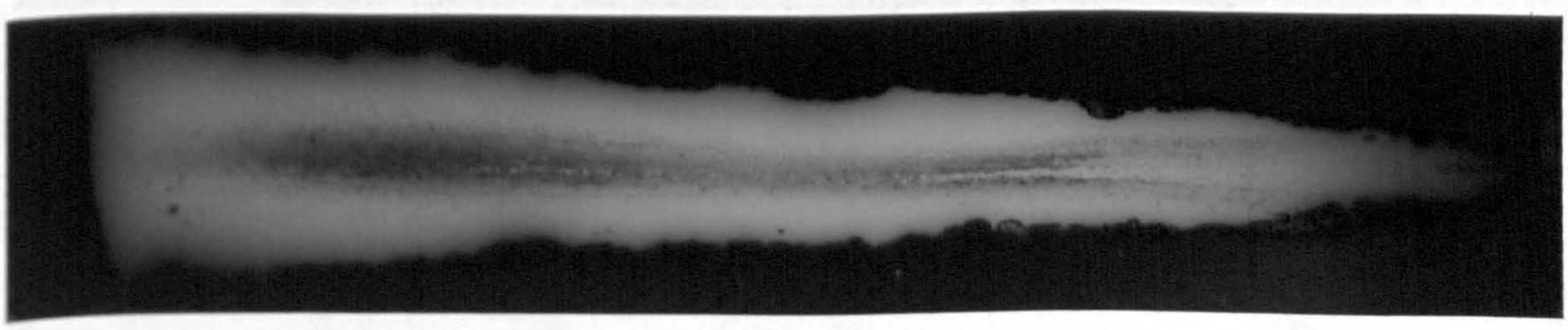

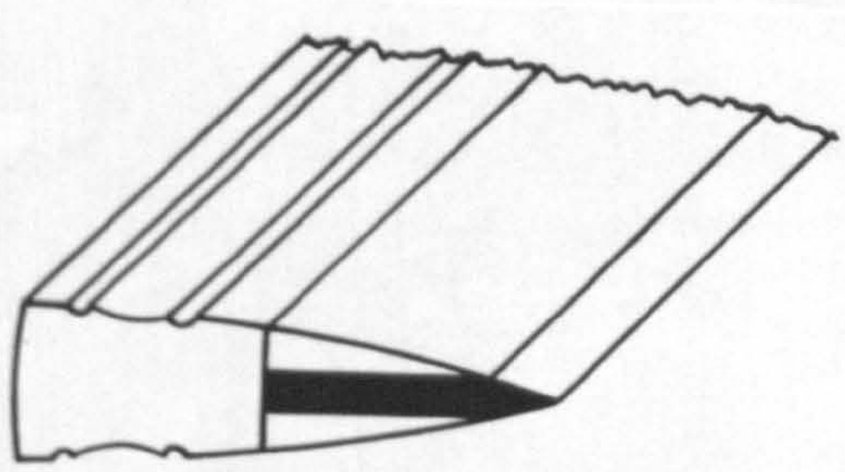

Fig 56 Scramasax S37, from Kempsford: (a) and (b) sketch of section; (c) and (d) photomacrograph; (e) three-dimensional view

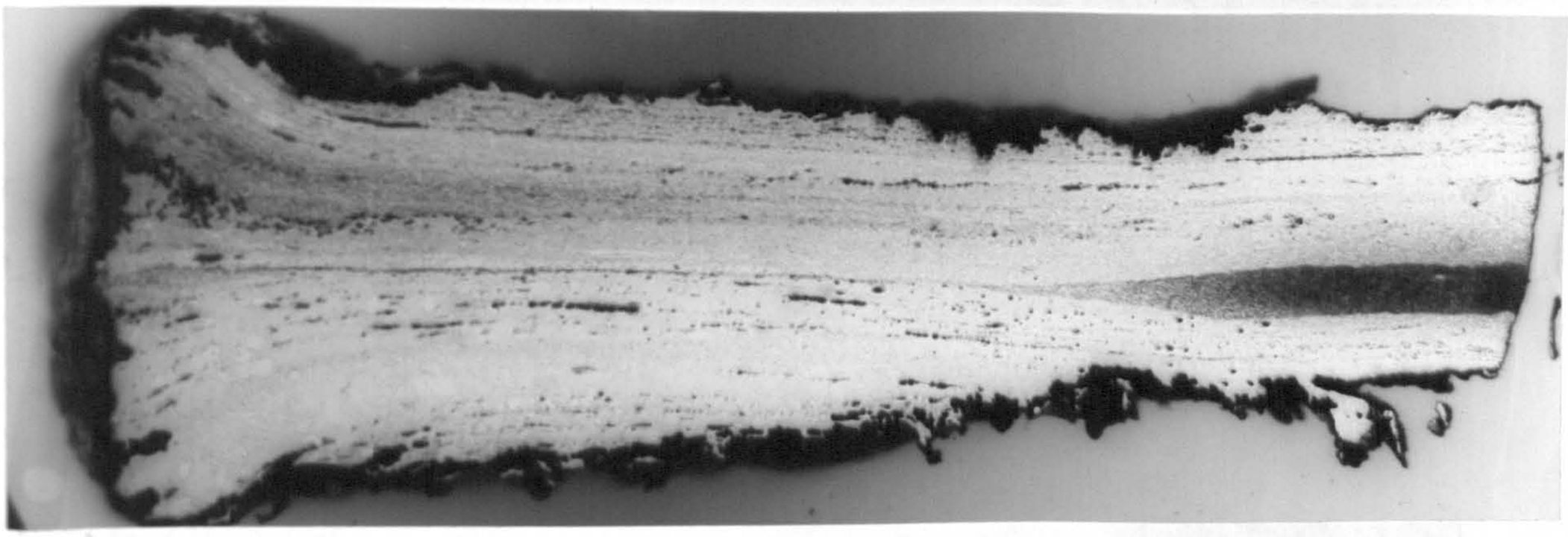

(a)

(b)

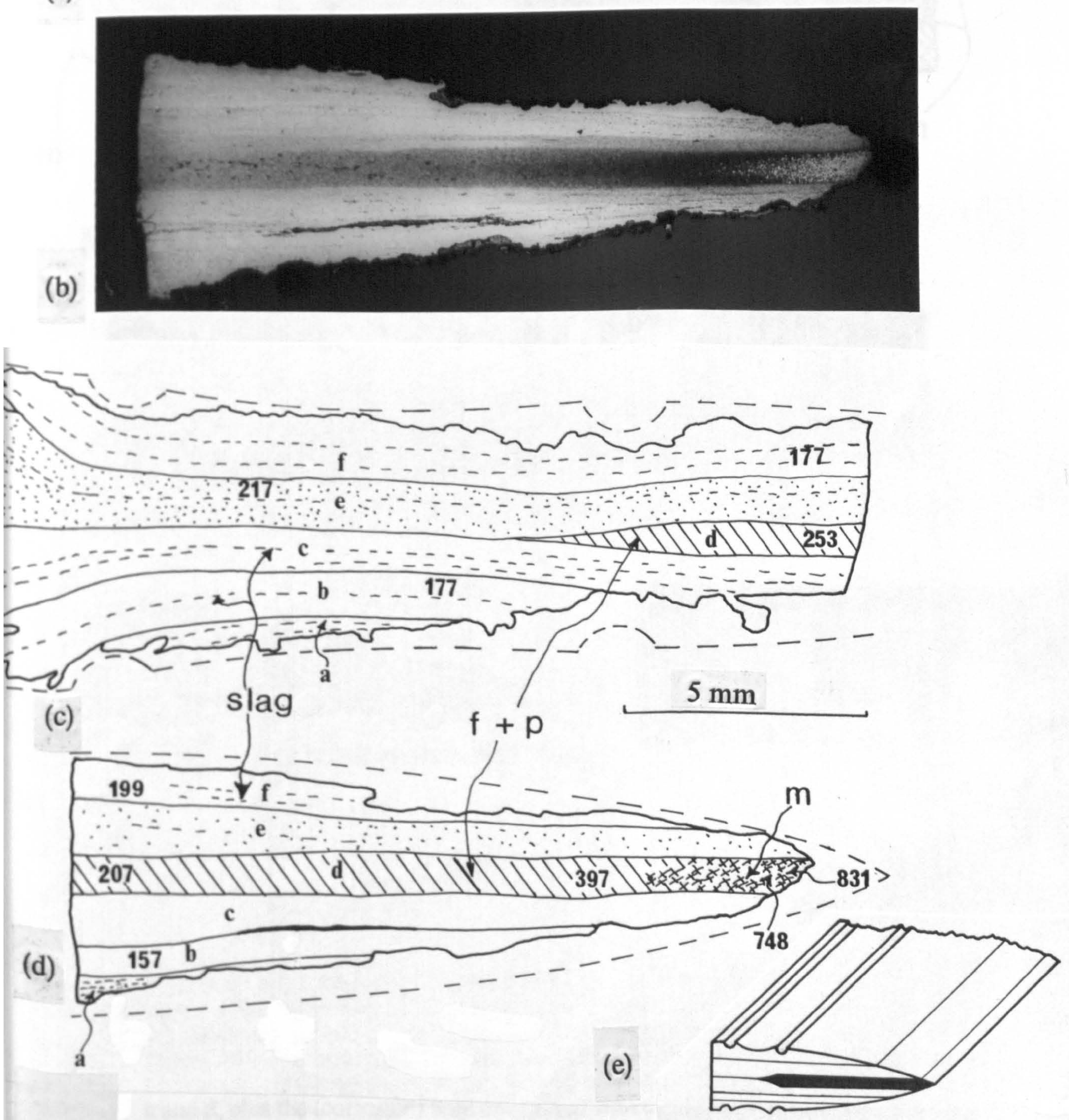

Fig 57 Scramasax S42, from the River Lea at Leyton: (a) and (b) photomacrographs; (c) and (d) sketches of sections; (e) three-dimensional view

(a)

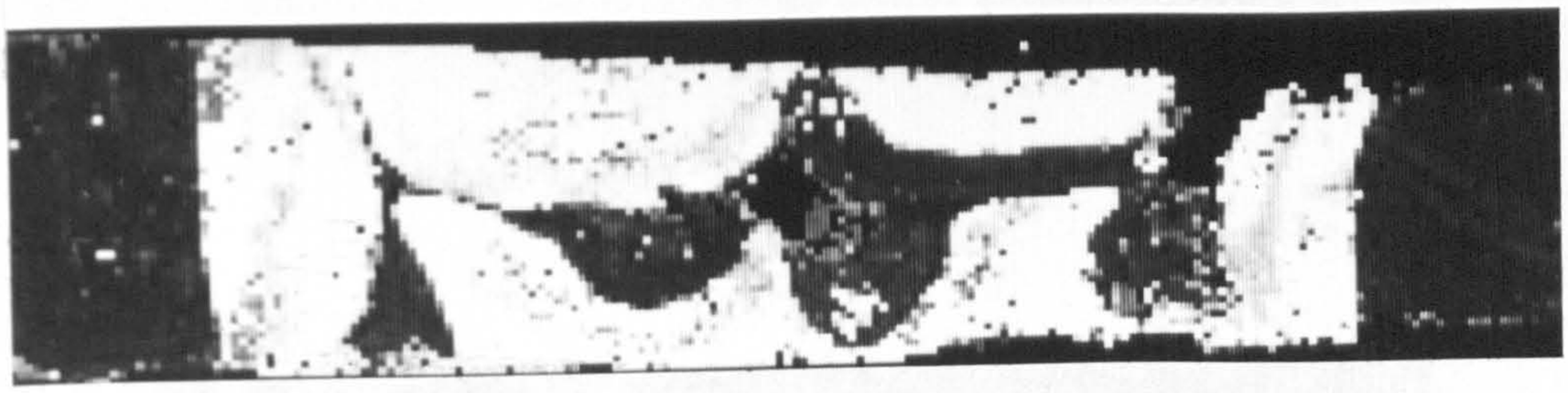

(b)

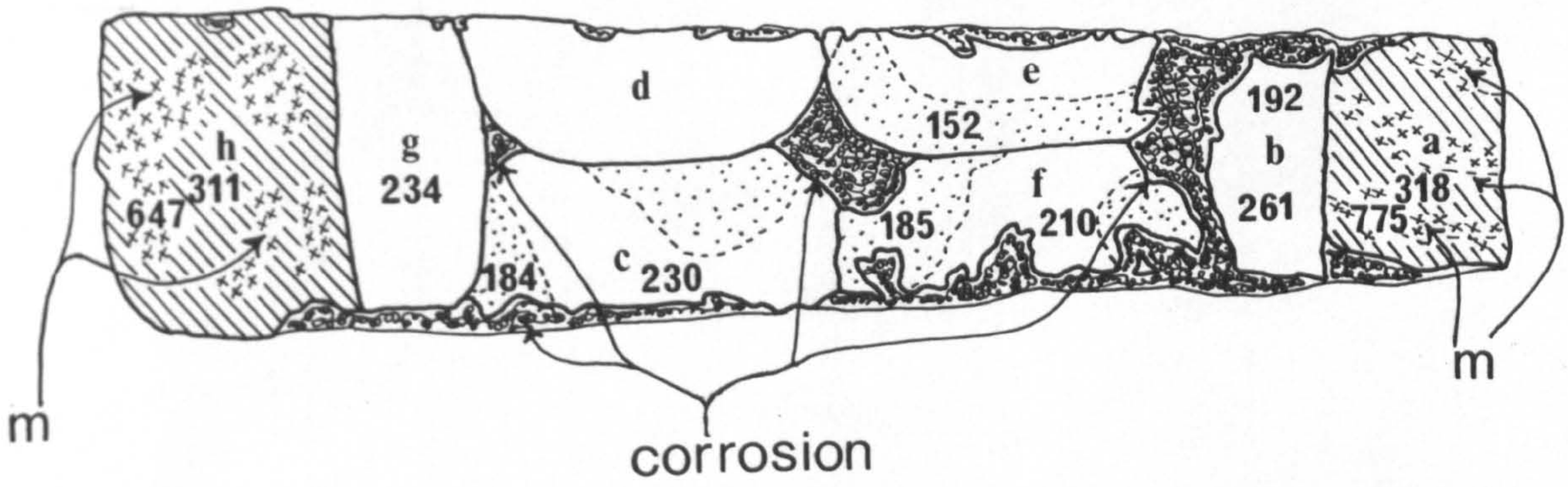

(c)

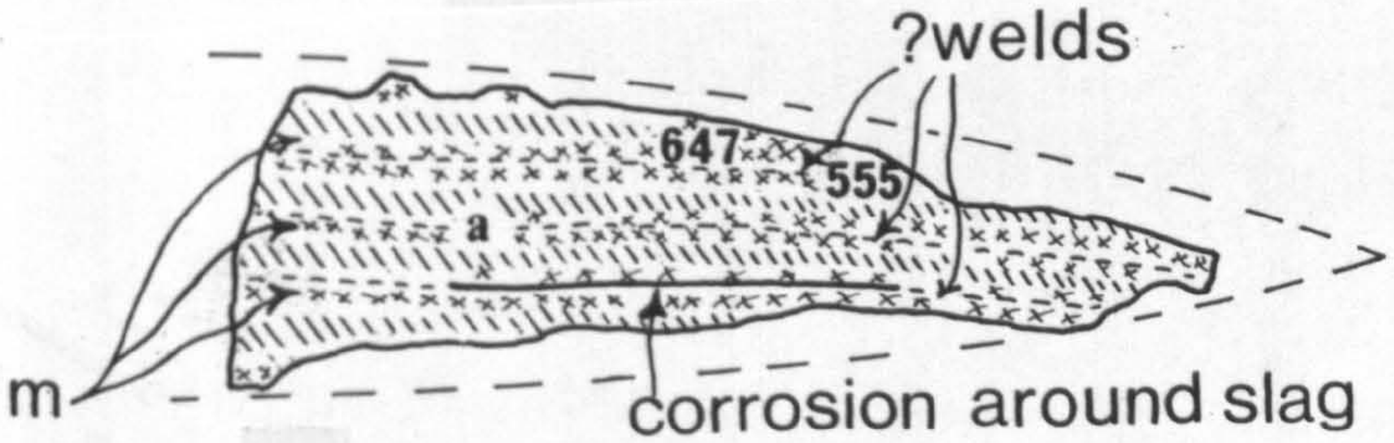

(d)

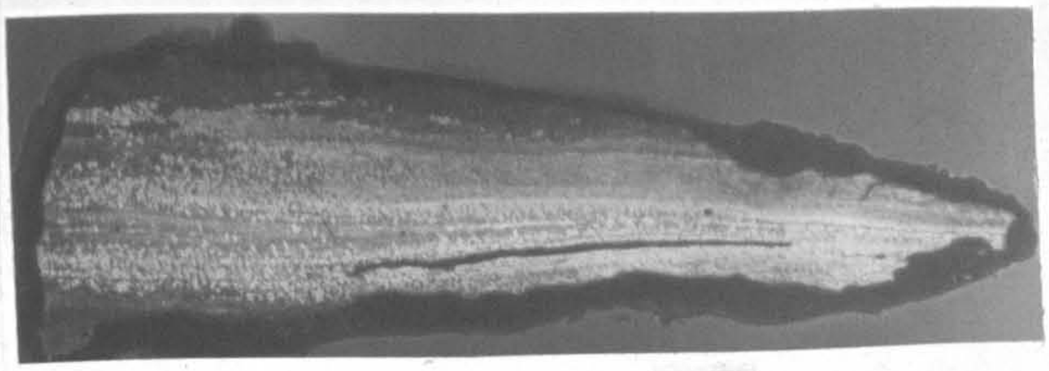

(e)

5 mm

Fig 58 Scramasax S4, from Dorset County Museum: (a) EPMA phosphorus map; (b) sketch of (back) section; (c) photomacrograph; (d) sketch of (cutting edge) section; (e) photomacrograph; (f) photomicrograph showing martensite and radial pearlite (troostite) in the back piece h; (g) photomicrograph showing fine grain (grey) low carbon and very large grain (white) high phosphorus parts of pattern-welded pieces c and d, plus the (corrosion) hold once filled with entrapped smithing slag with some slag surviving in the corner; (h) x-radiograph; (i) surface and three-dimensional reconstruction

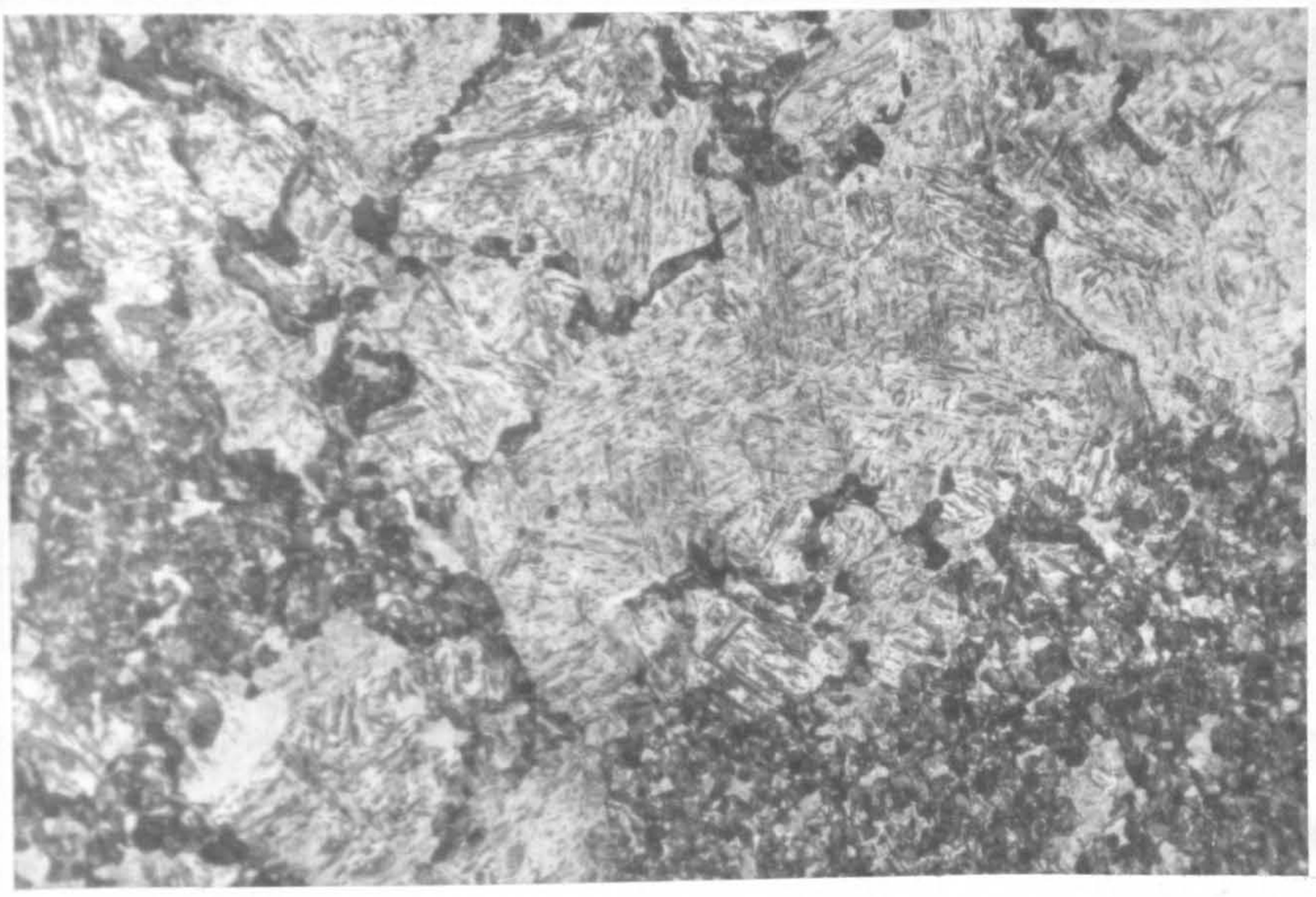

(f) x225

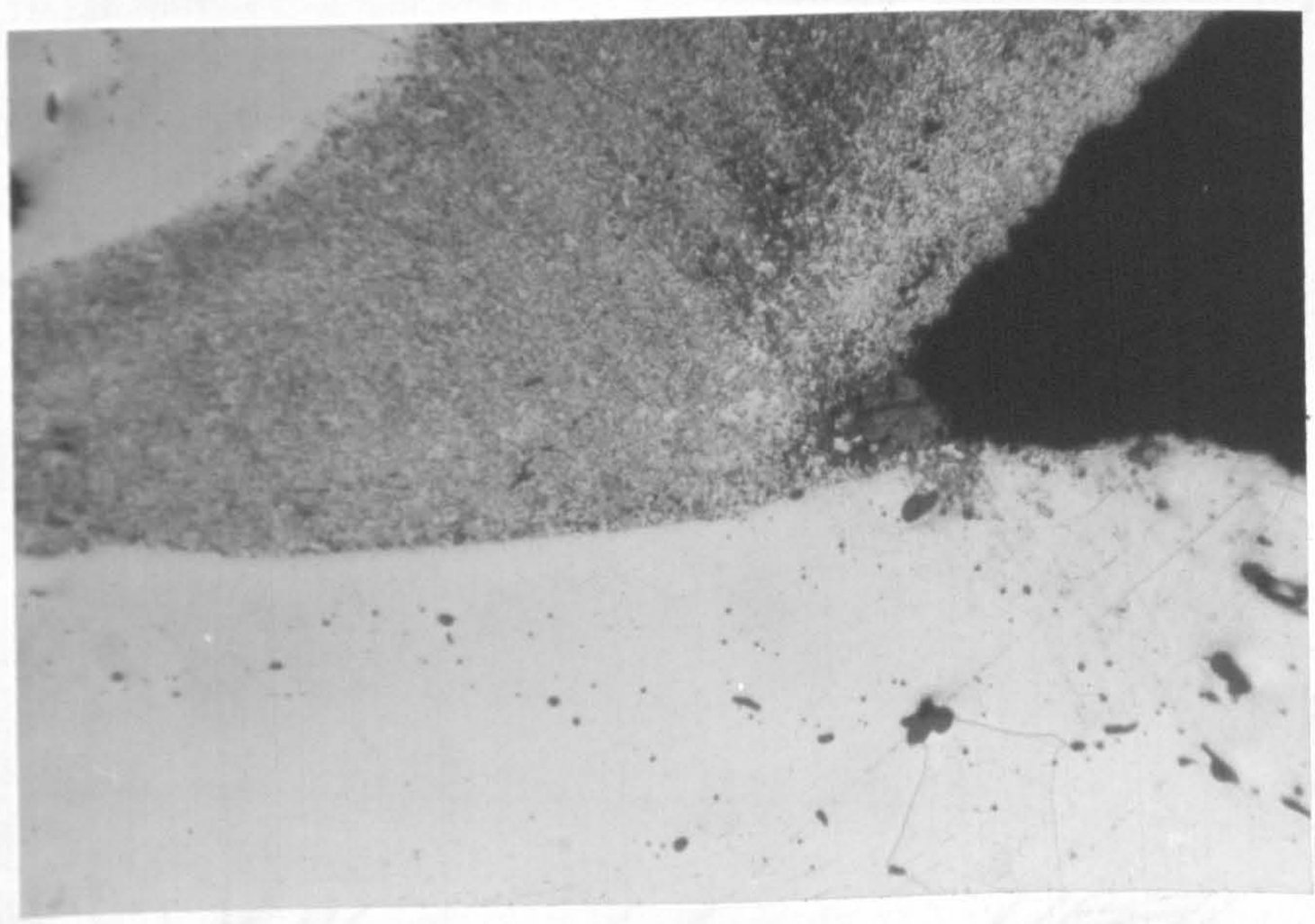

(g) x50

Fig 58 (continued)

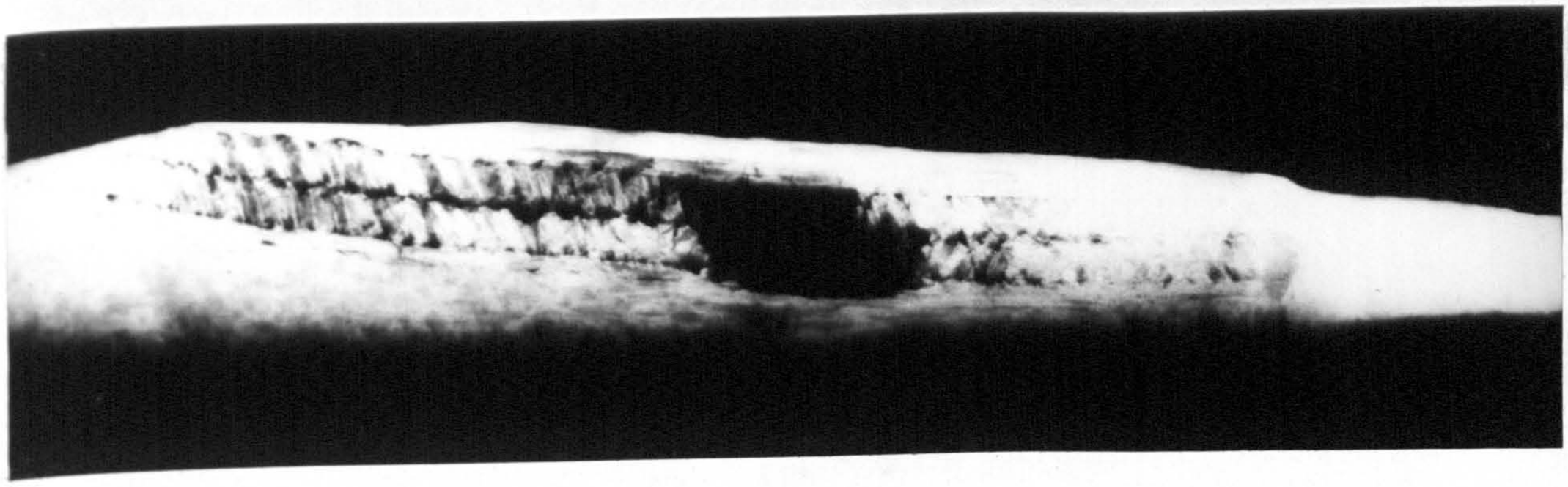

(h)

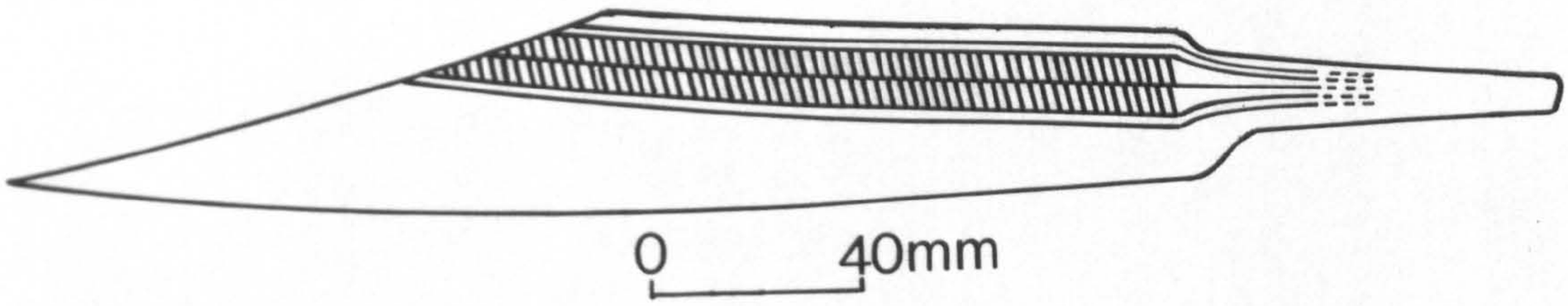

(i)

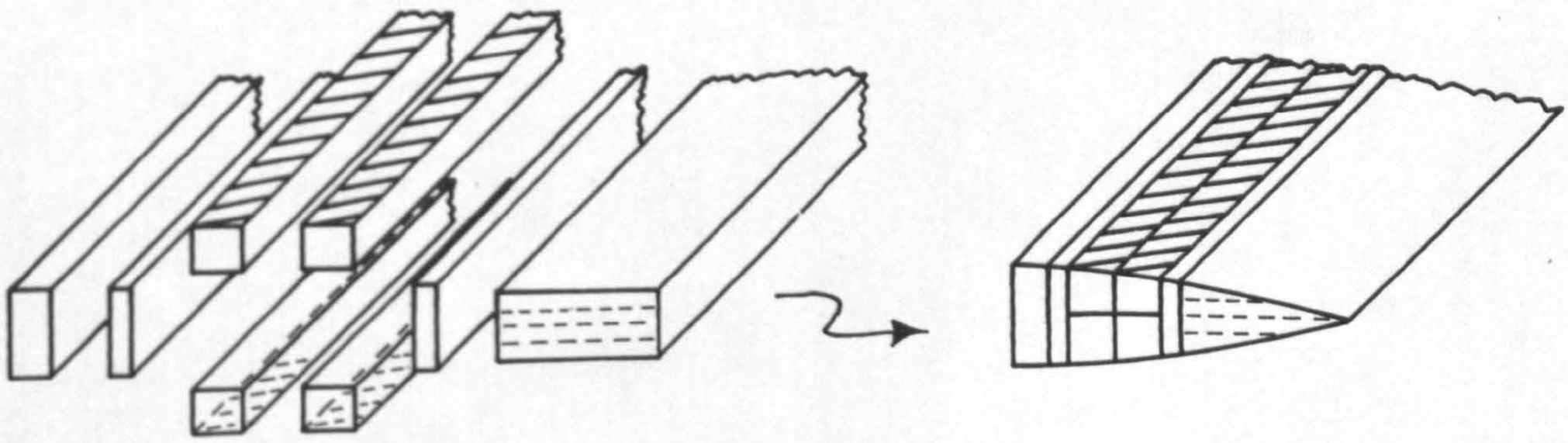

Fig 58 (continued)

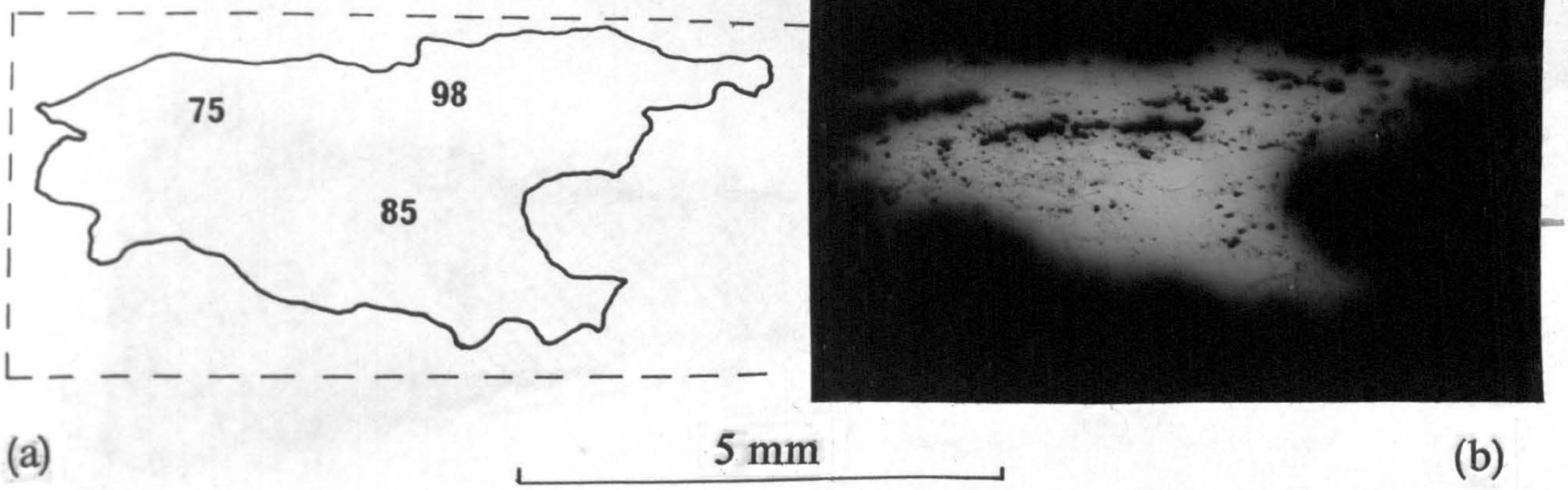

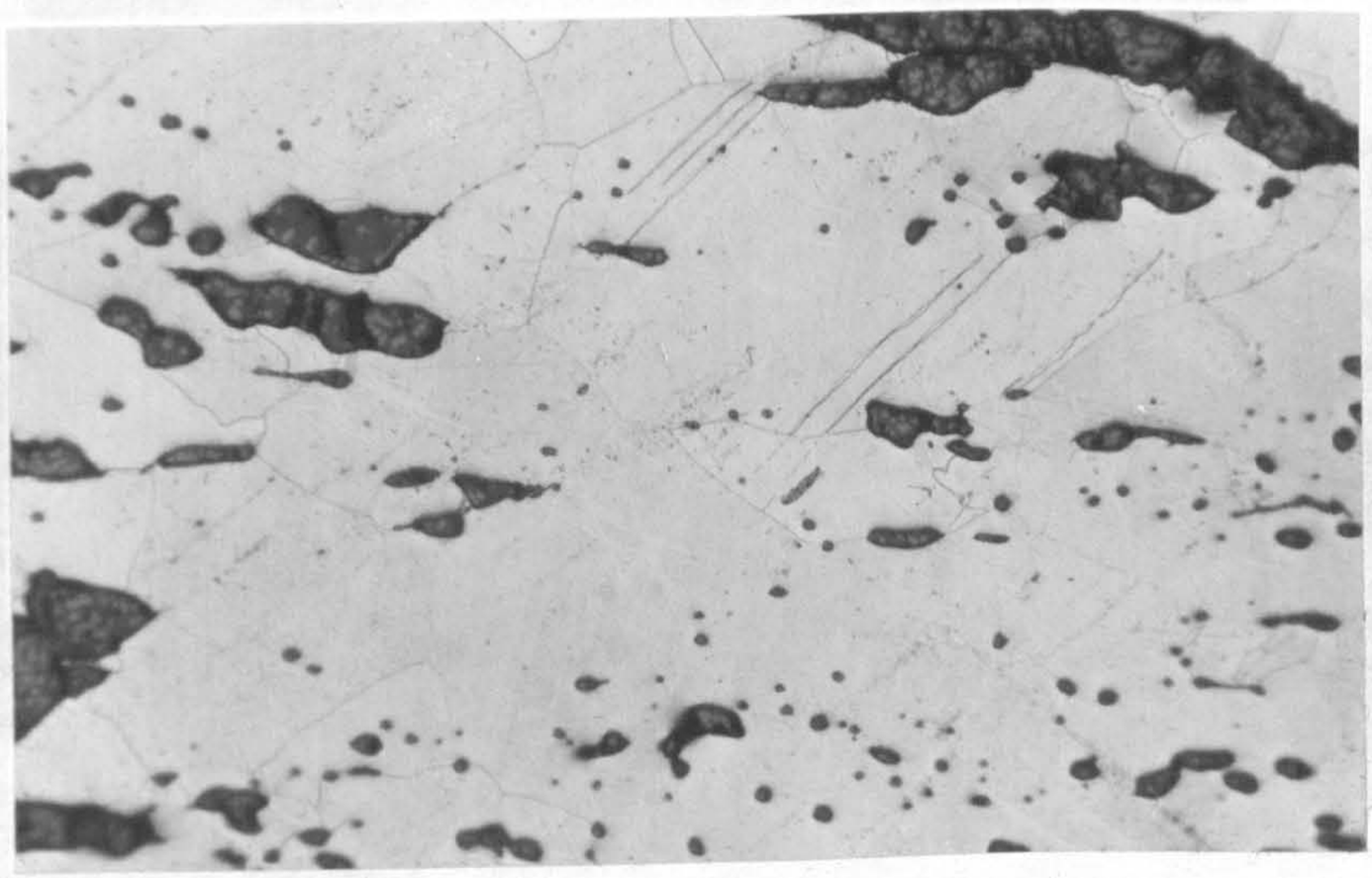

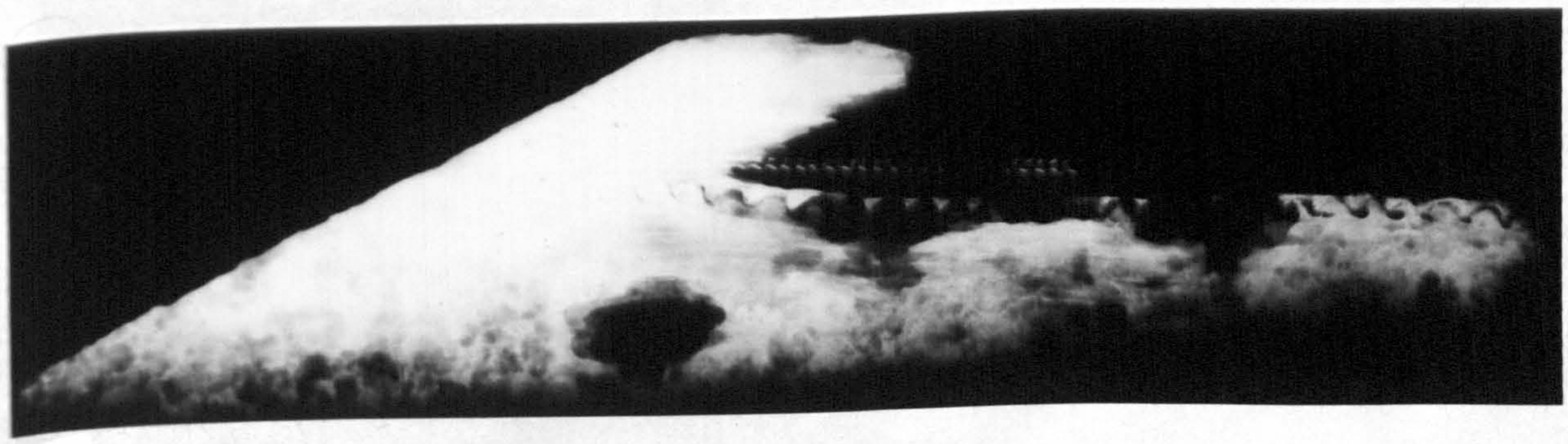

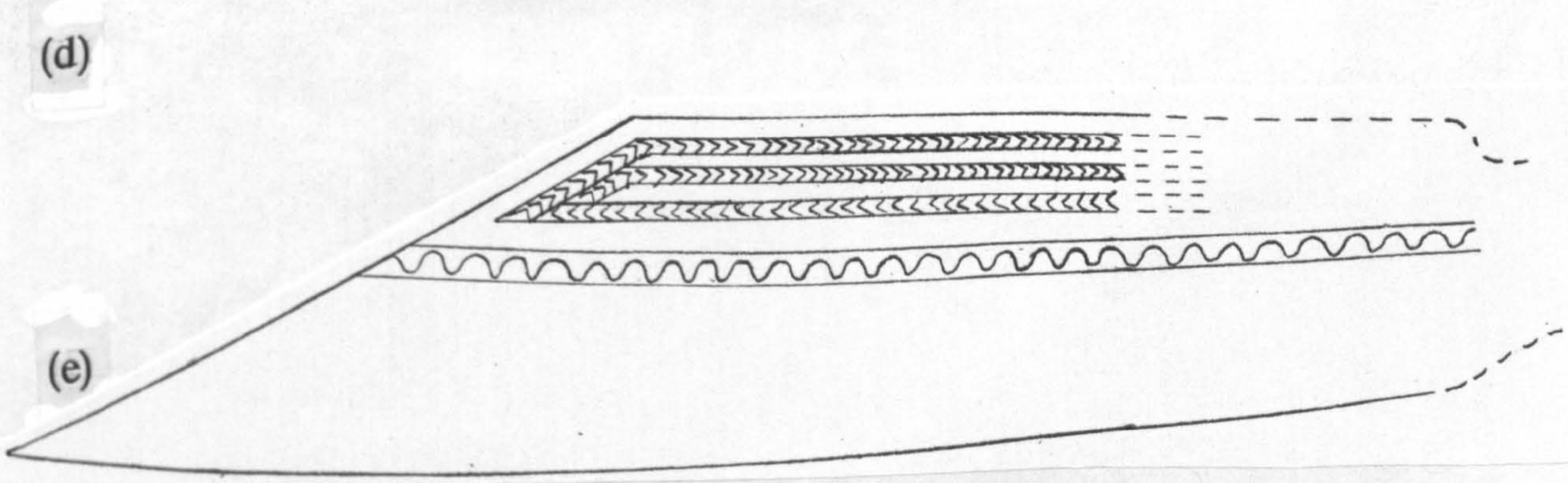

Fig 59 Scramasax S9, from the Thames at Hampton: (a) sketch of section; (b) photomacrograph; (c) photomicrograph showing ferrite plus slag inclusions and neumann bands; (d) x-radiograph; (e) surface view

(a)

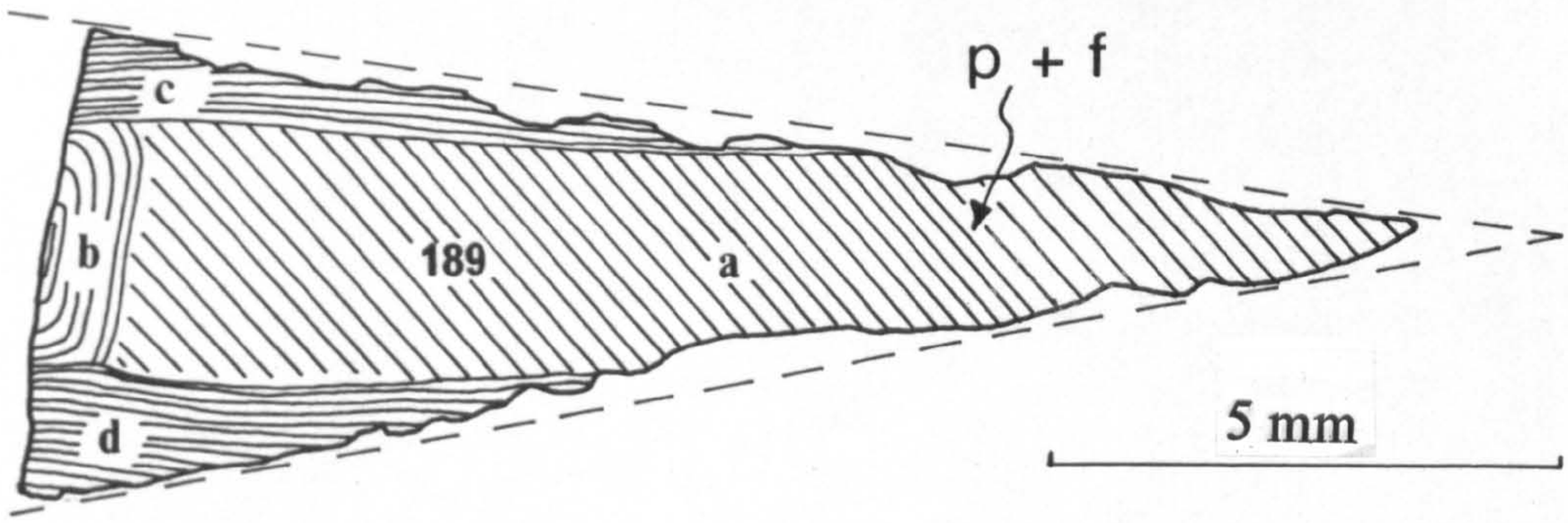

(b)

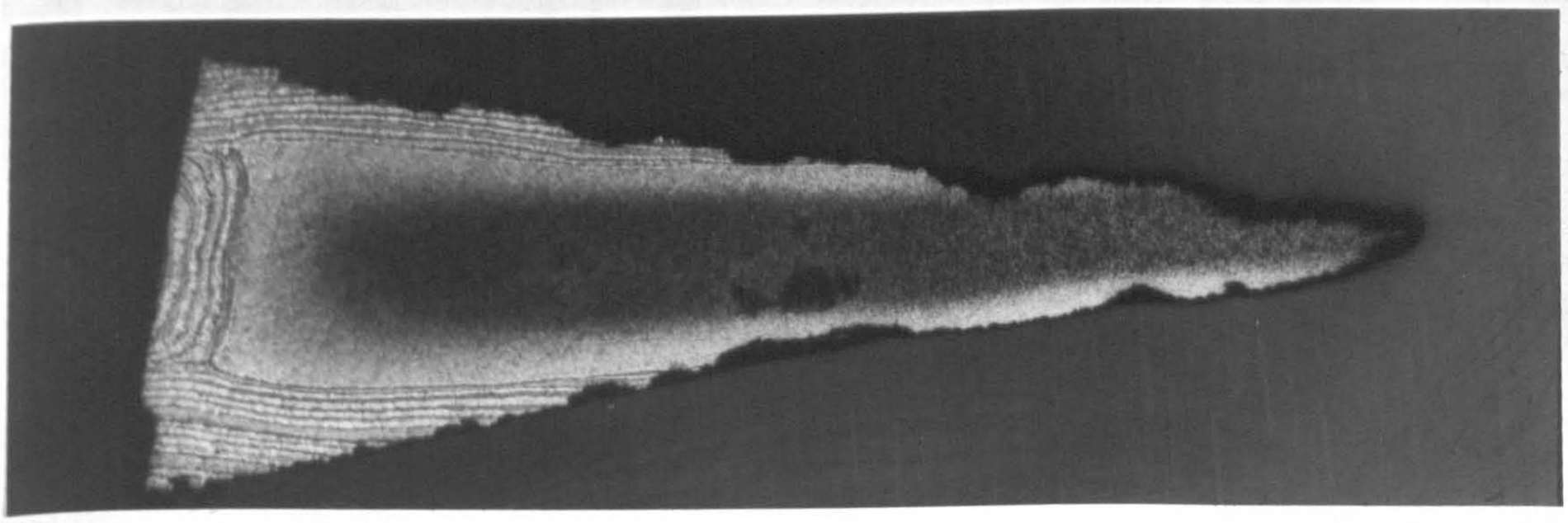

(c)

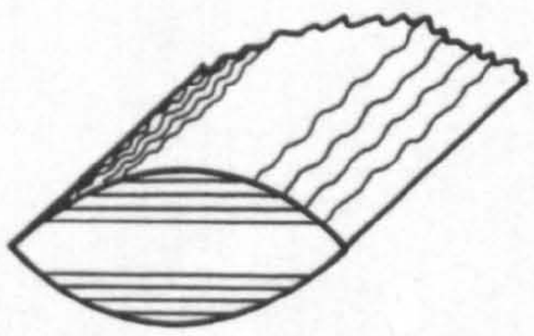

(d)

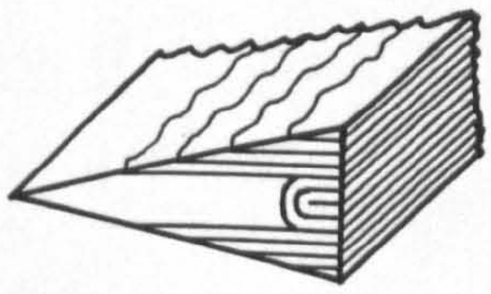

Fig 60 Kris S57 : (a) sketch of section; (b) photomacrograph; (c) three-dimensional views, (i) across projecting shoulder and, (ii) of main part of blade

Fig 61 Spearhead S38, from Kempsford: (a) photomacrograph (b) sketch of section; (c) three-dimensional view

(a)

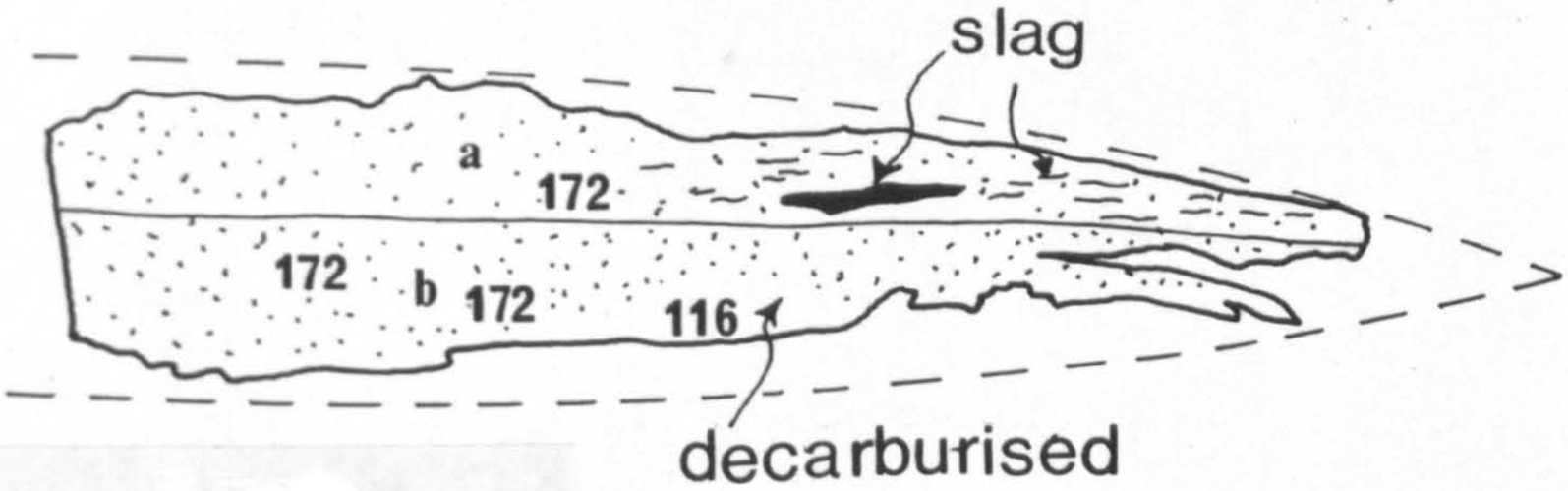

(b)

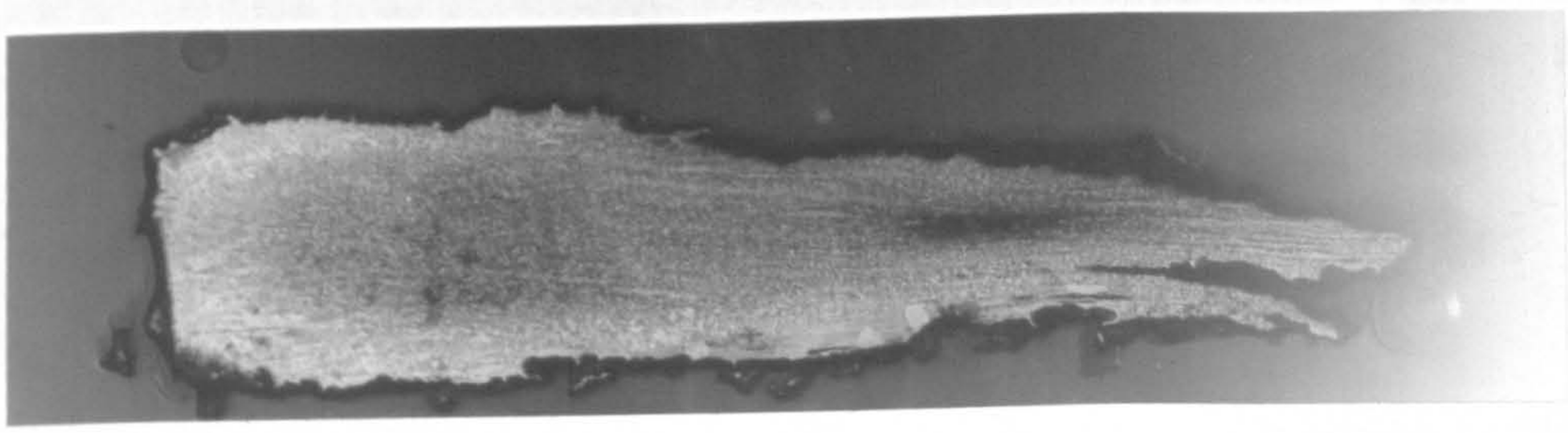

(c)

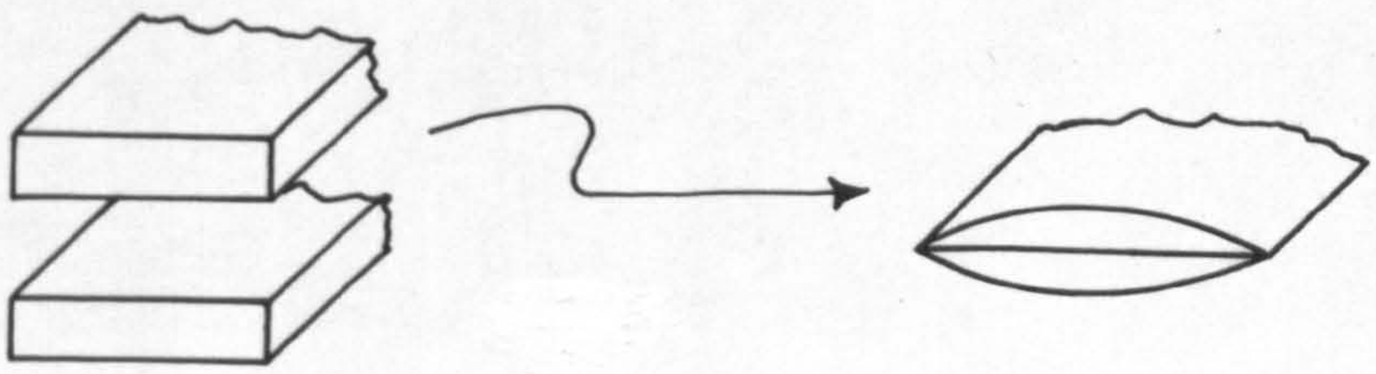

Fig 62 Spearhead S35, from Kempsford; (a) sketch of section; (b) photomacrograph; (c) three-dimensional reconstruction

(a)

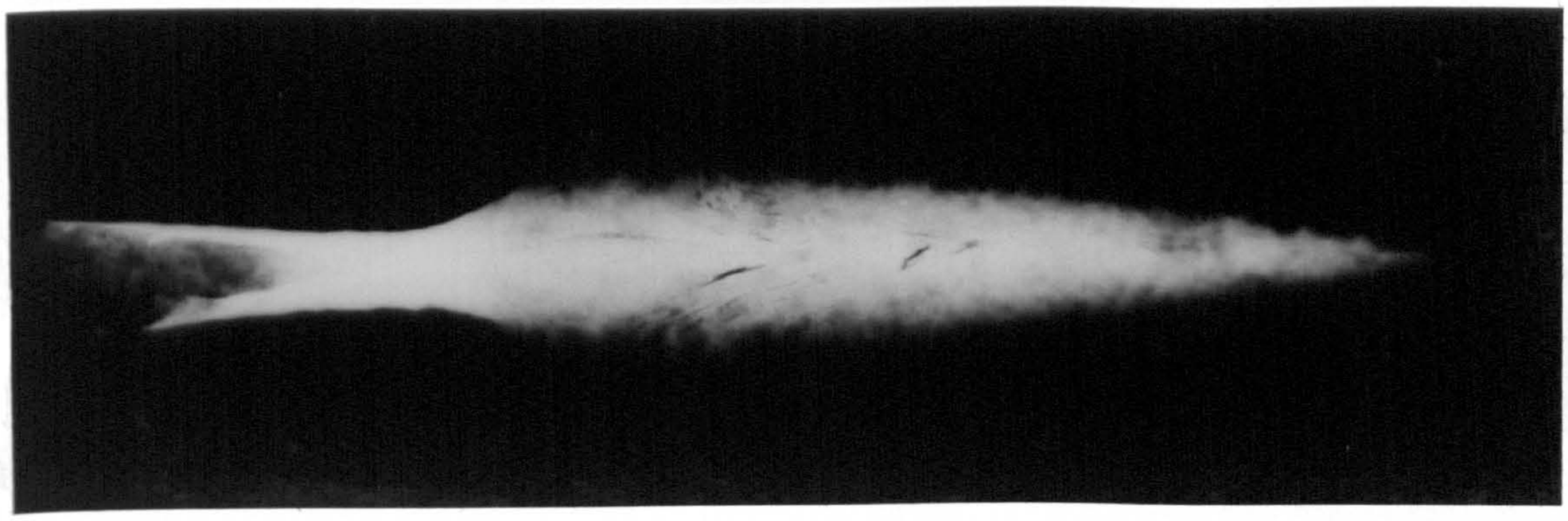

(b)

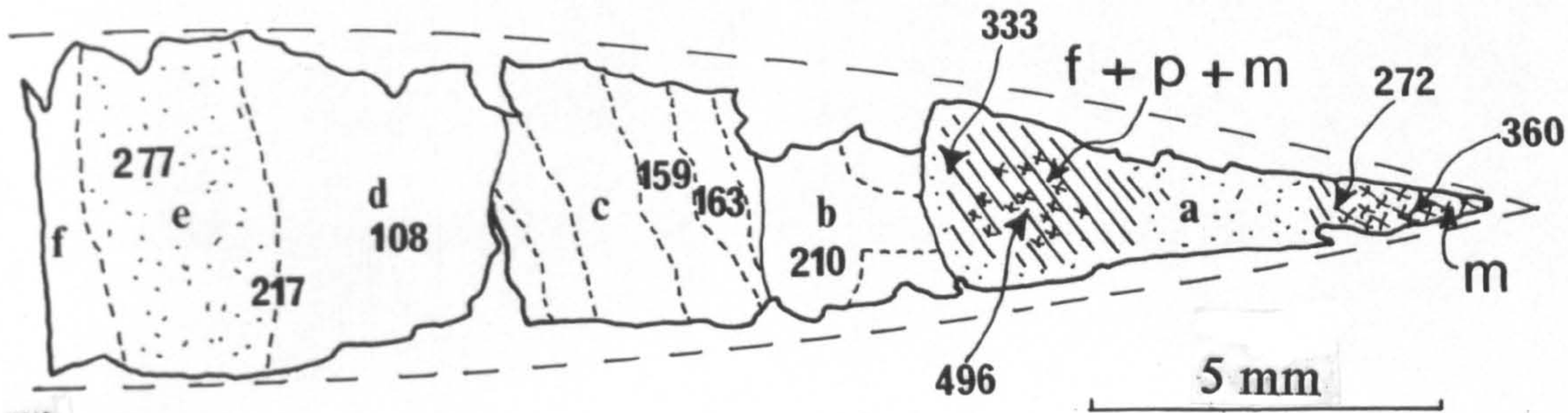

(c)

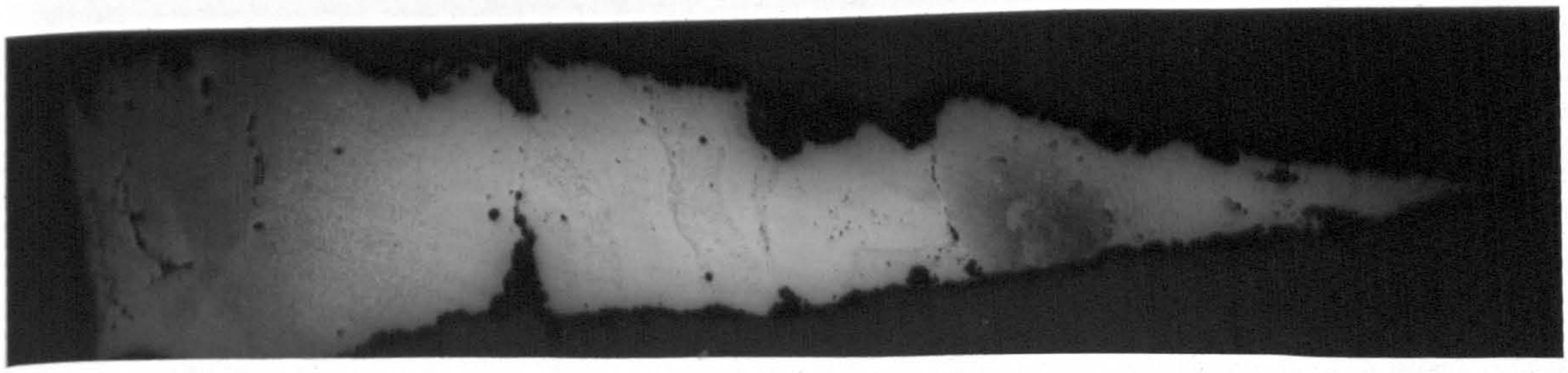

(d)

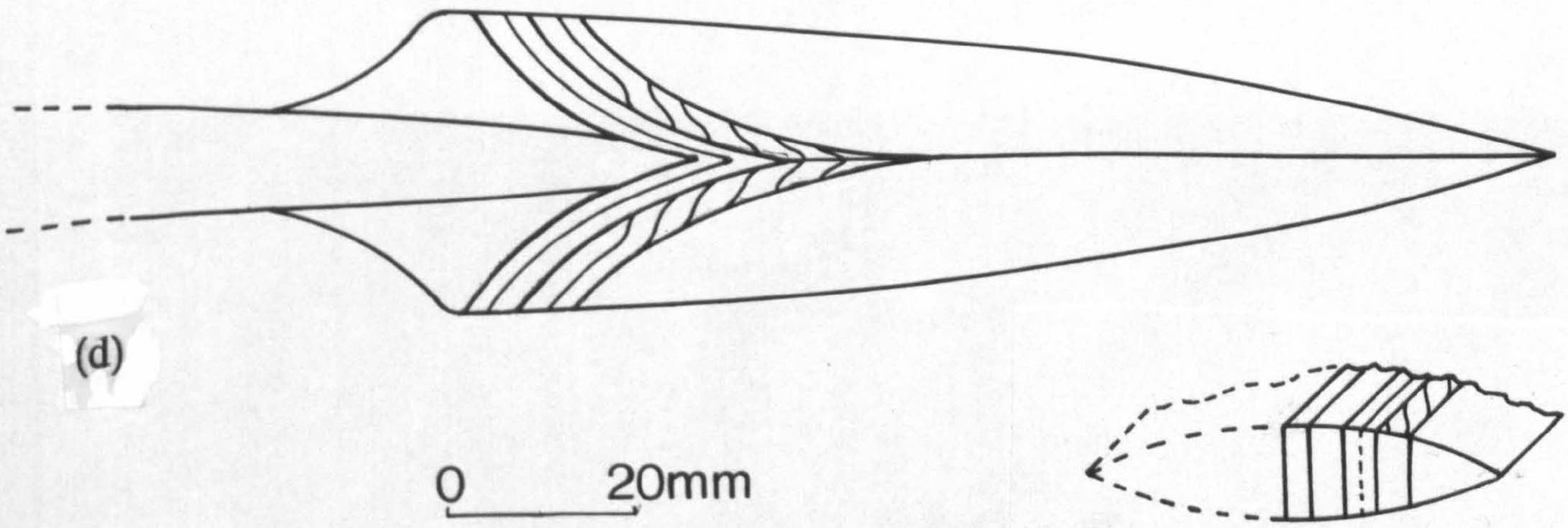

Fig 63 Spearhead S36, from Kempsford: (a) x-radiograph; (b) sketch of section; (c) photomacrograph; (d) surface detail and three dimensional view

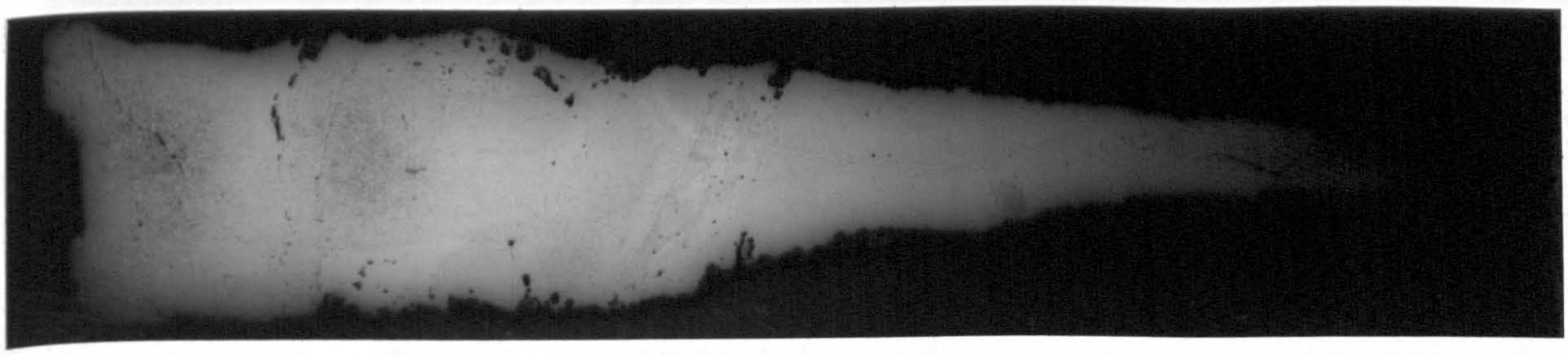

(a)

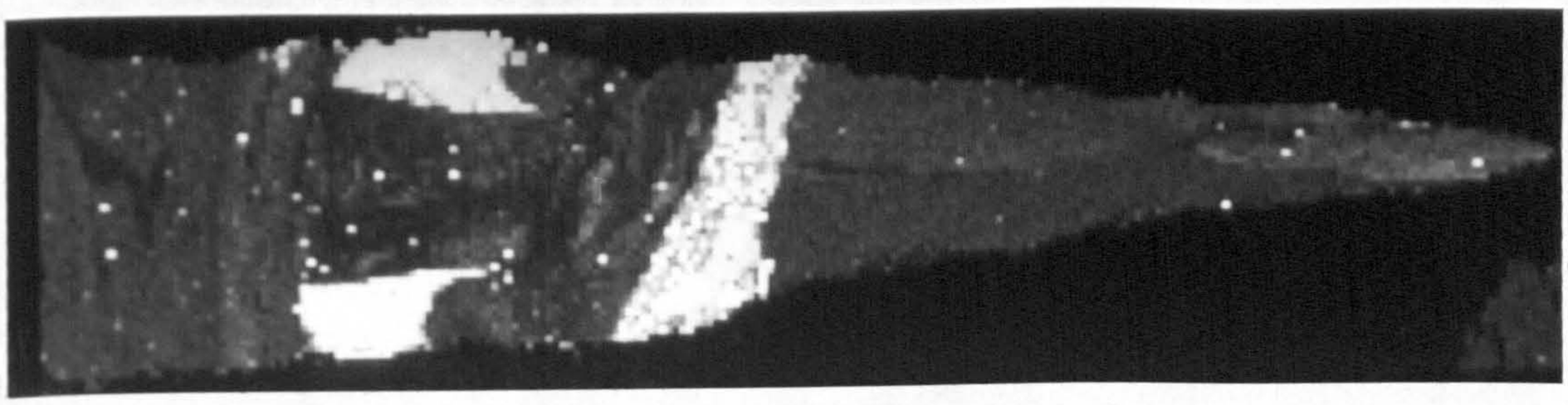

(b)

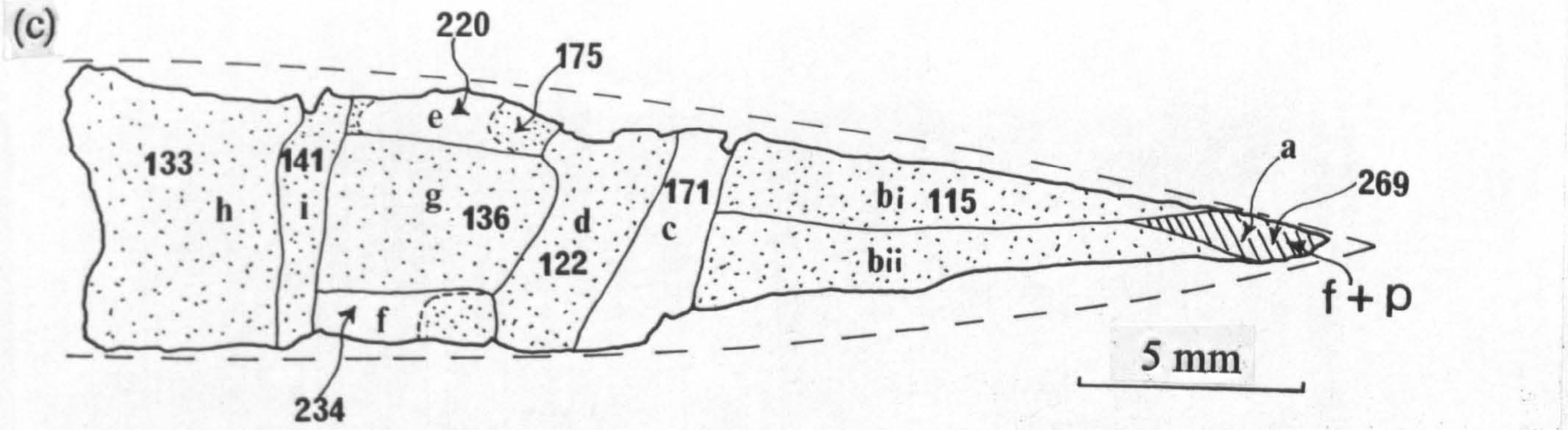

(d)

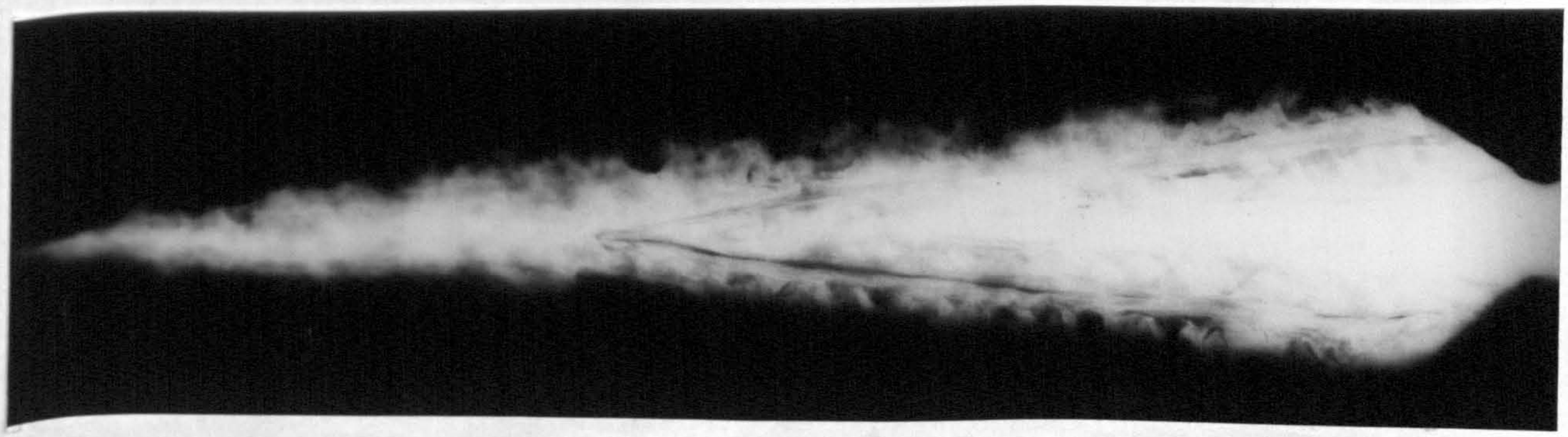

Fig 64 Spearhead S33, from Kempsford: (a) photomacrograph; (b) EPMA phosphorus map; (c) sketch of section; (d) x-radiograph; (e) surface detail; (f) three-dimensional view; (g) section mounted flat-wise to show surface detail especially the wavy weld.

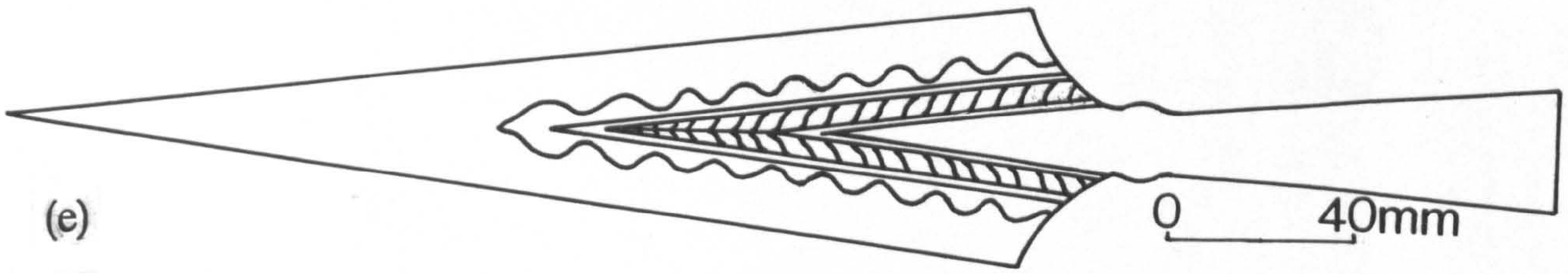

(e)

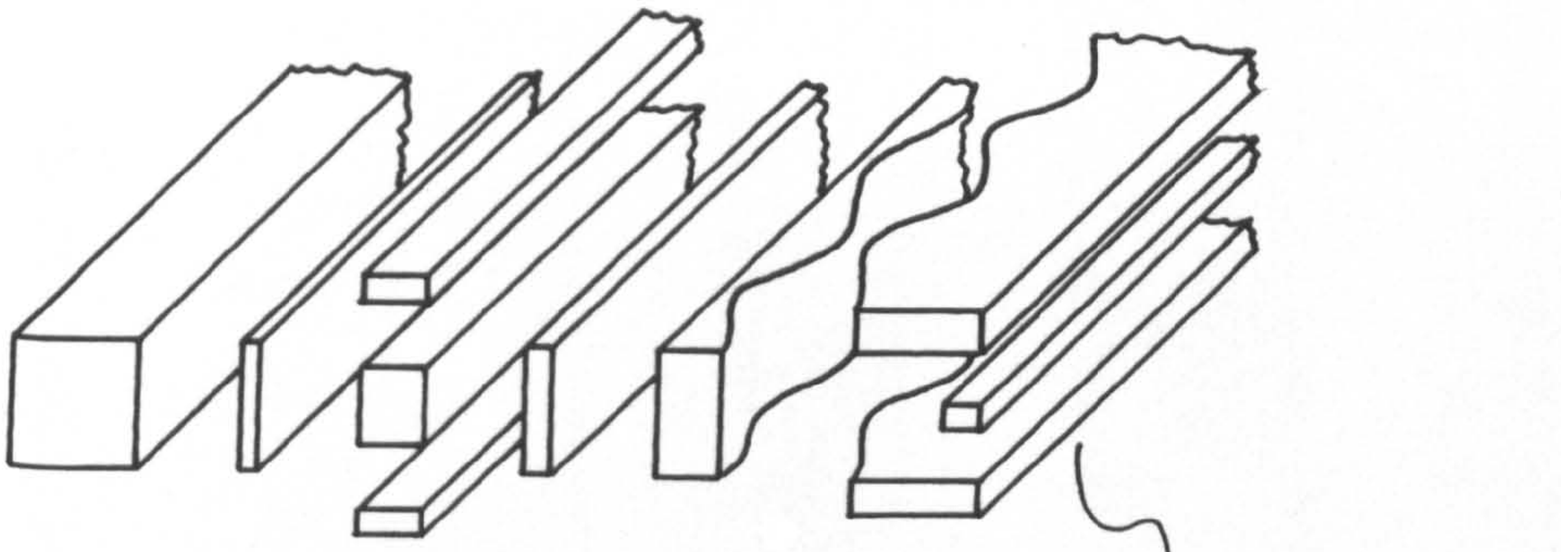

(f)

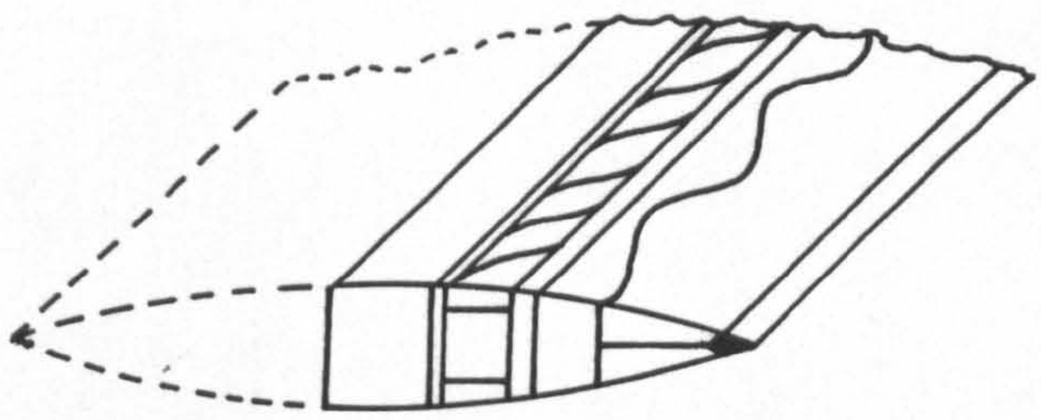

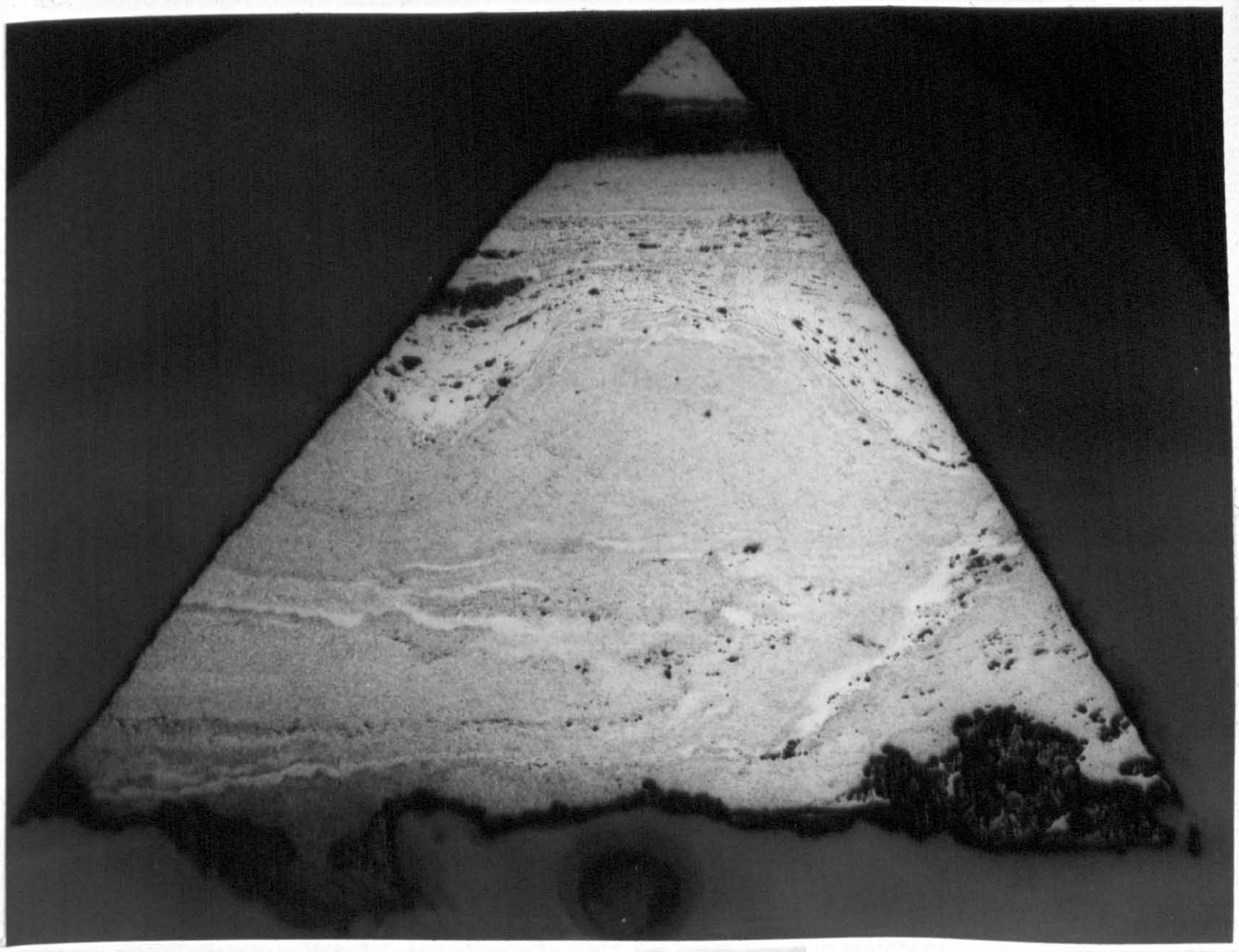

(g)

5 mm

Fig 64 (continued)

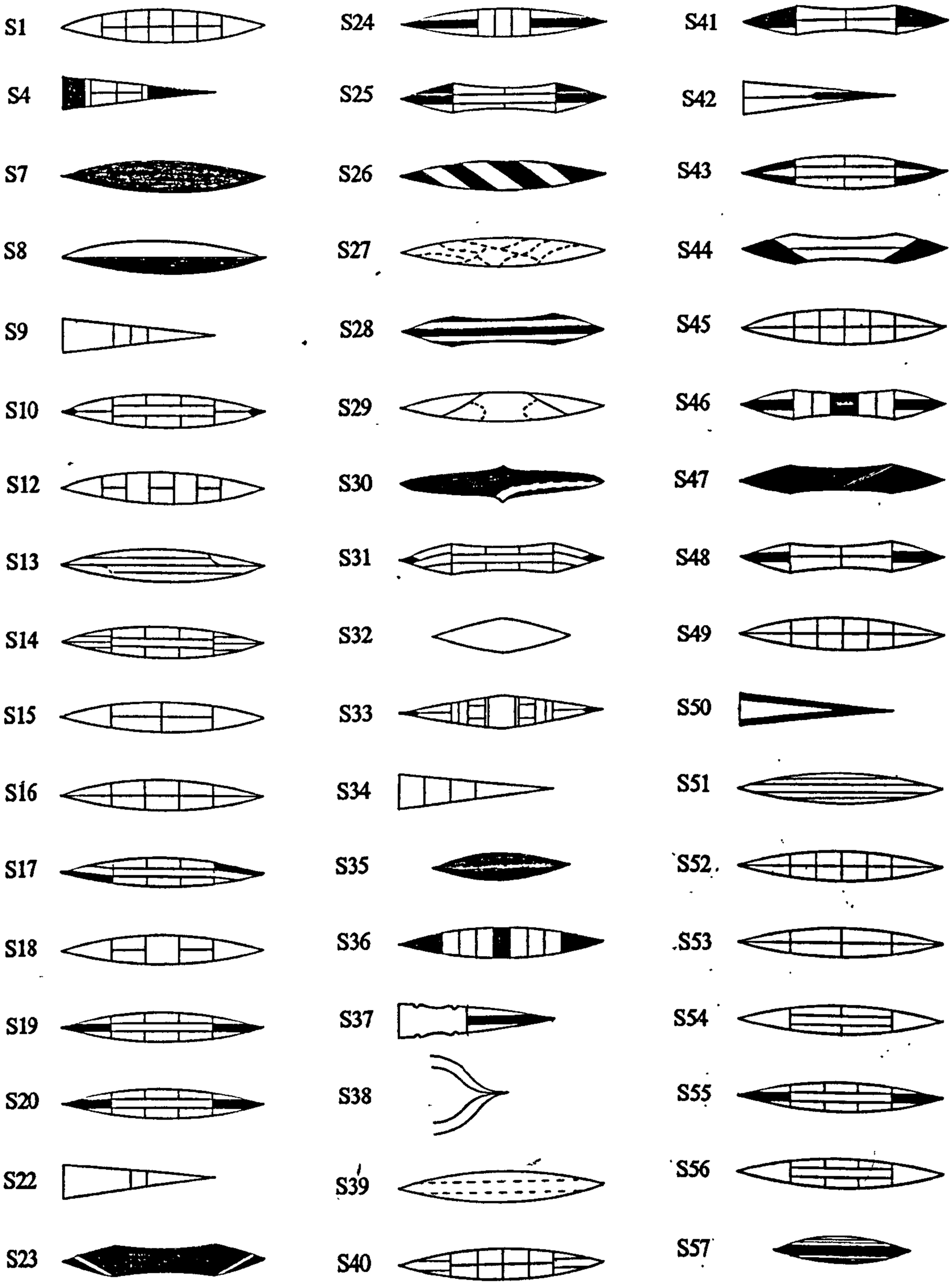

Fig 65 Summary of cross-sectional structures found (Chapters 6 and 7)

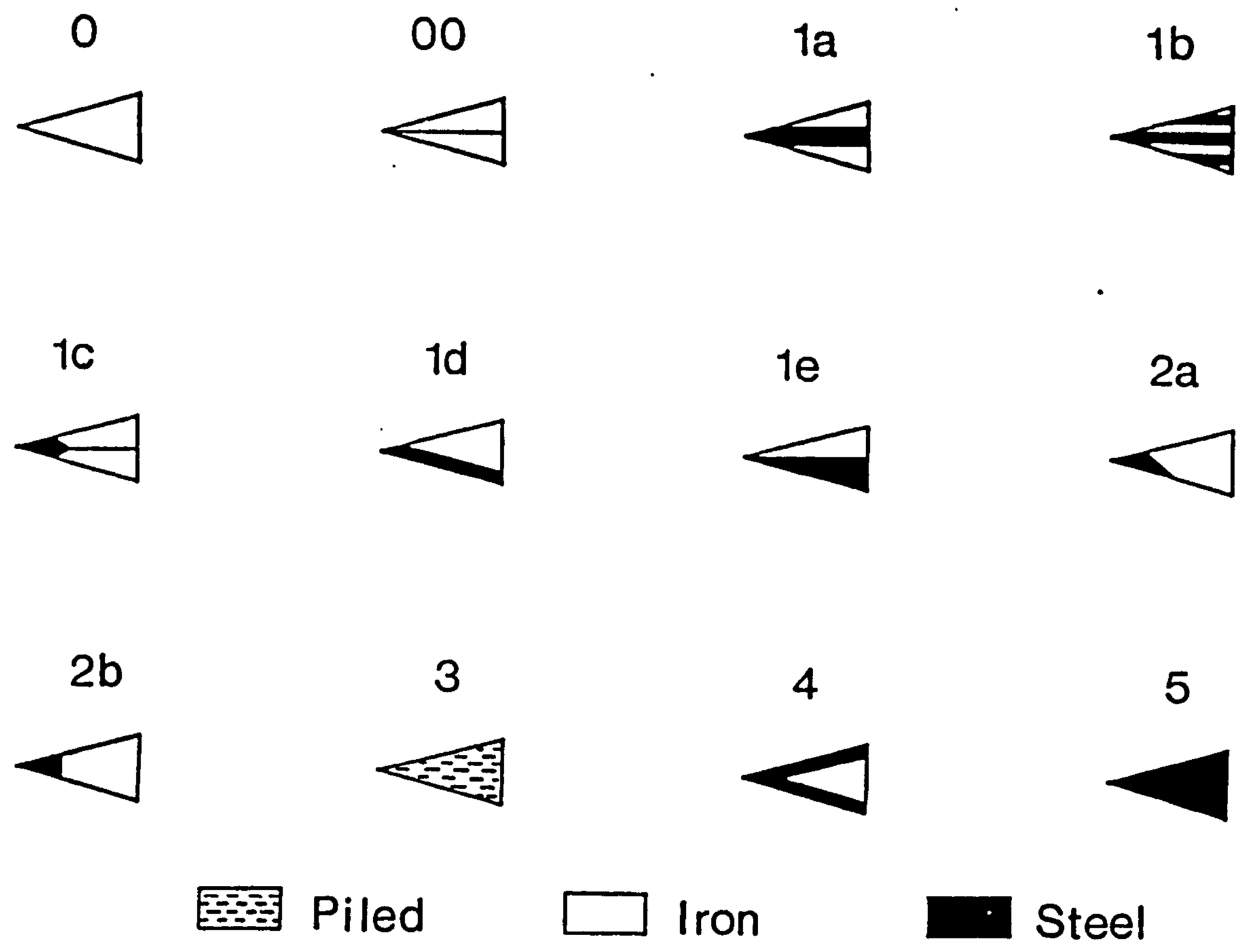

Fig 66 Methods of combining iron and steel to make blades (Chapters 6 and 7)

Main structural types found in pattern-welded blades

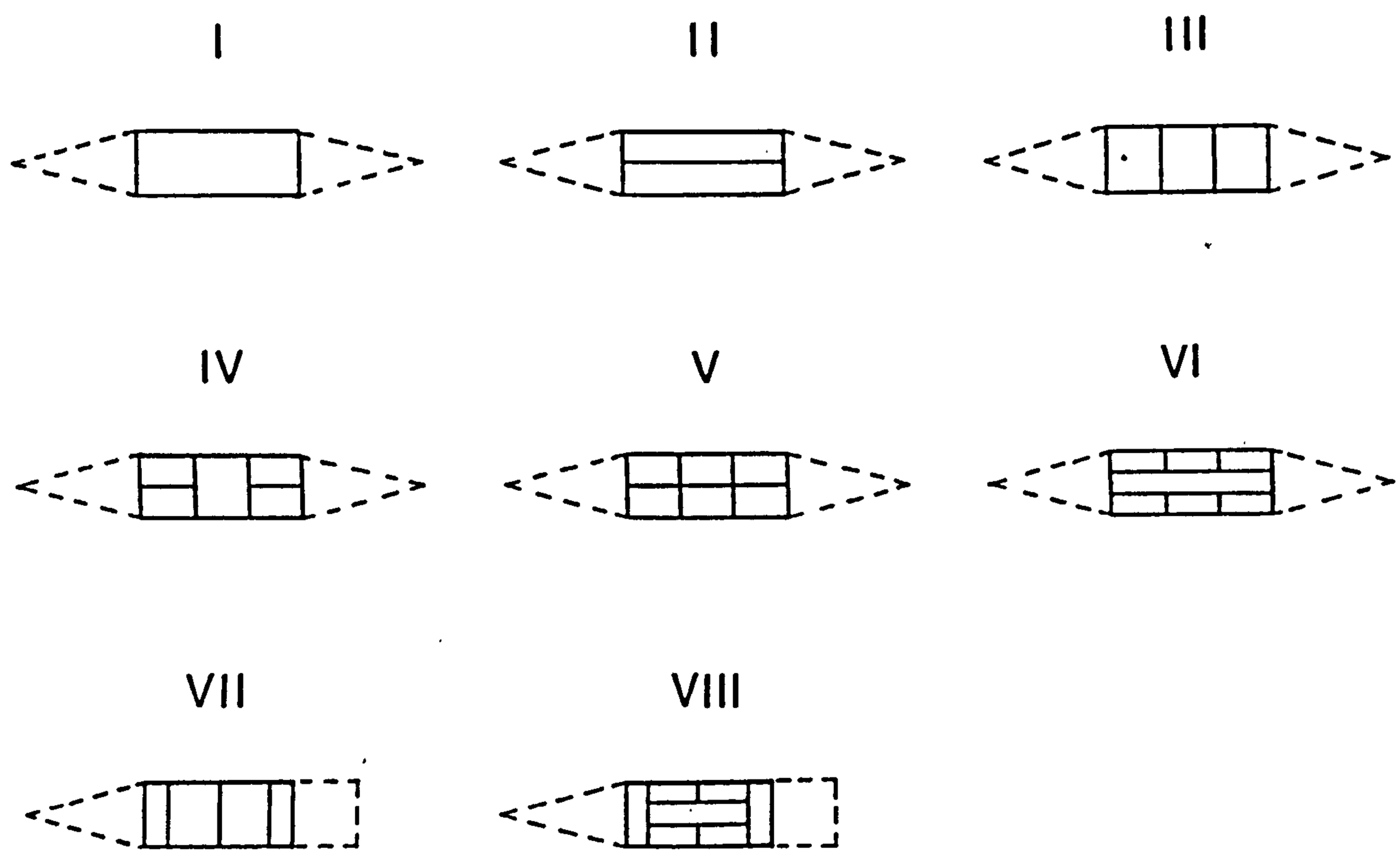

Fig 67 Main structural types found in pattern-welded blades (Chapters 6 and 7)

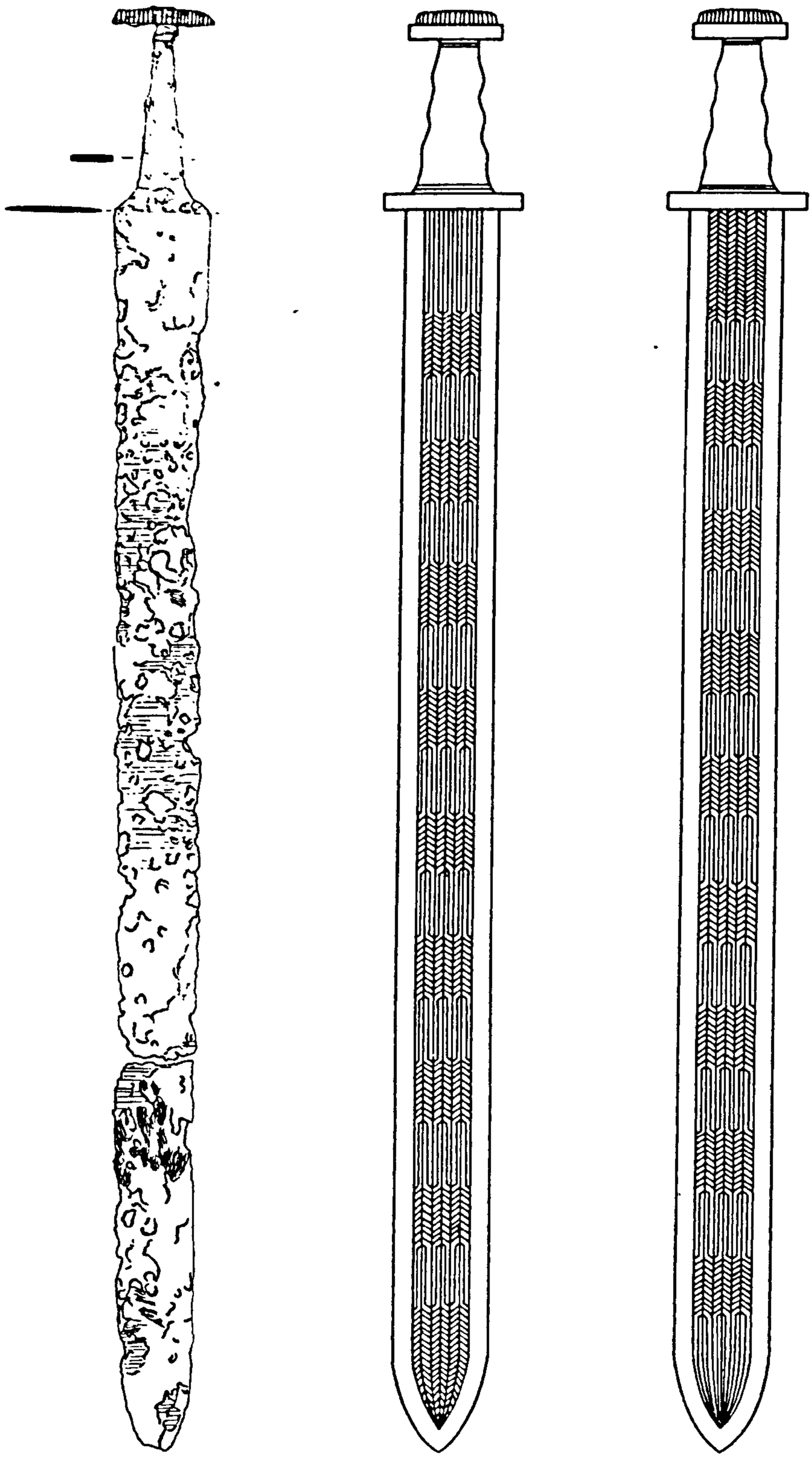

Fig 68 Acklam sword: reconstruction of both sides of the blade, drawn from a radiograph (Chapter 7.4.5)

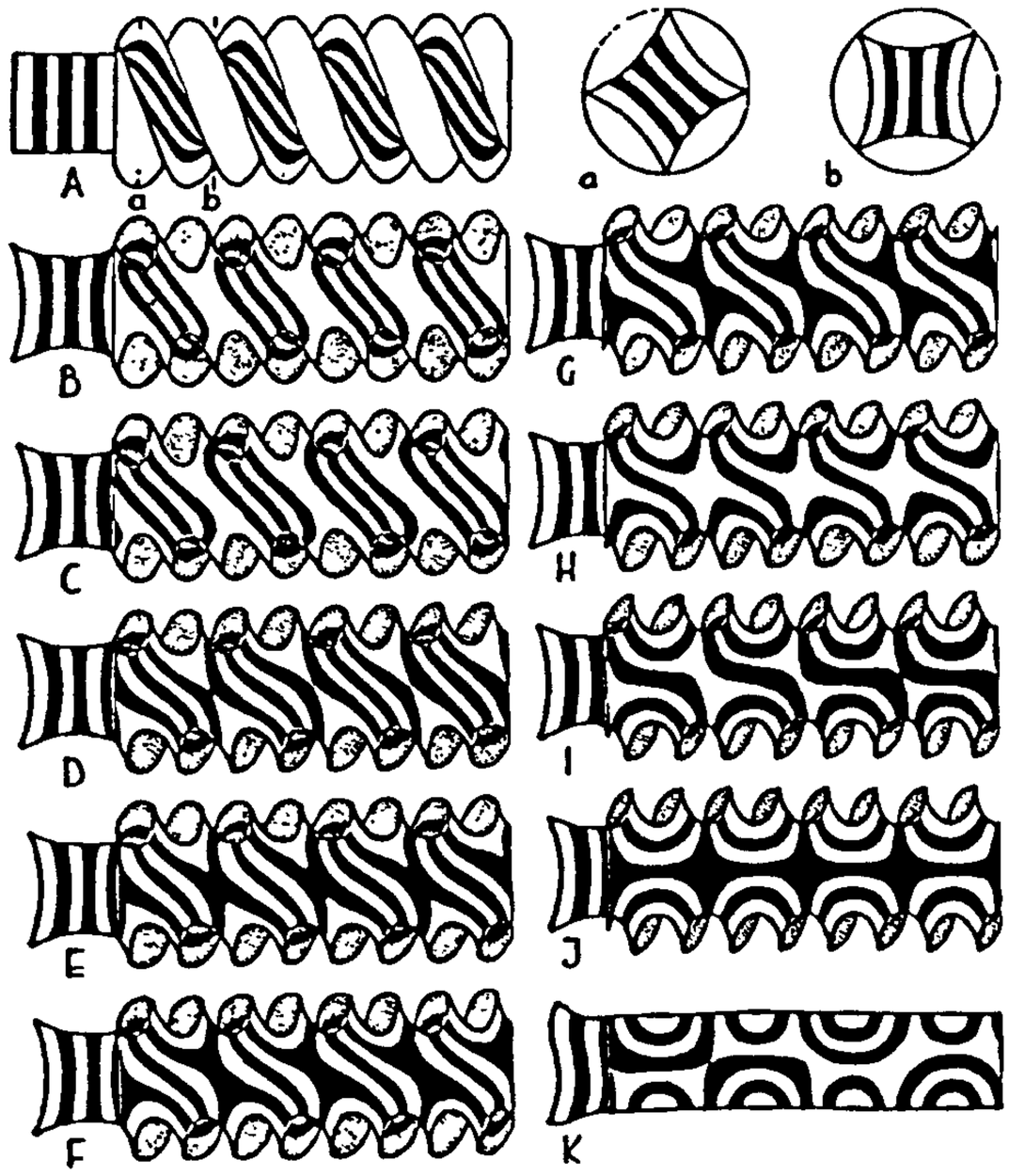

Fig 69 Variation of pattern through the thickness of a twisted laminated rod (Chapters 6 and 7)

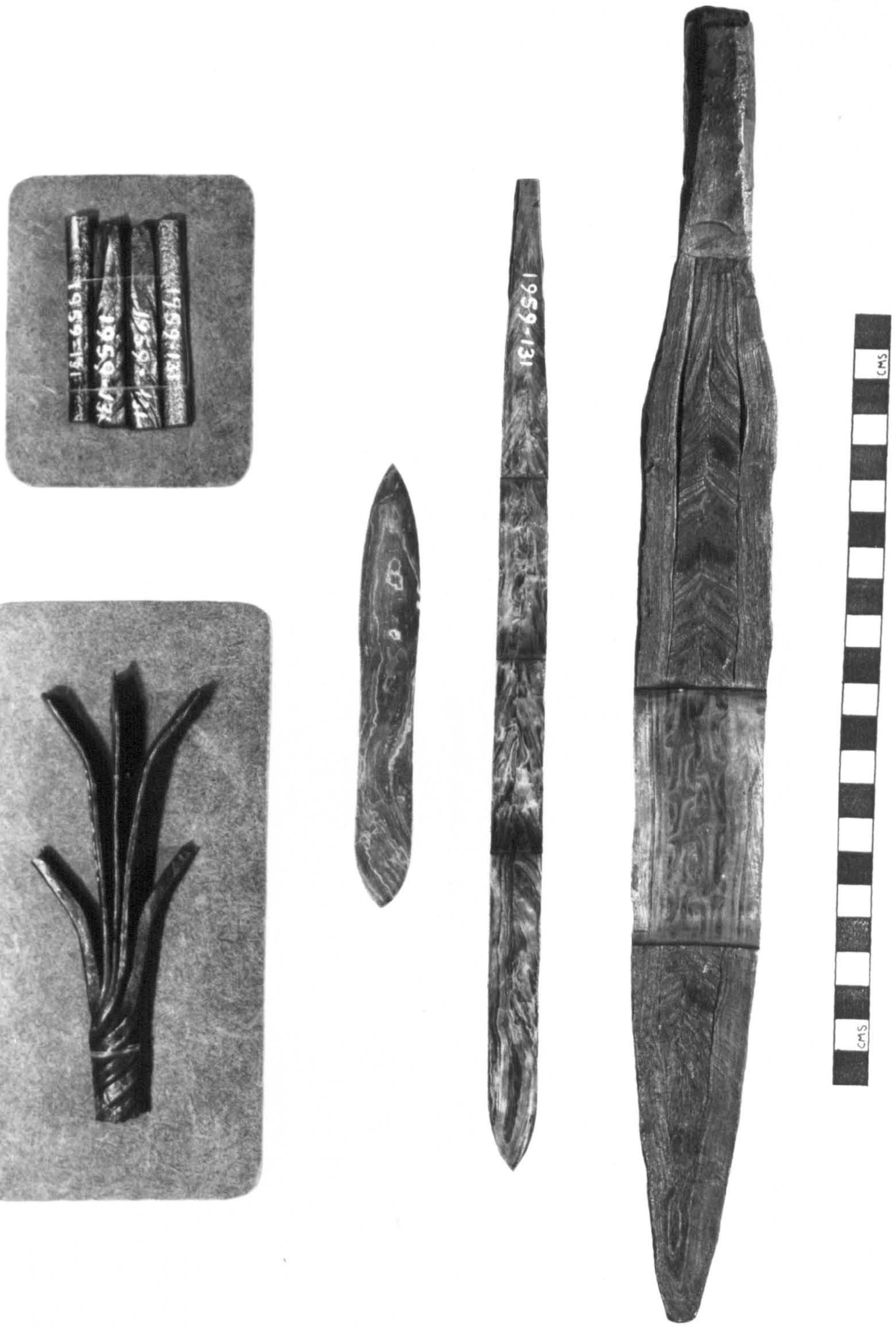

Fig 70 Pieces from different stages in Anstee's 1959 pattern-welding experiments (Chapter 7.4.1)

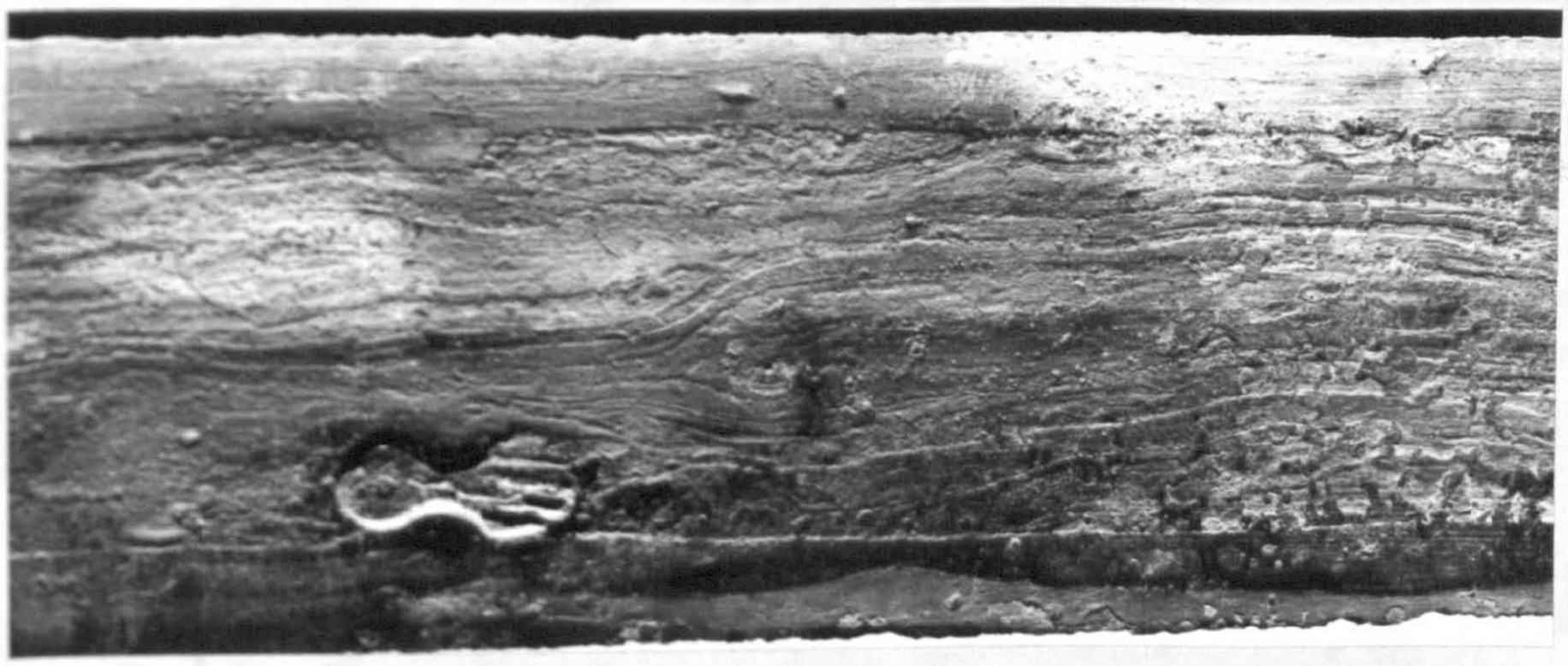

Fig 71 Peterborough Sword, surviving surface detail: heavily etched structural pattern with resist protected edges and remains of inlaid makers mark

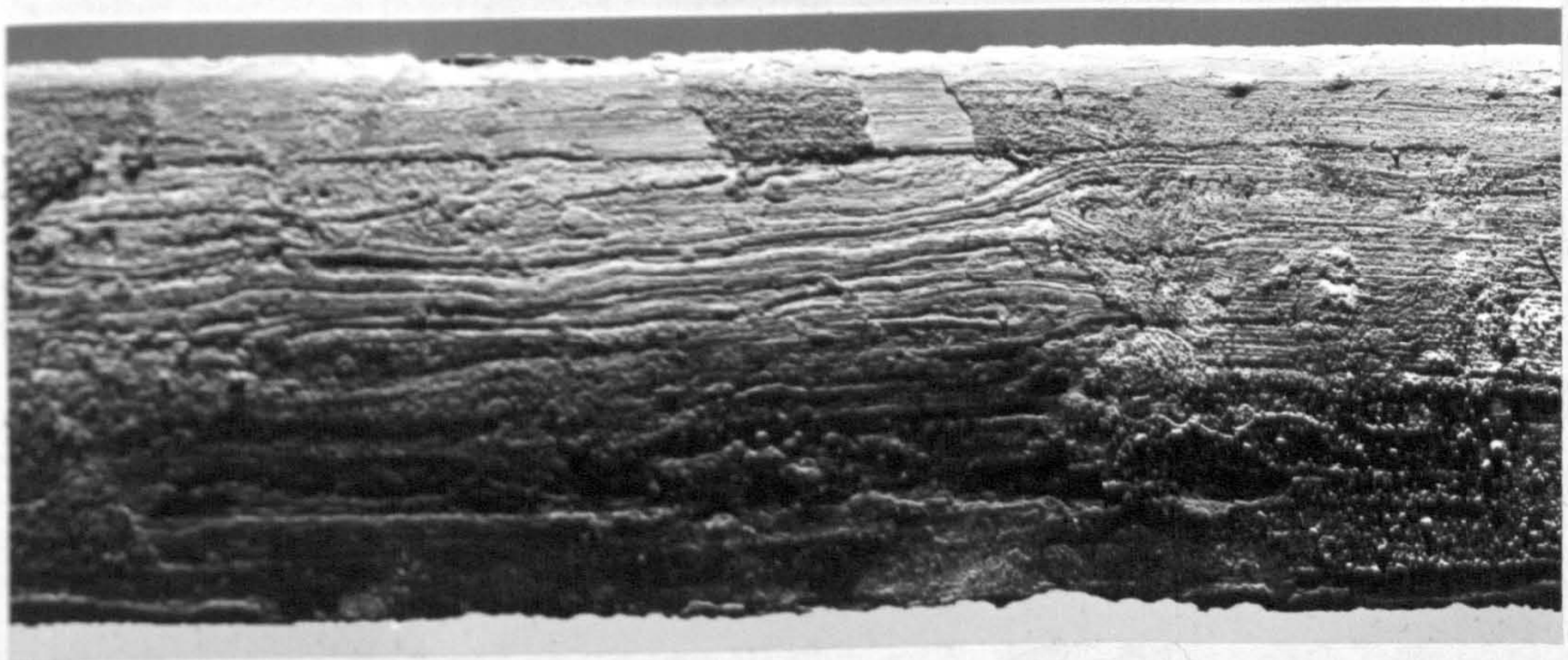

Fig 72 Peterborough Sword, surviving surface detail: pattern enhanced by oblique lighting

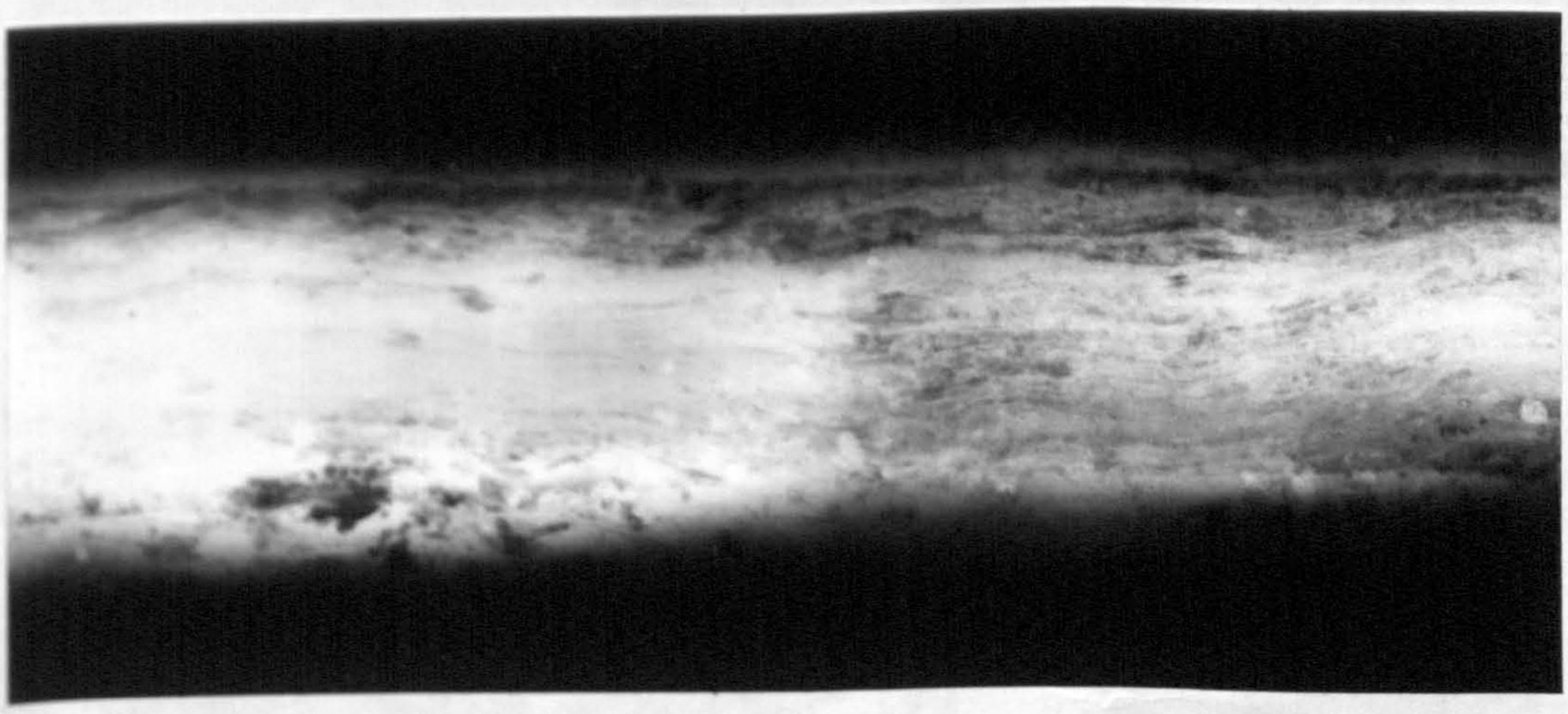

Fig 73 Peterborough Sword, x-radiograph showing the coarse-grain pattern running across the full width of the blade

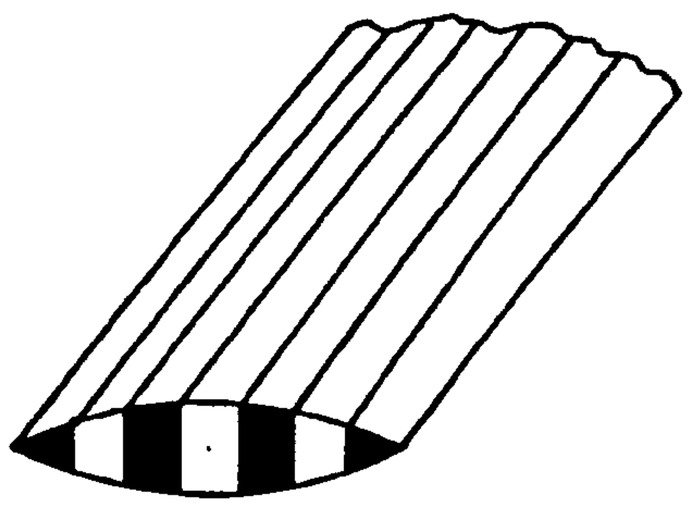

Fig 74 Simple (Stage 2b) pattern-welded structure seen in a sword blade from Llyn Cerrig Bach (see Chapter 7.4.2)

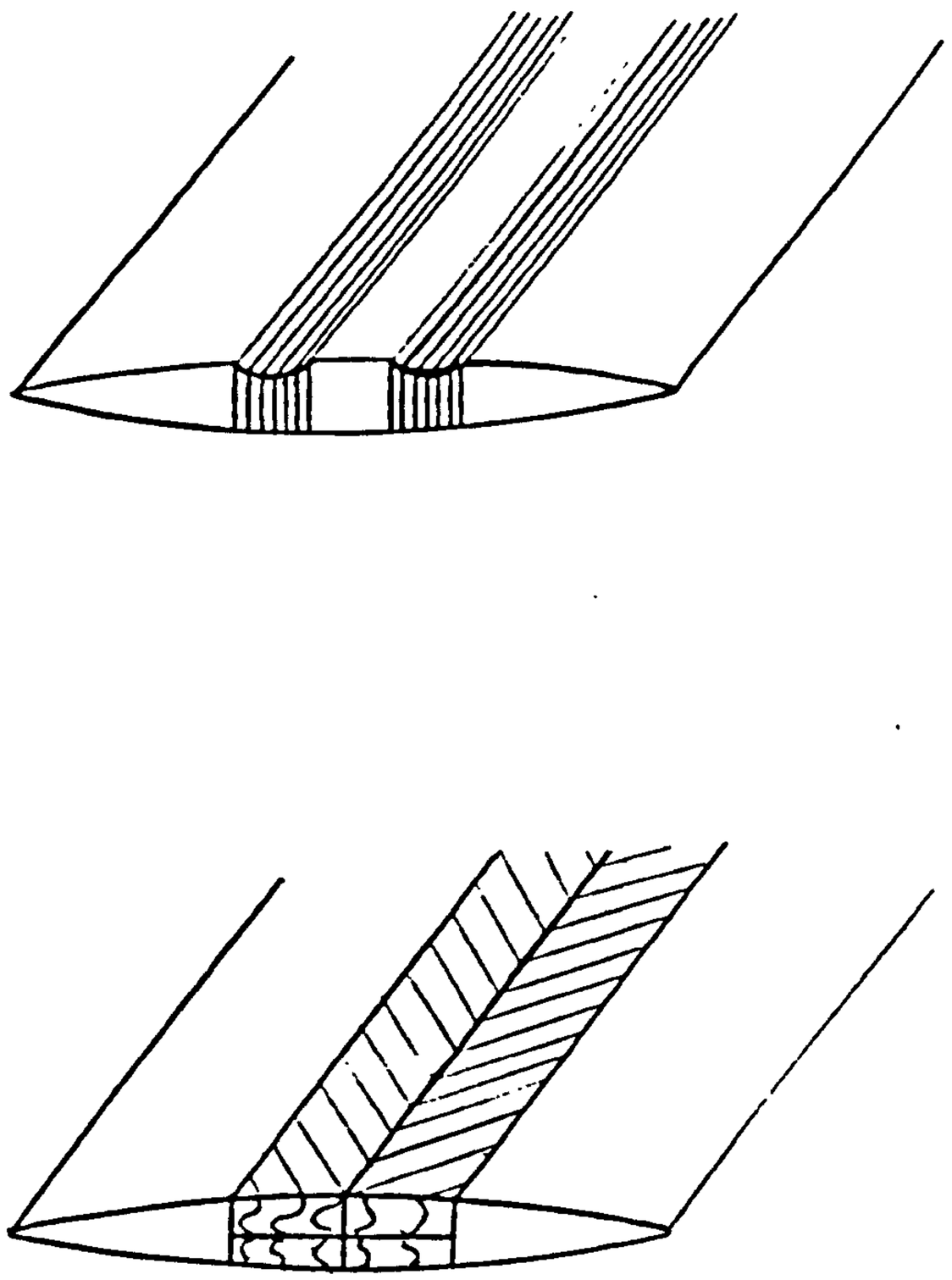

Fig 75 3rd century (Stage 3b) pattern-welded swords from Canterbury: (i) blade with a (Type 3) non-twisted pattern; (ii) blade with a (? Type 5) twisted pattern (see Figs 67 and 73); radiographs of Canterbury blades (i) and (ii)

(i)

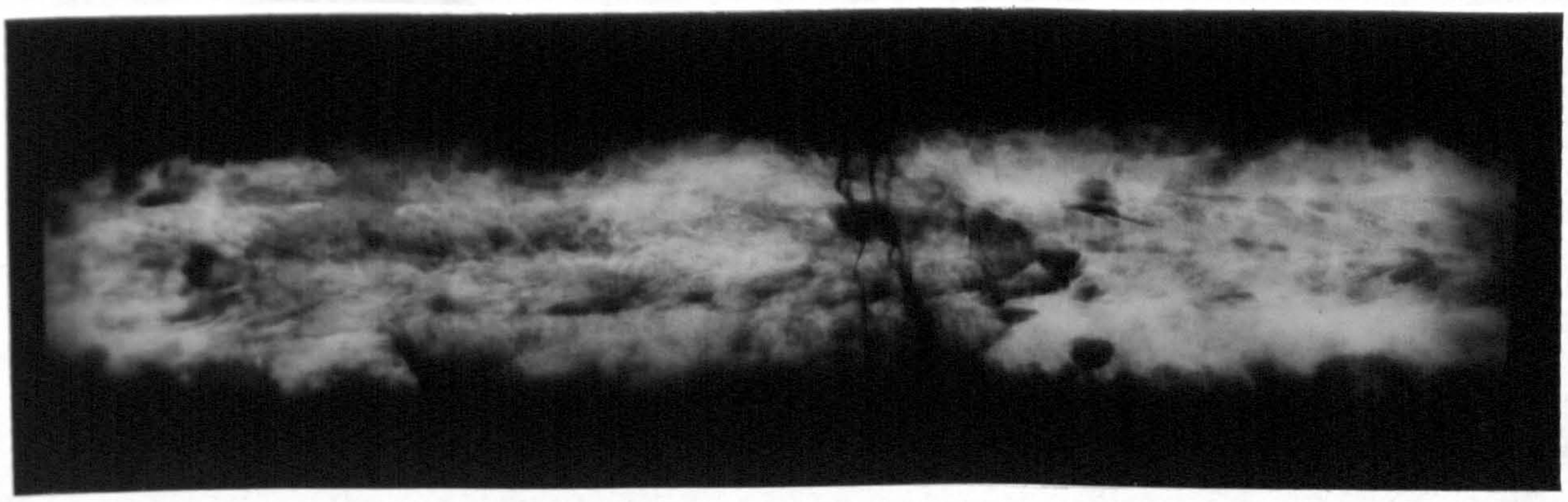

(ii)

Fig 75 (continued)

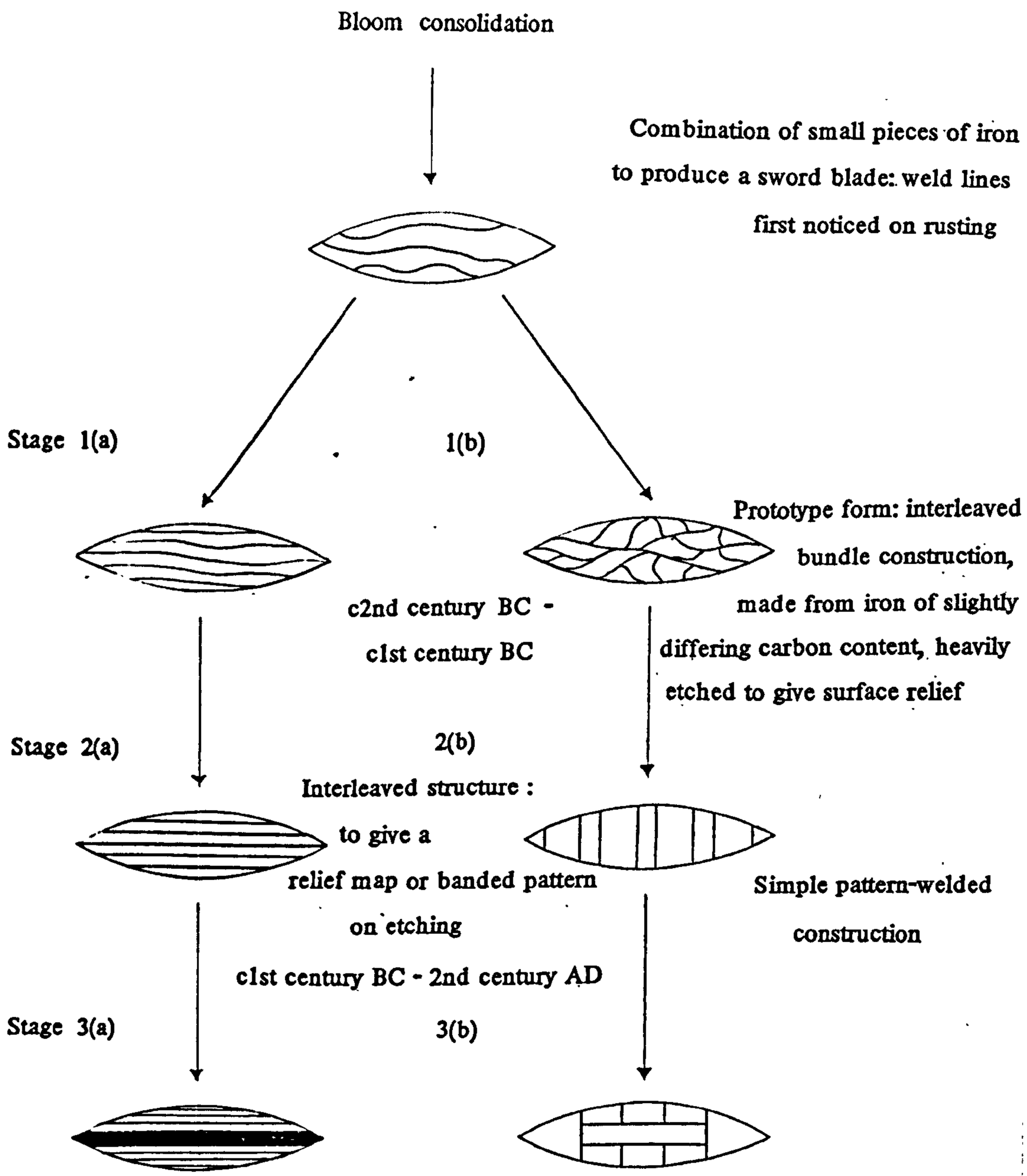

Fig 76 Development of pattern-welding (Chapter 7.4.2)

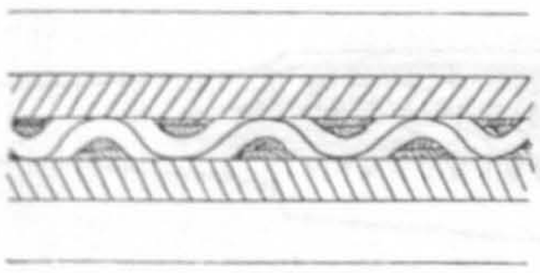

After Ypey (1972)

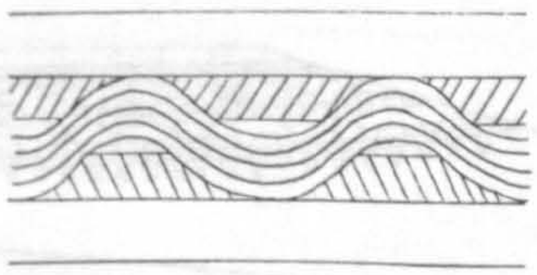

After Leppaaho (1964)

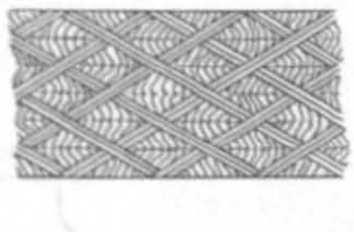

Nydam/Ashmolean Museum, ?3-4th c
(see Appendix 1)

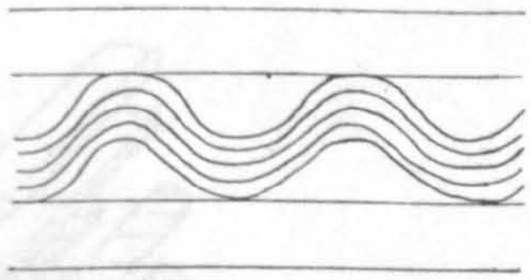

West Heslerton, 6-7th c
(see Appendix 1)

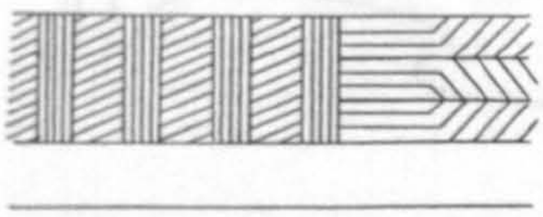

Howletts, Kent, 6th c
(see Appendix 1)

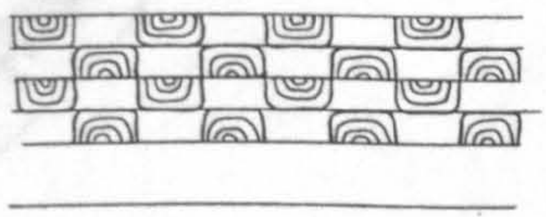

After Leppaaho (1964)

Fig 77 Some unusual forms of pattern-welding found on sword blades (Chapter 7.4.2)

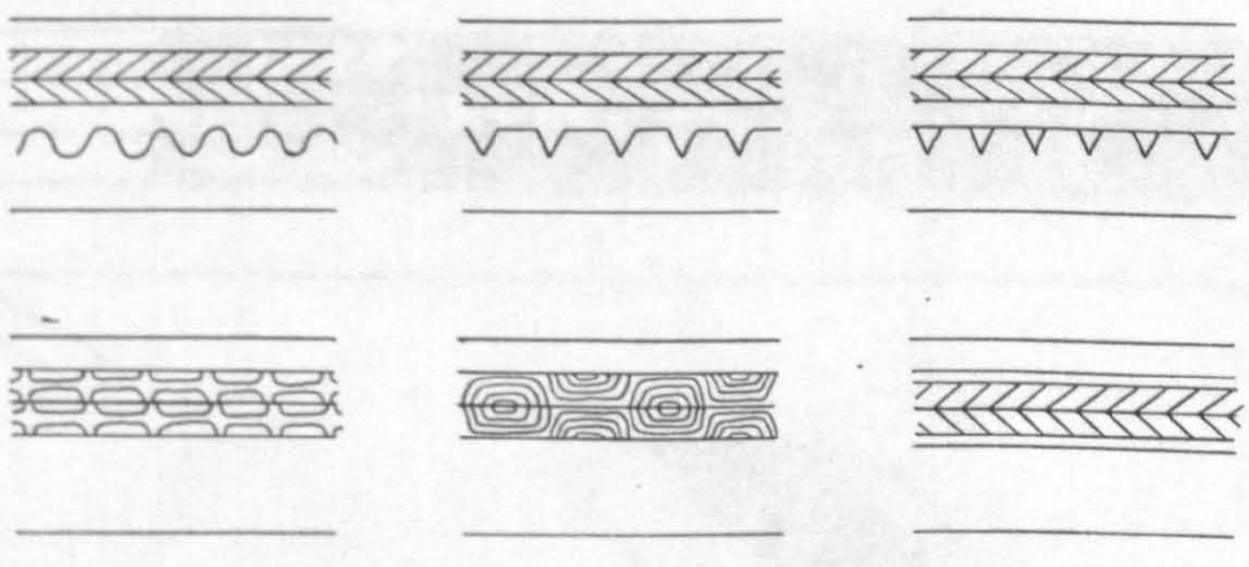

Fig 78 Combinations of weld pattern found on scramasaxes and/or spearheads of the Late Saxon period (Chapter 7.4.4)

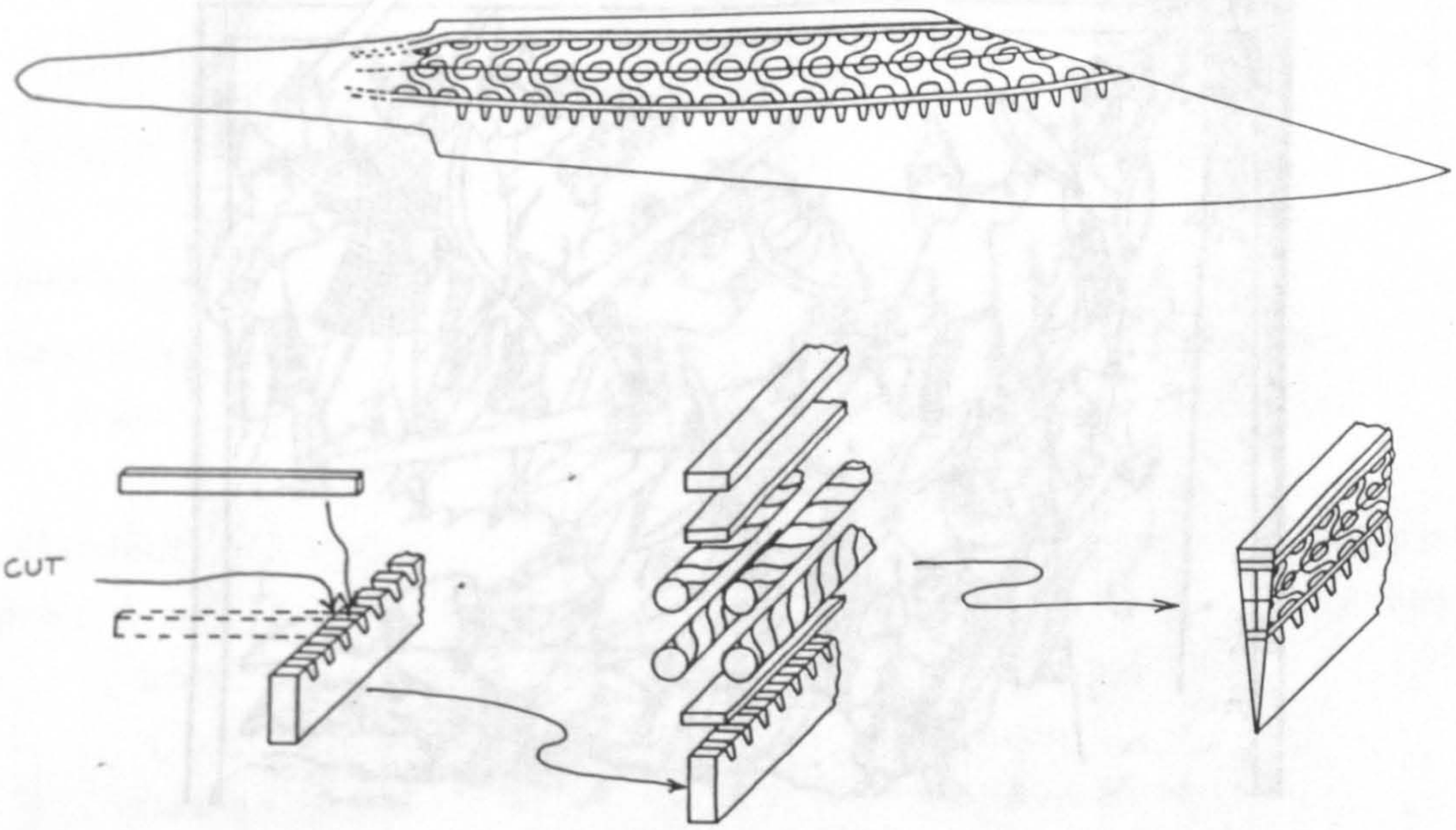

Fig 79 Aldersgate scramasax or knife: conjectural method of construction for this individual toothed type of weld pattern (Chapter 7.4.4)

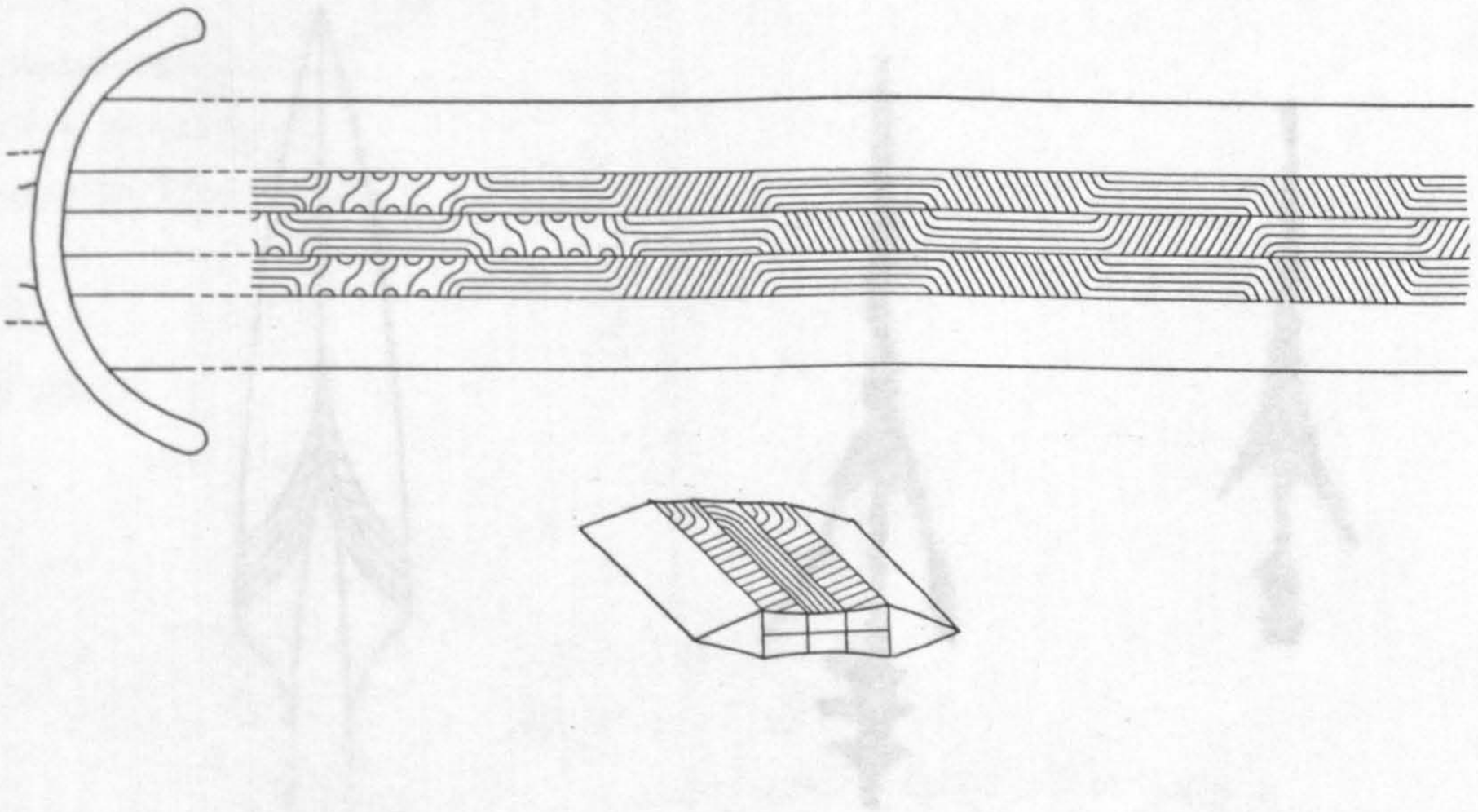

Fig 80 Gilling sword: pattern partially distorted by grinding (Chapter 7.4.5)

Fig 81 An eleventh century manuscript illustration showing barbed spearheads - British Museum, Cotton M.S Claudius Biv (see Chapter 7.4.5)

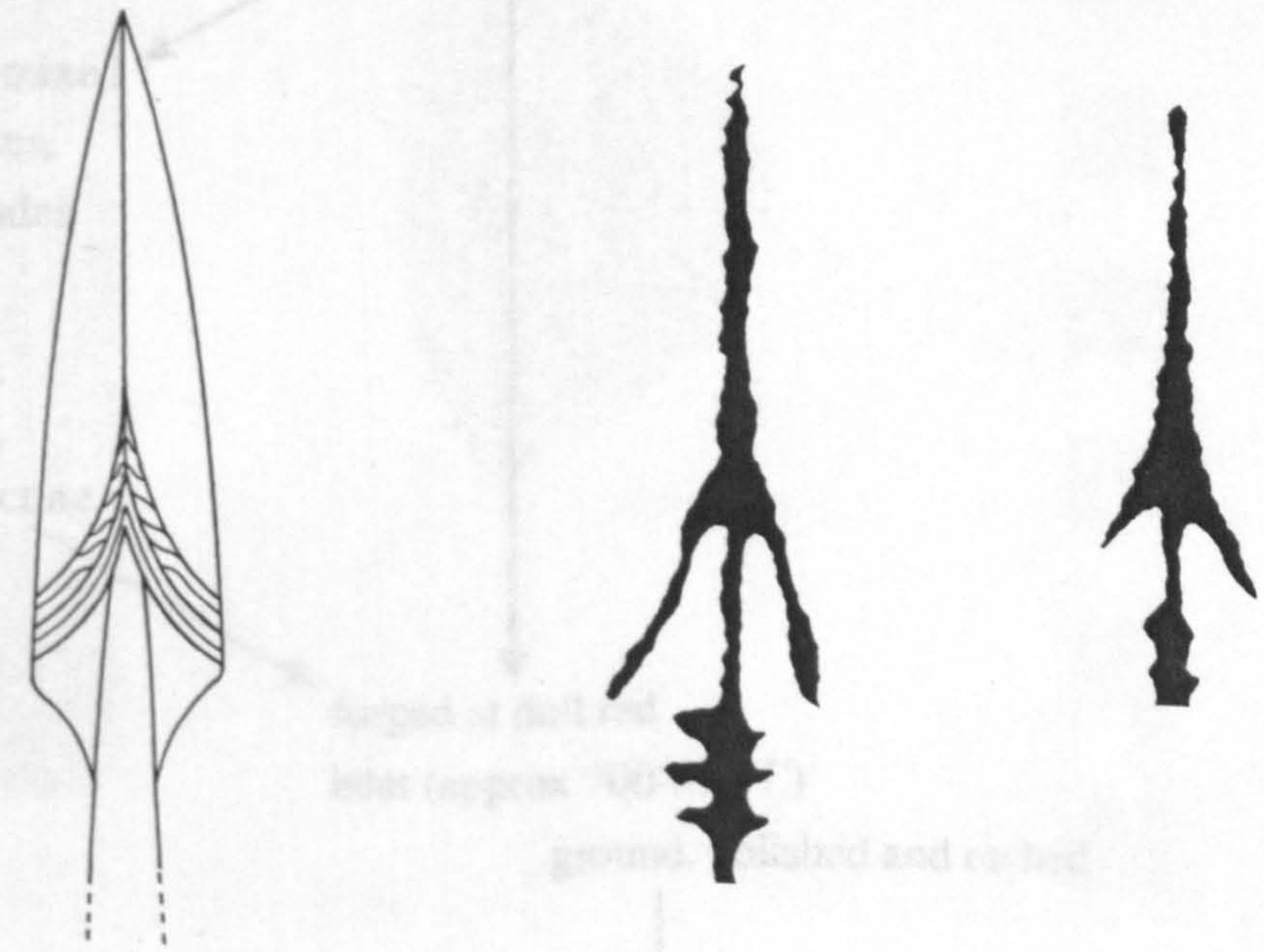

Fig 82 A comparison between a typical form of Late Saxon pattern-welded spearhead (6.50 from Kempsford) and one of the spearheads shown in the eleventh century illustration (Fig 81) (See Chapter 7.4.5)

Fig 83. The Wootz to Watered Crucible Steel Process

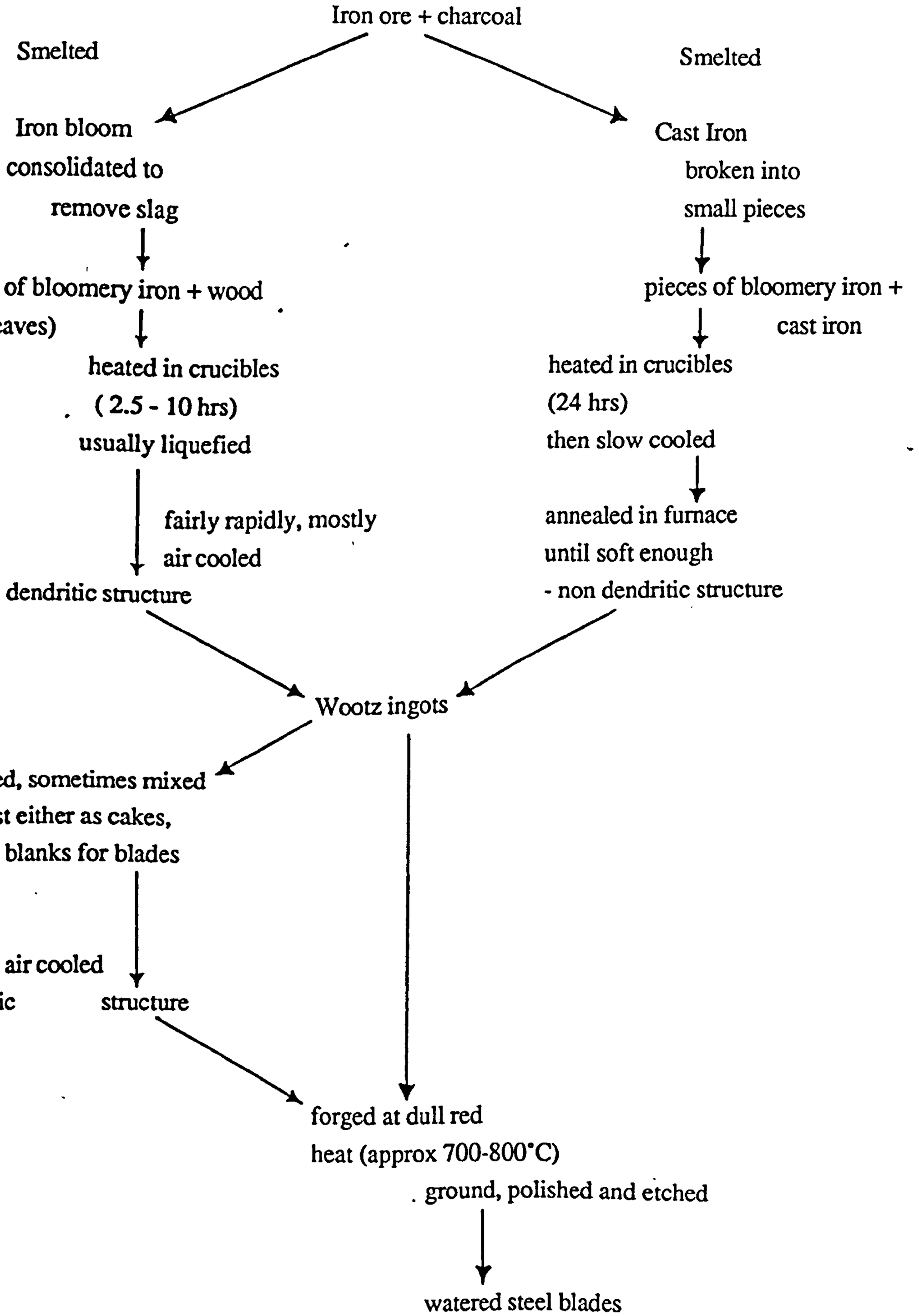

Fig 83 The wootz to watered crucible steel process (Appendix 2: A2.5.2)

Fig 84 Two wootz ingots and a bar forged from a wootz ingot (from the Science Museum, Percy Collection) (see Appendix 2 : A2.3)

Table 1

Effect of carbon on the average hardening temperature and the critical cooling rate of plain carbon steel

Carbon %	0.2	0.3	0.4	0.5	0.6	0.7	0.8	1.0
Average Hardening Temperature °C	870	850	830	810	790	770	760	760
Critical Cooling Rate °C/Sec	1200	1000	800	700	600	550	500	400

Table 2

Variation of Temper Colour with Temperature

TINT OF OXIDE ON SURFACE OF STEEL	TEMPERATURE °C	SUITABLE FOR
Dark blue	316	Hand saws
Blue	293	Fine saw blades, augers
Bright blue	288	Watch springs, swords
Purple	277	Table knives, large shears wood turning tools
Brown, beginning to show purple	266	Axes, Planes and Wood - working tools
Brown	254	Scissors, Shears, Cold Chisels
Golden Yellow	243	Penknives, Hammers, Taps
Straw	230	Razor blades
Pale Yellow	221	Small edge tools

Table 3

Effect of phosphorus on the diffusion of carbon

Starting material	% C absorbed in a given time
Fe	0.94
Fe + 0.6% P	0.60
Fe + 1.2% P	0.52

Table 4

Effect of temperature on the thickness of the carburised layer after two hours

minimum carbon content = 0.3%

Temperature, °C	Thickness, mm
950	1.14
1000	1.64
1050	1.90
1100	2.66

Table 5

Effect of carbon and phosphorus on the hardness of iron

	%	Hardness - HV			
		Carbon		Phosphorus	
(a)	0	*	75	*	75
	0.05		-		78
	0.15		100		91
	0.31		-		113
	0.23	+	110	+	145
	0.60		180		216
	0.90		200		250
	1.20		260		287
	1.50		-		270
(b)	0.58		-	x	183
	0.58		-		204
	0.59		-		149
	0.61		-		177
	0.67		-		197
	0.69		-		191
	0.71		-		167
	0.74		-		200
	0.76		-		203
	0.77		-		204
	0.78		-		204
	0.86		-		203

(a) * and + relate to annealled iron

\+ Based on experimental work of J.G. McDonnell using less pure materials

x Approximate correlations of hardness and percentage of phosphorus from the present work. NB. The hardness figures are corrected assuming an error of 15% on the original results of microhardness testing

Table 6

Colour Changes of Iron with Temperature

Colour	Temperature °C
Just Visible Red	500 - 600
Dull Cherry Red	700 - 750
Cherry Red	750 - 825
Bright Cherry Red	825 - 875
Brightest Red	900 - 950
Orange	950 - 1000
Light Orange	1000 - 1050
Lemon	1100 - 1200
White	1200 - 1300
Bright White	1300 - 1400

Table 7 **Summary of Metallographic Analyses (Chapter 6)**

Catalogue No.	Sample No.	Site	Swords Site Ref No.	Date	Structure/Hardness HV Edge	Back/Core	Remarks
1	S 32	Unknown (Reading Museum)	131-61	EIA	F+P/112-129		
2	S 27	Thames at Little Wittenham	106.61(1)	LIA	F+P/178-F/120		
3	S 29	Thames at Little Wittenham	Reading	LIA	F+P/214-329		
4	S 39	Whittlesey, Cambridge	Peterborough	R-B	F+P+/185	F+P/149	Type 1
5	S 17	Sarre, Kent	Maidstone KAS 830	6-7th	M+T (564	F+P/236	PW
6	S 49	Bifrons, Kent (?)	Maidstone Tomlinson Coll. KAS620, 1954.20	"	F/158	F/118-178	PW
7	S 51	Sarre, Kent	Maidstone KAS820	"	F+P/156-189		-
8	S 52	Sarre, Kent	Maidstone KAS823	"	F/187	F+P/159-162	PW
9	S 53	Sarre, Kent	Maidstone KAS 825	"	F/144	F+P/159-217	PW
10	S 54	Sarre or Bifrons, Kent	Maidstone KA834	"	F(P)164-197	F/172	PW
11	S 55	Sarre or Bifrons, Kent	Maidstone KAS836	6-7th	M+T/581	F/181	PW
12	S 56	Bifrons, Kent	Maidstone	"	F/152	F/164-214	PW
13	S 12	Wickhambreux, Kent (?)	Maidstone	"	F+P/206	F/177-202	PW
14	S 13	Kent	Maidstone Tomlinson Collection KAS 620, 1954.17	5 - 7th	F+P/171-230		
15	S 14	Eastrey, Kent	Maidstone A-S. 121	6-7th	F/234	F/230-243	PW
16	S 15	Holborough, Kent	Maidstone	7th cent	F/114	?F/129-217	PW
17	S 18	Aylesford, Kent	Maidstone	6-7th	F+P/212	P+F/187-212	PW

Catalogue No.	Sample No.	Site	Swords Site Ref No.	Date	Structure/Hardness HV Edge	Back/Core	Remarks
18	S 19	Wickhambreux, Kent (?)	Maidstone	"	F+P/241	F/138-185	PW
19	S 20	Lenham Kent	Maidstone 3.1977	6th cent	P/298	F+P/179	PW
20	S 1	Lovedon Hill, Lincs	Lincoln; 6.66	6-7th	F+P/165	F/199-202	PW
21	S 40	Chesterton, Camb.	Peterborough 16/1979/1	5-6th	P+T/272	F/230-243	PW
22	S 10	Mitcham, Surrey	56.106/14	6th	F+P/203	F/96-123	PW
23	S 45	Mitcham, Surrey	Mus London 56.106/13	"	F+P/200-221	F+P/215	PW
24	S 16	Sarre Kent	Maidstone KAS818	6th-7th	F(P)/170	F+P/163-172	PW
25	S 31	Caversham, Reading (SU 73867511)	Reading 51.80	7-9th	M+T/775	F/149-217	PW
26	S 46	Brentford, Middx	Mus. Lond 0.2112	"	TM/647	M/788-F/212	PW
27	S 7	Unknown (Thames?)	Mus. Lond. C2260	9-10th	M+T/477	M+T+P/268	Steel
28	S 8	Unknown (Thames?) C2258	Mus. Lond.	"	F+SC/172	F/81	Steel/Iron
29	S 43	Thames, nr London	Mus. Lond.	10-11th	P/256	P+F/179	PW
30	S 48	Rochester, Kent	Maidstone	9-10th	M/564	F/163	PW
31	S 23	Thames	Reading	"	TM+P/762	P/428	Inlaid
32	S 47	Thames, London Waterloo Bridge	Mus. London A3670	10th	P(F)/239	F+P/144	Steel
33	S 24	Cleeve, Goring on Thames	Reading 256:636 (TCB)	9-11th	M+T/647	F/221	PW
34	S 41	Thames, Vauxhall	Mus. London. A.13591	8-10th	TM/490	F/305	PW
35	S 25	Reading, Oxford Rd	Reading 16:26	10-11th	P(F)/272	P+F/170	Inlaid
36	S 44	Thames at Brentford	Mus. London A.24419	11th	P/325	F/157	PW
37	S 26	Thames at Wallingford Bridge	Reading 1608:64	12-14th	P+F/195	F/133	Iron

Catalogue No.	Sample No.	Site	Swords Site Ref No.	Date	Structure/Hardness HV Edge	Back/Core	Remarks
38	S 28	Unknown	Reading 56:80 (HL)	13-14th	TM/496	TM/393	
39	S 30	Sunbury Weir, Middx	Reading	Late Med	P+F/236-171		
40	S 50	Barham Down	Maidstone	6-8th	P+F/248	F/171	Knife Type 4
41	S 22	R. Thames Reading	52.80 Reading	9-11th	F/152	F/184	PW
42	S 34	R. Thames Kempsford	Swindon Mus 790308	10-11th	P+F/204	F/165	PW
43	S 37	R. Thames Kempsford	Swindon Mus	9-10th	M/737	F+P/236-174	Knife Type 1
44	S 42	Leyton	0.2275	8-10th	M/831	F/157	Knife Type 1
45	S 4	Dorset	Dorset Mus	9-10th	TM/775	F/152	PW
46	S 9	R. Thames Hampton	A.27086	10-11th		F/98-75	
47	S57	Malasia	1. Glover	19-20th	P+F/189		PW Kris
48	S 38	R. Thames, Kempsford	Swindon Mus	c600BC	F+P/149	F/112	Knife Type 0
49	S 35	R. Thames, Kempsford	Swindon Mus	6-11th	F+P/172	F/116	Knife Type 0
50	S 36	R. Thames, Kempsford	Swindon Mus	10-11th	TM/496-272	F+P/277-108	PW
51	S 33	R. Thames	Swindon Mus	9-10th	P+F/269	F/178	PW

Table 8 - Electron probe micro-analysis (EPMA): Results, percentage of minor elements by weight

Object	Analysis no	P	S	Co	NI	Cu	As
S4a	1	0.709	0.008	n.d.	0.014	0.012	0.003
	2	0.037	0.011	0.117	0.127	0.004	n.d.
	3	0.048	0.011	0.043	0.071	n.d.	0.001
	4	0.77	0.003	n.d.	0.026	0.004	n.d.
	5	0.752	0.014	n.d.	0.025	0.007	n.d.
	6	0.78	0.002	0.005	0.03	n.d.	0.022
	7	0.754	0.01	0.004	0.022	n.d.	0.039
	8	0.06	0.006	0.03	0.049	n.d.	n.d.
	9	0.033	0.008	0.035	0.081	0.008	n.d.
	10	0.035	0.006	0.026	0.043	n.d.	0.009
	11	0.046	0.003	0.017	0.029	0.009	0.006
	12	0.766	0.01	n.d.	0.031	n.d.	0.029
	13	0.584	0.004	0.003	0.03	n.d.	n.d.
	14	0.583	0.013	n.d.	0.032	0.002	n.d.
	15	0.042	0.01	0.029	0.022	0.006	0.012
	16	0.027	0.012	0.042	0.029	0.001	0.022
	17	0.712	n.d.	0.008	n.d.	n.d.	0.053
	18	0.008	0.004	0.016	0.031	0.006	n.d.
S33	19	0.073	0.005	0.005	0.002	0.038	n.d.
	20	0.033	0.011	n.d.	0.012	n.d.	0.051
	21	0.043	0.006	n.d.	0.031	n.d.	0.037
	22	0.591	0.014	0.02	0.073	0.002	0.112
	23	0.031	0.007	n.d.	0.009	n.d.	n.d.
	24	0.035	0.009	n.d.	0.022	0.009	0.037
	25	0.857	0.021	0.002	0.034	n.d.	0.018
	26	0.062	0.007	n.d.	0.03	n.d.	0.1
	27	0.052	0.007	n.d.	0.02	0.001	0.074
	28	0.688	0.013	n.d.	0.043	0.02	0.048
S15	29	0.354	0.015	n.d.	0.032	n.d.	0.016
	30	0.532	0.023	n.d.	0.021	0.001	0.06
	31	0.613	0.021	n.d.	0.036	0.002	0.033
	32	0.109	0.016	n.d.	0.017	0.006	0.063
	33	0.109	0.004	n.d.	0.017	0.006	0.039
	34	0.115	0.009	n.d.	0.029	0.007	n.d.
S14	35	0.01	0.019	0.011	0.03	0.016	0.002
	36	0.672	0.007	n.d.	0.009	0.043	0.044
	37	0.047	n.d.	0.001	0.027	0.021	0.01
	38	0.11	n.d.	0.022	0.067	0.04	0.12
	39	0.086	0.003	n.d.	0.016	0.019	n.d.
	40	0.109	0.015	n.d.	0.01	0.057	0.028
S34a	41	0.025	0.007	0.009	0.043	n.d.	0.11
	42	0.763	0.009	0.008	0.59	n.d.	0.31
	43	0.036	0.009	n.d.	0.027	0.003	0.016
	44	0.782	0.18	0.01	0.046	n.d.	0.043
	45	0.46	0.006	0.001	0.027	n.d.	0.047
	46	0.081	0.008	0.002	0.044	0.001	0.093
	47	0.737	0.007	0.007	0.07	n.d.	0.032
	48	0.745	0.01	0.017	0.058	n.d.	0.045